CAMBRIDGE AEROSPACE SERIES 4

FLIGHT MECHANICS OF HIGH-PERFORMANCE AIRCRAFT



Nguyen X. Vinh

This text, written at a level accessible to advanced undergraduate and beginning graduate students, covers all aspects of flight performance of modern day high-performance aircraft, from take-off to landing, through different phases of flight in climb, cruise, turning and ascent.

The book begins with an introduction to equations of motion, aerodynamic forces, and propulsion systems and then goes on to apply what has been learned to performance during descent and glide, cruising, climb, turning, and take-off and landing. A final chapter discusses the performance of hypervelocity reentry vehicles. Challenging exercises are included at the ends of chapters. These are designed to give readers a deeper understanding of the material covered in the text. This text will serve as an introductory text for advanced under-graduates and beginning graduate students. It will also be of value to researchers in universities and industry. The author is an internationally recognised teacher and researcher in this subject and has received the Excellence in Teaching and Excellence in Research Awards from the College of Engineering at the University of Michigan.

Cambridge Aerospace Series

1. J. M Rofle and K. J. Staples (ed.): *Flight Simulation*
2. P. Berlin: *The Geostationary Applications Satellite*
3. M. J. T. Smith: *Aircraft Noise*
4. N. X. Vinh: *Flight Mechanics of High-Performance Aircraft*
5. W. A. Mair and D. L. Birdsall: *Aircraft Performance*

Cambridge Aerospace Series 4

General editors: David L. Birdsall, Peter Barker

Flight Mechanics of High-Performance Aircraft

Flight Mechanics of High-Performance Aircraft

Nguyen X. Vinh

Professor of Aerospace Engineering
The University of Michigan

CAMBRIDGE
UNIVERSITY PRESS

Published by the Press Syndicate of the University of Cambridge
The Pitt Building, Trumpington Street, Cambridge CB2 1RP
40 West 20th Street, New York, NY 10011-4211, USA
10 Stamford Road, Oakleigh, Melbourne 3166, Australia

© Cambridge University Press 1993

First published 1993
First paperback edition 1995

A catalogue record for this book is available from the British Library

Library of Congress cataloguing in publication data

Vinh, Nguyen X.
Flight mechanics of high-performance aircraft/Nguyen X. Vinh.
p. cm. — (Cambridge aerospace series)
Includes bibliographical references and index.
ISBN 0 521 34123 X
1. Airplanes—Performance. 2. Aerodynamics. I. Title.
II. Series.
TL671.4.V56 1993
629.132'3—dc20 91-18833 CIP

ISBN 0 521 34123 X hardback
ISBN 0 521 47852 9 paperback

Transferred to digital printing 1999

Contents

Foreword *page* xi

1 Introduction **1**

1.1 Flight mechanics 1

1.2 Plan of study 3

1.3 Objective 5

2 Equations of motion **8**

2.1 Introduction 8

2.2 Relative angular motion 9

2.3 Equations for flight over a rotating spherical earth 11

2.4 Equations for flight over a flat earth 22

Exercises 25

3 Aerodynamic forces **27**

3.1 Introduction 27

3.2 The earth's atmosphere 28

3.3 Aerodynamic forces 33

3.4 The drag polar 35

3.5 Effect of Mach number 41

3.6 Airspeed measurement 44

3.7 The equivalent airspeed 52

Exercises 54

4 Propulsion systems **59**

4.1 Introduction 59

4.2 Rocket 60

8.5 Numerical application 240
8.6 Non-steady turn 243
Exercises 248

9 Turning flight of jet aircraft 253
9.1 Turning flight in general 253
9.2 The maneuvering limit 256
9.3 The thrust required for turning 261
9.4 Optimum turn 265
9.5 Numerical application 270
9.6 Steady turn with constant thrust setting 273
9.7 Non-steady turn 279
9.8 Three-dimensional turn 281
9.9 Turning in a vertical plane 286
Exercises 290

10 Take-off and landing performance 298
10.1 Introduction 298
10.2 Description of a take-off 298
10.3 Equations of motion 301
10.4 Practical solutions for the ground run 305
10.5 Ground effect and wind effect on ground run 309
10.6 The transition phase 312
10.7 Description of a landing 317
10.8 Transition to touch-down 318
10.9 The ground run during landing 320
Exercises 322

11 Performance of hypervelocity reentry vehicles 332
11.1 Introduction 332
11.2 Dimensionless equations of motion 334
11.3 Gliding entry at small flight path angles 339
11.4 Ballistic entry at large flight path angles 344
11.5 Skip entry 348
11.6 Aerodynamic heating 353
11.7 Comparative analysis of performance 359
Exercises 362

Appendices 369
1 Atmospheric and gravity data 369
2 Typical aircraft characteristics 371
3 Conversion table 374

References 375

Index 377

Foreword

After its initial phase of qualitative evaluation, the Theory of Flight of aircraft has for many years entered the rigorous domain of rational mechanics.

Due to the strong development of computational fluid dynamics in analyzing the known equations for real gases, and due to progress in wind tunnel testing and flow measurements without interference on the ground and in test flights, the physical phenomena concerning aircraft motion from low speeds to very high speeds are accurately known except perhaps in some hypersonic domain. This is indeed an excellent area for modeling with continuous improvement toward perfection.

But the power of electronic computing machinery and the refined programs for performance evaluation should not deter the engineers from the theoretical foundations of rational mechanics and at the same time from the physical meaning and consequently the influence of each term in the system of equations governing the motion of the flight vehicle. The continuous iteration between the physical phenomena, the results from experience, and the governing theory constitutes the intellectual and fundamental progress of our profession.

It is in this spirit that Flight Mechanics should be taught. Having done it in the past, I can appreciate the volume of knowledge and the amount of effort that Professor Nguyen X. Vinh, my friend and colleague at the French Académie Nationale de l'Air et de l'Espace, has accumulated in the present text to assure its clarity based on a solid foundation.

Being a rated instrument flying pilot in France, a chief of staff of the Vietnamese Air Force for many years, with doctor's degrees in Aerospace Engineering and in Mathematics respectively from the

United States and from France, and now a professor in a prestigious American university, the author of this text has focused the required experience and intellectual capability to achieve his goal.

As a prolific writer, the author has already written two books in Flight Mechanics, the first one in hypersonic reentry trajectories published by the University of Michigan where he has taught for over twenty years, and the second one in optimal trajectories in atmospheric flight published by Elsevier Scientific Publishing Company in the Netherlands. In addition, he is the author of 16 official reports published by government agencies in the United States and in Europe and more than 70 technical papers in refereed journals.

With my salutation for the author's exceptional career and his gentle character, I am happy and honored to introduce the present treatise.

André Turcat
Former Pilot and Director of
Flight Tests for the SST Concorde
General Secretary of the
Académie Nationale de l'Air
et de l'Espace

1

Introduction

1.1 Flight mechanics

Atmospheric flight mechanics is the study of the motion of a vehicle inside a planetary atmosphere.

With respect to an inertial frame of reference, let $\mathbf{r}$ be the vector defining the position of the center of mass of the flying object and $\mathbf{V}$ its velocity vector. They are related by the kinematic relation

$$\frac{d\mathbf{r}}{dt} = \mathbf{V} \tag{1.1}$$

This book is restricted to performance analysis. In this respect, we follow the motion of the center of mass under the application of various forces. This involves the force equation

$$m\frac{d\mathbf{V}}{dt} = \mathbf{T} + \mathbf{A} + m\mathbf{g} \tag{1.2}$$

where m is the mass, $\mathbf{T}$ the propulsive force, $\mathbf{A}$ the aerodynamic force and $\mathbf{g}$ the acceleration due to the gravitational attraction of the planet which, in our case, is the earth. Some performance characteristics of interest are the range of variation of speed, from a minimum value to a maximum value, the ceiling which is the maximum altitude attainable by the vehicle, its maneuverability in terms of the rate of climb, the turning radius and the turning rate, the time of flight and the distance travelled for a given amount of fuel. This leads to including the

equation for the variation of mass in the form

$$\frac{dm}{dt} = -\beta \tag{1.3}$$

where β is the fuel mass flow rate and is a characteristic of the propulsion system.

A typical flight trajectory of a vehicle, which may also be an orbital vehicle, is shown in Fig. 1.1, from the initial time t_0 to the final time t_f. The type of vehicle considered in this book is invariably a winged vehicle with a plane of symmetry. It leaves the ground by taking off along a horizontal runway and lands at the end of the mission in the same manner. In between, the vehicle, which we refer to as the aircraft except in the last chapter on reentry trajectories, first proceeds to climb to a cruise altitude to accomplish the mission and near the end, descends to make an approach for landing. During the flight, the aircraft is expected to perform some turning maneuvers. Each of these segments of the flight mission is a topic for performance analysis.

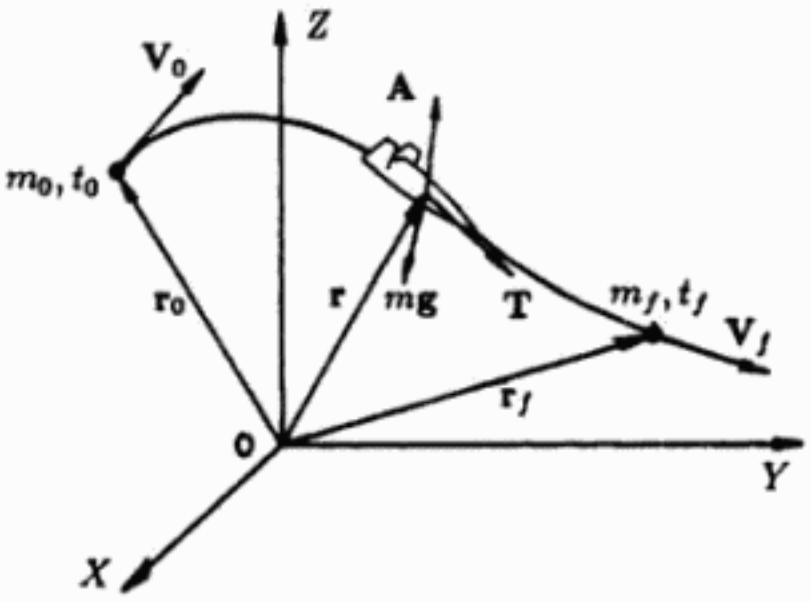

Figure 1.1: Typical flight trajectory.

In flight, the aircraft constitutes a dynamic system, and in evaluating its performance, we consider all possible achievements. This is done by controlling the flight trajectory through the propulsive thrust **T** and the aerodynamic force **A**. Through the analysis, the ultimate

objective is to display clearly, in some way, the peak performance. For example, starting from an initial mass m_0, at the initial time t_0, and for a prescribed final mass m_f, the range problem consists of evaluating the distance travelled along a ground track which is a great circle with its plane passing through the initial position vector $\mathbf{r}_0$. Of all the possible distances, there exists a maximum range which is attained by an appropriate selection of the flight altitude, the propulsive control and the aerodynamic control. Likewise, in a coordinated turn at constant altitude, the heading change can be controlled at various rates, and the maximum rate is the peak performance achieved.

The analysis in this book will be based on the three equations listed above. At first, they look deceptively simple, but in fact, they constitute a set of seven non-linear differential equations for the three components of the position vector, three components of the velocity vector and the mass. Furthermore, the aircraft with its propulsion system installed, is a physical object, and as such its operation inside an atmosphere is subject to several laws of physics, and the inherent relationships must be well understood before the actual analysis can be carried out. Once the preliminary discussion of the physical phenomena and their range of validity is properly completed, the rest of the analysis is a problem of theoretical mechanics. This is the reason for selecting as the title of this book, *Flight Mechanics of High-Performance Aircraft*. The physical aspect of flight at high altitude and high speed and the theoretical mechanics of flight are both given due consideration.

1.2 Plan of study

After this introductory chapter, the seven equations of motion for performance analysis are derived in Chapter 2. For aircraft motion, it is sufficient to consider the gravitational acceleration as uniform. Then, by using a rectangular coordinate system with the z-axis along the local vertical and a moving coordinate system with the origin at the center of mass of the vehicle and the axes directed along the tangent, the normal and the binormal to the flight path, it is a simple matter to project the two vector equations (1.1) and (1.2) onto the axes of these systems. But, in recognizing the fact that future aircraft may fly faster and higher, in the speed range where the curvature of the earth must be considered in the analysis, we have derived the general equations

for flight around a rotating, spherical earth. Then, by introducing the appropriate simplification for the case of aircraft motion, at a relatively low speed and low altitude range, the relevant equations for uniform gravitational field are deduced.

For high performance aircraft, operating at high subsonic and supersonic speeds, the influence of Mach number is an important factor to be considered in the analysis. Since Mach number depends on the speed of sound, which in turn depends on the altitude, the characteristic properties of an idealized earth's atmosphere, namely the Standard Atmosphere, are presented in some detail in Chapter 3. In the same chapter, we discuss the various measurements of airspeed. In particular, we aim to make clear explicitly the distinction between true airspeed, calibrated airspeed and equivalent airspeed. The notions of a realistic lift–drag relationship, and the assumed parabolic drag polar with its limitation and its Mach number dependance are conveniently presented in this chapter.

It is a matter of fact that aircraft performance depends on both the aerodynamic characteristics and the propulsion system. The various aircraft engines currently in use are analyzed in Chapter 4. Then, starting with Chapter 5, we undertake the analysis of performance in each segment of the flight trajectory.

In most flight manuals for test pilot schools, take-off performance is discussed first. This assumes a basic knowledge of flight mechanics by the reader. Here, in the analytical presentation of the theory, we use the progressive approach and start in Chapter 5 with the simplest problem, namely the steady glide and descent in which the weight is nearly constant. Cruising flight at constant or nearly constant altitude is the topic for discussion in Chapter 6. In the discussion, we strongly emphasize the influence of Mach number in the search for the optimum speed and altitude giving maximum range and maximum endurance. After going through the chapter and working on the exercises at the end, the reader should have a clear understanding of why most transport aircraft cruise near the tropopause at subsonic speeds, and why supersonic transport aircraft fly in the stratosphere. We discuss climb performance in Chapter 7. Based on the explicit formulas obtained, we show the various influences of altitude, weight and Mach number on the rate of climb and the climb angle. The notion of energy height is introduced to explain the zoom climb in which the aircraft dives to

accelerate before a direct ascent to high altitudes. Turning flight is the topic for discussion in Chapters 8 and 9. Chapter 8 starts with the general considerations for a turn in a horizontal plane. It ends with a discussion of optimum turning for a propeller driven aircraft. Because the turning performance of a fighter aircraft is of prime consideration in the evaluation of its superiority, a whole chapter, Chapter 9 is devoted to jet aircraft turning. Finally the take-off and the landing performances of conventional aircraft are discussed in Chapter 10. In anticipation of the appearance of future hypersonic vehicles, which can be propelled into the upper layer of the atmosphere, we have added Chapter 11 in which we discuss the different recovery modes for these vehicles.

1.3 Objective

This book is written first as a textbook. Its level is accessible to advanced undergraduate and beginning graduate students. To address these groups, and to make it useful teaching material, we have constructed a sufficient number of exercises at the end of each chapter. It is customary in an elementary text to have a large number of exercises for the instructor to select as weekly assignments to the students. But quite often these exercises are simply designed as numerical applications of the formulas derived in the text. Although in performance evaluation, we believe in quantitative results, the analytical investigation to prove a qualitative statement definitely is more challenging and perhaps more useful to the reader. For this reason, nearly all the exercises are analytical in nature. These are constructed to give the reader a deeper understanding of the material covered in the text. As for the numerical applications, we have added three appendices. In Appendix 1, we have reproduced the data for the Standard Atmosphere in the troposphere and in the stratosphere. In Appendix 2, with some fear of obsoleteness in the future, we reluctantly provide physical data for typical aircraft. They are purely representative for the intructor to use in making numerical assignments, and as such they do not correspond to any current aircraft in service. Finally, in Appendix 3, we list some conversion factors between the classical British system of units and the International system of units (SI).

In writing a text on Flight Mechanics, it is difficult to standardize the symbol and to settle on one definite system of measurements. First, in applying certain laws of physics, the SI system is enforced. But, in flight, altitude is shown in kilofeet while speed is indicated in knots or in mph. Furthermore, in adopting the British system of units, we can express the shaft power P_s of an engine simply in units of ft-lb/s. But the power of an engine is customarily given in horsepower and in that case we must use the conversion factor $k = 550$, and have to write in the equation containing the power 550 (HP) instead of simply P_s. Being both a former military pilot and a trained mathematician, I have adopted the simplest way of writing the equations and of evaluating the various performance parameters. For example, in evaluating the cruising speed in steady flight at constant altitude of a propeller driven aircarft, I consider the equation in the form

$$\eta_p P_s = TV \tag{1.4}$$

The factor $\eta_p < 1$, called the propeller efficiency, is needed because it expresses a physical property in converting, through the propeller, shaft power into thrust power. But it is rather cumbersome to write the left-hand side of this equation as $550\eta_p$ (HP). If in Eq. (1.4) P_s is expressed in units of ft-lb/s and the thrust T in lb, we have the speed V in ft/s. Then, by simply converting the length from feet into meters or other units, we can express the speed in km/hr or mph.

The other difficulty concerns symbol. For example, in thermodynamics, T is used to denote absolute temperature while in flight mechanics T is the favorite symbol for thrust. For bank angle, in deriving the general equations for flight over a spherical earth, we have used the symbol σ since ϕ already denotes latitude while ψ is reserved for heading. But σ is the standard symbol for the density ratio. Instead of burdening the text with a variety of symbols and using multiple subscripts to distinguish the parameters, we have stayed with the familiar symbol. Since each chapter treats a specific topic and is more or less self-contained, duplication and confusion are avoided at the expense of redefining the symbol when required. Sometimes it is still embarassing, as in Chapter 4 on Propulsion Systems where we used $\beta = -dm/dt$ as the fuel mass flow rate to satisfy the engine controllers and in the same chapter, in another section in discussing the propeller theory we use β as the blade angle in accordance with the familiar symbol used

by the propeller designers. There, a note of apology has been added to indicate that the section is an entity within the chapter.

It is my sincere hope that this text will also be useful to the practicing aeronautical engineer. Some of my colleagues who have extensive industrial experience have seen the material and have assured me that it is worth publishing.

2

Equations of motion

2.1 Introduction

In this chapter, we shall derive the equations of motion for use throughout the text. Although we shall be mainly concerned with altitude and speed ranges such that gravitational acceleration can be considered as uniform, in anticipation of future operations of hypervelocity vehicles such as the National Aero-Space Plane which may glide over a long range, we first derive the general equations for flight over a spherical, rotating earth. Then next, the simplified equations for flight over a flat earth with an atmosphere at rest will be deduced using the appropriate assumptions.

The motion of a vehicle, considered as a point mass, flying inside the earth's atmosphere, is defined, at each instant t, by

$$\begin{aligned} \mathbf{r}(t) &= \text{position vector} \\ \mathbf{V}(t) &= \text{velocity vector} \\ m(t) &= \text{mass} \end{aligned} \tag{2.1}$$

At each instant, it is subject to a total force $\mathbf{F}$ composed of the gravitational force $m\mathbf{g}$, the aerodynamic force $\mathbf{A}$ and a thrust force $\mathbf{T}$ provided by the propulsion system.

$$\mathbf{F} = \mathbf{T} + \mathbf{A} + m\mathbf{g} \tag{2.2}$$

The gravitational force is always present. For unpowered flight, the propulsive force is zero, while for flight in a vacuum the aerodynamic

force vanishes. As seen in the definition (2.1), in three-dimensional flight, the state of the vehicle, considered as a dynamic system, is defined, at each instant t, by seven variables: three for the position vector, three for the velocity vector, and the final variable is the mass.

With respect to an inertial system, we first have the kinematic vector equation

$$\frac{d\mathbf{r}}{dt} = \mathbf{V} \tag{2.3}$$

Then, by Newton's second law, we have the force equation

$$m\frac{d\mathbf{V}}{dt} = \mathbf{F} \tag{2.4}$$

By selecting a convenient set of coordinates to represent the vectors $\mathbf{r}$ and $\mathbf{V}$, we shall obtain six scalar equations from these two vector equations. The seventh equation is that describing the variation of mass.

It is convenient to use a reference system attached to the earth. Since the time derivative in Eq. (2.4) for Newton's second law is evaluated with respect to a fixed system and since the earth's system is rotating, we need to obtain a formula for transforming the time derivative from one system to another rotating system.

2.2 Relative angular motion

Consider a fixed system $OX_1Y_1Z_1$ and another system $Oxyz$ which is rotating with respect to the fixed system with angular velocity $\boldsymbol{\omega}$. Let $\mathbf{i}$, $\mathbf{j}$ and $\mathbf{k}$ be the unit vectors along the axes of the rotating system (Fig. 2.1). Let $\mathbf{A}$ be any arbitrary vector with components A_x, A_y and A_z along the rotating axes. Then

$$\mathbf{A} = A_x\,\mathbf{i} + A_y\,\mathbf{j} + A_z\,\mathbf{k} \tag{2.5}$$

Since $Oxyz$ is rotating, its associated unit vectors $\mathbf{i}$, $\mathbf{j}$ and $\mathbf{k}$ are functions of time. Hence, the time derivative of $\mathbf{A}$, taken with respect to the fixed system, is

$$\frac{d\mathbf{A}}{dt} = \left(\frac{dA_x}{dt}\,\mathbf{i} + \frac{dA_y}{dt}\,\mathbf{j} + \frac{dA_z}{dt}\,\mathbf{k}\right) + \left(A_x\frac{d\mathbf{i}}{dt} + A_y\frac{d\mathbf{j}}{dt} + A_z\frac{d\mathbf{k}}{dt}\right) \tag{2.6}$$

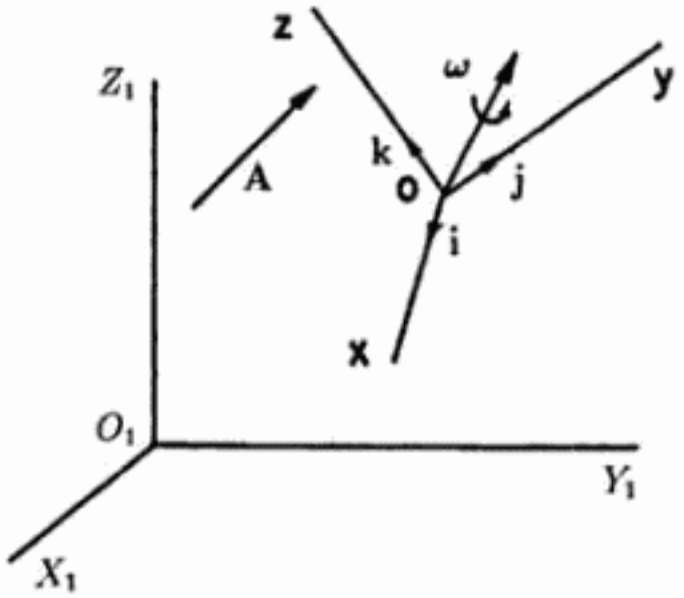

Figure 2.1: Relative angular motion.

Now, a point P with position vector $\mathbf{r}$, fixed in a system which is rotating with angular velocity ω, will have as linear velocity (Fig. 2.2).

$$\mathbf{V} = \frac{d\mathbf{r}}{dt} = \omega \times \mathbf{r} \tag{2.7}$$

If $\mathbf{r}$ is taken as the vector $\mathbf{i}$, $\mathbf{j}$ and $\mathbf{k}$ respectively, we have the Poisson's formulas

$$\begin{aligned} \frac{d\mathbf{i}}{dt} &= \omega \times \mathbf{i} \\ \frac{d\mathbf{j}}{dt} &= \omega \times \mathbf{j} \\ \frac{d\mathbf{k}}{dt} &= \omega \times \mathbf{k} \end{aligned} \tag{2.8}$$

Using these relations, together with the definition (2.5), it is seen that the second term on the right-hand side of Eq. (2.6) is

$$A_x \frac{d\mathbf{i}}{dt} + A_y \frac{d\mathbf{j}}{dt} + A_z \frac{d\mathbf{k}}{dt} = \omega \times \mathbf{A} \tag{2.9}$$

In Eq. (2.6), the first term on the right-hand side can be interpreted as the time derivative of the vector $\mathbf{A}$ if the vectors $\mathbf{i}$, $\mathbf{j}$ and $\mathbf{k}$ are constant

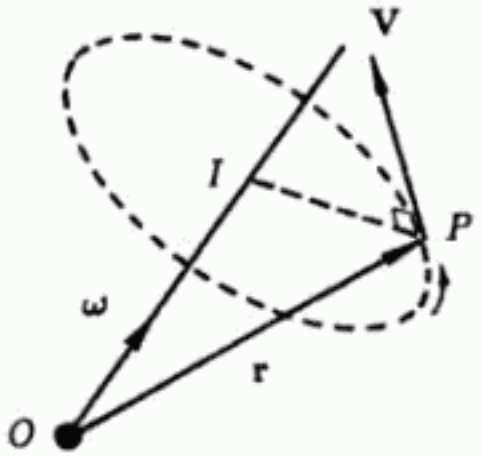

Figure 2.2: Kinematics of rotation.

unit vectors. Hence, it is the time derivative of **A** with respect to the rotating system $Oxyz$. We denote it by

$$\frac{\delta \mathbf{A}}{\delta t} = \frac{dA_x}{dt}\,\mathbf{i} + \frac{dA_y}{dt}\,\mathbf{j} + \frac{dA_z}{dt}\,\mathbf{k} \tag{2.10}$$

and write Eq. (2.6) as

$$\frac{d\mathbf{A}}{dt} = \frac{\delta \mathbf{A}}{\delta t} + \omega \times \mathbf{A} \tag{2.11}$$

This is the formula for transforming the time derivative from one system to another rotating system.

2.3 Equations for flight over a rotating spherical earth

The inertial reference frame $OX_1Y_1Z_1$ is taken such that O is at the center of the gravitational field of the spherical earth and the OX_1Y_1 plane is the equatorial plane. The $OXYZ$ reference frame is fixed with respect to the earth with OZ coinciding with OZ_1. It is assumed that the earth is rotating with constant angular velocity ω directed along the Z-axis. If the atmosphere is at rest with respect to the earth, then it rotates with the same angular velocity.

The vector equation (2.4) is written with respect to the inertial frame. In deriving the equations of motion we should use the earth-fixed axes $OXYZ$ as the reference frame since it is a convenient base

to follow the motion of the vehicle. Hence, putting $\mathbf{A} = \mathbf{r}$ in Eq. (2.11) and then taking its time derivative, we have the expression for the absolute acceleration $d\mathbf{V}/dt$

$$\frac{d\mathbf{r}}{dt} = \frac{\delta \mathbf{r}}{\delta t} + \boldsymbol{\omega} \times \mathbf{r}$$

$$\frac{d\mathbf{V}}{dt} = \frac{\delta}{\delta t}\left[\frac{\delta \mathbf{r}}{\delta t} + \boldsymbol{\omega} \times \mathbf{r}\right] + \boldsymbol{\omega} \times \left[\frac{\delta \mathbf{r}}{\delta t} + \boldsymbol{\omega} \times \mathbf{r}\right]$$

Since $\delta\boldsymbol{\omega}/\delta t = 0$, we have

$$\frac{d\mathbf{V}}{dt} = \frac{\delta^2 \mathbf{r}}{\delta t^2} + 2\boldsymbol{\omega} \times \frac{\delta \mathbf{r}}{\delta t} + \boldsymbol{\omega} \times (\boldsymbol{\omega} \times \mathbf{r}) \tag{2.12}$$

The vector equation (2.4) now becomes, with the earth-fixed system used as the reference frame

$$m\frac{\delta^2 \mathbf{r}}{\delta t^2} = \mathbf{F} - 2m\boldsymbol{\omega} \times \frac{\delta \mathbf{r}}{\delta t} - m\boldsymbol{\omega} \times (\boldsymbol{\omega} \times \mathbf{r}) \tag{2.13}$$

For convenience, we change the notation for the time derivative and write this vector equation as

$$m\frac{d\mathbf{V}}{dt} = \mathbf{F} - 2m\boldsymbol{\omega} \times \mathbf{V} - m\boldsymbol{\omega} \times (\boldsymbol{\omega} \times \mathbf{r}) \tag{2.14}$$

In this equation, $\mathbf{V}$ is the velocity of the vehicle with respect to the earth-fixed axes and the time derivative is taken with respect to these axes. From the equation, it is seen that as the earth is rotating with $\boldsymbol{\omega} \neq 0$, it gives rise to two additional forces, or proportionally to two additional accelerations. The term $-2\boldsymbol{\omega} \times \mathbf{V}$ is the Coriolis acceleration and the term $-\boldsymbol{\omega} \times (\boldsymbol{\omega} \times \mathbf{r})$ is the transport acceleration. For a given distance r, the transport acceleration depends on the direction of the vector $\mathbf{r}$, that is on the latitude of the vehicle. This acceleration is zero when $\mathbf{r}$ is collinear to $\boldsymbol{\omega}$, as when the vehicle is at the poles. It is a maximum with a value $\omega^2 r$ when the vehicle is in the equatorial plane (see Exercise 2-5). For the earth, this maximum value is of the order of $10^{-3} g_0$ where g_0 is the acceleration due to gravity at sea level. On the other hand, the Coriolis acceleration depends on the magnitude and the direction of the velocity of the vehicle with respect to the earth. It is zero when the flight path is parallel to the polar axis and reaches a maximum with a value $2\omega V$ when the flight path is

orthogonal to the polar axis. For orbital speed, this maximum value is of the order of $10^{-1}g_0$, and for lower speed, say in high subsonic cruise of jet aircraft, the maximum Coriolis acceleration is of the order of $10^{-3}g_0$. The maximum Coriolis acceleration for the earth is plotted versus speed in Fig. 2.3 for reference. For reentry vehicles, Coriolis acceleration should be retained for better accuracy while for aircraft operation the term can be neglected. Equation (2.14) and the kinematic relation

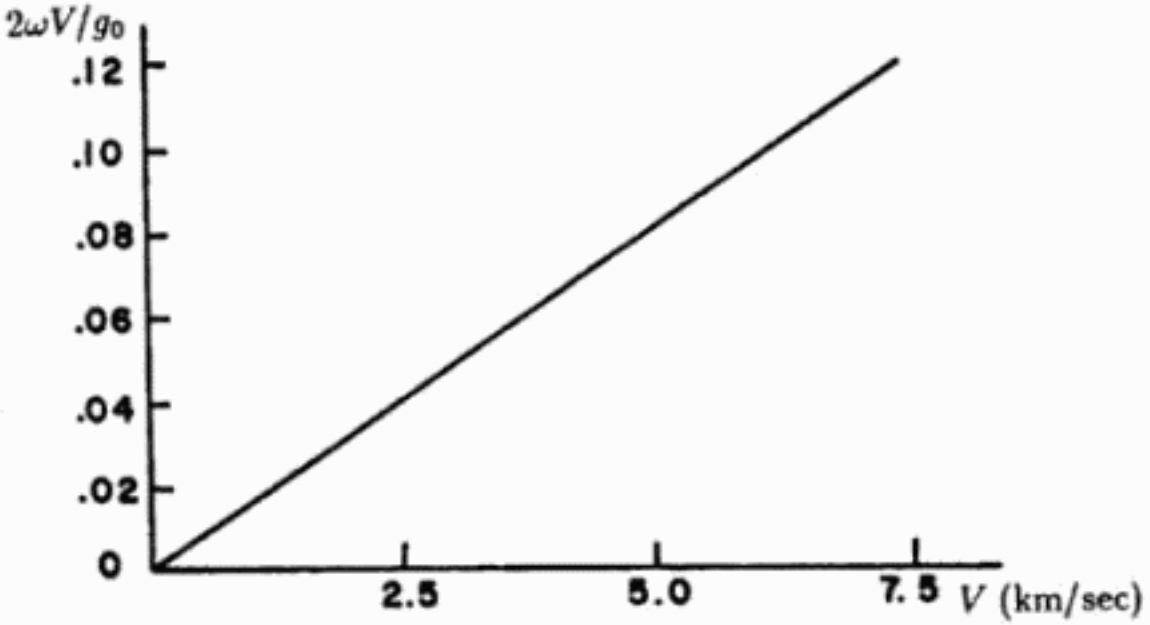

Figure 2.3: Maximum Coriolis acceleration as function of the speed.

$$\frac{d\mathbf{r}}{dt} = \mathbf{V} \tag{2.15}$$

constitute the vector equations for the position vector $\mathbf{r}$ and the velocity vector $\mathbf{V}$. They are equivalent to six scalar equations.

With respect to the earth-fixed system $OXYZ$ (Fig. 2.4), the position vector $\mathbf{r}$ is defined by its magnitude r, its longitude θ (measured from the X-axis, in the equatorial plane, positively eastward) and its latitude ϕ (measured from the equatorial plane, along a meridian, positively northward). It is convenient to evaluate the different vectors in Eqs. (2.14) and (2.15) by their components in a rotating coordinate system $Oxyz$ such that the x-axis is along the position vector, the y-axis is

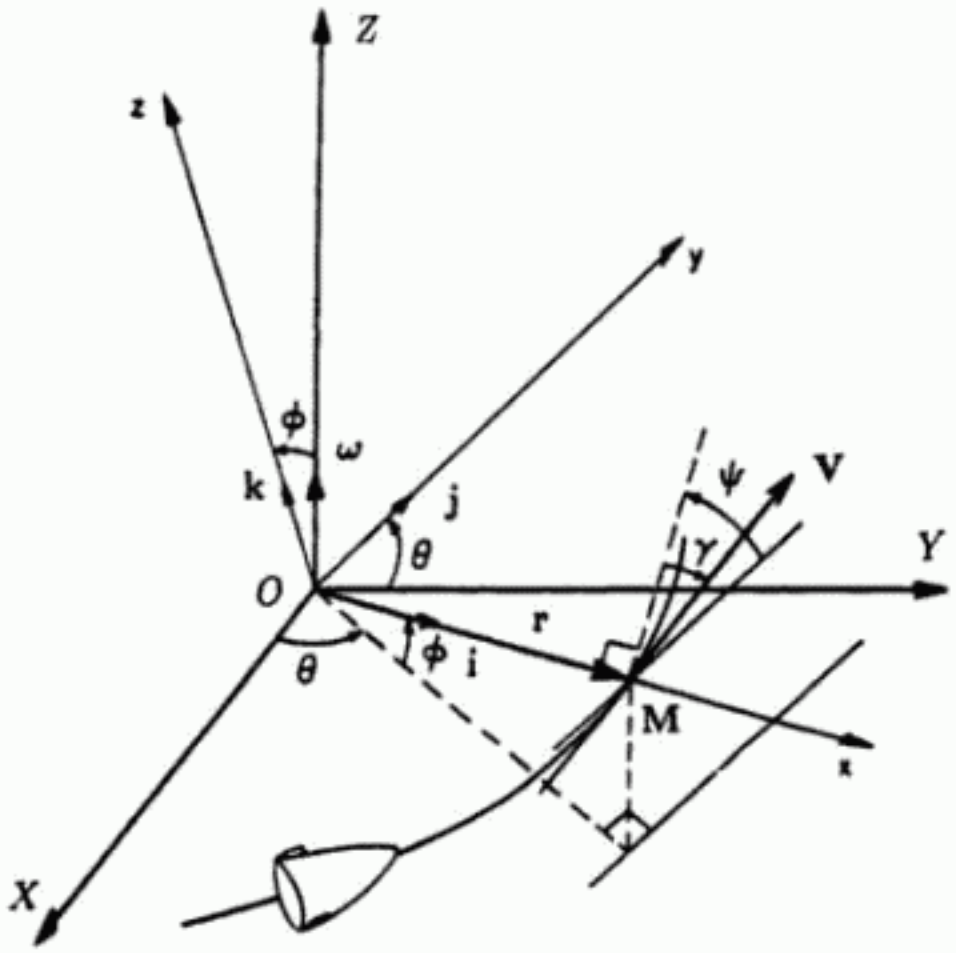

Figure 2.4: Coordinate systems.

in the equatorial plane, orthogonal to the x-axis and from it toward the eastward direction, and the z-axis completing a right-handed system. Let γ be the angle between the local horizontal plane, that is the plane passing through the vehicle located at the point M and orthogonal to the position vector $\mathbf{r}$, and the velocity vector $\mathbf{V}$. The angle γ is termed the flight path angle and is positive when $\mathbf{V}$ is above the horizontal plane. Let ψ be the angle between the local parallel of latitude and the projection of $\mathbf{V}$ on the horizontal plane. The angle ψ is termed the heading and is measured positively in the right-handed direction about the x-axis. Let $\mathbf{i}$, $\mathbf{j}$ and $\mathbf{k}$ be the unit vectors along the axes of the rotating system $Oxyz$. We have

$$\mathbf{r} = r\,\mathbf{i} \tag{2.16}$$

and

$$\mathbf{V} = V\sin\gamma\,\mathbf{i} + V\cos\gamma\cos\psi\,\mathbf{j} + V\cos\gamma\sin\psi\,\mathbf{k} \tag{2.17}$$

On the other hand, the angular velocity $\boldsymbol{\omega}$ can be represented by its components in the Oxz plane

$$\boldsymbol{\omega} = \omega\sin\phi\,\mathbf{i} + \omega\cos\phi\,\mathbf{k} \tag{2.18}$$

Hence (see Exercises 2-2 and 2-4)

$$\begin{aligned}\boldsymbol{\omega}\times\mathbf{V} = {} & -\omega V\cos\gamma\cos\phi\cos\psi\,\mathbf{i} + \omega V(\sin\gamma\cos\phi - \cos\gamma\sin\phi\sin\psi)\,\mathbf{j} \\ & + \omega V\cos\gamma\sin\phi\cos\psi\,\mathbf{k}\end{aligned} \tag{2.19}$$

and

$$\boldsymbol{\omega}\times(\boldsymbol{\omega}\times\mathbf{r}) = -\omega^2 r\cos^2\phi\,\mathbf{i} + \omega^2 r\sin\phi\cos\phi\,\mathbf{k} \tag{2.20}$$

In the total force $\mathbf{F}$, the gravity force for a central field is

$$m\mathbf{g} = -mg(r)\,\mathbf{i} \tag{2.21}$$

where $g(r)$ is a function of the distance. The aerodynamic force can be resolved into a drag force $\mathbf{D}$ opposite to the velocity vector $\mathbf{V}$ and a lift force $\mathbf{L}$ orthogonal to it. In symmetric flight, the thrust vector $\mathbf{T}$ is always in the lift–drag plane (Fig. 2.5). Then, we can resolve the thrust into a tangential component T_T along the velocity and a normal component T_N along the lift force. The direction of the thrust can be defined by the angle ε between the thrust and the velocity vector. This angle is called the thrust angle-of-attack. Then we have

$$\begin{aligned} T_T &= T\cos\varepsilon \\ T_N &= T\sin\varepsilon \end{aligned} \tag{2.22}$$

It is convenient for the derivation of the equations to group the components of aerodynamic and propulsive forces and define

$$\begin{aligned} F_T &= T\cos\varepsilon - D \\ F_N &= T\sin\varepsilon + L \end{aligned} \tag{2.23}$$

where F_T is the component of the combined aerodynamic and propulsive forces along the velocity vector and F_N is its component orthogonal to the velocity in the lift–drag plane.

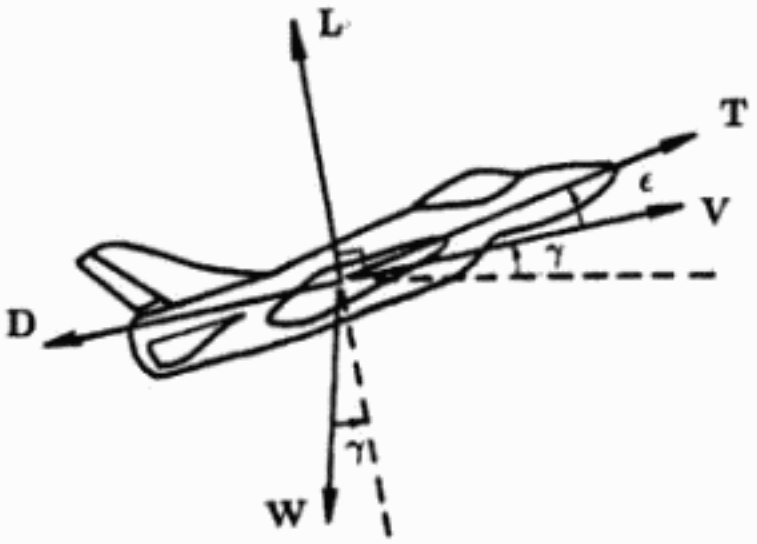

Figure 2.5: Aerodynamic and propulsive forces.

In vector form, since $\mathbf{F}_T$ is along $\mathbf{V}$, we can refer to Eq. (2.17) and replace V by F_T to obtain

$$\mathbf{F}_T = F_T \sin\gamma\, \mathbf{i} + F_T \cos\gamma \cos\psi\, \mathbf{j} + F_T \cos\gamma \sin\psi\, \mathbf{k} \qquad (2.24)$$

In planar flight, the vector $\mathbf{F}_N$ is in the $(\mathbf{r}, \mathbf{V})$ plane, that is the vertical plane, and there is no lateral force. By control action on the ailerons, if we rotate the vector $\mathbf{L}$, and hence also the vector $\mathbf{F}_N$, about the velocity vector $\mathbf{V}$ we create a lateral component of the force $\mathbf{F}_N$ that has the effect of changing the orbital plane. To resolve the force $\mathbf{F}_N$, or its collinear force $\mathbf{L}$, into components along the rotating axes, we refer to Fig. 2.6. The vertical plane considered is the $(\mathbf{r}, \mathbf{V})$ plane. Assume that the vector $\mathbf{L}$ is rotated out of this plane through an angle σ. The angle σ, which is the angle between the vector $\mathbf{L}$ and the $(\mathbf{r}, \mathbf{V})$ plane, will be referred to as the roll, or bank angle. The force $\mathbf{F}_N$ is resolved into a component $\mathbf{F}_N \cos\sigma$ in the vertical plane and orthogonal to $\mathbf{V}$ and a component $\mathbf{F}_N \sin\sigma$ orthogonal to the vertical plane. Let x', y' and z' be the axes, from the position M of the vehicle, parallel to the rotating axes x, y and z respectively. Let x_1, y_1 and z_1 be the axes from the point M, along the direction of $\mathbf{F}_N \cos\sigma$, $\mathbf{V}$ and $\mathbf{F}_N \sin\sigma$ respectively. The system $Mx_1y_1z_1$ is deduced from the system $Mx'y'z'$ by a rotation ψ in the horizontal plane, followed by a

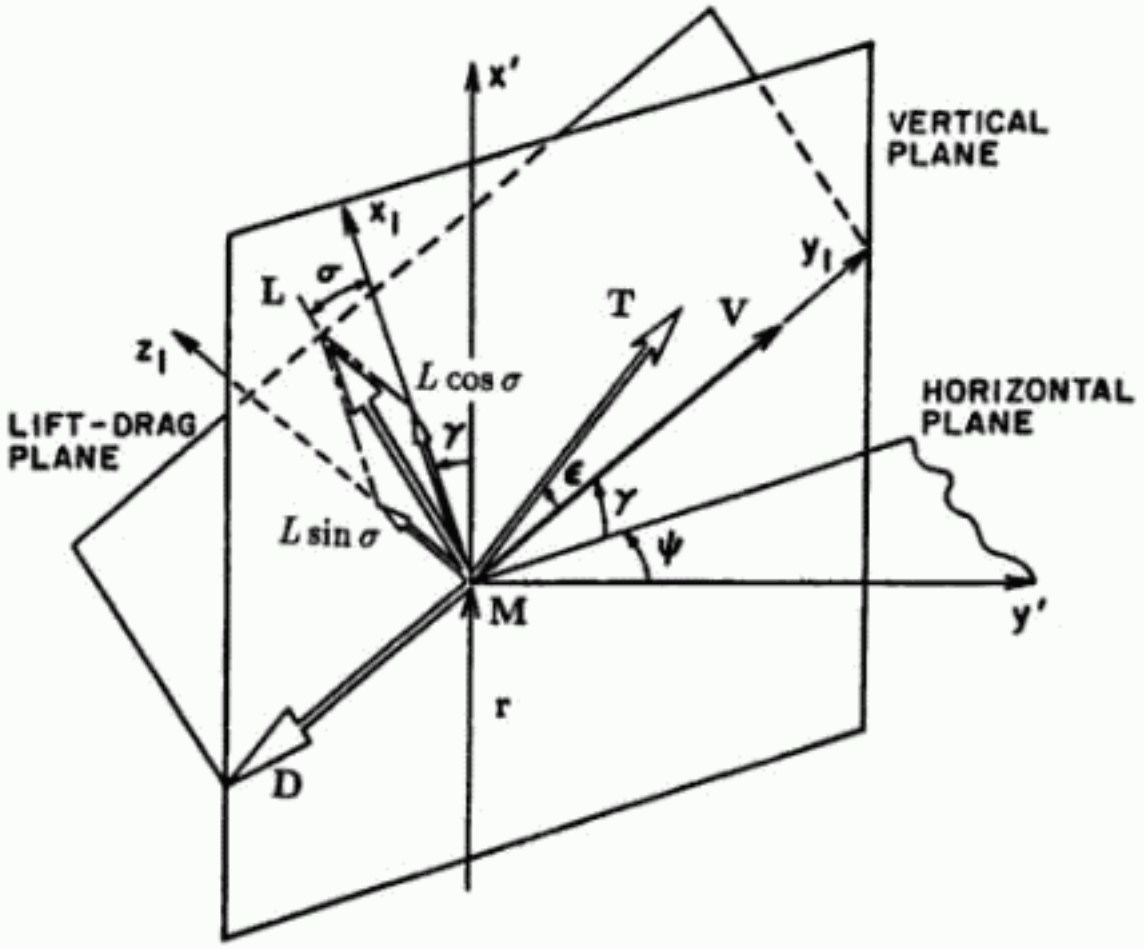

Figure 2.6: Aerodynamic forces.

rotation γ in the vertical plane. Hence, we have the matrix equation for the transformation

$$\begin{Bmatrix} x' \\ y' \\ z' \end{Bmatrix} = \begin{bmatrix} 1 & 0 & 0 \\ 0 & \cos\psi & -\sin\psi \\ 0 & \sin\psi & \cos\psi \end{bmatrix} \begin{bmatrix} \cos\gamma & \sin\gamma & 0 \\ -\sin\gamma & \cos\gamma & 0 \\ 0 & 0 & 1 \end{bmatrix} \begin{Bmatrix} x_1 \\ y_1 \\ z_1 \end{Bmatrix} \quad (2.25)$$

Carrying out the matrix multiplication

$$\begin{Bmatrix} x' \\ y' \\ z' \end{Bmatrix} = \begin{bmatrix} \cos\gamma & \sin\gamma & 0 \\ -\sin\gamma\cos\psi & \cos\gamma\cos\psi & -\sin\psi \\ -\sin\gamma\sin\psi & \cos\gamma\sin\psi & \cos\psi \end{bmatrix} \begin{Bmatrix} x_1 \\ y_1 \\ z_1 \end{Bmatrix} \quad (2.26)$$

Since the components of $\mathbf{F}_N$ in the $Mx_1y_1z_1$ system are $x_1 = F_N\cos\sigma$, $y_1 = 0$, $z_1 = F_N\sin\sigma$, we deduce the components of $\mathbf{F}_N$ along the

system $Mx'y'z'$, or what is the same, along the rotating system $Oxyz$.

$$\begin{aligned}\mathbf{F}_N = {} & F_N \cos\sigma\cos\gamma\,\mathbf{i} - F_N(\cos\sigma\sin\gamma\cos\psi + \sin\sigma\sin\psi)\,\mathbf{j} \\ & - F_N(\cos\sigma\sin\gamma\sin\psi - \sin\sigma\cos\psi)\,\mathbf{k}\end{aligned} \tag{2.27}$$

In summary, we have resolved all the vector terms in Eqs. (2.14) and (2.15) into components along the rotating axes $Oxyz$. In order to take the time derivative of the vectors $\mathbf{r}$ and $\mathbf{V}$ in Eqs. (2.14) and (2.15) with respect to the earth-fixed system $OXYZ$ using their components along the rotating system $Oxyz$ we need to evaluate the angular velocity $\boldsymbol{\Omega}$ of the rotating axes. The system $Oxyz$ is obtained from the system $OXYZ$ by a rotation θ about the positive Z-axis, followed by a rotation ϕ about the negative y-axis. Hence the angular velocity $\boldsymbol{\Omega}$ of the rotating system $Oxyz$, in terms of its components on this system, is

$$\boldsymbol{\Omega} = \sin\phi\frac{d\theta}{dt}\,\mathbf{i} - \frac{d\phi}{dt}\,\mathbf{j} + \cos\phi\frac{d\theta}{dt}\,\mathbf{k} \tag{2.28}$$

Using Eqs. (2.8) with $\boldsymbol{\Omega}$ instead of $\boldsymbol{\omega}$, we deduce the time derivatives of $\mathbf{i}$, $\mathbf{j}$ and $\mathbf{k}$ with respect to the earth-fixed system $OXYZ$

$$\begin{aligned}\frac{d\mathbf{i}}{dt} &= \boldsymbol{\Omega}\times\mathbf{i} = \cos\phi\frac{d\theta}{dt}\,\mathbf{j} + \frac{d\phi}{dt}\,\mathbf{k} \\ \frac{d\mathbf{j}}{dt} &= \boldsymbol{\Omega}\times\mathbf{j} = -\cos\phi\frac{d\theta}{dt}\,\mathbf{i} + \sin\phi\frac{d\theta}{dt}\,\mathbf{k} \\ \frac{d\mathbf{k}}{dt} &= \boldsymbol{\Omega}\times\mathbf{k} = -\frac{d\phi}{dt}\,\mathbf{i} - \sin\phi\frac{d\theta}{dt}\,\mathbf{j}\end{aligned} \tag{2.29}$$

If we take the derivative of $\mathbf{r}$, as given by Eq. (2.16), using the first of the Eqs. (2.29) for the derivative of $\mathbf{i}$, we have

$$\mathbf{V} = \frac{d\mathbf{r}}{dt} = \frac{dr}{dt}\,\mathbf{i} + r\cos\phi\frac{d\theta}{dt}\,\mathbf{j} + r\frac{d\phi}{dt}\,\mathbf{k} \tag{2.30}$$

Identifying this equation with Eq. (2.17) yields three scalar equations

$$\begin{aligned}\frac{dr}{dt} &= V\sin\gamma \\ \frac{d\theta}{dt} &= \frac{V\cos\gamma\cos\psi}{r\cos\phi} \\ \frac{d\phi}{dt} &= \frac{V\cos\gamma\sin\psi}{r}\end{aligned} \tag{2.31}$$

These equations are the kinematic equations.

On the other hand, if we take the derivative of the velocity vector **V**, as given by Eq. (2.17), using the Eqs. (2.29) for the derivatives of the unit vectors **i**, **j** and **k** and subsequently the Eqs. (2.31) for $d\theta/dt$ and $d\phi/dt$, we have

$$\begin{aligned}\frac{d\mathbf{V}}{dt} = &\left[\sin\gamma\frac{dV}{dt} + V\cos\gamma\frac{d\gamma}{dt} - \frac{V^2}{r}\cos^2\gamma\right]\mathbf{i}\\ &+\left[\cos\gamma\cos\psi\frac{dV}{dt} - V\sin\gamma\cos\psi\frac{d\gamma}{dt} - V\cos\gamma\sin\psi\frac{d\psi}{dt}\right.\\ &\left.+\frac{V^2}{r}\cos\gamma\cos\psi(\sin\gamma - \cos\gamma\sin\psi\tan\phi)\right]\mathbf{j}\\ &+\left[\cos\gamma\sin\psi\frac{dV}{dt} - V\sin\gamma\sin\psi\frac{d\gamma}{dt} + V\cos\gamma\cos\psi\frac{d\psi}{dt}\right.\\ &\left.+\frac{V^2}{r}\cos\gamma(\sin\gamma\sin\psi + \cos\gamma\cos^2\psi\tan\phi)\right]\mathbf{k} \qquad (2.32)\end{aligned}$$

By substituting into the basic vector equation (2.14), using the Eqs. (2.19)-(2.21), (2.24) and (2.27) and then identifying the components along the rotating axes, we obtain three scalar equations

$$\begin{aligned}&\sin\gamma\frac{dV}{dt} + V\cos\gamma\frac{d\gamma}{dt} - \frac{V^2}{r}\cos^2\gamma\\ &\quad= \frac{F_T}{m}\sin\gamma + \frac{F_N}{m}\cos\sigma\cos\gamma - g + 2\omega V\cos\gamma\cos\psi\cos\phi\\ &\qquad+\omega^2 r\cos^2\phi\\ &\cos\gamma\frac{dV}{dt} - V\sin\gamma\frac{d\gamma}{dt} - V\cos\gamma\tan\psi\frac{d\psi}{dt}\\ &\quad+\frac{V^2}{r}\cos\gamma(\sin\gamma - \cos\gamma\sin\psi\tan\phi)\\ &\quad= \frac{F_T}{m}\cos\gamma - \frac{F_N}{m}(\cos\sigma\sin\gamma + \sin\sigma\tan\psi)\\ &\qquad-\frac{2\omega V}{\cos\psi}(\sin\gamma\cos\phi - \cos\gamma\sin\psi\sin\phi) \qquad (2.33)\\ &\cos\gamma\frac{dV}{dt} - V\sin\gamma\frac{d\gamma}{dt} + \frac{V\cos\gamma}{\tan\psi}\frac{d\psi}{dt}\\ &\quad+\frac{V^2}{r}\cos\gamma\left(\sin\gamma + \frac{\cos\gamma\cos\psi\tan\phi}{\tan\psi}\right)\end{aligned}$$

$$= \frac{F_T}{m}\cos\gamma - \frac{F_N}{m}\left(\cos\sigma\sin\gamma - \frac{\sin\sigma}{\tan\psi}\right)$$
$$-2\omega V\frac{\cos\gamma\sin\phi}{\tan\psi} - \omega^2 r\frac{\sin\phi\cos\phi}{\sin\psi}$$

Solving for the derivatives dV/dt, $d\gamma/dt$ and $d\psi/dt$, we obtain

$$\begin{aligned}
\frac{dV}{dt} &= \frac{F_T}{m} - g\sin\gamma + \omega^2 r\cos\phi(\sin\gamma\cos\phi - \cos\gamma\sin\psi\sin\phi)\\
V\frac{d\gamma}{dt} &= \frac{F_N}{m}\cos\sigma - g\cos\gamma + \frac{V^2}{r}\cos\gamma + 2\omega V\cos\psi\cos\phi\\
&\quad + \omega^2 r\cos\phi(\cos\gamma\cos\phi + \sin\gamma\sin\psi\sin\phi) \qquad (2.34)\\
V\frac{d\psi}{dt} &= \frac{F_N}{m}\frac{\sin\sigma}{\cos\gamma} - \frac{V^2}{r}\cos\gamma\cos\psi\tan\phi\\
&\quad + 2\omega V(\tan\gamma\sin\psi\cos\phi - \sin\phi) - \frac{\omega^2 r}{\cos\gamma}\cos\psi\sin\phi\cos\phi
\end{aligned}$$

These three equations are the force equations. The presence of the ω terms is due to the rotation of the earth. If we assume that the atmosphere is at rest with respect to the earth, then it has the same rotation as the earth. As has been discussed above, for the earth, ω is small and the term $\omega^2 r$, which represents the transport acceleration, can be neglected. On the other hand, the term $2\omega V$, which represents the Coriolis acceleration, has an important effect in a high-speed, long-range flight. For an accurate analysis, especially in the problem of calculating the trajectory of a ballistic missile, the term should be retained.

In this book we shall mainly be concerned with flight regimes in the speed range well below orbital speed. As shown in Fig. 2.3, the Coriolis acceleration is of the order of $10^{-3}g_0$ and can be neglected. This is the assumption of a non-rotating earth. Then, the force equations become

$$\begin{aligned}
\frac{dV}{dt} &= \frac{F_T}{m} - g\sin\gamma\\
V\frac{d\gamma}{dt} &= \frac{F_N}{m}\cos\sigma - g\cos\gamma + \frac{V^2}{r}\cos\gamma \qquad (2.35)\\
V\frac{d\psi}{dt} &= \frac{F_N}{m}\frac{\sin\sigma}{\cos\gamma} - \frac{V^2}{r}\cos\gamma\cos\psi\tan\phi
\end{aligned}$$

where the force components F_T and F_N are defined in Eqs. (2.23).

For powered flight, $T \neq 0$, and the mass of the vehicle is varying. We have the equation for the mass flow rate

$$\frac{dm}{dt} = -\frac{c}{g}T \tag{2.36}$$

where T is the thrust magnitude and c is termed the specific fuel consumption. This parameter depends on the design of the propulsion system and on other variables such as speed and altitude as well as on the propellant.

The drag force D and the lift force L in the definitions (2.23) will be analyzed in Chapter 3. It will be shown that they can be expressed as

$$\begin{aligned} D &= \frac{1}{2}\rho S C_D V^2 \\ L &= \frac{1}{2}\rho S C_L V^2 \end{aligned} \tag{2.37}$$

where C_D and C_L are respectively the drag coefficient and the lift coefficient. The atmospheric density, ρ, is in general a function of the altitude, or in the case of a spherical earth, it is a function of the radial distance r. In differential form, we have

$$\frac{d\rho}{\rho} = -\beta(r)\, dr \tag{2.38}$$

where $\beta(r)$ is a function of the distance r. Within a small range of altitude, one can consider β as constant and deduce a strictly exponential law for ρ.

Finally, the acceleration due to gravity, g, is inversely proportional to the square of the distance, that is

$$g(r) = \frac{g_0 r_0^2}{r^2} \tag{2.39}$$

where subscript zero denotes the reference level, usually taken as sea level.

2.4 Equations for flight over a flat earth

We can use the same procedure as in the case of a spherical earth to derive the equations of motion when a simple flat earth model is used. For economy of thought we shall deduce these equations directly from the equations for flight over a spherical earth by using the appropriate simplifications. For convenience, we recall the equations for flight over a non-rotating spherical earth. We have the kinematic relations

$$\begin{aligned} \frac{dr}{dt} &= V \sin\gamma \\ \frac{d\theta}{dt} &= \frac{V \cos\gamma \cos\psi}{r \cos\phi} \\ \frac{d\phi}{dt} &= \frac{V \cos\gamma \sin\psi}{r} \end{aligned} \tag{2.40}$$

and the force equations

$$\begin{aligned} \frac{dV}{dt} &= \frac{F_T}{m} - g \sin\gamma \\ V\frac{d\gamma}{dt} &= \frac{F_N}{m}\cos\sigma - g\cos\gamma + \frac{V^2}{r}\cos\gamma \\ V\frac{d\psi}{dt} &= \frac{F_N}{m}\frac{\sin\sigma}{\cos\gamma} - \frac{V^2}{r}\cos\gamma\cos\psi\tan\phi \end{aligned} \tag{2.41}$$

These are the equations to be simplified. The equation for the mass flow rate, Eq. (2.36), remains unchanged.

First, atmospheric flight operation is conducted in a relatively thin layer of the atmosphere compared to the radius of the earth. Let h be the altitude of flight, and r_0 the radius of the earth. Then

$$r = r_0 + h \tag{2.42}$$

and, since h/r_0 is a small quantity, we can use binomial expansion to obtain

$$\frac{r_0}{r} = \frac{r_0}{r_0 + h} = 1 - \frac{h}{r_0} + \left(\frac{h}{r_0}\right)^2 - \cdots \tag{2.43}$$

On substituting into Eq. (2.39), we have for the acceleration of gravity as a function of altitude

$$g = g_0\left[1 - 2\frac{h}{r_0} + 3\left(\frac{h}{r_0}\right)^2 - \cdots\right] \tag{2.44}$$

For a flight up to the realm of the atmosphere, $h = 9.5 \times 10^4$ meters, taking the earth's radius as $r_0 = 6.37839 \times 10^6$ meters, we have the ratio $h/r_0 = 1.489 \times 10^{-2}$. Hence, even at such high altitude, by neglecting this term in Eq. (2.44) we commit only the same error as neglecting the Coriolis acceleration. Therefore, it is appropriate to consider g as a constant.

Next, let V be the speed of the vehicle and V_c the circular speed, that is the speed along a circular orbit, in a vacuum, at a distance r. In circular motion, the centrifugal acceleration equals the gravitational acceleration and we have

$$\frac{V_c^2}{r} = g \tag{2.45}$$

We consider the ratio

$$\frac{V^2}{V_c^2} = \frac{V^2}{gr} \tag{2.46}$$

Hence, when the flight speed is small compared to the orbital speed, we have

$$\frac{V^2}{gr} \ll 1 \tag{2.47}$$

More specifically, taking a circular speed of 7910 m/sec, for an aircraft flying at twice the speed of sound at sea level which corresponds to $V = 680$ m/sec we have the ratio $V^2/gr = 7.390 \times 10^{-3}$. Hence, for aircraft operation, we can neglect this term in the equations of motion.

With these simplifications, Eqs. (2.41) become

$$\begin{aligned} \frac{dV}{dt} &= \frac{F_T}{m} - g \sin\gamma \\ V\frac{d\gamma}{dt} &= \frac{F_N}{m}\cos\sigma - g\cos\gamma \\ V\frac{d\psi}{dt} &= \frac{F_N}{m}\frac{\sin\sigma}{\cos\gamma} \end{aligned} \tag{2.48}$$

Now, let $OXYZ$ be the reference system used in writing the equations (2.40) for flight over a spherical earth with the origin O at the center of the earth (Fig. 2.7) This system is called the geocentric coordinate system. For aircraft operation, it is convenient to use as reference system a coordinate system $Exyh$ with the origin E at the surface of the earth. This system, called the topocentric coordinate system is shown in Fig. 2.7. A flat earth model implies that the gravitational

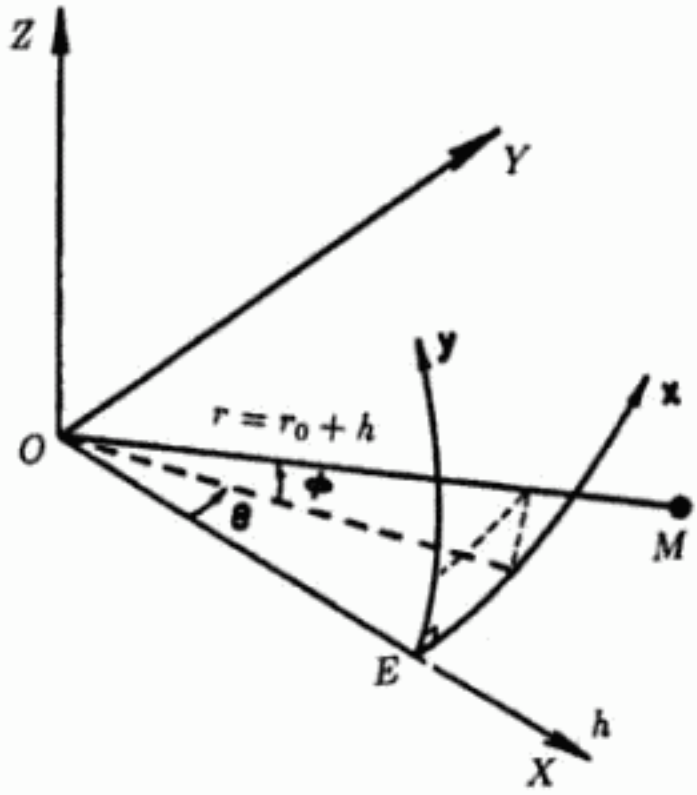

Figure 2.7: Geocentric and topocentric coordinate systems.

field is uniform, that is the vector **g** is constant in both magnitude and direction. Therefore, this assumes that both longitude θ and latitude ϕ, expressed in radians, are small. Hence, taking $\cos\phi = 1$, we can write the last two equations of the system (2.40)

$$\begin{aligned} r_0 \frac{d\theta}{dt} &= V \cos\gamma \cos\psi \left(1 - \frac{h}{r_0} + \cdots\right) \\ r_0 \frac{d\phi}{dt} &= V \cos\gamma \sin\psi \left(1 - \frac{h}{r_0} + \cdots\right) \end{aligned} \tag{2.49}$$

Neglecting the small term h/r_0 and considering that

$$\begin{aligned} x &= r_0\theta \\ y &= r_0\phi \\ h &= r - r_0 \end{aligned} \tag{2.50}$$

we can write the Eqs. (2.40) as

$$\frac{dx}{dt} = V \cos\gamma \cos\psi$$

$$\frac{dy}{dt} = V \cos\gamma \sin\psi \tag{2.51}$$
$$\frac{dh}{dt} = V \sin\gamma$$

Equations (2.48) and (2.51) together with Eq. (2.36) are the equations for flight over a flat earth.

Exercises

2-1. Let $\mathbf{i}, \mathbf{j}$ and $\mathbf{k}$ be the unit vectors along the axes of an orthogonal coordinate system. From the basic definitions of the dot product and the vector product, verify the identities

$$\mathbf{i}\cdot\mathbf{i} = \mathbf{j}\cdot\mathbf{j} = \mathbf{k}\cdot\mathbf{k} = 1$$
$$\mathbf{i}\cdot\mathbf{j} = \mathbf{j}\cdot\mathbf{k} = \mathbf{k}\cdot\mathbf{i} = 0$$
$$\mathbf{i}\times\mathbf{i} = \mathbf{j}\times\mathbf{j} = \mathbf{k}\times\mathbf{k} = 0$$
$$\mathbf{i}\times\mathbf{j} = \mathbf{k}, \quad \mathbf{j}\times\mathbf{k} = \mathbf{i}, \quad \mathbf{k}\times\mathbf{i} = \mathbf{j}.$$

2-2. Let

$$\mathbf{A} = A_x\,\mathbf{i} + A_y\,\mathbf{j} + A_z\,\mathbf{k}$$
$$\mathbf{B} = B_x\,\mathbf{i} + B_y\,\mathbf{j} + B_z\,\mathbf{k}$$

Using the identities in Exercise 2-1, show that

$$\mathbf{A}\cdot\mathbf{B} = A_xB_x + A_yB_y + A_zB_z$$
$$\mathbf{A}\times\mathbf{B} = \begin{vmatrix} \mathbf{i} & \mathbf{j} & \mathbf{k} \\ A_x & A_y & A_z \\ B_x & B_y & B_z \end{vmatrix}$$

2-3. Using the results of Exercise 2-2, show the following identity for the triple dot product

$$(\mathbf{A}\times\mathbf{B})\cdot\mathbf{C} = \begin{vmatrix} A_x & A_y & A_z \\ B_x & B_y & B_z \\ C_x & C_y & C_z \end{vmatrix}$$

where C_x, C_y and C_z are the components of the vector $\mathbf{C}$. Deduce that $(\mathbf{A}\times\mathbf{B})\cdot\mathbf{C} = (\mathbf{B}\times\mathbf{C})\cdot\mathbf{A} = (\mathbf{C}\times\mathbf{A})\cdot\mathbf{B}$.

2-4. Using the results of Exercise 2-2, verify the following indentity for the triple cross product,

$$\mathbf{A} \times (\mathbf{B} \times \mathbf{C}) = (\mathbf{A} \cdot \mathbf{C})\,\mathbf{B} - (\mathbf{A} \cdot \mathbf{B})\,\mathbf{C}$$

2-5. Using the identity in Exercise 2-4, consider the transport acceleration

$$\mathbf{a}_t = -\boldsymbol{\omega} \times (\boldsymbol{\omega} \times \mathbf{r}) = -(\boldsymbol{\omega} \cdot \mathbf{r})\boldsymbol{\omega} + \omega^2 \mathbf{r}.$$

By squaring this vector, show that

$$a_t^2 = \omega^2[\omega^2 r^2 - (\boldsymbol{\omega} \cdot \mathbf{r})^2].$$

Deduce that the minimum value of a_t is zero when $\mathbf{r}$ is collinear to $\boldsymbol{\omega}$, and its maximum value $a_t = \omega^2 r$ is reached when $\mathbf{r}$ is in the equatorial plane. Calculate this maximum value $\omega^2 r/g$ for the earth with $\omega = 2\pi/24$ hours, $r = 6.378 \times 10^6$ m, $g = 9.806$ m/sec.

2-6. Consider the Coriolis acceleration,

$$\mathbf{a}_c = -2\boldsymbol{\omega} \times \mathbf{V}.$$

It is a maximum when the flight path is parallel to the equatorial plane. Using the data in Exercise 2-5, calculate this maximum value $a_c/g = 2\omega V/g$, for orbital flight $V = \sqrt{gr}$, and for flight at sonic speed $V = 340$ m/sec.

2-7. Based on the geometry shown in Fig. 2.2, show that the two vectors $\mathbf{V}$ and $\boldsymbol{\omega} \times \mathbf{r}$ are collinear and have the same direction and furthermore they have the same magnitude. Hence, they satisfy Eq. (2.7).

2-8. Let

$$\boldsymbol{\omega} = \omega_x\,\mathbf{i} + \omega_y\,\mathbf{j} + \omega_z\,\mathbf{k}.$$

From the first of the Eq. (2.8) and the identity in Exercise 2-4, show that

$$\mathbf{i} \times \frac{d\mathbf{i}}{dt} = \boldsymbol{\omega} - \omega_x\,\mathbf{i}.$$

Derive similar expressions for $\mathbf{j}$ and $\mathbf{k}$ and deduce that

$$\boldsymbol{\omega} = \frac{1}{2}\left(\mathbf{i} \times \frac{d\mathbf{i}}{dt} + \mathbf{j} \times \frac{d\mathbf{j}}{dt} + \mathbf{k} \times \frac{d\mathbf{k}}{dt}\right).$$

3

Aerodynamic forces

3.1 Introduction

Besides the gravitational force of attraction, a vehicle in flight is also subjected to the propulsive forces developed by the engines on board and the aerodynamic forces which arise from the relative motion between the vehicle and the atmosphere. To evaluate the aerodynamic forces, it is necessary to know the properties of the atmosphere and, in particular, the local pressure and temperature at any point in the space in which the flights take place. The aerodynamic forces are most effective at low altitudes so that only a very thin layer in the lower reaches of the atmosphere need be considered. Many of the more complicated aspects of planetary atmospheres are of no consequence in aerodynamic calculations. For instance, though the atmosphere is composed of a mixture of a number of gases, it may be treated as a uniform gas of unvarying composition throughout the aerodynamically important altitudes.

For the air, which constitutes the atmosphere surrounding the earth, the physical properties of interest are the temperature, the pressure, the density and the viscosity. It is a fact that the values of these properties vary, not only with the geographic location and altitude, but also from day to day. In flight mechanics, we adopt a specific set of data representing some kind of average conditions. This set of figures giving the variations in altitude of the physical properties of the air is known as the International Standard Atmosphere (USAF, 1962). For

an analytical treatment of the equations of motion, the modeling of the physical properties of the air is based on this standard atmosphere.

3.2 The earth's atmosphere

For the earth's atmosphere, the 1962 U.S. Standard Atmosphere is universally adopted and it is based on the following assumptions:

3.2.1 Temperature

At sea level, the standard temperature of the air is 288.150°K. As the altitude increases the temperature decreases, initially at a constant rate. This range of altitude within which the temperature decreases steadily defines a region of the atmosphere called the troposphere. The surface which constitutes the layer of the atmosphere at an altitude slightly over 11 km, with a corresponding temperature of 216.650°K, is called the tropopause. Therefore, below the tropopause the temperature decreases at a constant rate of 6.5 deg/km. Above this altitude, the temperature remains constant. The corresponding region of the atmosphere is called the stratosphere. The stratosphere extends to an altitude slightly above 20 km. Above the stratosphere, the temperature increases with altitude, reaching values well above the sea level value before decreasing once again, then increasing to very high values on the outer fringe of the atmosphere. For all practical applications in this book, in powered flight, the properties of the atmosphere within the troposphere and the stratosphere are relevant. A schematic variation of temperature is shown in Fig. 3.1.

3.2.2 Pressure

At sea level, the standard pressure of the air is $1.01325 \times 10^5 \mathrm{N/m^2}$. The pressure at any point in a stationary fluid is determined by the weight of the fluid above the point considered. If follows that the pressure decreases as the altitude increases. At the tropopause the pressure is equal to 0.2234 of the pressure at sea level. The rate of change of pressure is associated with the rate of change of density, which will be considered next.

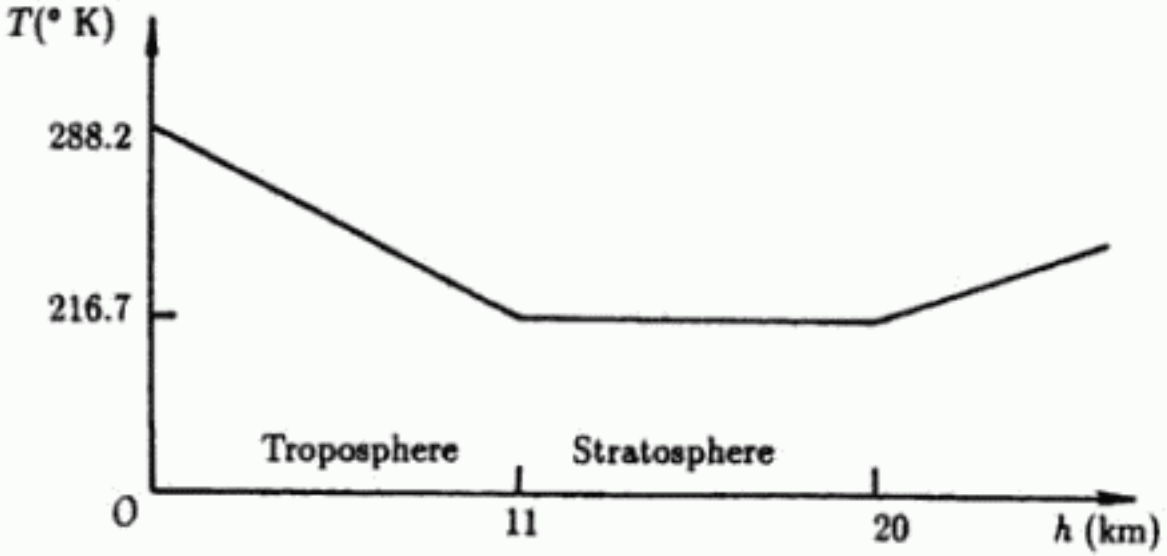

Figure 3.1: Variation of temperature with altitude.

3.2.3 Density

At sea level, the standard density of the air is 1.225kg/m^3. There are two basic equations governing density as a function of altitude. The first is the familiar equation of state for the atmosphere relating its pressure p, density ρ and temperature T

$$p = \rho RT \tag{3.1}$$

where R is the gas constant, equal to 287.053 joules/kg°K. The second basic equation states that the rate of change of pressure must equal the increased weight of the atmosphere supported, as the altitude changes. We have

$$dp = -\rho g dh \tag{3.2}$$

where g is the acceleration due to gravity.

From the equation of state comes

$$\frac{d\rho}{\rho} = \frac{dp}{p} - \frac{dT}{T} \tag{3.3}$$

which, combined with Eqs. (3.1) and (3.2), gives

$$\frac{d\rho}{\rho} = -\left(\frac{g}{RT} + \frac{1}{T}\frac{dT}{dh}\right)dh \tag{3.4}$$

This equation can be written as

$$\frac{d\rho}{\rho} = -\beta dh \tag{3.5}$$

where β, defined as the bracketed term in Eq. (3.4) is the reciprocal of the scale height. Using this differential form for the density, the atmosphere will be represented as a locally exponential atmosphere. If the coefficient β can be considered as constant over some small altitude interval, then the integrated density function is

$$\rho = \rho_0 e^{-\beta h} \tag{3.6}$$

where ρ_0 is the density at the reference level and h is the altitude measured from this level. We notice that, in the stratosphere, the temperature T is constant and hence $\beta = g/RT$ is constant if we neglect the variation of g with altitude. In the troposphere, T is a linear function of altitude, and hence β is a function of the altitude h and, as shown below, it is possible to have a rigorous integration of Eq. (3.5). Nevertheless, it is found convenient in flight mechanics to use the strictly exponential atmosphere as given in Eq. (3.6) for both the troposphere and the stratosphere. During each phase of the flight, the variation in altitude is small and it suffices, for each range of altitude, to adjust the value of β for agreement with the standard atmosphere. Throughout this text, we shall use Eq. (3.6) with subscript zero denoting the condition at sea level.

In some analyses, such as the one presented in Chapter 6, it is useful to have a direct relationship between pressure and density. With the standard atmosphere, in the stratosphere, since the temperature is constant, by the equation of state (3.1) p is simply proportional to ρ. Let subscript $*$ denote the condition at the tropopause. Then, we have the relation

$$\frac{p}{p_*} = \frac{\rho}{\rho_*} \tag{3.7}$$

To obtain the equivalent relation for the troposphere, let $T' = dT/dh$ be the constant temperature gradient. Again, by using subscript zero to denote the condition at sea level, we have

$$T = T_0 + T'h \tag{3.8}$$

By substituting into Eq. (3.4) and integrating from the condition at sea level, we obtain

$$\rho = \rho_0 \left(1 + \frac{T'}{T_0} h\right)^{-\frac{1}{T'}\left(\frac{g}{R} + T'\right)} \tag{3.9}$$

This is the law of variation of density with respect to altitude in the troposphere according to the standard atmosphere. By using Eq. (3.8) and with the constant value for R and keeping g constant at the value $g = 9.80665\,\mathrm{m/s^2}$, with $T' = -6.5 \times 10^{-3}\,\mathrm{deg/m}$, we have the equation in the form

$$\frac{\rho}{\rho_0} = \left(\frac{T}{T_0}\right)^{4.2558774} \tag{3.10}$$

By combining this equation with Eq. (3.1), we have the relation

$$\frac{p}{p_0} = \left(\frac{\rho}{\rho_0}\right)^b \tag{3.11}$$

where $b = 1.234969$. In the standard atmosphere, this equation is valid up to the tropopause. Hence, we can include Eq. (3.7) in the same formulation, by writing

$$\frac{p}{p_*} = \left(\frac{\rho}{\rho_*}\right)^b \tag{3.12}$$

with $b = 1.235$ in the troposphere and $b = 1$ in the stratosphere.

In performance analysis, for flight at high speeds, the aerodynamic forces depend on the Mach number, M, defined as the ratio of the actual airspeed, V, to the speed of sound, a,

$$M = \frac{V}{a} \tag{3.13}$$

It can be shown that the speed of sound is related to the pressure and the density by the relation

$$a^2 = \frac{kp}{\rho} \tag{3.14}$$

where k is the ratio of the specific heats, also called the adiabatic index of the gas, which is approximately 1.4 for air. Then, combining the Eqs. (3.1) and (3.14), we have the relation

$$a^2 = kRT \tag{3.15}$$

which shows that the speed of sound is a function of temperature.

3.2.4 Viscosity

Viscosity exists in the form of tangential stress distributed within the fluid whenever there is relative motion. Hence a velocity gradient exists, in particular where the fluid moves over the surface of the vehicle. It is measured by the dynamic viscosity, μ, defined as the ratio of the viscous stress to the velocity gradient. At sea level, the standard coefficient of viscosity of air is 1.7894×10^{-5} N-s/m^2. The coefficient μ, for any given gas, depends only on its temperature, and increases with temperature. Hence, μ decreases as the temperature decreases with altitude in the troposphere. At the tropopause its value is equal to 0.7945 the value at sea level. It becomes constant in the stratosphere.

An explicit formula for computing the value of μ is

$$\frac{\mu}{\mu_0} = 0.081480723 \frac{T^{3/2}}{T + 110.4} \tag{3.16}$$

Extensive data for the variations of temperature, speed of sound, dynamic viscosity, density and pressure in the Standard Atmosphere are given in the Reference. In Appendix 1, we have reproduced these values, normalized with respect to their values at sea level for every 5000 ft in the troposphere and the stratosphere. The values at sea level are given in both the English system of units and the international system (SI). If altitude is given in meters, a simple conversion to altitude in feet will allow the Table to be read. For an exact calculation at any specified altitude, we can also use the pertinent formulas given in this section.

As an example, consider a flight at 10,000ft which gives $h = 3048$m. With $T_0 = 288.150°$K and $T' = -6.5 \times 10^{-3}$ deg/m, from Eq. (3.8), the standard temperature at this altitude is $T = 268.338°$K. Hence, we have the ratio $T/T_0 = 0.931244$. From Eq. (3.15), we have for the speed of sound $a/a_0 = 0.965010$. For the dynamic viscosity, we obtain from Eq. (3.16), $\mu/\mu_0 = 0.945669$. For the density, we have from Eq. (3.10), $\rho/\rho_0 = 0.738479$. The pressure ratio is calculated from Eq. (3.11) with the value of b in the troposphere as $p/p_0 = 0.687704$. These values are in perfect agreement with the tabulated values.

If the flight altitude is 50,000 ft, in the stratosphere, with $h = 15,240$ m, the temperature, the speed of sound and the dynamic viscosity keep the same values as at the tropopause. For the density, Eq. (3.6) is used with the reference level at the tropopause. The constant value β is such that $1/\beta = RT_*/g = 6341.6184$ m. The altitude as measured from the tropopause is only $\Delta h = h - h_* = 4240$ m. This gives $\rho/\rho_* = p/p_* = 0.512426$. By normalizing with respect to the values at sea level using $\rho_*/\rho_0 = 0.297076$ and $p_*/p_0 = 0.223361$, we find that $\rho/\rho_0 = 0.152229$ and $p/p_0 = 0.114456$. Again, these values are in perfect agreement with the tabulated values. Explicit formulas for the computation will be given in Subsection 3.6.4.

3.3 Aerodynamic forces

Aerodynamic forces develop whenever there is relative motion between the fluid and the immersed body. A simple dimensional analysis will lead to the functional form for the aerodynamic force A. The aerodynamic force on a body depends on its shape and its attitude, that is its relative position with respect to the flow of the fluid. For a given shape and attitude, let us assume that A depends on the density, the free stream velocity, the size of the body, the viscosity and also the speed of sound in the fluid. Then we write

$$A \sim \rho^\alpha V^\beta l^\gamma \mu^\delta a^\epsilon \tag{3.17}$$

In dimensions, with M being the mass, L the length, and T the time, we express the equivalence

$$MLT^{-2} \sim (ML^{-3})^\alpha (LT^{-1})^\beta L^\gamma (ML^{-1}T^{-1})^\delta (LT^{-1})^\epsilon \tag{3.18}$$

Equating powers, we obtain the system

$$\begin{aligned} 1 &= \alpha + \delta \\ 1 &= -3\alpha + \beta + \gamma - \delta + \epsilon \\ -2 &= -\beta - \delta - \epsilon \end{aligned} \tag{3.19}$$

In terms of δ and ϵ, we solve for

$$\begin{aligned} \alpha &= 1 - \delta \\ \beta &= 2 - \delta - \epsilon \\ \gamma &= 2 - \delta \end{aligned} \tag{3.20}$$

If the effects of viscosity through μ, and compressibility through a, are neglected, we take $\delta = \epsilon = 0$ and have the form $A = C\rho l^2 V^2$. Then, the size of the body can be expressed through a reference area, S, and the expression for the aerodynamic force is given as

$$A = \frac{1}{2}\rho S V^2 C_A \tag{3.21}$$

where C_A is a certain dimensionless coefficient which is a function of the shape of the body and its attitude with respect to the relative velocity of the fluid. In this book, the vehicle considered will have a plane of symmetry and it will invariably operate under symmetric conditions. In other words, the velocity vector will be in the plane of symmetry. Then, the attitude of the vehicle is conveniently described by the angle-of-attack, α, which is the angle between the relative velocity vector and a reference line fixed with respect to the vehicle (Fig. 3.2). In deriving the equations of motion in the preceding chapter, we have seen that it is convenient to resolve the aerodynamic force into two forces: the drag force opposite to the direction of the motion, and the lift force orthogonal to it. Hence, from Eq. (3.21) we obtain

$$\begin{aligned} D &= \frac{1}{2}\rho S V^2 C_D \\ L &= \frac{1}{2}\rho S V^2 C_L \end{aligned} \tag{3.22}$$

where C_D and C_L, called the drag coefficient and the lift coefficient, respectively, are functions of the angle-of-attack.

Now, if we retain the effects of viscosity and compressibility, with $\delta \neq 0$ and $\epsilon \neq 0$, expression (3.17) will take the form

$$A \sim \rho S V^2 \left(\frac{\mu}{\rho V l}\right)^{\delta} \left(\frac{a}{V}\right)^{\epsilon} \tag{3.23}$$

The ratio V/a is the Mach number while the dimensionless quantity

$$R_e = \frac{\rho V l}{\mu} \tag{3.24}$$

is known as the Reynolds number. By comparing Eqs. (3.21) and (3.23), we conclude that, the expressions (3.22) for the aerodynamic

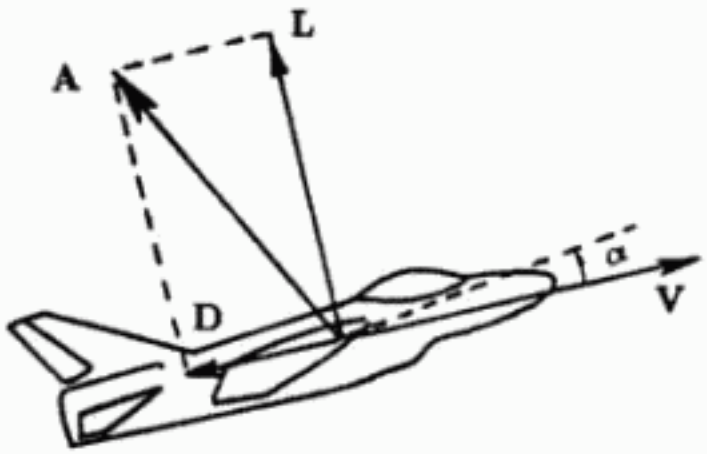

Figure 3.2: Aerodynamic forces in the plane of symmetry.

forces are still valid, but the drag and the lift coefficients are now functions of the angle-of-attack, of the Mach number, and the Reynolds number

$$\begin{aligned} C_D &= C_D(\alpha, M, R_e) \\ C_L &= C_L(\alpha, M, R_e) \end{aligned} \tag{3.25}$$

3.4 The drag polar

At given Mach number and Reynolds number, the drag and the lift coefficients are functions of the angle-of-attack. If the reference line, from which the angle-of-attack is measured, is taken such that $\alpha = 0$ corresponds to the zero-lift condition, typical variations of C_D and C_L are shown in Fig. 3.3.

At low angles-of-attack, the variation of C_L is linear. On the other hand, at relatively high angles-of-attack, the effect of flow separation is important, and the lift coefficient varies non-linearly with the angle-of-attack and depends strongly on the Reynolds number. It reaches a maximum value $C_L = C_{L_{max}}$, at an angle-of-attack $\alpha = \alpha_{max}$, called the stalling angle-of-attack. Generally speaking, flight is restricted to angles-of-attack less than α_{max}. Hence, we have the constraint $C_L \leq C_{L_{max}}$ restricting the lift coefficient.

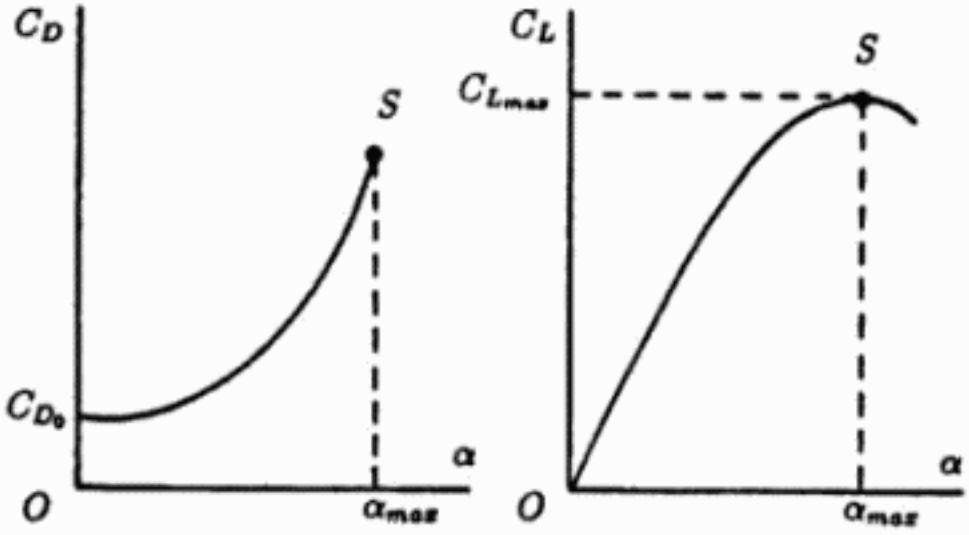

Figure 3.3: Variations of C_D and C_L with α.

By eliminating α between the two equations (3.25) we obtain a relation between C_D and C_L

$$C_D = C_D(C_L, M, R_e) \tag{3.26}$$

For each prescribed set of values for M and R_e, the plot of this equation is called the drag polar. A typical plot is shown in Fig. 3.4 with the scale for C_L generally about 10 times the scale for C_D.

For control of the flight, the pilot may vary the thrust throttle setting to change the propulsive force, and through the control surfaces, he may vary the angle-of-attack and the bank angle to change the aerodynamic force in magnitude and direction. Depending on the optimum performance to be achieved, the angle-of-attack during the flight varies as a selected function of the time between the values $\alpha = 0$ and $\alpha = \alpha_{max}$. For given Mach number and Reynolds number, Eqs. (3.25) are considered as the parametric equations for the drag polar in Fig. 3.4 with various values of α shown at several characteristic points on the plot. It will be shown in subsequent performance analyses that these points are the key optimum operating points for the conduct of the flight. We list below the corresponding angles-of-attack in increasing order of magnitude.

1. By convention, in this book, the value $\alpha = 0$ is the angle-of-attack

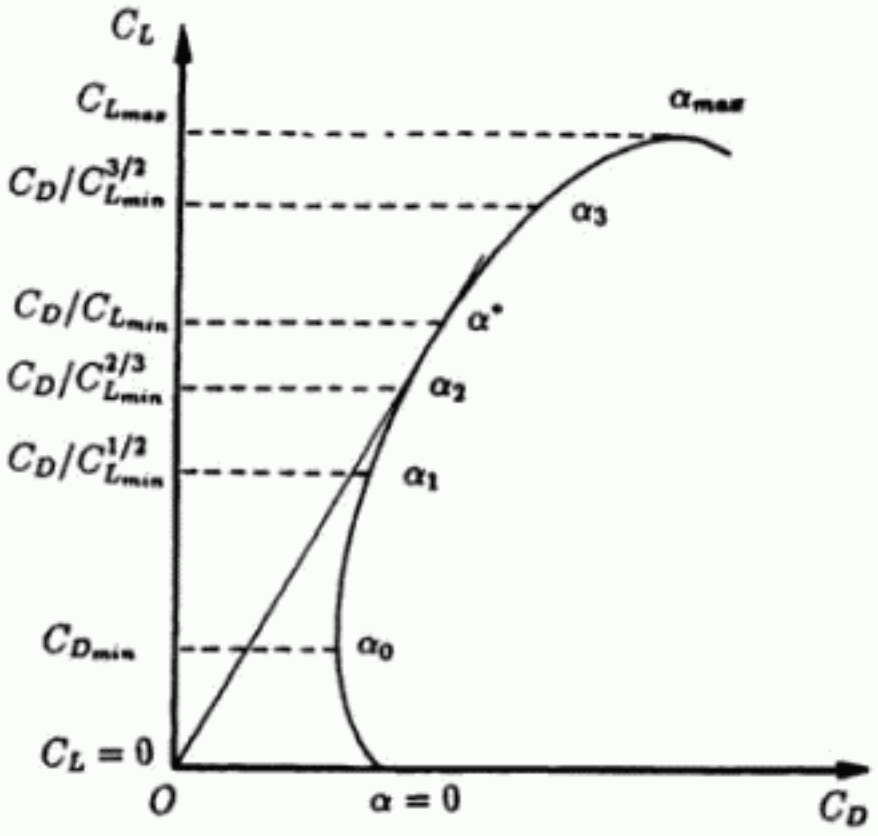

Figure 3.4: A realistic drag polar.

for zero-lift coefficient.

2. The value $\alpha = \alpha_0$ is the angle-of-attack for minimum drag coefficient.

3. The value $\alpha = \alpha_1$ is the angle-of-attack which minimizes the ratio $C_D/C_L^{1/2}$.

4. The value $\alpha = \alpha_2$ is the angle-of-attack which minimizes the ratio $C_D/C_L^{2/3}$.

5. The value $\alpha = \alpha^*$ is the angle-of-attack which minimizes the ratio C_D/C_L. We denote the corresponding lift coefficient and drag coefficient by C_L^* and C_D^*, respectively. This is an operating point of utmost importance in flight mechanics since it is the point where the lift-to-drag ratio is maximized. It is clear that the point is obtained by drawing a tangent from the origin of the coordinate system to the drag polar.

6. The value $\alpha = \alpha_3$ is the angle-of-attack which minimizes the ratio $C_D/C_L^{3/2}$.

7. Finally, the value $\alpha = \alpha_{max}$ is the stall angle-of-attack at the point of maximum lift coefficient.

For an analytical work, we need to make explicit the lift-drag relationship in Eq. (3.26). For high-performance aircraft, the main effect on the drag polar is the influence of Mach number. For most aircraft configurations, by experience, it is found that it is adequate to represent the main portion of the drag polar as a parabola with equation

$$C_D = C_{D_0}(M) + K(M)C_L^2 \tag{3.27}$$

where $C_{D_0}(M)$ and $K(M)$ are some appropriate functions of Mach number. With this representation, C_{D_0} is called the zero-lift drag coefficient and K, the induced drag factor. The drag polar is referred to as the parabolic drag polar. At low Mach number, generally for $M \leq 0.6$, C_{D_0} and K are practically constant. At higher Mach number, C_{D_0} and K vary in the direction which provides higher drag coefficient and smaller lift coefficient. Therefore, the maximum lift coefficient $C_{L_{max}}$ which is constant at low Mach number also decreases with higher Mach number. The parabolic drag polar for a typical jet transport aircraft is shown in Fig. 3.5.

In Eq. (3.27), the term KC_L^2 is the induced drag coefficient and for a subsonic aircraft it is mainly a pressure drag. Disregarding viscosity, for a wing with elliptical spanwise lift distribution, the induced drag factor K can be calculated from

$$K = \frac{1}{\pi \mathcal{AR}} \tag{3.28}$$

where $\mathcal{AR}$ denotes the aspect ratio defined as

$$\mathcal{AR} = \frac{b^2}{S} \tag{3.29}$$

for a wing with span b and planform area S. Taking into account the complete configuration of the aircraft including the non-ellipticity of the lift distribution over the wing, the skin friction drag and the interaction of the fuselage, the coefficient K is modified to

$$K = \frac{1}{e\pi \mathcal{AR}} \tag{3.30}$$

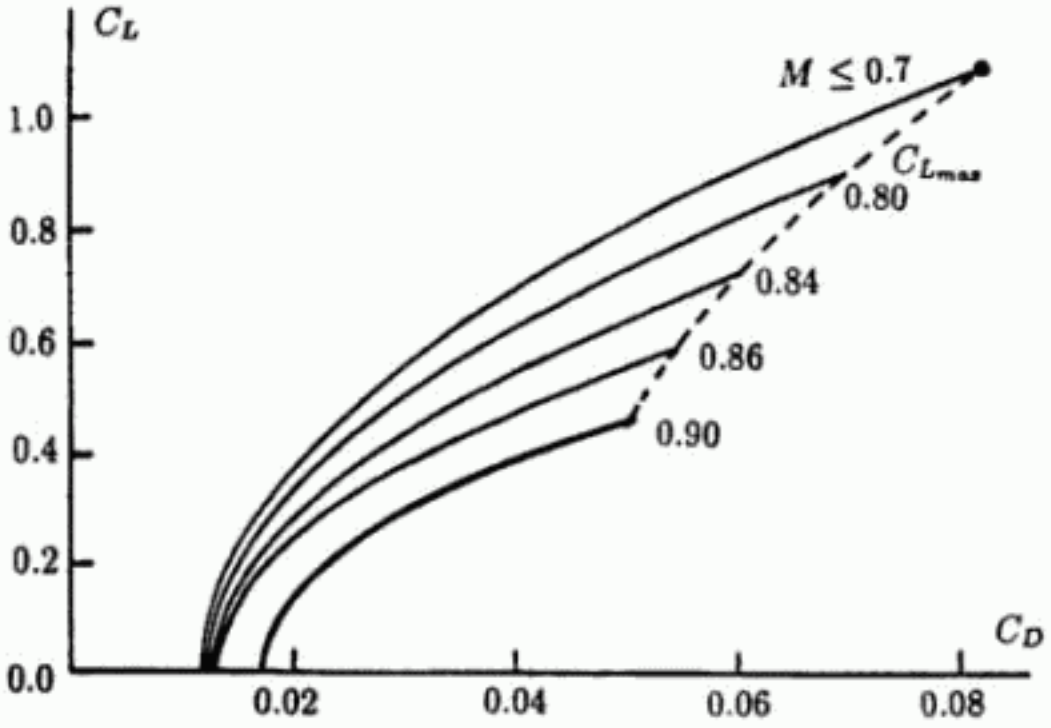

Figure 3.5: Parabolic drag polar of a typical high subsonic aircraft.

where the coefficient e is called the Oswald's efficiency factor and its practical range is 0.6–0.9.

If Eq. (3.27) is substituted in the equations of motion in Chapter 2, then since the lift coefficient is assumed to be a known function of the angle-of-attack, C_L can be used as a control for the flight. Sometimes, it is convenient to use the lift-to-drag ratio, also called the aerodynamic efficiency, as a control variable. It is defined as

$$E = \frac{L}{D} = \frac{C_L}{C_D} \tag{3.31}$$

Now, with the parabolic drag polar, as given in Eq. (3.27), we evaluate the lift coefficient at the various characteristic points shown in Fig. 3.4. In general, at any Mach number, we consider a function to be minimized of the form

$$C_D C_L^{-m} = C_{D_0} C_L^{-m} + K C_L^{2-m} = f(C_L) \tag{3.32}$$

where m is such that $0 \leq m < 2$. Hence, the points from α_0 to α_3 correspond to the values of m in the sequence 0, 1/2, 2/3, 1 and 3/2. By minimizing this function with respect to C_L, we are led to the conditions

$$\frac{df}{dC_L} = \frac{1}{C_L^{m+1}}[(2-m)KC_L^2 - mC_{D_0}] = 0$$
$$\frac{d^2f}{dC_L^2} = \frac{2(2-m)K}{C_L^m} > 0 \tag{3.33}$$

Therefore, we have the solution

$$C_L = \sqrt{\frac{m}{2-m}}\sqrt{\frac{C_{D_0}}{K}}$$
$$C_D = \frac{2}{2-m}C_{D_0} \tag{3.34}$$
$$E = \frac{\sqrt{m(2-m)}}{2\sqrt{KC_{D_0}}}$$

We first consider the particular point α^* at $m = 1$, where the lift-to-drag ratio is maximized. We have the solution

$$C_L = \sqrt{\frac{C_{D_0}}{K}} = C_L^*$$
$$C_D = 2C_{D_0} = C_D^* \tag{3.35}$$
$$E_{max} = \frac{C_L^*}{C_D^*} = \frac{1}{2\sqrt{KC_{D_0}}}$$

These formulas are frequently used in this text. We then calculate and summarize the relevant values for the other points in Table 3.1.

The use of a parabolic drag polar is convenient in deriving explicit formulas for the evaluation of flight performance. But it has a serious defect in that it is not valid near the stalling angle-of-attack. In subsequent chapters, whenever it is required, we shall supplement the analysis with the consideration of a realistic and non-parabolic drag polar near the stalling point.

Table 3.1: Characteristic values along a parabolic drag polar.

α	α_0	α_1	α_2	α^*	α_3	α_{max}
m	0	1/2	2/3	1	3/2	$\cdots$
C_L/C_L^*	0	$\sqrt{3}/3$	$\sqrt{2}/2$	1	$\sqrt{3}$	$C_{L_{max}}/C_L^*$
E/E_{max}	0	$\sqrt{3}/2$	$2\sqrt{2}/3$	1	$\sqrt{3}/2$	$(C_{L_{max}}/C_{D_{max}})/E_{max}$

3.5 Effect of Mach number

Within the parabolic formulation of the drag polar, the assumption of constant values for C_{D_0}, K and $C_{L_{max}}$ is only valid at low Mach number. Depending on the airfoil and the angle-of-attack, even for a free-stream Mach number as low as 0.7, a conventional airfoil may accelerate the flow to velocities that are locally supersonic over the forward or middle portion of the upper surface of the wing. The flow then decelerates rapidly through a relatively strong shock wave to subsonic conditions. This causes the boundary layer to thicken and, depending on the strength of the shock, to separate. The net result is that it produces a sharp increase in the zero-lift drag coefficient C_{D_0} as the speed is nearing the speed of sound. A typical variation of $C_{D_0}(M)$ as a function of Mach number for a supersonic aircraft is shown in Fig. 3.6. While the minimum value of the free stream Mach number for which the local flow becomes supersonic is known as the critical Mach number, the slightly higher value, by a few hundredths, which causes a sudden rise in the zero-lift drag coefficient is referred to as the drag-divergence Mach number. After a maximum, near to $M = 1$ or slightly higher, C_{D_0} decreases to a near constant value at supersonic speeds.

For flight dynamicists, it suffices to know the characteristic behavior of the three functions $C_{D_0}(M)$, $K(M)$ and $C_{L_{max}}(M)$. It is assumed that these quantities are known explicitly as functions of the Mach number. For any aircraft configuration, this is done by modeling these functions as polynomials in M, based on aerodynamic data obtained from wind tunnel measurements and flight tests.

Figure 3.7 shows the variations of these functions for a typical high

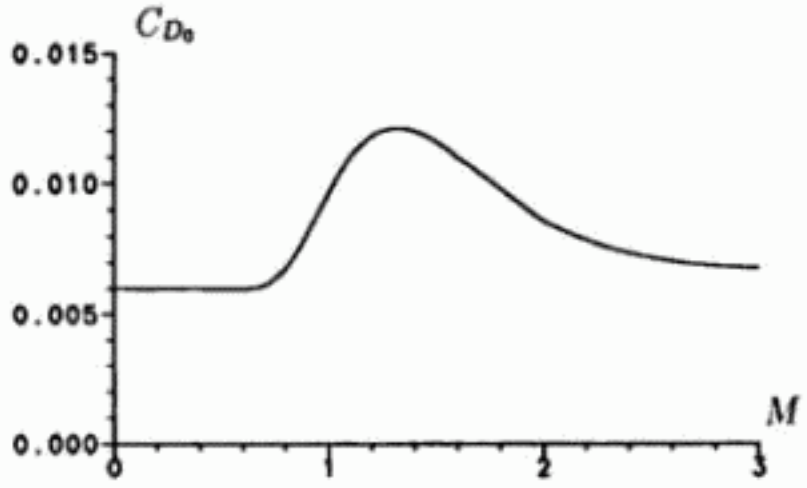

Figure 3.6: Variation of $C_{D_0}(M)$ for a supersonic aircraft.

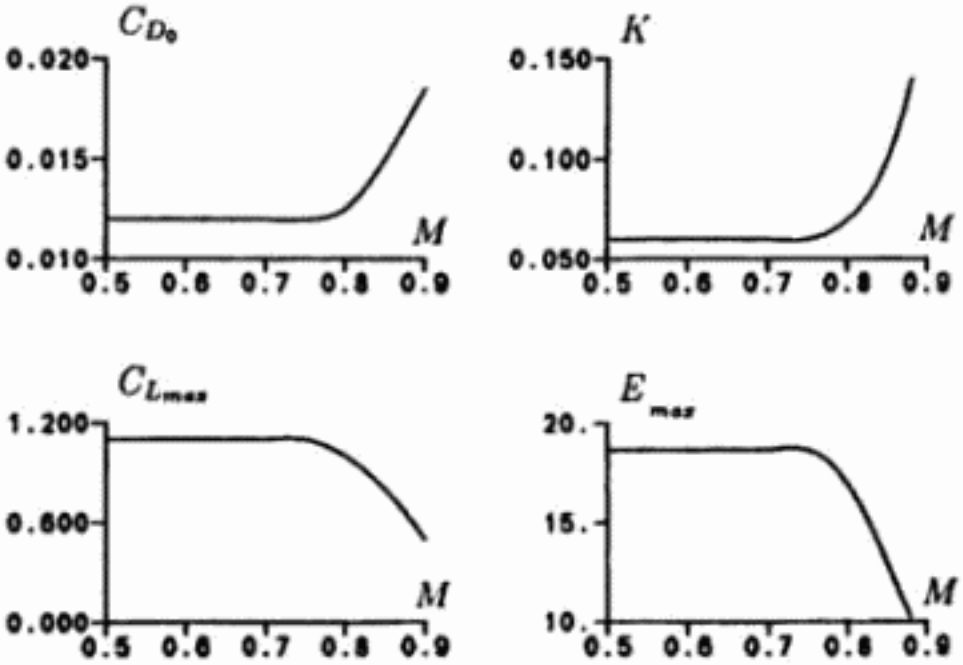

Figure 3.7: Variations of aerodynamic characteristics for a typical high subsonic transport aircraft.

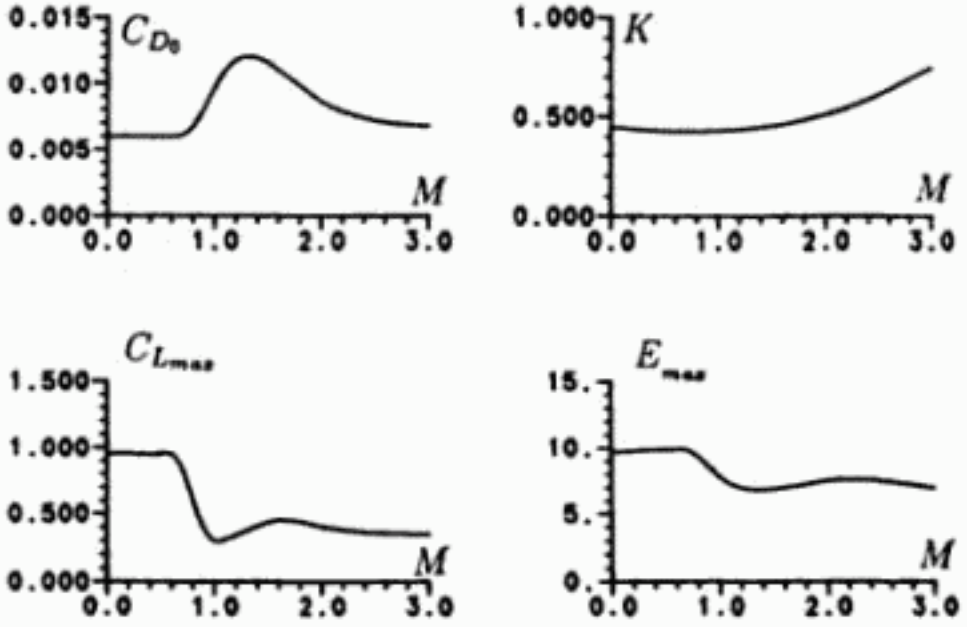

Figure 3.8: Variations of aerodynamic characteristics for a typical supersonic fighter aircraft.

subsonic jet transport aircraft. The variation of the maximum lift-to-drag ratio, E_{max}, as calculated from Eq. (3.35), is also plotted in the figure. At low Mach number, $M \leq 0.7$, the aerodynamic functions are nearly constant. When the speed increases, approaching the sonic speed, both C_{D_0} and K increase markedly and as a consequence the function E_{max} decreases. One important effect of compressibility is that the maximum lift coefficient, $C_{L_{max}}$, for a subsonic aircraft decreases drastically for speeds approaching the speed of sound. Since the lift coefficient, C_L, used as an aerodynamic control, is bounded by this upper limit, the domain of flight is strongly influenced by this function.

Figure 3.8 shows the variations of these elements for a typical supersonic fighter aircraft. The pertinent remark here is that while the induced drag factor K, increases monotonically with the Mach number, the zero-lift drag coefficient C_{D_0}, first increases and reaches a maximum value in the transonic region and then decreases at high supersonic speeds to a value higher than its low subsonic value. For a supersonic aircraft, the function $C_{L_{max}}$ first decreases and passes through a minimum value in the transonic region and then slightly increases to a near constant value at high supersonic speeds. For the majority of supersonic aircraft the value of $C_{L_{max}}$ at supersonic speeds is close to unity.

3.6 Airspeed measurement

For the evaluation of flight performance and in navigation, it would be ideal if there were an instrument on board the aircraft which gives a direct reading of the relative speed V of the aircraft with respect to the surrounding atmosphere. This speed will be generally referred to as the airspeed, or the true airspeed. But this speed can only be measured indirectly and thus its evaluation is made through the use of the standard atmosphere as will be explained in this important section.

3.6.1 The Pitot-static system

The Pitot-static system, shown schematically in Fig. 3.9 is a device which collects the static pressure of the undisturbed atmosphere p, and the total or stagnation pressure p_t. While the total pressure is collected through the mouth of the Pitot tube, assumed parallel to the relative velocity, the static pressure is obtained through the openings on the side of the tube or from another location. These two pressures are fed to a differential pressure gauge which is the airspeed indicator. Therefore, it is important to notice that the airspeed indicator measures the pressure difference $\Delta p = p_t - p$.

The relationship between p, p_t and the true airspeed V is given by Bernouilli's equation for compressible fluid flow

$$\frac{k}{k-1}\frac{p}{\rho} + \frac{1}{2}V^2 = \text{constant} = \frac{k}{k-1}\frac{p_t}{\rho_t} \tag{3.36}$$

where again ρ is the density of the air and k is the ratio of the specific heats with value $k = 1.4$ for air. This equation assumes that the air is brought to rest at the stagnation point, where $V = 0$, adiabatically. In subsonic speeds, the stagnation conditions are reached isentropically, and we have an additional relation between the pressure and the density,

$$\frac{\rho_t}{\rho} = \left(\frac{p_t}{p}\right)^{1/k} \tag{3.37}$$

Solving for V^2 from Eq. (3.36) and on using this equation, we obtain

$$V^2 = \frac{2kp}{(k-1)\rho}\left[\left(\frac{p_t}{p}\right)^{(k-1)/k} - 1\right] \tag{3.38}$$

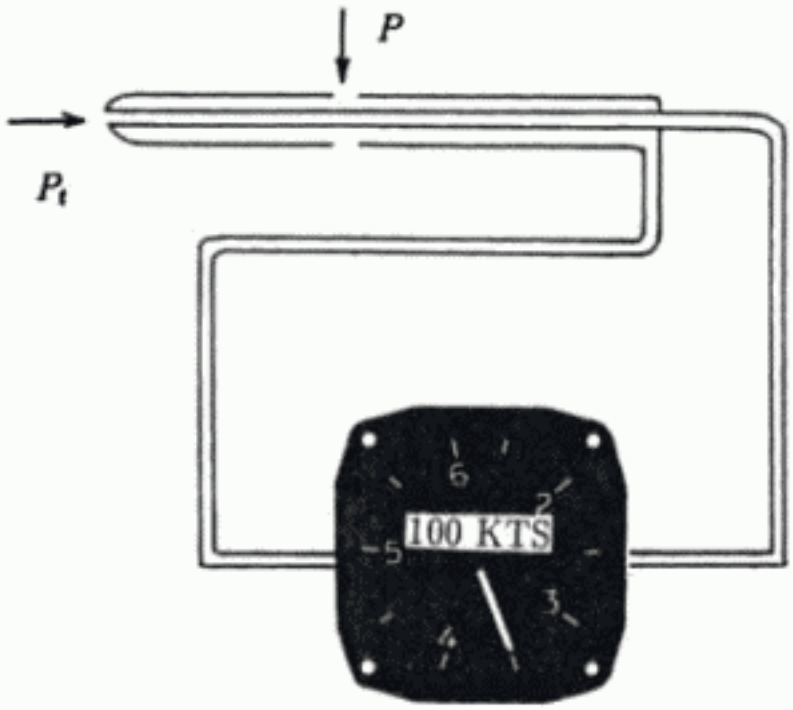

Figure 3.9: The Pitot–static system.

By observing that $p_t/p = (\Delta p/p) + 1$ and using Eq. (3.14) for the speed of sound we have the relation for evaluating the true airspeed at subsonic speeds

$$V^2 = \frac{2a^2}{k-1}\left[\left(\frac{\Delta p}{p} + 1\right)^{(k-1)/k} - 1\right] \tag{3.39}$$

3.6.2 The calibrated airspeed

As a differential pressure gauge, the airspeed indicator measures the pressure difference Δp. If, in addition, we have the ambient pressure p and the ambient speed of sound a, Eq. (3.39) will give the true airspeed V. But with Δp as the only measurement, for a reading showing the speed, this instrument is calibrated with constant values for p and a, taken as the standard values at sea level. Hence, we define the

calibrated airspeed V_c according to the formula

$$V_c^2 = \frac{2a_0^2}{k-1}\left[\left(\frac{\Delta p}{p_0}+1\right)^{(k-1)/k} - 1\right] \tag{3.40}$$

A perfect airspeed indicator is an instrument which gives this speed V_c. But, because of possible instrument errors from various sources, the speed read on the instrument, called the indicated airspeed V_i, is slightly different. In this text, we use V_i with the meaning that it is precisely the calibrated airspeed V_c as defined by Eq. (3.40).

At this stage, with a reading of V_i, which we take as exactly equal to V_c, it is possible to calculate the true airspeed at the flight altitude within the framework of the standard atmosphere. This is because if V_c is known, Δp is evaluated from Eq. (3.40). Then, as shown previously in Section 3.2, at the flight altitude h, the standard values for p and a can be evaluated. The true airspeed is then obtained from Eq. (3.39). Of course, this is the actual speed only if the atmosphere varies with altitude as in the standard atmosphere.

We shall return to the relationship $V_c \rightarrow V$ at the end of this section.

3.6.3 The Machmeter

At high subsonic and supersonic speeds, the airspeed indicator is of little use and the Machmeter becomes the instrument for assessing the speed. A Machmeter is similar to the speed indicator but it includes both the measurement of the pressure difference $\Delta p = p_t - p$, and also the measurement of the static pressure p.

At subsonic speed, from Eq. (3.39) with $M = V/a$, we have the so-called Saint-Venant formula

$$M^2 = \frac{2}{k-1}\left[\left(\frac{\Delta p}{p}+1\right)^{(k-1)/k} - 1\right] \tag{3.41}$$

This is the calibration formula for Machmeters at subsonic speeds, with the quantity $\Delta p/p$ being measured directly by the Pitot–Machmeter system. With $k = 1.4$, we rewrite this equation in the simple form

$$\frac{\Delta p}{p} = (1 + 0.2M^2)^{3.5} - 1 \tag{3.42}$$

A Pitot tube, extended into a supersonic flow, will produce a normal shock ahead of its mouth, and hence will collect the total pressure p_{t_1} aft of the shock. Experimental data reveal that the true ambient pressure can be collected if the openings on the side of the tube are located at a distance more than ten times the diameter behind the mouth of the tube. Hence, at supersonic speeds, the Pitot–Machmeter system measures directly $\Delta p = p_{t_1} - p$ and p. If can be shown that, in this case, the relation between p_{t_1}, p and the Mach number M is

$$p_{t_1} = p\left(\frac{k+1}{2}\right)^{(k+1)/(k-1)}\left(\frac{2}{k-1}\right)^{1/(k-1)}\frac{M^{2k/(k-1)}}{\left(\frac{2k}{k-1}M^2-1\right)^{1/(k-1)}} \tag{3.43}$$

Numerically, with $k = 1.4$ we write this equation as

$$\frac{\Delta p}{p} = \frac{166.92158M^7}{(7M^2-1)^{2.5}} - 1 \tag{3.44}$$

This is the Lord Rayleigh formula for supersonic calibration of Machmeters. It is used when $\Delta p/p$ has a value in excess of 0.893, while for lower values of the ratio, the Saint-Venant formula (3.42) is used.

In conclusion, allowing for instrument errors from various sources, at the flight altitude, a Machmeter gives the true Mach number both at subsonic and supersonic speeds. The Machmeter is calibrated based on the measurements of $\Delta p = p_t - p$, and p, or actually on the ratio $\Delta p/p$. The relationship used is the Saint-Venant formula (3.42) for subsonic speeds and the Rayleigh formula (3.44) for supersonic speeds.

On the other hand, allowing for instrument errors from various sources, at the flight altitude, a speed indicator does not give the true airspeed V, but a speed V_c called the calibrated airspeed. This is purely a conventional speed based on Eq. (3.40) to transform Δp into V_c for subsonic speeds. With $k = 1.4$, we can rewrite this equation for calibration as

$$\frac{\Delta p}{p_0} = \left[1 + 0.2\left(\frac{V_c}{a_0}\right)^2\right]^{3.5} - 1 \tag{3.45}$$

If the speed indicator is also calibrated for supersonic speeds, the relevant formula is

$$\frac{\Delta p}{p_0} = \frac{166.92158(V_c/a_0)^7}{[7(V_c/a_0)^2-1]^{2.5}} - 1 \tag{3.46}$$

3.6.4 Relation between calibrated airspeed and true airspeed

In flight, from the reading of the speed indicator, we have the calibrated airspeed V_c. It is proposed to calculate the true airspeed at the flight altitude h. This altitude is given by the altimeter which is simply an instrument which measures the ambient static pressure p. Its calibration in height is based on the standard atmosphere. For example, if the altimeter shows an altitude of 36,089 ft, it simply means that at this flight altitude the static pressure is such that $p/p_0 = 0.223361$, with $p_0 = 1.01325 \times 10^5\,\mathrm{N/m^2}$ being the standard pressure at sea level. This altitude is known as the pressure altitude and it is equal to the true altitude only if the actual variation of pressure with altitude is the same as in the standard atmosphere. Therefore, all the calculations in this sub-section are based on the formulas for the standard atmosphere.

If V_c is known, say in knots, then with the speed of sound in the standard atmosphere at sea level $a_0 = 661.471\,\mathrm{kt}$, Δp can be evaluated from Eq. (3.45) for subsonic speeds or Eq. (3.46) for supersonic speeds. There are Tables for this relationship, with some discrete values shown below

V_c (kt)	200	400	600	800	1000
$\Delta p\,(\mathrm{N/m^2})$	6634	28395	71369	145406	249057

With the pressure difference Δp known, the Mach number M can be evaluated from Eq. (3.42) or Eq. (3.44) with the input of the static pressure p. In the standard atmosphere, the temperature, the speed of sound, the pressure and also the density can be evaluated at the flight altitude h by the equations in Section 3.2, rearranged below for convenience.

Below the altitude of 11,000 m, with h expressed in meters, we have

$$\frac{T}{T_0} = 1 - \frac{6.5 \times 10^{-3}}{288.150} h \tag{3.47}$$

$$\frac{a}{a_0} = \left(\frac{T}{T_0}\right)^{0.5} \tag{3.48}$$

$$\frac{p}{p_0} = \left(\frac{T}{T_0}\right)^{5.2558774} \tag{3.49}$$

$$\frac{\rho}{\rho_0} = \left(\frac{T}{T_0}\right)^{4.2558774} \tag{3.50}$$

For the reference values, we use $T_0 = 288.150°\text{K}$, $a_0 = 340.294$ m/s, $p_0 = 1.01325 \times 10^5$ N/m^2 and $\rho_0 = 1.225$ kg/m^3.

Above the altitude of 11,000 m and within the stratosphere, the temperature and the speed of sound keep their constant values at the tropopause as $T_* = 216.650°\text{K}$ and $a_* = 295.070$ m/s, while for the pressure and the density the following formulas are relevant.

$$\frac{p}{p_0} = 0.223361 \exp\left(-\frac{h - 11000}{6341.6184}\right) \tag{3.51}$$

$$\frac{\rho}{\rho_0} = 0.297076 \exp\left(-\frac{h - 11000}{6341.6184}\right) \tag{3.52}$$

With the calculated Mach number, and the speed of sound at the flight altitude, the true airspeed is simply

$$V = Ma \tag{3.53}$$

In the case of a reading of the Mach number from the Machmeter, it suffices to calculate the speed of sound and use this equation for conversion to the true airspeed.

As an example, let us compare the speeds at two flight regimes with the calibrated airspeeds of $V_{c_1} = 200$ kt and $V_{c_2} = 400$ kt, respectively.

If the flight is at sea level and if the atmospheric condition is identical to the condition of the standard atmosphere, then these speeds are the true airspeeds V_1 and V_2 and their ratio is $V_2/V_1 = 2$.

If the flight is at the tropopause, $h = 11,000$ m, then we evaluate $p = 22632\ N/m^2$, $a = 295.070$ m/s.

For the case of $V_c = 200$ kt, $\Delta p = 6634\ N/m^2$. Then

$$\frac{\Delta p}{p} = \frac{6634}{22632} = 0.293125$$

From Eq. (3.42), this gives $M = 0.617$, and hence $V_1 = 182.058$ m/s.

For the case of $V_c = 400$ kt, $\Delta p = 28395\ N/m^2$. Then

$$\frac{\Delta p}{p} = \frac{28395}{22632} = 1.254639$$

Since $\Delta p/p > 0.893$, the speed is supersonic and by iteration, Rayleigh formula (3.44) gives $M = 1.1458$. Hence, we obtain for the true airspeed $V_2 = 338.09$ m/s. The ratio of the speeds is $V_2/V_1 = 1.857$.

Figure 3.10 shows the relationship between the calibrated airspeed and the true airspeed at various standard altitudes. The construction of the graph is explained in Exercises 3-1 and 3-2. By inspection of the plots, we have the following observations:

The true airspeed is equal to the calibrated airspeed at sea level in the standard atmosphere. For the same calibrated airspeed, the true airspeed is higher at higher standard altitude. The corresponding Mach number is also higher. Therefore, for the same reading of the calibrated airspeed V_c, flight may be subsonic at low altitude or it can be supersonic at high altitude. This is because as the true airspeed increases with altitude, the speed of sound decreases in the troposphere and is constant in the stratosphere and hence the Mach number increases with altitude.

Although the exact relationship between V_c and V is not simple, an approximate formula can be obtained at low speeds. In Eq. (3.42), by replacing $0.2 = (k-1)/2$ and $3.5 = k/(k-1)$, we can use binomial expansion to obtain

$$\frac{\Delta p}{p} = \frac{1}{2}kM^2\left(1 + \frac{1}{4}M^2 + \frac{1}{40}M^4 + \frac{1}{1600}M^6 + \cdots\right) \tag{3.54}$$

The value of the quantity inside the brackets, for $M = 0.2$ is 1.0100 and for $M = 0.3$ is 1.0227. Therefore, at low Mach numbers, by using Eqs. (3.13) and (3.14) we have the approximation

$$\Delta p \approx \frac{kpM^2}{2} = \frac{kpV^2}{2a^2} = \frac{1}{2}\rho V^2 \tag{3.55}$$

The quantity $\rho V^2/2$ is termed the dynamic pressure and in incompressible fluid, when we neglect the effect of the Mach number it is equal to the pressure difference Δp. If this formula with the standard density at sea level is used to calibrate the speed indicator, we shall have

$$\Delta p = \frac{1}{2}\rho_0 V_c^2 \approx \frac{1}{2}\rho V^2 \tag{3.56}$$

The relation between the calibrated airspeed and the true airspeed

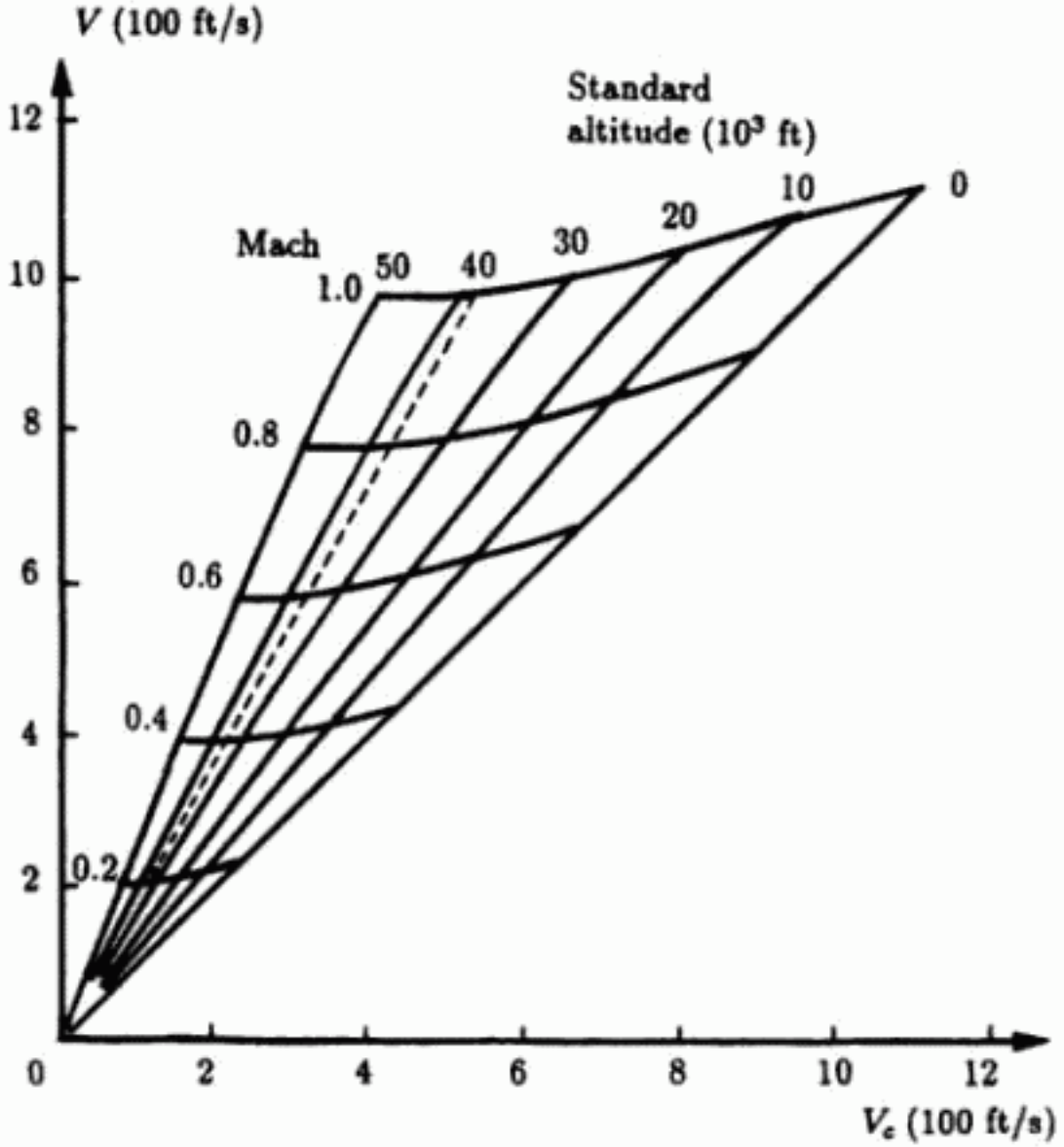

Figure 3.10: Relationship between calibrated airspeed and true airspeed in the standard atmosphere.

at low speed is approximately

$$V \approx \frac{V_c}{\sqrt{\rho/\rho_0}} \tag{3.57}$$

3.7 The equivalent airspeed

We introduce the concept of the equivalent airspeed, V_e, in a separate section and not in the section on Airspeed Measurement because there are instances when one may confuse this speed with the calibrated airspeed V_c.

By definition, the equivalent airspeed is given by

$$V = \frac{V_e}{\sqrt{\rho/\rho_0}} \tag{3.58}$$

where V is the true airspeed, ρ the density at the flight altitude and ρ_0 is the density at sea level for any arbitrary atmosphere. This equation is simply a mathematical transformation. Another way to view this is to go back to the definition (3.40) of the calibrated airspeed V_c. It is evident that V_c is obtained from the measurement of the pressure difference Δp, while from Eq. (3.58), the equivalent airspeed V_e is not derived from any physical measurement. It simply stands on its definition which is another way, that is an equivalent way, to write the true airspeed. The confusion comes from the fact that by comparing Eqs. (3.57) and (3.58), it is seen that, at very low speed, for incompressible fluid, and in the standard atmosphere, V_e is nearly equal to V_c. To clarify this statement a numerical example is in order.

In the previous section, we have considered the case of a reading of calibrated airspeed $V_c = 200$ kt $= 102.889$ m/s. We have found that, if the flight is at the tropopause, in the standard atmosphere calculation, the true airspeed is $V = 182.058$m/s. At this altitude, $\rho/\rho_0 = 0.297076$. If we use Eq. (3.58) to calculate the equivalent airspeed, we find that $V_e = 99.230$ m/s and it is not the same as V_c. This is because we are dealing with a high Mach number at $M = 0.617$. Now, if we recalculate the speeds at the flight altitude of $h = 2000$m we will be dealing with a

low Mach number. From Eqs. (3.47–3.48), we obtain $a = 332.529$ m/s, $p = 79495$ N/m^2 and $\rho/\rho_0 = 0.821625$. Then

$$\frac{\Delta p}{p} = \frac{6634}{79495} = 0.083452$$

From Eq. (3.42), this gives a low Mach number of $M = 0.340$. Therefore, the true airspeed is $V = 113.060$ m/s. By using the definition (3.58) to compute the equivalent airspeed with the density ratio evaluated above, we find that $V_e = 102.482$ m/s. It is now closer to V_c.

The usefulness of the equivalent airspeed will be made clearer when we analyze aircraft performance, but the general idea is that it is used for the transformation

$$\frac{1}{2}\rho V^2 = \frac{1}{2}\rho_0 V_e^2 \tag{3.59}$$

The immediate conclusion is that if the flight is at constant dynamic pressure, then the equivalent airspeed is the same at all altitudes. Furthermore, it is found convenient for the interpretation of the results in performance analysis to replace the product $\rho V^2/2$ by its equivalent in certain formulas. For example, in rectilinear steady flight at constant altitude, the lift is used to balance the weight and we can write that

$$\frac{1}{2}\rho S V^2 C_L = W \tag{3.60}$$

At the stall, with $C_L = C_{L_{max}}$, if we use the equivalent airspeed, then

$$V_e = \sqrt{\frac{2W}{\rho_0 S C_{L_{max}}}} \tag{3.61}$$

For an average known value of the weight, since the stall is at low speed, when the altitude is low enough so that the corresponding Mach number is not too high, $C_{L_{max}}$ is constant and, as a consequence, the equivalent airspeed at stall is the same. Furthermore, if the condition of low Mach number prevails, V_e is nearly the same as the calibrated airspeed V_c read from the speed indicator. Therefore, the speed indicator is a good instrument to indicate the stall speed, and it is a flight instrument particularly useful at low speeds such as during a take-off or a landing.

Exercises

It is the intention of the author to familiarize the readers with the various unit systems in use in flight operations. Therefore, the numerical exercises in this chapter deal with a variety of units of speed and altitude.

3-1. It is proposed to generate the plots in Fig. 3.10 with the calibrated airspeed V_c as abcissa in ft/s and the true airspeed V as ordinate also in ft/s. The parameter used is the standard altitude in kft.

a) For subsonic speeds, let

$$F = \left[1 + 0.2\left(\frac{V}{a}\right)^2\right]^{3.5}$$

$$F_c = \left[1 + 0.2\left(\frac{V_c}{a_0}\right)^2\right]^{3.5}$$

Use Eqs. (3.42) and (3.45) to show that the relationship between F_c and F is

$$F = 1 + \frac{p_0}{p}(F_c - 1)$$

b) Take the constant altitude at intervals of 10 kft from sea level and use the data in Appendix 1 to evaluate the pressure ratio p/p_0, and the speed of sound a, with the value at sea level $a_0 = 1116.45$ ft/s. For each value of V_c, compute F and then V/a and finally V. Write a routine program to generate the plots at constant altitude.

3-2. Figure 3.10 is restricted to subsonic speeds at $M \leq 1$. It is proposed to generate the plots at constant Mach number. Hence, at a given Mach number

$$F = (1 + 0.2M^2)^{3.5}$$

is constant.

a) Show that for each value of $V_c \geq Ma_0$, the pressure ratio is computed from

$$\frac{p}{p_0} = \frac{F_c - 1}{F - 1}$$

Then, show that if $p/p_0 \geq p_*/p_0 = 0.223361$, the corresponding true airspeed is obtained from

$$V = Ma_0\left(\frac{p}{p_0}\right)^{0.095132}$$

with $a_0 = 1116.45$ ft/s, while when $p/p_0 < p_*/p_0$, it is simply

$$V = Ma_*$$

with $a_* = 968.08$ ft/s.

b) Write a routine program to generate the plots at constant Mach number.

3-3. By going over the process in Exercises 3-1 and 3-2, deduce that if V_c and V are expressed in another unit system, say in m/s, we have identical plots, and to use the graph, we can simply add a metric scale on the two axes.

3-4. It is of interest to have a graph with the true airspeed V as abcissa, and the altitude h as ordinate. To fix the idea, express V in m/s and h in km and size the graph for V between O and 500 m/s and h between O and 14 km. In this graph, we propose to plot lines of constant calibrated airspeed V_c in knots and lines of constant Mach number.

a) Show that, in the stratosphere with $h \geq 11$ km, the iso-Mach number lines are the vertical lines with abcissa

$$V = Ma_*$$

with $a_* = 295.070$ m/s.

b) Show that, in the troposphere with h expressed in km, the iso-Mach number lines are the parabolas with equation

$$V = Ma_0\left(1 - \frac{6.5h}{288.150}\right)^{1/2}$$

with $a_0 = 340.294$ m/s. If you carry out the plotting, although theoretically the curves are parabolas, they look quite linear. This is because of the small variation of h in km. Show that, approximately we have

$$V = Ma_0\left(1 - \frac{3.25h}{288.150}\right)$$

Plot the curves with M from 0.2 to 1.4 at 0.2 Mach interval.

c) By going over the process in parts a) and b), deduce that if V and h are expressed in another unit system, say with V in ft/s and h in kft, we have identical plots, and hence to use the graph, we can simply add a new scale on each of the coordinate axes.

3-5. In continuing the previous exercise, it is now proposed to plot lines of constant calibrated airspeed V_c in knots on the same graph. With the previous exercise, the (V, h) space is divided into two regions, one for subsonic speeds with $M \leq 1$, and one for supersonic speeds with $M > 1$.

a) Show that, at subsonic speeds, and in the tropopause, with $h \leq 11$ km, the relevant equations are

$$F_c = \left[1 + 0.2\left(\frac{V_c}{a_0}\right)^2\right]^{3.5}$$

$$F = \left[1 + 0.2\left(\frac{V}{a_0}\right)^2\left(\frac{a_0}{a}\right)^2\right]^{3.5}$$

$$F = 1 + \frac{p_0}{p}(F_c - 1)$$

$$\frac{a}{a_0} = \left(1 - \frac{6.5h}{288.150}\right)^{0.5}$$

$$\frac{p}{p_0} = \left(1 - \frac{6.5h}{288.150}\right)^{5.2558774}$$

with h in km.

b) For each value of V_c from 200 kt to 600 kt at 100 kt interval, multiply V_c by the conversion factor $k = 1852/3600$ to express it in m/s, and calculate the constant value F_c. Then for each altitude h, compute a/a_0, p/p_0, F and deduce V/a_0 and finally V for the plot. Write a routine program for plotting.

c) Show that in the stratosphere where $h > 11$ km, for the computation, we delete the equation for a/a_0, and replace F and p/p_0 by

$$F = \left[1 + 0.2\left(\frac{V}{a_*}\right)^2\right]^{3.5}$$

$$\frac{p}{p_0} = 0.223361 \exp\left(-\frac{h - 11}{6.3416184}\right)$$

Then, as before, with constant F_c for each altitude input in km, compute p/p_0, F and then V/a_* and deduce V with $a_* = 295.070$ m/s.

3-6. Discuss the necessary modification to extend the plotting in Exercise 3-5 for the case of supersonic speeds.

This graph is called the Chevalier graph and it is used to obtain the true airspeed V at any flight altitude and Mach number, or any flight altitude and calibrated airspeed.

3-7. Although it has been said that the equivalent airspeed V_e as defined in Eq. (3.58) is not derived from any physical measurement, within the assumption of the standard atmosphere, at any pressure altitude the true airspeed V can be obtained from a reading of a calibtated air speed V_c and hence from Eq. (3.58) the equivalent airspeed itself can be obtained.

a) At subsonic speeds, show that the relationship between V_c and V_e can be obtained through the equations

$$F_c = \left[1 + 0.2\left(\frac{V_c}{a_0}\right)^2\right]^{3.5}$$

$$F_e = \left[1 + 0.2\left(\frac{V_e}{a_0}\right)^2 \frac{p_0}{p}\right]^{3.5}$$

$$F_e = 1 + \frac{p_0}{p}(F_c - 1)$$

The relationship depends only on the pressure ratio.

b) It is proposed to generate a graph of V_c as abcissa, say in mph, and V_e as ordinate also in mph. Take the speed of sound at sea level as $a_0 = 761.216$ mph.

At any standard altitude, in kft, use the corresponding pressure ratio in the Table in Appendix 1. For each value of V_c, compute F_c, then F_e and deduce V_e/a_0 and finally V_e.

As a numerical example, at 10 kft where $p/p_0 = 0.6877$ deduce that for $V_c = 300$ mph and 500 mph, the corresponding values of V_e are 297.528 mph and 489.741 mph, respectively.

c) Write a routine program for the plotting at $h = 0$, 10, 20, 30 and 40 kft, and for V_c up to 700 mph.

d) At high altitude, the plots may enter the supersonic domain. Show that along the sonic line where $M = 1$, we have the relationship

$F_e = 1.2^{3.5}$ and hence

$$F_c = 1 + 0.892929\frac{p}{p_0}$$

At each altitude, use this relation to delimit the subsonic domain of V_c.

4

Propulsion systems

4.1 Introduction

In the equations of motion derived in Chapter 2, besides the aerodynamic forces, the other key force necessary to sustain flight is the propulsive force expressed as the thrust T delivered by the propulsion system installed in the vehicle. This force is obtained at the expense of the fuel consumption, at the rate expressed as

$$\frac{dm}{dt} = -\frac{c}{g}T \tag{4.1}$$

where c is termed the thrust specific fuel consumption and g is the constant gravitational acceleration. Hence, the parameter c, which is a performance characteristic of the propulsion system, is defined as the fuel weight flow rate per hour per pound of thrust. Numerically, for performance evaluation, it can be given in units of inverse hours.

In general, the thrust T is a function of the Mach number M, the altitude z, and the way that the engine is operating. This is represented by a parameter N referred to as the engine throttle setting. The specific fuel consumption c depends on the same parameters. Since $M = V/a$ where V is the true airspeed and a is the speed of sound at the flight altitude, and for any specified atmosphere a is a function of the altitude, we have the functional dependence

$$\begin{aligned} T &= T(V, z, N) \\ c &= c(V, z, N) \end{aligned} \tag{4.2}$$

It is the purpose of this chapter to describe the various propulsion systems that might be used currently or in the near future. For performance analyses, it is not necessary to get into a detailed discussion of the inner workings of each propulsion system. The main objective is to make explicit the functional relationship in Eqs. (4.2) so that the optimum flight conditions can be derived in subsequent chapters.

The propulsion systems of practical use can be classified into two groups: the single-flow systems and the multi-flow systems. A single-flow system is one in which the thrust is produced by the acceleration of one propulsive stream. In this category we have the rocket engine, the turbojet engine and the ramjet engine. A multi-flow system is one in which the thrust is produced by the acceleration of more than one propulsive stream. In this category we have the reciprocating piston engine and propeller combination, the turboprop system and the turbofan engine.

4.2 Rocket

In a rocket engine, either with solid propellant or a combination of liquid propellant and oxidizer, both carried in tanks on board, the burned mass is ejected through a nozzle, thus creating a reaction force which is the thrust. This thrust can be written as

$$\mathbf{T} = -\beta \mathbf{V}_{re} + (p - p_e) A_e \mathbf{n}_e \tag{4.3}$$

where $\beta = -dm/dt$ is the overall mass flow rate, $\mathbf{V}_{re}$ the average relative velocity, p_e the average pressure and A_e the engine exit area. It is assumed that the tangential stress over the exit area is negligible. The unit vector $\mathbf{n}_e$ normal to the area A_e is positively directed inward. Finally, p is the average free stream pressure. For simplicity, we may assume that all the vectors in Eq. (4.3) are collinear and write the one-dimensional equation as

$$T = \beta V_{re} + (p_e - p) A_e \tag{4.4}$$

By comparing Eq. (4.1) and Eq. (4.4) it is seen that the specific fuel consumption for rocket engines is given by

$$\frac{1}{c} = \frac{V_{re}}{g} + \frac{p_e - p}{g\beta} A_e = I_{sp} \tag{4.5}$$

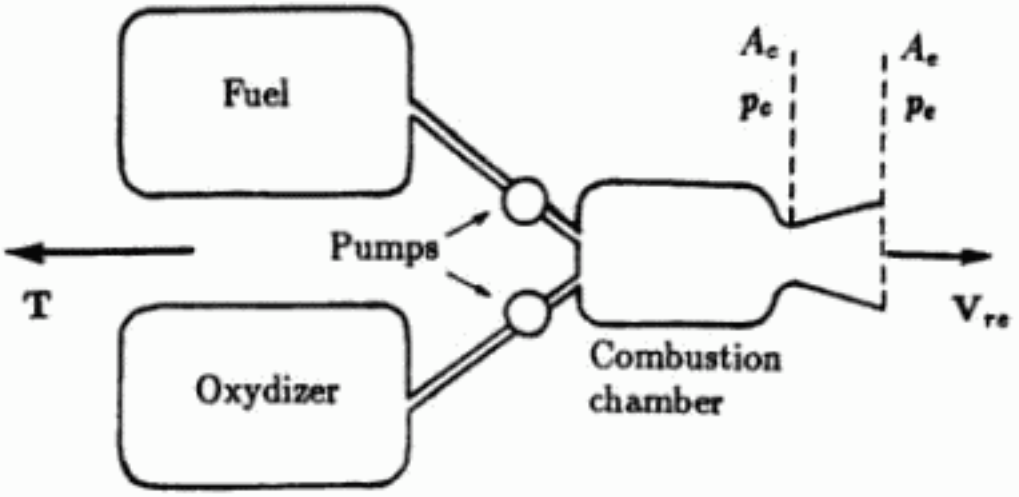

Figure 4.1: Diagram of rocket engine.

It is customary to use the parameter I_{sp} as the inverse of the thrust specific fuel consumption, and it is called the specific impulse. It has the dimension of time and is usually given in seconds in measuring the performance of rocket engines.

In Eq. (4.5), the mass flow rate β can be calculated from

$$\beta = C_\beta p_c A_c \tag{4.6}$$

where

C_β = mass flow coefficient, a propellant parameter.
p_c = average pressure in the combustion chamber. This pressure is also called the operating pressure.
A_c = area of the throat of the nozzle.

Hence

$$I_{sp} = \frac{V_{re}}{g} + \frac{p_e - p}{g C_\beta p_c} \frac{A_e}{A_c} \tag{4.7}$$

The ratio of the areas A_e/A_c can be expressed in terms of the expansion factor p_c/p_e as

$$\frac{A_c}{A_e} = \left(\frac{k+1}{2}\right)^{\frac{1}{k-1}} \left(\frac{p_e}{p_c}\right)^{\frac{1}{k}} \sqrt{\frac{k+1}{k-1}\left(1 - \frac{p_e}{p_c}\right)^{\frac{k-1}{k}}} \tag{4.8}$$

where k is the ratio of the specific heats, which is determined by the internal temperature and chemical composition of the exhaust and is normally less than the value of 1.4 for ordinary air.

From these relations, we see that the specific impulse is a function of the following four factors

1. The nature of the propellant (C_β, V_{re}, k).
2. The operating pressure p_c.
3. The expansion factor p_c/p_e.
4. The altitude of flight (g and p are functions of altitude).

For a given type of propellant, we can evaluate its specific impulse under some reference conditions. These conditions are:

For a solid propellant, $p_c = 70$ atm, $p_c/p_e = 70/1$ at sea level.

For a liquid propellant, $p_c = 25$ atm, $p_c/p_e = 25/1$ at sea level.

For liquid propellants, the highest specific impulse values are obtained by using hydrogen as a fuel and burning it either with oxygen or fluorine. Specific impulses ranging from 200 seconds to 300 seconds are obtained practically with a variety of combinations of propellants including solid propellants. In vacuum where $p = 0$ or at a specified operating altitude with constant value for p, the specific fuel consumption is constant. Since the mass flow rate as shown in Eq. (4.6) is constant, the thrust is independent of the forward speed of the vehicle. It is also practically independent of the altitude, at very high altitude where p is negligibly small.

Since the operation of a rocket engine does not depend on the surrounding atmosphere, it is the propulsion system for flight in a vacuum. But it has the disadvantage that all the mass creating the propulsive thrust must be carried on board. For aircraft operations, it is only used on some prototypes designed to have a high rate of climb. Also, it is used occasionally for a short time interval to add more thrust to the

main propulsion system such as in the case of a take-off from a short runway.

The propulsion systems we consider below are air-breathing.

4.3 Reciprocating engine and propeller system

In this classical propulsion system, an internal combustion reciprocating engine burns gasoline and air and produces a shaft power P. Hence, by analogy with Eq. (4.1), we can write the fuel mass flow rate as

$$\frac{dm}{dt} = -\frac{c_p}{g} P \tag{4.9}$$

where now c_p is termed the power specific fuel consumption.

4.3.1 Shaft power

For piston engines, the power is usually given in units of horsepower. If the thrust is expressed in lb and the speed in ft/s, by multiplying the horsepower (hp) by the conversion factor $k = 550$, we express the shaft power in ft-lb/s. In the SI system of units a conversion factor of $k = 7.457 \times 10^2$ transforms the horsepower into watts.

For a given throttle setting, a regular piston engine, which we refer to as an aspirated engine, produces a power which decreases as the altitude increases. As a first order approximation, we can consider it as proportional to a power of the density ratio. Hence, with respect to the reference value at sea level we have

$$\frac{P}{P_0} = \left(\frac{\rho}{\rho_0}\right)^x \tag{4.10}$$

In the troposphere, the exponent x has a value of the order of 0.7, while in the stratosphere $x = 1$, starting with the reference condition at the tropopause. To ease discussion, such as the one carried in Chapter 6, it is appropriate to use $x = 1$ uniformly.

The performance at altitude of a piston engine can be improved by supercharging. In this process, the air entering the intake manifold is compressed by means of a compressor which is driven by a gear train from the engine crankshaft. As the aircraft is gaining in altitude,

the throttle is opened progressively to keep constant manifold absolute pressure. Since at constant engine rotational speed, the power produced is purely a function of the manifold absolute pressure, the shaft power remains constant. Actually the power of a supercharged engine increases slightly with altitude. The supercharged engines of today use a turbine driven by the exhaust gases to increase the density of the air entering the cylinders to maintain constant output power. The advantage of the turbosupercharger compared with the gear-driven supercharger is clear in that the compressor does not extract power from the engine but uses the exhaust gases that would normally be wasted for its operation. Furthermore, the turbosupercharger is able to maintain sea level power to a much higher altitude. This altitude, called the critical altitude, has a maximum value of the order of 20,000 ft. Above the critical altitude, the power of a turbocharged piston engine decreases with altitude in the same manner as an aspirated piston engine. Hence, in performance analysis, with a supercharged engine, at constant throttle setting, the power is constant up to the critical altitude. Above the critical altitude, Eq. (4.10) is used with the reference condition at this altitude.

4.3.2 Propeller efficiency

The engine shaft power is used to drive a propeller for producing the thrust necessary to sustain flight. Within the specific objective of this text, namely the theory of flight mechanics, we shall first use the simple momentum theory to explain the process of thrust producing.

For a general propulsion system, the thrust T is produced according to Newton's second law

$$m\frac{dV}{dt} = T \tag{4.11}$$

where here, m is the mass involved in the process. For a rocket, m is essentially the mass of the fuel and oxidizer, and although it is relatively small, a high thrust is produced with a high acceleration dV/dt. For a jet engine, both m and dV/dt are moderate, and their product gives adequate values for the thrust. With a propeller, the increase in speed is small, but the mass involved is relatively large because it includes a large mass of the air that the propeller processes. This, in turn, will produce sufficient thrust. Hence, in matching the propulsion system to

the flying vehicle, the engines equipped with propellers are efficient at speeds lower than 500 mph, the jet engines function well at subsonic, transonic and supersonic speeds while for rocket engines their range of application is in the high supersonic and hypersonic domain.

For the operation of the propeller, in the simple theory, we assume that it is approximated by a thin actuator disk capable of producing a uniform change in the velocity of the air stream passing accross it. According to Fig. 4.2, let p be the free stream pressure and V the free stream speed. As the air stream approaches the front disk face, its speed increases to the value $V + v$ at the disk. Let p' be the pressure at the front disk face. By Bernoulli's equation for incompressible fluid

$$p + \frac{1}{2}\rho V^2 = p' + \frac{1}{2}\rho(V + v)^2 \tag{4.12}$$

Hence, the pressure has decreased from its free stream value to a lower value p' at the front disk face. Across the disk, the energy is added in the form of an increase in pressure Δp. Far behind the disk, the pressure drops to the free stream pressure and this is converted into an increase in speed to $V + v_1$. Then, we can again write the Bernoulli's equation as

$$p' + \Delta p + \frac{1}{2}\rho(V + v)^2 = p + \frac{1}{2}\rho(V + v_1)^2 \tag{4.13}$$

By adding the last two equations and simplifying we deduce the average pressure increase over the actuator disk

$$\Delta p = \rho v_1\left(V + \frac{1}{2}v_1\right) \tag{4.14}$$

Now, if A is the area of the actuator disk, the thrust produced by this disk is $T = A\Delta p$, and we have

$$T = \rho A v_1\left(V + \frac{1}{2}v_1\right) \tag{4.15}$$

This force can also be evaluated by Eq. (4.11). To this effect, the mass flow through the disk is $m = \rho A(V + v)dt$ while the total change in the speed is $dV = v_1$. Hence, from Eq. (4.11), we obtain

$$T = \rho A(V + v)v_1 \tag{4.16}$$

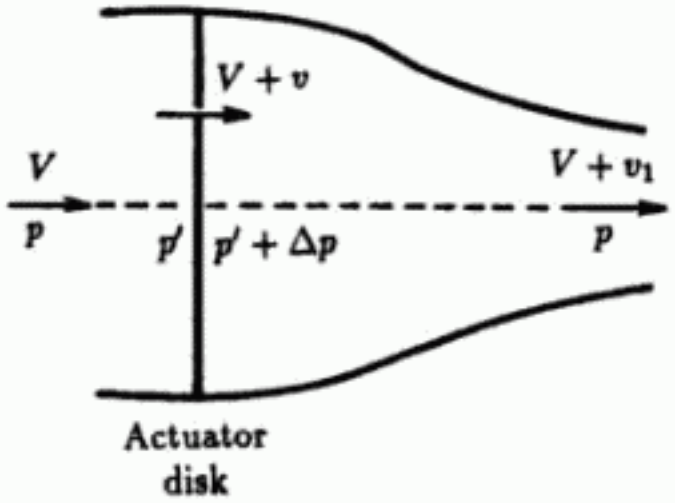

Figure 4.2: Stream tube across a propeller.

By equating the last two equations and solving for the total speed change, we obtain

$$v_1 = 2v \tag{4.17}$$

Therefore, according to this simple momentum theory, one half of the speed increase occurs in front of the disk and one half behind it. We define the propeller efficiency η_p as the ratio of the output power to the input power. The output power is the power available to propel the aircraft and it is the product of the thrust produced and the airspeed. Hence, we represent it by

$$P_a = TV \tag{4.18}$$

The input power is the engine shaft power, and it is used to produce the total pressure $A\Delta p = T$ on the disk with a speed equal to the speed accross the disk. Hence

$$P = T(V + v) \tag{4.19}$$

The propeller efficiency is then

$$\eta_p = \frac{P_a}{P} = \frac{V}{V + v} \tag{4.20}$$

While the definition of propeller efficiency as the ratio of the output power to the input power stands in general, the efficiency as given in

Eq. (4.20) is known as the ideal efficiency and it cannot be attained in practice since the momentum theory is too idealized. It does not account for the energy loss in slip-stream rotation, the propeller profile-drag losses, the decrease of pressure due to non-uniform thrust loading, the losses due to blade interference, and the drag rise in high-speed, compressible flow. The theory of propellers is available from many sources such as listed in the bibliography. For the present text, it suffices to use the definition (4.20) to write Eq. (4.9) for fuel consumption in the case of a propeller-driven aircraft as

$$\frac{dW}{dt} = -\frac{c_p}{\eta_p} P_a \tag{4.21}$$

where, by definition, P_a is the power available as given in Eq. (4.18).

The propeller efficiency, as evaluated from Eq. (4.20) represents the theoretical upper limit. In practice, it is a function of the forward airspeed, the angular rotational speed of the propeller and its design. The maximum efficiency is in range 0.80 to 0.85, and for a well designed blade it is reached with constant angular speed and variable pitch propellers.

4.3.3 Blade element theory

Although Eq. (4.21), with assigned values for the power specific fuel consumption c_p and the propeller efficiency η_p, is sufficient for evaluating aircraft performance such as the range attained and the endurance achieved for a given amount of fuel, a brief discussion of propeller blade element theory would help in the understanding of the way to achieve the optimum value for the propeller efficiency. In order to keep the familiar notation used in presenting blade element theory in classical texts, the various definitions we shall introduce are restricted to the present sub-section.

If we consider two cylinders with the same axis as the axis of rotation of the rotor and with radii r and $r + dr$, these surfaces cut a section of the propeller blade as shown in Fig. 4.3.

This section is viewed by an observer at the tip of the blade and aligning along the axis of rotation. Hence, if ω is the angular speed of the propeller, it is moving to the right with circumferential speed ωr and at the same time forward with airspeed V. By drawing the

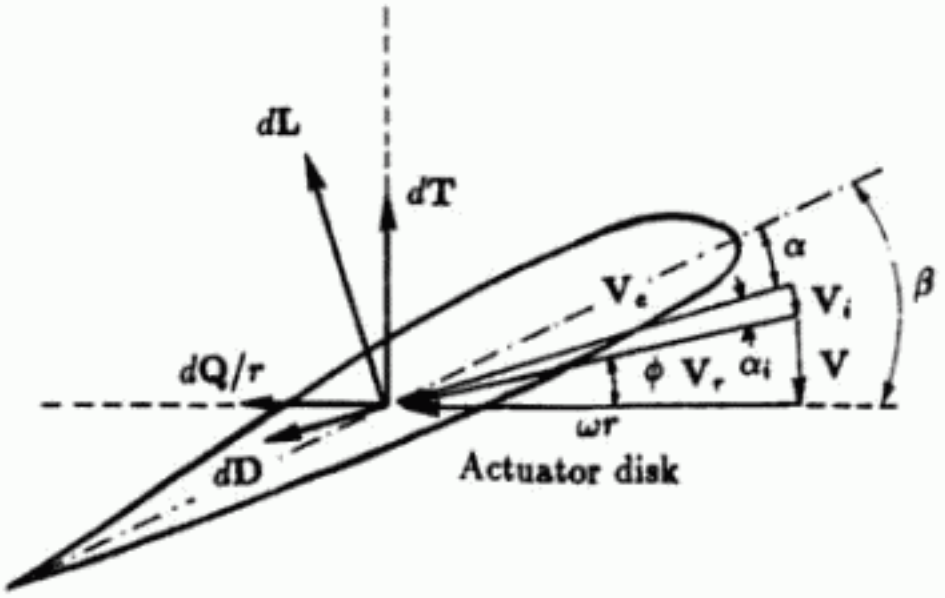

Figure 4.3: Velocities and forces acting on an element of a propeller blade.

velocity diagram, it appears that the relative velocity $\mathbf{V}_r$ is inclined at an angle ϕ such that

$$\tan \phi = \frac{V}{\omega r} \tag{4.22}$$

With respect to the idealized actuator disk, the zero-lift line of the airfoil section is inclined at an angle β, called the geometric pitch angle. Because of the induced velocity $\mathbf{V}_i$, the effective relative velocity is $\mathbf{V}_e$, and its direction is obtained by rotating the velocity $\mathbf{V}_r$ through a very small induced angle-of-attack α_i. From the velocity diagram shown in Fig. 4.3, the effective angle-of-attack is then

$$\alpha = \beta - \phi - \alpha_i \tag{4.23}$$

The distance r varies from a hub distance r_h, where the blade effectively begins, to the radius R of the propeller. Therefore, from Eq. (4.22), the angle ϕ starts with a large value near the hub and progressively decreases toward the tip of the blade. From Eq. (4.23), to obtain an efficient angle-of-attack at all distances, it is necessary to twist the

blade so that β is high at r_h and decreases to a smaller value at the tip. Although β varies along the blade, this is a feature of the aerodynamic design of the propeller. The term "variable pitch" which we shall discuss at the end of this section will have a different meaning, in the sense that for a given propeller system, we have a mechanism which allows the rotation in flight of the whole rigid blade about an axis along the blade (feathering axis).

Let dL and dD be the lift and the drag components of the element of aerodynamic force created by the motion of the blade element. Their projections in the direction normal to the actuator disk provide the thrust element while the force in the circumferential direction, if multiplied by the lever arm r will provide the torque element which must be overcome by the shaft power. Therefore, we have the elemental equations for each blade section

$$dT = dL\cos(\phi + \alpha_i) - dD\sin(\phi + \alpha_i) \tag{4.24}$$

and

$$dQ = r[dL\sin(\phi + \alpha_i) + dD\cos(\phi + \alpha_i)] \tag{4.25}$$

If C_l and C_d are the lift coefficient and the drag coefficient of the blade element, at the angle-of-attack as given in Eq. (4.23), and c is the chord of the airfoil section, a function of r, we can use $c\,dr$ to represent the reference area for the blade element and have

$$\begin{aligned} dL &= \frac{1}{2}\rho V_e^2 C_l c\,dr \\ dD &= \frac{1}{2}\rho V_e^2 C_d c\,dr \end{aligned} \tag{4.26}$$

We can use the simple momentum theory to evaluate the induced angle-of-attack at each distance r. First, since α_i is very small, in radians, we can take $V_e \approx V_r$, and $V_i \approx V_r\alpha_i$. Furthermore, we can assume that C_d/C_l is very small and hence, approximately, the thrust element for B blades is

$$dT = \frac{1}{2}Bc\rho V_r^2 C_l\cos\phi\,dr \tag{4.27}$$

Now, if we use momentum theory to evaluate dT through equation (4.16), we have the following:

1. The area of the annular stream tube is $dA = 2\pi r\,dr$.

2. The axial speed at the propeller disk is $V + V_i \cos(\phi + \alpha_i) \approx V + V_r \alpha_i \cos\phi$.

3. The total speed change through the propeller disk is $2V_i \cos(\phi + \alpha_i) \approx 2V_r \alpha_i \cos\phi$.

Therefore, we have, by applying Eq. (4.16)

$$dT = 4\pi\rho r(V + V_r\alpha_i \cos\phi)V_r\alpha_i \cos\phi \, dr \tag{4.28}$$

Since the reference line of the blade section is the zero-lift line, the lift coefficient of the section is evaluated from

$$C_l = C_{l_\alpha}\alpha = a(\beta - \phi - \alpha_i) \tag{4.29}$$

where $a = C_{l_\alpha}$ is the slope of the lift curve. On substituting in Eq. (4.27) and then equating with Eq. (4.28) we have a quadratic equation in α_i

$$\alpha_i^2 + \left(\tan\phi + \frac{\sigma a}{8x\cos\phi}\right)\alpha_i - \frac{\sigma a}{8x\cos\phi}(\beta - \phi) = 0 \tag{4.30}$$

where by definition

$$x = \frac{r}{R}, \qquad \sigma = \frac{Bc}{\pi R} \tag{4.31}$$

Thus, x is the dimensionless distance, defining the blade element station and it varies from $x_h = r_h/R$ to 1. The dimensionless parameter σ is called the solidity, and if the chord c is constant , that is for a rectangular blade, σ is the ratio of the total propeller area to the area of the propeller disk. In reality, c is a function of r, and hence σ varies with x. Likewise, the slope of the lift curve, a, is a function of the thickness ratio and it varies slightly along the blade. The geometric pitch angle of the blade, β, is a given function of the dimensionless distance x. As for the angle ϕ of the relative velocity, it is conveniently expressed in terms of x and the ratio

$$J = \frac{V}{2nR} \tag{4.32}$$

called the advance ratio. In this definition n is the number of revolutions per second and hence $\omega = 2\pi n$ rad/s. Then, by using this definition in Eq. (4.22), it is clear that

$$\tan\phi = \frac{J}{\pi x} \tag{4.33}$$

Finally, it is customary to evaluate the thrust and the power in dimensionless form. Hence, we define the thrust coefficient C_T and the power coefficient C_P as

$$C_T = \frac{T}{\rho n^2 (2R)^4} \tag{4.34}$$

and

$$C_P = \frac{P}{\rho n^3 (2R)^5} = \frac{2\pi n Q}{\rho n^3 (2R)^5} \tag{4.35}$$

In this way, it is seen that $2nR$ is the reference speed while $4R^2$ is the reference area in defining C_T and C_P.

With the definition of the dimensionless parameters and by noticing that in using Eqs. (4.26) in Eqs. (4.24) and (4.25) we can take $V_e \approx V_r = V/\sin\phi$, we have the thrust coefficient and the power coefficient, for B blades, in the form

$$C_T = \frac{\pi}{8} \int_{x_h}^{1} \sigma (J^2 + \pi^2 x^2)[C_l \cos(\phi + \alpha_i) - C_d \sin(\phi + \alpha_i)]\, dx \tag{4.36}$$

and

$$C_P = \frac{\pi}{8} \int_{x_h}^{1} \sigma x (J^2 + \pi^2 x^2)[C_l \sin(\phi + \alpha_i) + C_d \cos(\phi + \alpha_i)]\, dx \tag{4.37}$$

In summary, to perform the integration for C_T and C_P, one would be given $\beta(x)$ and $\sigma(x)$. Then, with the selected aerodynamic characteristics for the blades, the slope of the lift curve, a, is also known. For any advance ratio J, the angle ϕ can be calculated from Eq. (4.33) at each value of x. The induced angle-of-attack α_i is evaluated at the blade section from Eq. (4.30). The lift coefficient C_l is obtained from Eq. (4.29). The drag coefficient C_d is deduced from the drag polar for the airfoil. The two coefficients C_T and C_P are evaluated numerically. The propeller efficiency is evaluated from its definition

$$\eta_p = \frac{P_a}{P} = \frac{TV}{P} = \frac{C_T V}{C_P (2nR)}$$

Hence, finally

$$\eta_p = \frac{C_T}{C_P} J \tag{4.38}$$

By going over the evaluation of C_T and C_P, it has been recognized that, as seen from Eq. (4.29), the blade must be twisted to have the function

$\beta(x)$ decreasing with the function $\phi(x)$ along the blade, so that the angle-of-attack is optimum at each section. But the angle ϕ depends on the advance ratio J, and as such, when $\beta(x)$ is given, there exists a value of J for the maximum value of the propeller efficiency. But J varies with the forward speed V, and in this case it is optimum to have β varying proportionally. This can be done with a mechanism that allows the whole blade to rotate in flight along an axis along the blade. This propeller system is called a variable-pitch propeller. In practice, one may use constant-speed propellers. This system is equipped with governors to maintain constant angular speed as the engine throttle is varied. When the power increases, the angular speed tends to increase, the blade pitch angles are automatically increased to keep constant angular speed. Hence this is essentially an automatic variable-pitch propeller.

For performance evaluation we assume that at the desired forward speed, the value η_p used is its optimum value.

4.4 Gas turbine engine

A gas turbine engine is shown schematically in Fig. 4.4. Basically, this type of engine consists of a diffuser, a compressor, a combustion chamber and a turbine, but the flow of the air and of the burned gas varies with the specific type of engine designed for producing the thrust and the power.

As shown in the figure, the air enters the inlet, and is diffused and slightly compressed. It then passes through a compressor. After the compressed air leaves the compressor section, a part of it enters the combustion chamber. Atomized fuel is sprayed through fuel nozzles and the mixture of the air and the fuel is burned. Here, we take note that, on the average, the ratio of the mass of the air to the mass of the fuel is about 60. But only approximately 25% of the air is used for the combustion. The remainder of the air bypasses the fuel nozzles and is mixed downstream of the burner with the hot gases to obtain a cooler product for the operation of the turbine. This is because a temperature in excess of 3000°F can be reached in the combustion process and such a temperature would quickly destroy the turbine blades. A flow of cooler gas at a temperature of about 1600°F permits continuous operation of the turbine at maximum rating with present-day metallurgical blades.

The mixed air and burned gas expand through the turbine and the energy extracted from the moving gases furnishes the power required to drive the compressor. Nearly 75% of the combustion energy is used to drive the compressor. The remaining 25% represents the kinetic energy of the exhaust and is used to produce the thrust.

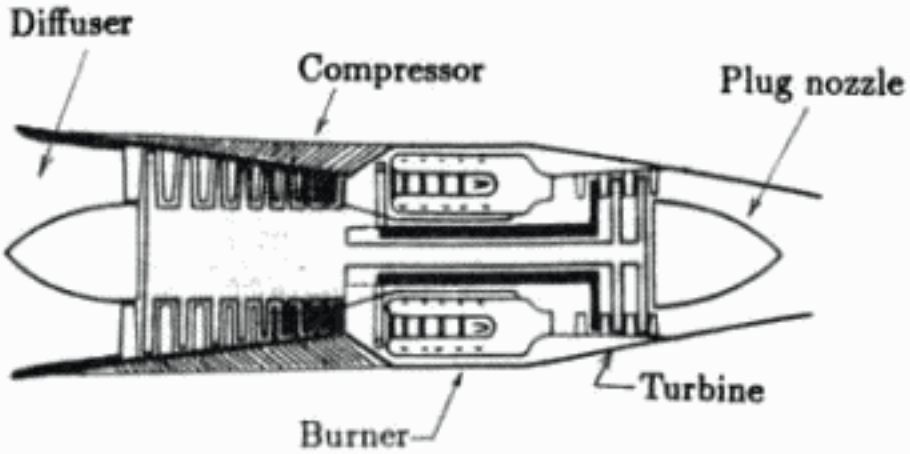

Figure 4.4: Schematic diagram of a gas turbine engine.

4.4.1 Turbojet

The turbojet engine produces the propulsive thrust T by expanding hot combustion gases through a nozzle. In its operation, a part of the hot combustion products is expanded in the turbine to develop power to drive the compressor and other aircraft accessories. The full expansion of combustion gases to atmospheric pressure in the jet nozzle serves to increase their speed to a value well above that of the forward airspeed of the aircraft. The process produces the propulsive force by reaction.

As before, we can write the one-dimensional equation for the thrust as

$$T = \beta_e V_{re} - \beta_a V + (p_e - p)A_e \tag{4.39}$$

where now β_e is the exit mass flow rate at relative speed V_{re} and β_a is the mass flow rate of the air entering with airspeed V. Again, as

in Section 4.2 for the analysis of a rocket engine, p is the free stream pressure while p_e is the average pressure at the exit of the nozzle with area A_e. Again, by denoting $\beta = -dm/dt$ to be the fuel mass flow rate, we have obviously

$$\beta = \beta_e - \beta_a \tag{4.40}$$

Then, the expression for the thrust is

$$T = \beta_a(V_{re} - V) + \beta V_{re} + (p_e - p)A_e \tag{4.41}$$

Just as for the operation of the rocket engine, the last term depends on the expansion nozzle and the operating pressure. If sonic conditions are not encountered at the nozzle exit such as in the case at low altitude where the ambient pressure p is sufficiently high to limit the nozzle pressure ratio to values less than those capable of creating sonic conditions, we may assume that the flow in the nozzle is fully expanded to free stream condition and neglect this term for an approximate evaluation of the thrust. By comparing Eqs. (4.1) and (4.41), we have the expression for the inverse of the thrust specific fuel consumption, using a standard constant value for the gravity acceleration

$$\frac{1}{c} = \frac{\beta_a}{\beta g}(V_{re} - V) + \frac{V_{re}}{g} + \frac{(p_e - p)A_e}{g\beta} \tag{4.42}$$

The thrust specific fuel consumption, or simply called the specific fuel consumption, is expressed in the English system as pounds of fuel per hour per pound of thrust. In the SI system, it is given as N/hr/N. Mathematically, it has the dimension of inverse of time. For an efficient turbojet engine, values of c as low as 0.75 pound of fuel per hour per pound of thrust are attainable. Realistically, many turbojet engines are operating in the neighborhood of $c = 1$/hr. Since the ratio of the mass flow rates β_a/β is high, and V_{re} is large, as compared to V, the first term in Eq. (4.42) accounts for most of the value of $1/c$. Similarly, to obtain an estimate of the value of the thrust, we can just consider the first term in Eq. (4.41). In inspecting this equation, it is clear that a high relative exhaust velocity produces a higher thrust. Since the thrust is approximately proportional to the mass flow rate of the air, β_a, it can be assumed that the thrust is proportional to a power of the density ratio, ρ/ρ_0. Hence it decreases as the altitude increases. As for the effect of the forward speed V, when the airspeed increases from

zero, the thrust starts with its static value and slightly decreases at first. Then, at higher speeds, with both an increase in V_{re} and a much higher increase in the air mass flow rate, β_a, the net thrust increases.

If we apply dimensional analysis to the operation of a turbojet engine, we find that the thrust and the thrust specific fuel consumption are functions of the flight Mach number, the Reynolds number, the ambient pressure ratio and a quantity called the referred rpm, $N/\sqrt{\theta}$, where θ is the ratio of the ambient temperature to the reference temperature and N is the rotational speed. Therefore, we have the dependence as shown in Eq. (4.2) since both the speed of sound and the temperature at the flight altitude are functions of the altitude. In flight mechanics, N is then the engine control parameter and for a gas turbine engine, we can conveniently express it as the percentage of the maximum rotational speed allowable. By Eq. (4.1), the fuel efficiency depends on the values of the thrust and the specific fuel consumption. It is assumed that data concerning the variations of these parameters, in terms of the airspeed V, the altitude z and the engine control, which we refer to as the throttle setting N, are available. Then, an approximate method is to assume a functional dependence of the form

$$\begin{aligned} T &= T_0(V,N)\left(\frac{\rho}{\rho_0}\right)^x \\ c &= c_0(V,N)\left(\frac{\rho}{\rho_0}\right)^y \end{aligned} \tag{4.43}$$

where subscript zero denotes the condition at sea level, and x and y are two exponents appropriately selected in accordance with engine performance data. In general N has some specified value in the range 0.8 to 1.0, and T_0 and c_0 can be adequately modeled as quadratic functions in the forward speed V. For a well designed turbojet engine properly matched to the aircraft in which it is installed, the function T_0 first decreases slightly with V and then increases slightly at higher subsonic speeds. Hence, in the subsonic regime, at any throttle setting, we can consider T_0 as practically independent of the airspeed. For high thrust engines operating at supersonic speeds thrust shows a marked increase with the Mach number if afterburning is used. This is because only about 25% of the air is used to support combustion in the combustion chamber. Therefore, there is sufficient oxygen in the turbine exhaust

for additional burning of fuel sprayed in a stovepipe attached to the rear of the engine. The additional heat further expands the exhaust gases, providing an increased exhaust velocity V_{ve} and hence an increased thrust. With afterburning, although the thrust is approximately doubled, the corresponding value of the thrust specific fuel consumption also increases to the range 2–4/hr and the increase in fuel consumption is considerable. As a consequence, engines with afterburners are installed on supersonic aircraft, and afterburning is used only when it is required.

If the flight is at constant altitude, or in the stratosphere where the speed of sound is constant, it is appropriate to model T_0 and c_0 as functions of the true airspeed as shown in Eq. (4.43). Since these quantities are actually functions of Mach number, at times it is more accurate to consider $T_0(M, N)$ and $c_0(M, N)$ instead, for performance evaluation. In Eq. (4.43) the exponent x is approximately 0.7 in the troposphere and we can set it as $x = 1$ in the stratosphere. As for the specific fuel consumption, within a certain speed range, we can assume that it is independent of the speed. It is a minimum for a value of N in the range of 0.8–0.95 of maximum rotational speed and in the tropopause. In the troposphere, the value for the exponent y is in the neighborhood of 0.1. It is practically zero in the stratosphere.

The Eqs. (4.43) can be used for modeling thrust and specific fuel consumption for flight operations such as the cruise or the climb in the troposphere. For flight at high altitude, it is more convenient to use the reference level at the tropopause and model the functions in the form

$$\begin{aligned} T &= T_*(M, N)\left(\frac{\rho}{\rho_*}\right)^x \\ c &= c_*(M, N)\left(\frac{\rho}{\rho_*}\right)^y \end{aligned} \tag{4.44}$$

with different values for x and y in the two layers of the atmosphere. For the discussion of aircraft performance in subsequent chapters, we shall use a constant average value for c with the knowledge that it is a minimum at the tropopause. As for the variation of thrust, we use a typical variation of T_0 with respect to airspeed, or to Mach number, as described above and the value $x = 1$ in Eq. (4.43), for both the troposphere and the stratosphere.

4.4.2 Ramjet

The near constant thrust produced by turbojet engines at subsonic speeds is an attractive feature of this type of engine since its power, $P = TV$, increases nearly linearly with the forward airspeed. With a properly designed entrance diffuser this characteristic is valid in the supersonic range. Since, as will be discussed in Chapter 6, at supersonic speeds, a slight increase in the thrust can produce a marked increase in the cruise Mach number, turbojet engines are the favorite propulsion system for aircraft operating in the range of speed from subsonic to supersonic speeds, up to about Mach 3.

The ramjet engine functions essentially on the same thermodynamic cycle as the turbojet. But as its name implies, all the compression portion of the cycle occurs at the inlet diffuser. In this entrance, the incoming airspeed decreases and produces a rise in the static pressure. At supersonic speeds, a compression shock is developed either in the diffuser or just ahead of the inlet of the ramjet. At Mach 2 or above, the shock compression of a ramjet is sufficient for fuel burning process and thus it is an acceptable substitute for mechanical compression. Therefore, the weight of the engine is greatly reduced. Furthermore, since there is no need for a turbine to drive the compressor, the temperature limit due to the heat resistance of the turbine blades is considerably higher than in the case of the turbojet engine. Continuing effort is being made to find a practical use for ramjet engines at high supersonic speeds.

4.4.3 Turboprop

A turbopropeller engine is a gas turbine engine in which the gases are nearly fully expanded in the turbine which, in turn, develops considerably more shaft power than is just required to drive the compressor and aircraft accessories. The excess power is used to drive a conventional propeller just as with the classical reciprocating engine. In this system, most of the thrust to sustain flight comes from the propeller, which is equipped with a speed-regulated pitch control, but present day turboprop engines are designed to operate with appreciable gas exit velocity to produce additional thrust in the same way as the turbojet engine. Hence, the evaluation of the engine performance

for a turboprop engine is in a mixed form, combining shaft power and thrust power.

Let T_j be the additional jet thrust which amounts to between 10 and 15 per cent of the total thrust. The shaft power is given in horsepower, as for a piston engine. After conversion, let P_s be its value expressed in ft-lb/s. If η_p is the propeller efficiency, the total power produced by the turboprop system and available to produce the thrust is

$$P_a = \eta_p P_s + T_j V \tag{4.45}$$

Since a turboprop engine is primarily a power generator, we can use the same Eq. (4.9), as in the case of a piston engine to evaluate fuel consumption. It is convenient to define the equivalent shaft power for a turboprop as

$$EP_s = P_s + \frac{T_j V}{\eta_p} = \frac{P_a}{\eta_p} \tag{4.46}$$

Then by analogy with Eq. (4.9), we have the equation for the fuel consumption

$$\frac{dW}{dt} = -c_p(EP_s) \tag{4.47}$$

where EP_s is expressed, say in ft-lb/s, and c_p is termed the equivalent power specific fuel consumption. The turboprop is used to extend the speed range of the piston-prop aircraft up to approximately $M = 0.70$.

In the analysis, at any given altitude, at a prescribed throttle setting with well regulated rpm, we can assume constant values for T_j, P_s and η_p in Eq. (4.45). Hence, when we evaluate the thrust produced, such as in the case of take-off performance analysis in Chapter 10, we obtain

$$T = \frac{\eta_p P_s}{V} + T_j \tag{4.48}$$

For a piston-prop, $T_j = 0$, and with constant propeller efficiency and constant shaft power, the thrust decreases as the speed increases during the take-off ground run. For a turboprop, with T_j at about 15% of the total thrust, the decrease in the thrust is less severe.

4.4.4 Turbofan

We have mentioned that the turboprop is used in the moderate speed range up to Mach number of about 0.70. This is because at

higher Mach number the tips of the propeller blades have near sonic relative speed and the propeller efficiency decreases sharply. In the Mach range between 0.70 and 0.85, turbofan engines are substituted for fuel economy. In a turbofan, a duct or shroud is placed around the jet engine and air is pumped through the annular passage to go through a fan. The primary hot airflow passes through the gas generator and the secondary cold airflow passes through the fan. The ratio of the secondary airflow to the primary airflow is called the bypass ratio and in present day engines, it attains a value of about 5. This multi-flow system produces thrust by acceleration of the airflow.

In evaluating the power of a turbofan, we can use the same Eq. (4.45) as for a turboprop, with the coefficient η_p denoting the efficiency of the fan. Although with very high bypass ratios the fan may produce more shaft power than the power due to the jet thrust, because of the fact that turbofans are operating in the speed range comparable to pure turbojet engines at high subsonic speeds, it is customary to treat the turbofan as a turbojet. Therefore, for turbofans we use the same Eq. (4.1) as for the turbojet to describe the fuel mass flow rate with the coefficient c called the equivalent thrust specific fuel consumption. In this equation the thrust is given by Eq. (4.48). If P_s is zero, we have the turbojet with T_j being the thrust which is nearly constant. For a turbofan, with significant shaft power, by considering P_s and η_p as nearly constant, the total thrust as shown in this equation decreases as the airspeed increases.

4.4.5 Comparative analysis

The four types of propulsion systems in current use are the pure turbojet, the piston-prop, the turboprop and the turbofan. As has been mentioned above, in evaluating the fuel consumption, we use the power equation for the piston-prop and the turboprop and the thrust equation for the turbojet and the turbofan. The selection of the type of engine to be used on any type of aircraft depends primarily on the cruising speed. As a rule, the piston-prop engines are used in low-speed aircraft while the turbojet engines and the turbofan engines with very low bypass ratios are used in high-speed aircraft. The turboprop engines and the turbofan engines with high bypass ratios are the favorite propulsion systems between these two extreme speed ranges.

In terms of the fuel consumption, the piston-prop engines are the most economical. The powers they produce are relatively small, from around 50 hp to around 600 hp because they are the heaviest of the four types of engines. Except for several types of fighter aircraft in World War II, in commercial aircraft these reciprocating engines are used with airspeeds up to around 300 mph.

Next in the speed range are the turboprop engines. They are also much lighter with the same horsepower. Hence for a given total weight, aircraft installed with a turboprop engine have a greater range with additional fuel. The turboprop has a low specific fuel consumption, slightly higher than that of the piston-prop.

A turbofan with a high bypass ratio is close to a turboprop while a turbofan with a low bypass ratio performs like a turbojet. In general, the turbofan combines the advantage of good propulsive efficiency of the turboprop and the high thrust production of the turbojet. As a consequence, the turbofan can be used on both civilian and military aircraft at airspeeds in high subsonic regime and up to and including low supersonic regime.

The exercises from 4-6 to 4-10 explain the calculation of the cruise airspeed for flight with these types of engines. To have an idea of the fuel economy, typical values of the equivalent thrust specific fuel consumption, all expressed in units of lb/hr/lb are shown in Table 4.1 for the four types of propulsion systems.

Table 4.1: Typical values of equivalent thrust specific fuel consumption.

Engines	c (lb/hr/lb)
Piston-prop	0.4–0.5
Turboprop	0.5–0.6
Turbofan (high bypass ratios)	0.6–0.7
Turbofan (low bypass ratios)	0.7–0.8
Turbojet	0.8–1.3
Turbojet (with afterburner)	1.9–2.4

4.5 Effect of altitude on engine performance

In analyzing aircraft performance, it is necessary to know the power produced and the thrust produced. In general, at any throttle setting, they vary with the airspeed and the altitude.

First, for a rocket, thrust is independent of airspeed and it is practically independent of altitude.

In this text, for uniformity, we shall call the thrust available, T_a, the total thrust produced by the propulsion system. Hence $T_a = T$. On the other hand, the term power available, P_a, is used to designate the product of thrust and airspeed, that is $P_a = TV$ as defined in Eq. (4.18). This relation is for the purpose of relating the output power P_a, the airspeed V and the corresponding thrust T. As for the value of P_a itself, for a piston-prop and a turboprop, it is calculated by Eq. (4.45). For a piston-prop, $T_j = 0$ and with constant optimum value for the propeller efficiency η_p, P_a varies with the shaft power. For a given throttle setting, with respect to altitude, its variation has been discussed in Sub-section 4.3.1.

For a turboprop, since the speed is in the subsonic range, for a prescribed throttle setting, P_a is a linear function of V. At constant V, the shaft power P_s and the jet thrust T_j both decrease as a power law in the density ratio and we can use Eq. (4.10) to describe the variation of P_a with respect to altitude. This is for the case of an aspirated engine. A turboprop can be made to keep its output power constant by derating the power. This is achieved by using a propeller such that it can not use all of the shaft power developed by the engine at low altitude. In this way, the output power, being derated at low altitude, is lower, but it can be kept constant by continuously increasing the shaft power to balance the loss in the jet power T_jV as the aircraft gains in altitude. Then the power of the turboprop has the same characteristics in altitude dependance as a turbocharged piston-prop with a critical altitude of the order of 20,000 ft. Above this altitude, the power decreases with density ratio.

For turbojet and turbofan engines, we consider the output thrust, or the thrust available, as given in Eq. (4.48). With constant P_s, η_p and nearly constant T_j, the thrust decreases as the speed increases as shown in the equation. At constant speed, for a given throttle setting, since both P_s and T_j vary as a power law in the density ratio, we can

use the law of variation, Eq. (4.43), for these propulsion systems.

Exercises

4-1. In the simple momentum theory, show that the speed increase at the actuator disk is

$$v = \frac{1}{2}\left(\sqrt{V^2 + \frac{2T}{\rho A}} - V\right)$$

Thus, show that according to this theory, the ideal propeller efficiency is

$$\eta_p = \frac{2}{1 + \sqrt{1 + \dfrac{2T}{\rho A V^2}}}$$

4-2. We can define the propeller disk thrust coefficient C_T by the equation

$$T = \frac{1}{2}\rho A V^2 C_T$$

Therefore, the ideal propeller efficiency is

$$\eta_p = \frac{2}{1 + \sqrt{1 + C_T}}$$

To have an idea of the value of C_T, consider the case of constant speed cruise at constant altitude where

$$T = D = \frac{1}{2}\rho S V^2 C_D,$$

where S is the reference area for the aircraft and C_D is the drag coefficient. Then deduce that

$$C_T = \frac{S}{A} C_D$$

Discuss the influence of the relative size of the propeller disk A/S and of the aircraft drag coefficient C_D on propeller efficiency.

4-3. Show that for very small induced angle-of-attack we have approximately

$$\alpha_i = \frac{\beta - \phi}{1 + \dfrac{8x}{a\sigma}\sin\phi}$$

By observing that $\alpha = \beta - \phi - \alpha_i$, show that an alternative form is

$$\alpha_i = \frac{\sigma C_l}{8x \sin\phi}$$

As a numerical application, consider an advance ratio of $J = 1.8$ and assume constant solidity $\sigma = 0.10$ and constant lift coefficient $C_l = 0.340$ throughout the blade. Evaluate the induced angles-of-attack at stations of $x = 0.2, 0.4, \cdots, 1.0$.

4-4. Each blade section at a distance r has a helicoidal motion and, without slipping, it would move forward in one revolution a distance d called the linear pitch, or simply the pitch.

a) Show that

$$d = 2\pi R x \tan\beta \tag{1}$$

b) If the induced angle α_i is neglected, show that the angle-of-attack is given by the equation

$$\tan\alpha = \frac{\dfrac{d}{2R} - J}{\pi x + \dfrac{dJ}{2R\pi x}} \tag{2}$$

c) In a preliminary design, we can twist the blade angle β by using Eq. (1) with a constant value for d. Such a propeller is called a constant linear pitch propeller. As a numerical verification, take $J = 1.8$. At the blade station $x = 0.4$, calculate the ratio $d/2R$ to obtain an angle of attack of $\alpha = 4°$. Then, with this value, use Eq. (2) to plot the variation of the angle-of-attack in the interval of x from 0.4 to 1.0. Observe that α is nearly constant, and has a maximum at a certain value of x. Calculate this maximum value.

4-5. For an analytical evaluation of the coefficients C_T and C_P as given in Eqs. (4.36) and (4.37), we take $\alpha_i = 0$, $x_h = 0$ and use average

constant values for the solidity σ and the lift and the drag coefficients C_l and C_d.

a) Show that we have the integrals

$$C_T = \frac{J^3\sigma}{8}\int_0^{\pi/J} y\sqrt{1+y^2}\left(C_l - \frac{C_d}{y}\right)dy$$

$$C_P = \frac{J^4\sigma}{8}\int_0^{\pi/J} y^2\sqrt{1+y^2}\left(\frac{C_l}{y} + C_d\right)dy$$

where y is a new variable of integration appropriately defined.

b) Perform the integration and show that

$$C_T = \frac{1}{8}\pi^3\sigma C_d\left[\frac{1}{3}\frac{C_l}{C_d}f(\epsilon) - g(\epsilon)\right]$$

and

$$C_P = JC_T + \frac{1}{32}\pi^4\sigma C_d[f(\epsilon) + \epsilon^3 + 3\epsilon g(\epsilon)]$$

where

$$\epsilon = \frac{J}{\pi}$$

is the rescaled advance ratio and f and g are two functions of ϵ, defined as

$$f(\epsilon) = (1+\epsilon^2)^{3/2} - \epsilon^3$$

$$g(\epsilon) = \frac{\epsilon}{2}\left[\sqrt{1+\epsilon^2} + \epsilon^2\,\mathrm{Log}\,\frac{1+\sqrt{1+\epsilon^2}}{\epsilon}\right]$$

c) By using Eq. (4.38) for the propeller efficiency show that

$$\eta_p = \frac{\epsilon}{\epsilon + F\left(\epsilon, \frac{C_l}{C_d}\right)}$$

where

$$F = \frac{f(\epsilon) + \epsilon^3 + 3\epsilon g(\epsilon)}{4\left[\frac{1}{3}\frac{C_l}{C_d}f(\epsilon) - g(\epsilon)\right]}$$

This expression for η_p is still too ideal, but it shows explicitly the effect of the aerodynamic characteristics of the propeller, in terms of the

average lift-to-drag ratio C_l/C_d, and especially of the advance ratio $J = \pi\epsilon$.

Write a numerical program to plot η_p versus ϵ in the range from 0 to 1, with several lift-to-drag ratios, $C_l/C_d = 18, 24, 30, 36$. Observe that, in each case, there exists a value of ϵ for maximum propeller efficiency.

4-6. For a steady cruise at constant altitude, we have equilibrium of the forces

$$T = \frac{1}{2}\rho S V^2 C_D$$
$$W = \frac{1}{2}\rho S V^2 C_L$$

Use a parabolic drag polar

$$C_D = C_{D_0} + K C_L^2$$

For a turbojet, at a prescribed throttle setting, by assuming that the thrust is independent of the speed, show that the cruising speed is obtained from the quadratic equation

$$S^2 C_{D_0} q^2 - STq + KW^2 = 0 \tag{1}$$

where $q = \rho V^2/2$ is the dynamic pressure.

Show that the solution exists if

$$T \geq \frac{W}{E_{max}} = T_{min} \tag{2}$$

This condition gives the lower limit of the thrust for steady cruise. When we use $T = T_{min}$, we have the maximum endurance. Show that the corresponding optimum speed is

$$V_1^* = \sqrt{\frac{2W}{\rho S C_L^*}} \tag{3}$$

where $C_L^* = \sqrt{C_{D_0}/K}$.

Notice that the condition for minimum thrust is the condition for the quadratic equation to have a double root.

4-7. Use the same conditions as in Exercise 4-6, but this time with a piston-prop providing a power available $\eta_p P_s = TV$ where P_s is the shaft power and η_p is the propeller efficiency. These are assumed constant for any prescribed throttle setting at the flight altitude.

Show that the cruising speed is obtained by solving the quartic equation

$$f(V) = \frac{1}{2}\rho S C_{D_0} V^4 - \eta_p P_s V + \frac{2KW^2}{\rho S} = 0 \tag{1}$$

To discuss the existence of the roots, first verify that at $V = 0$, $f > 0$ and $df/dV < 0$. Also, $df/dV = 0$ at only one positive value of V. Therefore, if we plot the function $f(V)$ versus V, it behaves like a parabola with an upward concavity and it may pass through zero twice, providing two positive roots for V if its minimum is less than zero.

Calculate the minimum of the function $f(V)$ and show that for the real roots to exist, we must have the condition

$$\eta_p P_s \geq \frac{2}{3^{3/4} E_{max}} \sqrt{\frac{2W^3}{\rho S C_L^*}} \tag{2}$$

This condition gives the lower limit for the power available for steady cruise. Show that when $\eta_p P_s$ is at its minimum value, and hence for maximum endurance, the corresponding optimum speed is

$$V_2^* = \sqrt{\frac{2W}{\rho S \sqrt{3} C_L^*}} \tag{3}$$

By comparing with the optimum speed in Exercise 4-6 for a turbojet, notice that $V_2^* < V_1^*$.

This problem will be discussed again in Chapters 6 and 7, but the present approach is geared toward solving the following two exercises. For this, notice that V_2^* is the double root of Eq. (1).

4-8. Again, we use the same conditions as in Exercise 4-6, but this time with a turbofan with the total thrust available as given in Eq. (4.48) as

$$T = \frac{\eta_p P_s}{V} + T_j$$

where η_p is now the fan efficiency, P_s the shaft power and T_j the jet thrust. We assume a constant η_p, and at the flight altitude P_s and T_j are functions of the engine control N.

a) Show that the cruising speed is obtained by solving the quartic equation

$$f(V) = \frac{1}{2}\rho S C_{D_0} V^4 - T_j V^2 - \eta_p P_s V + \frac{2KW^2}{\rho S} = 0 \qquad (1)$$

Notice that, when $P_s = 0$, we have Eq. (1) in Exercise 4-6 for a pure turbojet and when $T_j = 0$, we have Eq. (1) in Exercise 4-7 for a propeller driven aircraft.

b) In the case of a turboprop, the total power available is given by

$$P_a = \eta_p P_s + T_j V = TV$$

where now η_p is the propeller efficiency, assumed constant and the shaft power P_s and the jet thrust T_j are functions of the engine control N at the cruise altitude. Show that the cruising speed is given by the same equation (1).

c) As in the previous exercise, consider the derivative

$$\frac{df}{dV} = 2\rho S C_{D_0} V^3 - 2T_j V - \eta_p P_s \qquad (2)$$

Then, from Eqs. (1) and (2), verify that at $V = 0$, $f > 0$, and $df/dV < 0$. Furthermore, from Eq. (2), it can be assessed that this derivative vanishes for one and only one positive value of V. Therefore, in the positive V, the plot of $f(V)$ versus the speed V behaves like a parabola with an upward concavity, and it may pass through zero twice, providing two positive cruising speeds if its minimum is less than zero.

The condition for steady cruise with minimum thrust of a turbofan or minimum power of a turboprop is then obtained by solving Eq. (1) together with the equation

$$2\rho S C_{D_0} V^3 - 2T_j V - \eta_p P_s = 0 \qquad (3)$$

for the optimum speed V^* and the corresponding engine control N.

4-9. To summarize the results in Exercises 4-6, 4-7 and 4-8, it has been shown that the airspeed for steady cruise at constant altitude is obtained by solving the quartic equation

$$\frac{1}{2}\rho S C_{D_0} V^4 - T_j V^2 - \eta_p P_s V + \frac{2KW^2}{\rho S} = 0 \tag{1}$$

Also, it has been shown that if the thrust, or the power, or a combination of shaft power and jet thrust power, is sufficiently high, the equation provides two positive roots for the airspeed V.

For a pure turbojet, $P_s = 0$ and explicit solution is obtained. For a piston-prop, $T_j = 0$, or for a turbofan or a turboprop, with both P_s and T_j as functions of the engine control N non-vanishing, the quartic equation has to be solved numerically since the analytic solution requires some complicated transformation.

Furthermore, for minimum thrust or power, we have the condition

$$2\rho S C_{D_0} V^3 - 2T_j V - \eta_p P_s = 0 \tag{2}$$

which can be solved together with Eq. (1) for the optimum speed, and the minimum thrust or minimum power.

Explicit solutions are obtained for the turbojet and the piston-prop. The case of a turbofan and the case of a turboprop are more difficult to solve. We can proceed as follows.

a) By multiplying Eq. (2) by $V/4$ and substracting the result from Eq. (1), show that we have the equation

$$2T_j V^2 + 3\eta_p P_s V - \frac{8KW^2}{\rho S} = 0 \tag{3}$$

Hence, solving for V, we have

$$V = \frac{3}{4T_j}\left[\sqrt{\eta_p^2 P_s^2 + \frac{64KT_jW^2}{9\rho S}} - \eta_p P_s\right] \tag{4}$$

By using this solution in Eq. (2), show that

$$V^3 = \frac{1}{4\rho S C_{D_0}}\left[3\sqrt{\eta_p^2 P_s^2 + \frac{64KT_jW^2}{9\rho S}} - \eta_p P_s\right] \tag{5}$$

By raising Eq. (4) to the power 3 and equating the result with Eq. (5), we have a relation to be satisfied by the minimum thrust or power. The solution can only be obtained numerically if the dual variation T_j and P_s in terms of the throttle setting is available from engine data.

b) By taking hints from Exercise 4-6 for a pure jet aircraft and Exercise 4-7 for a pure prop aircraft, let

$$\begin{aligned} \tau &= \frac{E_{max} T_j}{W} \\ \pi &= \frac{3^{3/4} \eta_p P_s E_{max}}{2} \sqrt{\frac{\rho S C_L^*}{2W^3}} \end{aligned} \tag{6}$$

Then, for a given aircraft weight and aerodynamic characteristics C_{D_0} and K, and at the flight altitude, the engine data allow the evaluation of τ and π at any throttle setting. Show that the condition for minimum thrust or power is such that τ and π at the minimum throttle setting must satify the equation

$$\left(\sqrt{\pi^2 + \frac{4\sqrt{3}\tau}{3}} - \pi\right)^3 = \frac{4\sqrt{3}\tau^3}{9}\left(3\sqrt{\pi^2 + \frac{4\sqrt{3}\tau}{3}} - \pi\right) \tag{7}$$

For a pure jet aircraft, $\pi = 0$ and the solution is $\tau = 1$. For a pure prop aircraft, $\tau = 0$ and the solution is $\pi = 1$. To show this, expand the left-hand side of Eq. (7) in powers of τ and simplify the equation by the common factor τ^3 before using the limit $\tau \to 0$. The turbofan and the turboprop constitute the intermediate cases.

4-10. It is possible to assess qualitatively the optimum speed for minimum thrust of a turbofan and minimum power of a turboprop as follows.

Consider the equations for optimum condition

$$\frac{1}{2}\rho S C_{D_0} V^4 - T_j V^2 - \eta_p P_s V + \frac{2KW^2}{\rho S} = 0 \tag{1}$$

and

$$2\rho S C_{D_0} V^3 - 2T_j V - \eta_p P_s = 0 \tag{2}$$

a) For a turbofan, by eliminating T_j between the equations, show that the equation for the optimum speed is

$$f_1(V) = \frac{1}{2}\rho S C_{D_0} V^4 + \frac{1}{2}\eta_p P_s V - \frac{2KW^2}{\rho S} = 0 \tag{3}$$

Then, it is obvious that $f_1(0) < 0$ while if we use the speed V_1^* as obtained in Exercise 4-6 we have $f_1(V_1^*) > 0$. The optimum speed for a turbofan is less than the optimum speed for a turbojet.

b) For the case of a turboprop, by eliminating $\eta_p P_s$ between the equations, show that the equation for the optimum speed is

$$f_2(V) = \frac{3}{2}\rho S C_{D_0} V^4 - T_j V^2 - \frac{2KW^2}{\rho S} = 0 \tag{4}$$

Then, verify that if we use the speed V_2^* as obtained in Exercise 4-7, we have $f_2(V_2^*) < 0$, while it is obvious that $f_2 > 0$ for very large values of the airspeed V. Therefore the optimum speed for minimum power of a turboprop is greater than the optimum speed for a pure propeller aircraft.

c) Since for both the turbofan and the turboprop, we use the same system of equations (1) and (2) for evaluating their respective optimum speeds, there is no distinction between these speeds. Nevertheless by the analysis in part a) and part b) we can definitely conclude that their optimum speeds are always between V_2^* and V_1^*.

5

Descent and glide performance

5.1 Introduction

In the first four chapters we have developed the necessary mathematical tools for analyzing the performance of a vehicle in atmospheric flight. After the introductory chapter, the general equations of motion of the vehicle, considered as a point mass subject to gravitational, aerodynamic and propulsive forces, flying above a spherical, rotating earth, are first developed in Chapter 2. For relatively short range and/or low speed flight, the gravity acceleration vector is nearly constant. This leads to the notion of a flat earth and the resulting simplified equations of motion. Chapter 3 presents the analysis of the atmosphere and the aerodynamic forces resulting from the motion of the vehicle in this environment. To sustain flight, the vehicle is equipped with a propulsion system. The analysis of the different propulsion systems and their mathematical modeling is the subject of Chapter 4.

Starting with this chapter, we shall analyze the performance of a lifting vehicle equipped with a propulsion system. The speed range considered is such that it is much smaller than the orbital speed range. Hence, the equations used are those for flight over a flat earth presented in Chapter 2. In terms of Mach number, it ranges from low subsonic to moderate supersonic values. As discussed in Chapter 3, the main effect is that at a low subsonic speed, the drag polar remains practically unchanged while at a higher Mach number, generally for $M > 0.6$, the drag polar is a function of Mach number. The general plan adopted for each of the following chapters is that low speed flight is analyzed

first. Then, the same problem is investigated with the influence of Mach number.

From another point of view, flight can be treated as steady or non-steady. In steady flight, certain elements of the flight trajectory remain constant while in non-steady flight, nearly all of the flight elements are functions of time. Hence, in each chapter, we shall first study the case of steady flight. Whenever it is possible analytically, the more complicated case of non-steady flight will then be analyzed. Through Chapter 10, the vehicle will be referred to as the aircraft. The last chapter will be devoted to the analysis of a hypervelocity reentry vehicle.

In this chapter, we are concerned with several problems relative to descent and glide performance. The distinction between descent and glide is that the former condition may be powered, whereas the latter is performed without the engine operating. The flight is performed in a vertical plane. Hence, the equations of motion are the Eqs. (2.48) and (2.51) rewritten here for convenience. We have

$$\begin{aligned} \frac{dx}{dt} &= V\cos\gamma \\ \frac{dz}{dt} &= V\sin\gamma \\ \frac{dV}{dt} &= \frac{g}{W}(T\cos\varepsilon - D) - g\sin\gamma \\ V\frac{d\gamma}{dt} &= \frac{g}{W}(T\sin\varepsilon + L) - g\cos\gamma \end{aligned} \tag{5.1}$$

where x denotes the longitudinal distance, z the altitude, V the speed, γ the flight path angle, W the weight, D the drag, L the lift, T the thrust set at the angle ε with respect to the velocity vector and g the constant gravity acceleration. These equations can be derived directly by considering the force diagram in Fig. 5.1 (see Exercise 5-1). A glide corresponds to engine power-off, $T = 0$, while a descent generally requires only a small fraction of the maximum power to maintain a small rate of descent. In this case, the change in weight can be assumed to be negligible and it is adequate to assume a constant weight throughout this chapter. Hence, we shall take

$$W = \text{constant} \tag{5.2}$$

From now on, except when it is specified, the atmosphere is assumed to be at rest. Hence, we simply use speed instead of airspeed to denote the various airspeeds involved in the discussion.

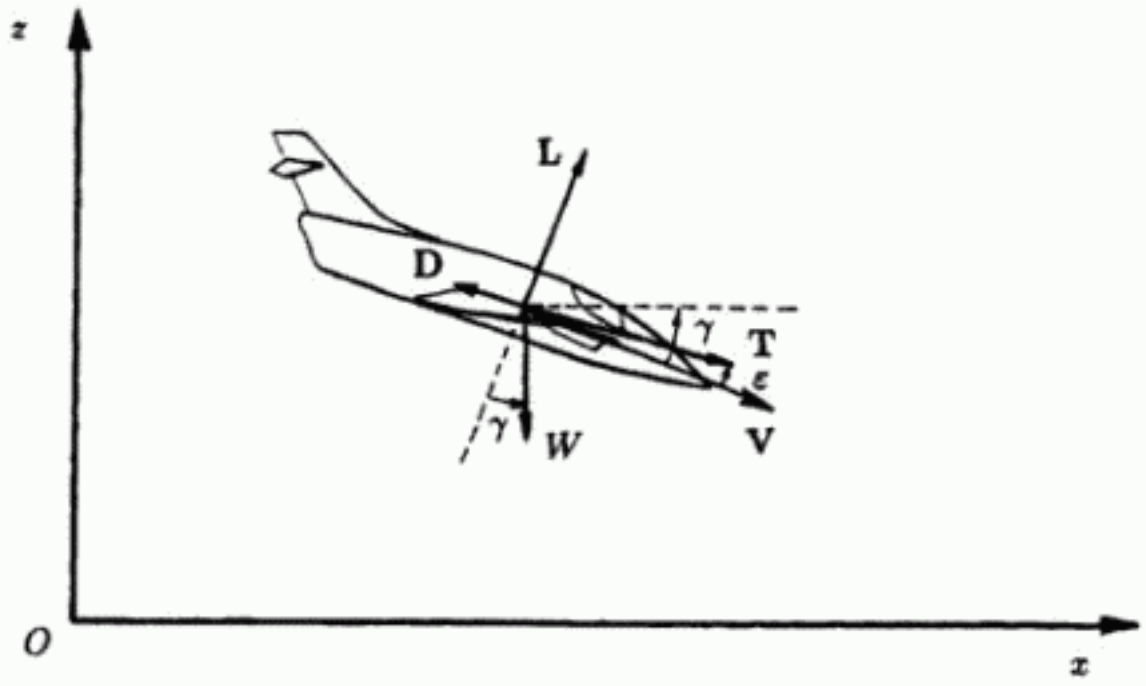

Figure 5.1: Descent in a vertical plane.

5.2 Steady glide at small flight path angle

The glide is performed with engine power-off. Hence, $T = 0$. It is assumed that the flight path angle is small so that

$$\begin{aligned} \sin\gamma &\approx \gamma \\ \cos\gamma &\approx 1 \end{aligned} \tag{5.3}$$

It is further assumed that the glide is steady, that is both the speed V and the flight path angle γ remain unchanged throughout the glide. This is purely an approximation since without the thrust, it is not possible to keep both the speed and the flight path angle constant. It is more appropriate to say that both the speed and the flight path angle

vary slowly so that the inertia terms dV/dt and $d\gamma/dt$ are negligible and can be neglected. The flight is termed quasi-steady glide.

Under these assumptions, the general equations (5.1) reduce to

$$\begin{aligned} \frac{dx}{dt} &= V \\ \frac{dz}{dt} &= V\gamma \\ -W\gamma &= D \\ W &= L \end{aligned} \tag{5.4}$$

We shall use a parabolic drag polar of the form

$$C_D = C_{D_0} + KC_L^2 \tag{5.5}$$

where at low Mach number, the zero-lift drag coefficient C_{D_0} and the induced drag factor K are constant.

5.2.1 Glide at minimum glide angle

By sign convention, the flight path angle γ is negative when the velocity is directed below the horizontal plane. By the third of the Eqs. (5.4), the glide angle, defined as the negative of the flight path angle, is given by

$$-\gamma = \frac{D}{W} \tag{5.6}$$

Hence, $\gamma < 0$, and the glide is descending. Among the possible glide conditions, glide with the smallest absolute value of γ is of obvious interest. We shall refer to this glide as glide at minimum glide angle. The glide is also called the flattest glide.

Since W is constant, by Eq. (5.6), the flattest glide corresponds to using the minimum drag. Defining the dynamic pressure

$$q = \frac{1}{2}\rho V^2 \tag{5.7}$$

and writing the last of the Eqs. (5.4)

$$W = qSC_L \tag{5.8}$$

On the other hand, using a parabolic drag polar we have for the drag

$$D = qS(C_{D_0} + KC_L^2) \tag{5.9}$$

Solving for C_L in Eq. (5.8) and substituting into Eq. (5.9), we obtain

$$D = qSC_{D_0} + \frac{KW^2}{qS} \tag{5.10}$$

Hence, the drag D is a function of the dynamic pressure q and the condition of minimum drag is

$$\frac{dD}{dq} = 0$$

Explicitly, we have

$$q = \frac{W}{S}\sqrt{\frac{K}{C_{D_0}}} \tag{5.11}$$

Flattest glide is conducted at constant dynamic pressure. By comparing Eqs. (5.8) and (5.11), we see that the lift coefficient for the smallest glide angle is

$$C_L = \sqrt{\frac{C_{D_0}}{K}} = C_L^* \tag{5.12}$$

The glide is performed using the maximum lift-to-drag ratio. By combining Eqs. (5.10) and (5.11), we have the corresponding minimum drag

$$D = 2W\sqrt{KC_{D_0}} \tag{5.13}$$

This minimum drag is also constant. We recall from Chapter 3 that, for parabolic drag polar, the maximum lift-to-drag ratio is $E_{max} = (4KC_{D_0})^{-1/2}$. Hence, from Eqs. (5.6) and (5.13), we have the minimum glide angle

$$(-\gamma)_{min} = \frac{1}{E_{max}} \tag{5.14}$$

The flattest glide is designed to achieve longer range. This is seen by eliminating the time between the first two equations of system (5.4). We have

$$\frac{dx}{dz} = \frac{1}{\gamma} \tag{5.15}$$

For any given altitude drop, we maximize the distance travelled by minimizing the glide angle. Using the solution, Eq. (5.14), and integrating from the initial altitude z_i to the final altitude z_f, we obtain the maximum range

$$x = E_{max}(z_i - z_f) \tag{5.16}$$

According to this formula, the maximum glide distance is independent of the wing loading W/S. It is proportional to the value E_{max}, which is an aerodynamic characteristic of the glider, and to the altitude difference $\Delta z = z_i - z_f$.

At this point, the following pertinent remarks are in order.

Without using the small angle approximation, we consider the drag and the lift equations

$$\begin{aligned} -W\sin\gamma &= D \\ W\cos\gamma &= L \end{aligned} \tag{5.17}$$

Hence the glide angle is given by

$$-\tan\gamma = \frac{D}{L} = \frac{1}{E} \tag{5.18}$$

In this form, it is seen that for the smallest glide angle , we still use $E = E_{max}$. We refer to Exercise 5-2 for the calculation of the corresponding minimum drag.

Next, from the solution (5.11) for minimum glide angle, the dynamic pressure $q = \rho V^2/2$ is constant. Hence this optimum glide is performed with constant equivalent speed V_e which, at low speed, is the same as the calibrated speed V_c. But, during the glide, as the atmospheric density ρ increases, the true speed V decreases. This apparently is in violation of the assumption of steady glide, $dV/dt = 0$. In fact, in the analysis, to a first order approximation, we have neglected the inertia term. To include this non-steady effect, we return to the system (5.1) and consider

$$m\frac{dV}{dt} + mg\sin\gamma = -D$$

But

$$\frac{dV}{dt} = \frac{dV}{dz}\frac{dz}{dt} = V\sin\gamma\frac{dV}{dz}$$

Hence

$$W\sin\gamma\left(1 + \frac{V}{g}\frac{dV}{dz}\right) = -D \tag{5.19}$$

This equation replaces the first equation in system (5.17) while the second equation remains the same. Then the glide angle, with the effect of the variation of speed included, is now

$$-\tan\gamma = \left[E\left(1+\frac{V}{g}\frac{dV}{dz}\right)\right]^{-1} \tag{5.20}$$

Concerning the control of the flight, to minimize the glide angle, we still use $E = E_{max}$. As for the non-steady effect, we use an exponential atmosphere and consider

$$q = \frac{1}{2}\rho_0 e^{-\beta z} V^2$$

For constant q, we have the relation for the variations

$$V\frac{dV}{dz} = \frac{1}{2}\beta V^2 = \beta\frac{q}{\rho} \tag{5.21}$$

Therefore, from Eq. (5.20), we have for the glide angle, with constant dynamic pressure

$$-\tan\gamma = \left[E\left(1+\frac{\beta q}{g\rho}\right)\right]^{-1} \tag{5.22}$$

The non-steady effect should be included at high altitude where ρ is small.

5.2.2 Glide at minimum rate of descent

The negative of the vertical component of the velocity is called the rate of descent or sinking speed

$$V_z = -V\sin\gamma = \frac{VD}{W} \tag{5.23}$$

Another glide program of particular interest is the glide at minimum rate of descent. Obviously, this glide corresponds to the minimum value of the product VD, that is, of the power developed by the drag. Using Eqs. (5.7) and (5.10) we have

$$V_z = \left(\frac{2q}{\rho}\right)^{1/2}\left[\frac{qSC_{D_0}}{W} + \frac{KW}{qS}\right] \tag{5.24}$$

The expression for V_z is a function of both ρ and q, or what is the same, of both ρ and V. At each altitude, we search for its minimum by evaluating the optimum speed, or correspondingly the optimum dynamic pressure. This leads to the condition $\partial V_z/\partial q = 0$ which is expressed as

$$q = \frac{W}{S}\sqrt{\frac{K}{3C_{D_0}}} \tag{5.25}$$

Again, glide at minimum rate of descent is conducted at constant dynamic pressure and the above remarks regarding the decrease in the true speed and the constancy of the equivalent speed apply. Comparing the two optimal laws (5.11) and (5.25) we obtain

$$\frac{V_{\text{min rate}}}{V_{\text{min glide angle}}} = \frac{1}{3^{1/4}} = 0.7598 \tag{5.26}$$

Relative to the speed for minimum glide angle, the true speed for minimum rate of descent, and proportionally the equivalent speed, is slower by 24%. If this speed is lower than the stalling speed, then minimum rate of descent is conducted at near stall. By comparing Eq. (5.25) with Eq. (5.8) we deduce the optimum law for the lift coefficient

$$C_L = \sqrt{\frac{3C_{D_0}}{K}} = \sqrt{3}C_L^* \tag{5.27}$$

Glide at minimum rate of descent is at a higher angle-of-attack than glide at minimum glide angle. In terms of the lift-to-drag ratio, we have

$$E = \frac{C_L}{C_D} = \frac{\sqrt{3}C_L^*}{C_{D_0} + KC_L^2} = \frac{\sqrt{3}C_L^*}{2C_D^*} = 0.866E_{max} \tag{5.28}$$

The drag is obtained by using the optimum condition (5.25) in Eq. (5.10)

$$D = \frac{2}{\sqrt{3}}\frac{W}{E_{max}} \tag{5.29}$$

Hence, the glide angle is

$$-\gamma = \frac{2}{\sqrt{3}}\frac{1}{E_{max}} \tag{5.30}$$

and, compared with the minimum glide angle, it is steeper by 15%.

Since the glide angle is constant, the trajectory is a straight line. Integrating Eq. (5.15) with the solution (5.30), we have the range as a function of the altitude

$$x = \frac{\sqrt{3}}{2} E_{max}(z_i - z) \tag{5.31}$$

From the second of the Eqs. (5.4)

$$\frac{dt}{dz} = \frac{1}{V\gamma} = -\frac{1}{V_z} \tag{5.32}$$

The integration of this equation provides the time of flight, also called the endurance. It is clear that the maximum endurance is obtained by using the minimum rate of descent. The speed being obtained from Eq. (5.25) we have, on using Eq. (5.30) for γ, the minimum rate of descent

$$\min V_z = \frac{2}{E_{max}} \sqrt{\frac{2W}{\rho S}} \left(\frac{K}{27 C_{D_0}} \right)^{1/4} \tag{5.33}$$

With this smallest rate of descent, we rewrite Eq. (5.32)

$$\frac{dt}{dz} = -\frac{E_{max}}{2} \left(\frac{27 C_{D_0}}{K} \right)^{1/4} \sqrt{\frac{\rho S}{2W}} \tag{5.34}$$

If an exponential atmosphere of the form

$$\rho = \rho_0 e^{-\beta z} \tag{5.35}$$

is used, we can change the independent variable from z to ρ to have

$$\frac{dt}{d\rho} = \frac{E_{max}}{2\beta} \left(\frac{27 C_{D_0}}{K} \right)^{1/4} \sqrt{\frac{S}{2W}} \frac{1}{\rho^{1/2}} \tag{5.36}$$

Integrating from the initial altitude, depicted by ρ_i, we have the maximum endurance as a function of the instantaneous atmospheric density

$$t = \frac{E_{max}}{\beta} \left(\frac{27 C_{D_0}}{K} \right)^{1/4} \sqrt{\frac{S}{2W}} (\rho^{1/2} - \rho_i^{1/2}) \tag{5.37}$$

The total maximized time of flight is obtained by using the final atmospheric density $\rho = \rho_f$ in this equation. From this equation, it

is seen that the maximum endurance depends on the maximum lift-to-drag ratio, E_{max}, the lift coefficient for maximum lift-to-drag ratio, $\sqrt{C_{D_0}/K}$, and the wing loading, W/S. High maximum lift-to-drag ratio and low wing loading favor maximum endurance. Also, the time of flight is not proportional to the altitude difference Δz, but rather to $(\sqrt{\rho_f} - \sqrt{\rho_i})$ (see Exercise 5-4).

5.3 Descent at small flight path angle

Both the glide angle and the minimum rate of descent can be reduced with the assistance of a small thrust level produced by the engine. It is again appropriate to use the small angle approximation and furthermore to assume that the flight path angle remains nearly constant, that is $d\gamma/dt = 0$. Descent with engine power-on is generally used to control the speed and the altitude, as in the case of descent to make an approach before landing in an airport. Hence, in this analysis, when it is deemed necessary, we shall retain the inertia term dV/dt. On the other hand, the thrust angle ϵ is generally small and we can use the approximation

$$T \sin \epsilon \approx 0 \qquad T \cos \epsilon \approx T \tag{5.38}$$

With these assumptions, the general equations (5.1) are reduced to

$$\begin{aligned} \frac{dx}{dt} &= V \\ \frac{dz}{dt} &= V\gamma \\ \frac{dV}{dt} &= \frac{g}{W}(T - D) - g\gamma \\ L &= W \end{aligned} \tag{5.39}$$

We shall assume throughout this section that the thrust is held constant. Several problems associated with descent with engine power-on will be examined.

5.3.1 Maximum range for a specified altitude drop

This is the problem of descending from an initial altitude to a prescribed final altitude with a certain thrust setting while the range is maximized. If the change in speed is negligible, the third of the Eqs. (5.39) becomes

$$-\gamma = \frac{D-T}{W} \tag{5.40}$$

In level flight, $\gamma = 0$, and the thrust equals the drag. During descent we have $T < D$. The glide angle is controlled by the thrust and the drag. If the thrust is held constant, the glide angle is controlled by the drag, and the minimum value of $-\gamma$ is obtained by minimizing the drag. Since the equation for lift is the same as in the case for a glide with engine power-off, the dynamic pressure for minimizing the drag is the same as in the case of a glide. It is given by the same Eq. (5.11). For flattest descent we shall use maximum lift-to-drag ratio and the corresponding descent angle is

$$(-\gamma)_{min} = \frac{1}{E_{max}} - \frac{T}{W} \tag{5.41}$$

The equation for range is still Eq. (5.15), and flattest descent provides the maximum range. Using the relation (5.41) in Eq. (5.15) and integrating from the initial altitude z_i, we have the maximum range as a function of altitude

$$x = \frac{E_{max}(z_i - z)}{1 - (T/W)E_{max}} \tag{5.42}$$

It is seen that high maximum lift-to-drag ratio and high thrust-to-weight ratio favor maximum range. The maximum range for a specified altitude drop is obtained by using the prescribed final altitude $z = z_f$ in this equation.

5.3.2 Maximum endurance for a specified altitude drop

Again, in this problem, if the assumption of nearly constant speed for the descent is used, we have the same Eq. (5.40) for the flight path angle γ and the rate of descent is

$$V_z = \frac{V(D-T)}{W} \tag{5.43}$$

The solution for minimum rate of descent is slightly different compared with the case of a glide, $T = 0$, since here to minimize V_z, we minimize $V(D - T)$ and not simply the product VD. As before, we write the expression in terms of the dynamic pressure q,

$$V_z = \left(\frac{2q}{\rho}\right)^{1/2}\left[\frac{qSC_{D_0}}{W} + \frac{KW}{qS} - \frac{T}{W}\right] \tag{5.44}$$

The condition for minimum rate of descent, $\partial V_z/\partial q = 0$, is expressed as

$$3S^2C_{D_0}q^2 - TSq - KW^2 = 0 \tag{5.45}$$

If $T = 0$, we have the solution (5.25). When $T \neq 0$, we have a quadratic equation in q which on solving yields the positive root

$$q = \frac{W}{3S}\sqrt{\frac{K}{C_{D_0}}}\left[\sqrt{3 + E_{max}^2\tau^2} + E_{max}\tau\right] \tag{5.46}$$

where

$$\tau = \frac{T}{W} \tag{5.47}$$

is the thrust-to-weight ratio.

Equation (5.46) shows that minimum rate of descent is conducted at constant dynamic pressure, that is at constant equivalent speed. This value is slightly higher than the corresponding value for a glide due to the effect of the thrust. Although the speed is higher than in the case of the glide with power-off, the actual rate of descent is smaller due to the fact that the flight path angle is smaller. To show this, we combine Eqs. (5.44) and (5.45) to eliminate T and obtain

$$V_z = \frac{2W}{S}\left(\frac{2}{q\rho}\right)^{1/2}\left(K - \frac{S^2C_{D_0}q^2}{W^2}\right) \tag{5.48}$$

In this form, it is seen that a higher value of the dynamic pressure decreases the minimum rate of descent (Also see Exercise 5-5). This minimum rate of descent is zero when

$$W = \frac{1}{2}\rho SV^2C_L^* \tag{5.49}$$

It corresponds to a thrust

$$T = \frac{W}{E_{max}} \tag{5.50}$$

just sufficient to maintain level flight at maximum lift-to-drag ratio. On the other hand, the minimum rate of descent reaches a maximum value for $\tau = 0$. For the value of the thrust-to-weight ratio such that

$$0 \leq \tau < \frac{1}{E_{max}} \tag{5.51}$$

we write Eq. (5.32) for the endurance, using the solution (5.48) for V_r

$$\frac{dt}{dz} = -\left(\frac{S}{2W}\right)\left(\frac{q\rho}{2}\right)^{1/2}\left(K - \frac{S^2 C_{D_0} q^2}{W^2}\right)^{-1} \tag{5.52}$$

where the constant value of q is given by the general expression (5.46). Again using an exponential atmosphere as given by Eq. (5.35), changing the independent variable from z to ρ and integrating from the initial value ρ_i, we have for the endurance

$$t = \frac{1}{\beta}\left(\frac{S}{W}\right)\left(\frac{q}{2}\right)^{1/2}\left(K - \frac{S^2 C_{D_0} q^2}{W^2}\right)^{-1}(\rho^{1/2} - \rho_i^{1/2}) \tag{5.53}$$

This solution uses the minimum rate of descent and hence yields the maximum endurance.

To display the effect of different flight parameters, we use the solution (5.46) for q to rewrite this expression in the form

$$t = \frac{E_{max}}{\beta}\left(\frac{C_{D_0}}{K}\right)^{1/4}\sqrt{\frac{3S}{2W}}\,\frac{3[\sqrt{3 + E_{max}^2\tau^2} + E_{max}\tau]^{1/2}(\rho^{1/2} - \rho_i^{1/2})}{3 - E_{max}^2\tau^2 - E_{max}\tau\sqrt{3 + E_{max}^2\tau^2}} \tag{5.54}$$

Then, it is seen that low wing loading W/S and high maximum lift-to-drag ratio, E_{max}, favor maximum endurance. Also, the endurance increases with τ. When $\tau = 0$, the endurance reduces to its smallest value as given by Eq. (5.37).

For descent with engine power-on, from Eqs. (5.37) and (5.54), we deduce that endurance is increased by the factor

$$\frac{t_{descent}}{t_{glide}} = F = \frac{3[\sqrt{3 + E_{max}^2\tau^2} + E_{max}\tau]^{1/2}}{3^{1/4}[3 - E_{max}^2\tau^2 - E_{max}\tau\sqrt{3 + E_{max}^2\tau^2}]} \tag{5.55}$$

For any two prescribed terminal altitudes, and assigned time of descent, this equation can be solved for the required thrust-to-weight ratio (see Exercise 5-6).

5.3.3 *Maximum range for a specified speed change*

During an approach at small flight path angle with a reduced thrust setting, the aircraft may be required to reduce its speed to a desired final value. If we neglect the small component of gravity $g\gamma$ along the tangent to the flight path, we can combine the expressions for x and V in system (5.39) to have

$$\frac{dx}{dV} = \frac{V}{(T-D)g/W} \tag{5.56}$$

Since $W = L$, we can write this equation as

$$\frac{dx}{dV^2} = \left[2g\left(\frac{T}{W} - \frac{C_D}{C_L}\right)\right]^{-1} \tag{5.57}$$

In this form, it is seen that if the thrust is maintained constant, the range is maximized by using the maximum lift-to-drag ratio. Using this optimum law, we have on integrating from the initial speed V_i

$$x = \frac{E_{max}(V_i^2 - V^2)}{2g(1 - E_{max}\tau)} \tag{5.58}$$

Thus, high maximum lift-to-drag ratio favors maximum range in the problem of deceleration.

5.4 Deceleration in level flight

Within the assumption of a parabolic drag polar independent of the Mach number, the last problem investigated is an example of non-steady flight. The equations are now integrated rigorously under the assumption of coasting flight, $T = 0$, at constant altitude, $\gamma = 0$.

With $T = 0$, we write Eq. (5.56)

$$\frac{dV^2}{dx} = -\frac{\rho S V^2}{m}(C_{D_0} + KC_L^2) \tag{5.59}$$

The difference here is that, with engine power-off, we cannot use maximum lift-to-drag ratio to maintain constant altitude. As the speed decreases, the lift coefficient increases such that the equation for the lift

$$W = \frac{1}{2}\rho S V^2 C_L \tag{5.60}$$

is constantly satisfied. Using this equation in Eq. (5.59), we obtain

$$\frac{dV^2}{dx} = -\frac{\rho S V^2}{m}\left(C_{D_0} + \frac{4KW^2}{\rho^2 S^2 V^4}\right) \tag{5.61}$$

The final value of the speed is the stall speed, that is the speed corresponding to the maximum value of C_L. Hence, from Eq. (5.60),

$$V_f^2 = \frac{2W}{\rho S C_{L_{max}}} \tag{5.62}$$

The range attained in this deceleration coasting flight is obtained by integrating Eq. (5.61) from the initial speed V_i to this final speed V_f. We have

$$x_f = \left(\frac{E_{max} V_i^2}{2g}\right) \Omega \, \mathrm{Log}\left[\frac{\lambda_{max}^2}{1+\lambda_{max}^2}\left(1+\frac{1}{\Omega^2}\right)\right] \tag{5.63}$$

where we have defined the dimensionless wing loading

$$\Omega = \frac{2W}{\rho S C_L^* V_i^2} \tag{5.64}$$

and the rescaled maximum lift coefficient

$$\lambda_{max} = \frac{C_{L_{max}}}{C_L^*} \tag{5.65}$$

with C_L^* being the lift coefficient corresponding to maximum lift-to-drag ratio. It is obvious from the solution (5.63) that high initial speed V_i , high maximum lift-to-drag ratio E_{max} and high maximum lift coefficient λ_{max} improve the range. What is less apparent is the way that the coasting flight altitude influences the range. The altitude, or what is the same, the atmospheric density, enters the equation through the wing loading Ω considered as a parameter. It can be shown rigorously that there exists a value of Ω, and only one, such that x_f is maximized. This value is obtained by writing the equation $dx_f/d\Omega = 0$. We have a transcendental equation for evaluating Ω^2,

$$\frac{2}{1+\Omega^2} = \mathrm{Log}\left[\frac{\lambda_{max}^2}{1+\lambda_{max}^2}\left(1+\frac{1}{\Omega^2}\right)\right] \tag{5.66}$$

The optimum value of Ω is plotted as function of λ_{max} in Fig. 5.2. For each value of λ_{max}, we can deduce the optimal value Ω^* of Ω and

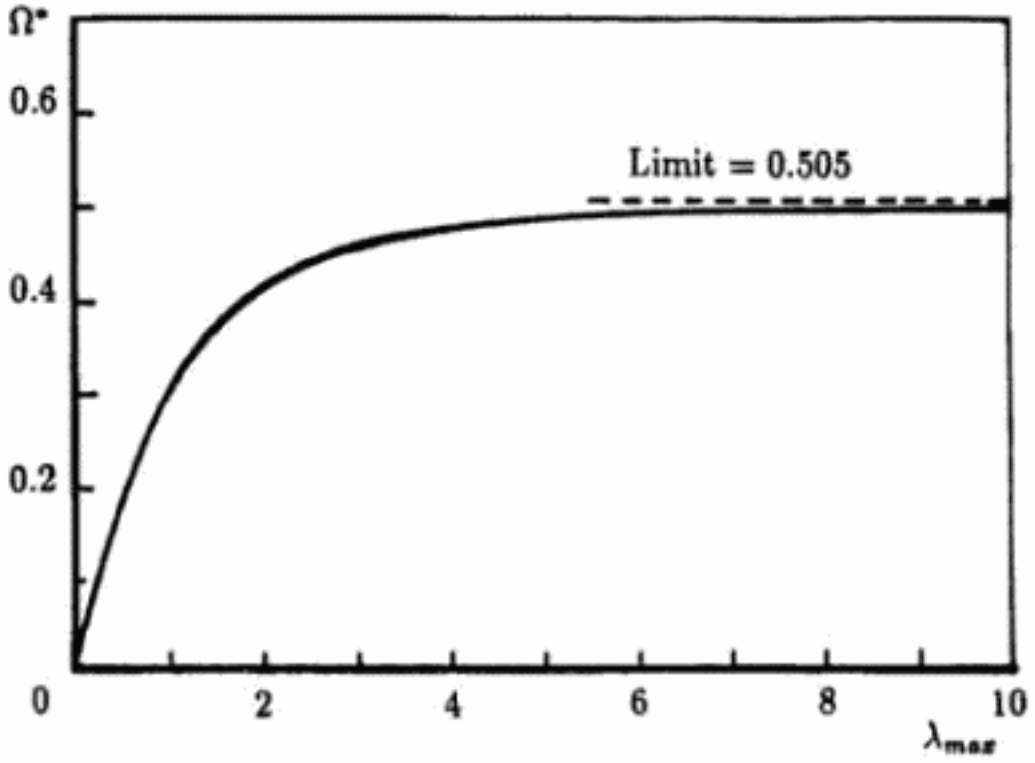

Figure 5.2: Variation of Ω^* with λ_{max}.

from the definition (5.64) we have the optimum altitude for maximum range in the problem of deceleration in level flight

$$\rho^* = \frac{2W}{SV_i^2\Omega^*}\sqrt{\frac{K}{C_{D_0}}} \tag{5.67}$$

This altitude exists when $\rho^* \leq \rho_0$, the value of ρ at sea level (see Exercise 5-9).

Exercises

5-1. Using the fact that tangential acceleration is dV/dt, project all the forces in Fig. 5.1 onto the tangent to the flight path to obtain

$$m\frac{dV}{dt} = T\cos\varepsilon - D - mg\sin\gamma$$

Next, using the fact that the normal acceleration is V^2/r where r is the radius of curvature, project all the forces into the normal to the flight path to obtain

$$m\frac{V^2}{r} = T\sin\varepsilon + L - mg\cos\gamma$$

Along a planar curve, if s is the arc length and γ is the turning angle, that is the angle between a fixed direction and the unit vector along the tangent, the curvature is defined as the inverse of the radius of curvature and is given by

$$\frac{1}{r} = \frac{d\gamma}{ds}$$

Use this equation and the kinematic relation $ds/dt = V$ to obtain the force equation along the normal to the flight path

$$mV\frac{d\gamma}{dt} = T\sin\varepsilon + L - mg\cos\gamma$$

5-2. If the flight path angle is not small, from the equations for the drag and the lift in quasi-steady state glide, show that the glide angle is

$$-\sin\gamma = \frac{D}{W}$$

and the drag is obtained from

$$D^2 + \frac{qS}{K}D - \left(W^2 + \frac{q^2S^2C_{D_0}}{K}\right) = 0$$

By minimizing D with respect to q, show that the solution for minimum glide angle is

$$q = \frac{W}{S}\sqrt{\frac{K}{C_{D_0}}}\frac{1}{\sqrt{1+4KC_{D_0}}}$$

and the corresponding minimum drag is

$$\frac{D}{W} = \frac{2\sqrt{KC_{D_0}}}{\sqrt{1+4KC_{D_0}}}$$

Show that for large value of E_{max}, these solutions reduce to Eqs. (5.11) and (5.13). Also show that the expression for the minimum glide angle is

$$-\tan\gamma = \frac{1}{E_{max}}$$

5-3. In quasi-steady state glide, if the flight path angle is not small, the rate of descent is

$$V_z = -V \sin\gamma = \frac{VD}{W} = \frac{\rho S C_D V^3}{2W}$$

Using the equations for lift and drag, show that

$$V_z = \sqrt{\frac{2W}{\rho S}} \frac{C_D}{(C_D^2 + C_L^2)^{3/4}}$$

Using a parabolic drag polar, show that

$$V_z = \sqrt{\frac{2W}{\rho S}} f(C_D)$$

where $f(C_D)$ is function of C_D. Deduce the condition for minimum rate of descent

$$2KC_D^2 - C_D + 4C_{D_0} = 0$$

From this equation derive the following solutions, valid for glide at minimum rate of descent when the small angle approximation is not used,

$$C_D = \frac{1}{4KE_{max}}(E_{max} - \sqrt{E_{max}^2 - 8})$$

$$\frac{C_L}{C_D} = \frac{2\sqrt{E_{max}^2 - 1 - E_{max}\sqrt{E_{max}^2 - 8}}}{E_{max} - \sqrt{E_{max}^2 - 8}}$$

$$q = \frac{W}{S}\sqrt{\frac{K}{3C_{D_0}}}\left[\frac{2}{E_{max}^2 - 2 - E_{max}\sqrt{E_{max}^2 - 8}}\right]^{1/2}$$

Show that when E_{max} is large, we have the approximate solution for small flight path angle as derived in the text,

$$C_D = 4C_{D_0}$$

$$\frac{C_L}{C_D} = \frac{\sqrt{3}}{2}E_{max}$$

$$q = \frac{W}{S}\sqrt{\frac{K}{3C_{D_0}}}$$

[*Hint: Put* $\epsilon = 1/E_{max}$ *and use series expansion in* ϵ.]

5-4. Consider Eq. (5.37) with $\rho = \rho_f$ for maximum endurance. Using the exponential atmosphere as given in Eq. (5.35), show that

$$t_f = \frac{E_{max}}{\beta}\left(\frac{27C_{D_0}}{K}\right)^{1/4}\sqrt{\frac{S\rho_i}{2W}}\,(e^{\beta\Delta z/2} - 1)$$

where $\Delta z = z_i - z_f$. For small altitude change, we have

$$t_f = \frac{E_{max}}{2}\left(\frac{27C_{D_0}}{K}\right)^{1/4}\sqrt{\frac{S\rho_i}{2W}}\,(z_i - z_f)$$

In this form, although the time of flight is proportional to Δz, it depends on the initial altitude through ρ_i. Show that this equation is the same as the one obtained by using the solution (5.33) with constant density, $\rho = \rho_i$, in Eq. (5.32) and integrating with respect to the altitude z.

5-5. (a) From Eqs. (5.33) and (5.48), deduce that the minimum rate of descent, for both glide and descent, decreases along the flight path.

(b) Let subscript 0 denote the glide condition and subscript 1 the descent condition in the problem of maximum endurance. Show that

$$q_1 = kq_0$$

where

$$k = \sqrt{1+\eta^2} + \eta \geq 1, \qquad \eta = \frac{E_{max}\tau}{\sqrt{3}} \geq 0$$

(c) Show that

$$\frac{V_{z_1}}{V_{z_0}} = \frac{3}{2k^{1/2}}\left(1 - \frac{1}{3}k^2\right)$$

Show that this function decreases as k increases and hence $V_{z_1} \leq V_{z_0}$ with the equality holding for $k = 1$, that is when $\tau = 0$.

(d) Show that when $V_{z_1} = 0$, we have the solution (5.50).

5-6. In the problem of descent to a specified altitude with maximum endurance it is proposed to evaluate the dimensionless thrust $E_{max}\tau$ so that the endurance is increased by a factor $F > 1$ as compared to the glide solution. Let

$$x = \frac{1}{3}[E_{max}\tau + \sqrt{3 + E_{max}^2\tau^2}], \qquad k = \frac{27^{1/4}}{2}F$$

From the definition (5.55) of the factor F, show that the solution is obtained by solving the equation

$$\frac{x^{1/2}}{1-x^2} = k$$

where of course k is given.

Let $x^{1/2} = y$ and write the equation as

$$y = \left(1 - \frac{y}{k}\right)^{1/4}$$

This equation is of the form $y = f(y)$ and it can be shown that the sequence $y_1 = f(y_0)$, $y_2 = f(y_1)$, $\cdots$, where y_0 is an estimated root, converges to the unique solution y.

With $F = 3$, use the procedure to obtain the following solution

$$y = 0.92424140$$
$$x = 0.85422218$$
$$E_{max}\tau = 0.69600546$$

5-7. Let

$$\lambda = \frac{C_L}{C_L^*}, \qquad \delta = \frac{C_D}{C_D^*}$$

where C_L^* and C_D^* are the lift and the drag coefficients for maximum lift-to-drag ratio. Show that the equation for parabolic drag polar has the universal form

$$\delta = \frac{1}{2}(1 + \lambda^2)$$

Plot this polar and locate the operating point for minimum glide angle and for minimum rate of descent with $T = 0$.

If the drag polar is of the form (generalized drag polar),

$$C_D = C_{D_0} + KC_L^n$$

show that its equivalent universal form is

$$\delta = \frac{(n-1) + \lambda^n}{n}$$

5-8. Find the limit of Eq. (5.66) when $\lambda_{max} \to \infty$. In this limiting equation, use the transformation

$$x = \frac{\Omega^2}{1 + \Omega^2}$$

to obtain the equation

$$x = e^{2(x-1)}$$

This equation is of the form $x = f(x)$ and near the unique root x^*, the sequence $x_1 = f(x_0)$, $x_2 = f(x_1)$, $\cdots$, where x_0 is an estimated solution converges to the exact solution. Use this iteration to obtain the solution $x^* = 0.20318787$, $\Omega^* = 0.50497621$.

5-9. Consider the two equations (5.66) and (5.67). From Eq. (5.66), and as shown in Fig. 5.2, the value Ω^* is only a function of λ_{max}, that is of the aerodynamic characteristic of the glider. Then, when Ω^* is obtained, from Eq. (5.67), the condition $\rho^* \leq \rho_0$ for the existence of an optimum coasting altitude can always be satisfied by starting with a relatively high initial speed V_i. Let V_f be the stall speed at sea level as computed from Eq. (5.62) with $\rho = \rho_0$. Show that to have an optimum altitude above sea level, the necessary and sufficient condition is

$$\frac{V_i^2}{V_f^2} > \frac{\lambda_{max}}{\Omega^*} = f(\lambda_{max})$$

Plot the limiting ratio

$$\frac{V_i}{V_f} = \sqrt{f(\lambda_{max})}$$

versus λ_{max}.

6

Cruise performance

6.1 Introduction

In general, cruise performance is characterized by flight in a vertical plane at small flight path angles with small changes in speed and altitude. In this chapter, we shall first consider the equations for cruise at constant altitude. The case of descent where the altitude slowly decreases has been analyzed in the previous chapter. The problem of cruise-climb where the altitude slowly increases involves only a slight modification in the analysis.

Within the assumption of a constant gravity field we have the equations of motion, as derived in Chapter 2, for $\gamma = 0$, $\psi = 0$, $\sigma = 0$,

$$\begin{aligned} \frac{dx}{dt} &= V \\ m\frac{dV}{dt} &= T\cos\varepsilon - D \\ mg &= T\sin\varepsilon + L \\ \frac{dm}{dt} &= -\frac{c}{g}T \end{aligned} \tag{6.1}$$

In the equations, x is the longitudinal distance or the range, V the speed, m the mass, D the drag, L the lift and T the magnitude of the thrust set at an angle ε with respect to the velocity vector. The parameter c is the thrust specific fuel consumption and is a characteristic of the engine. The Eqs. (6.1) for flight at constant altitude can be derived directly by considering the force diagram in Fig. 6.1.

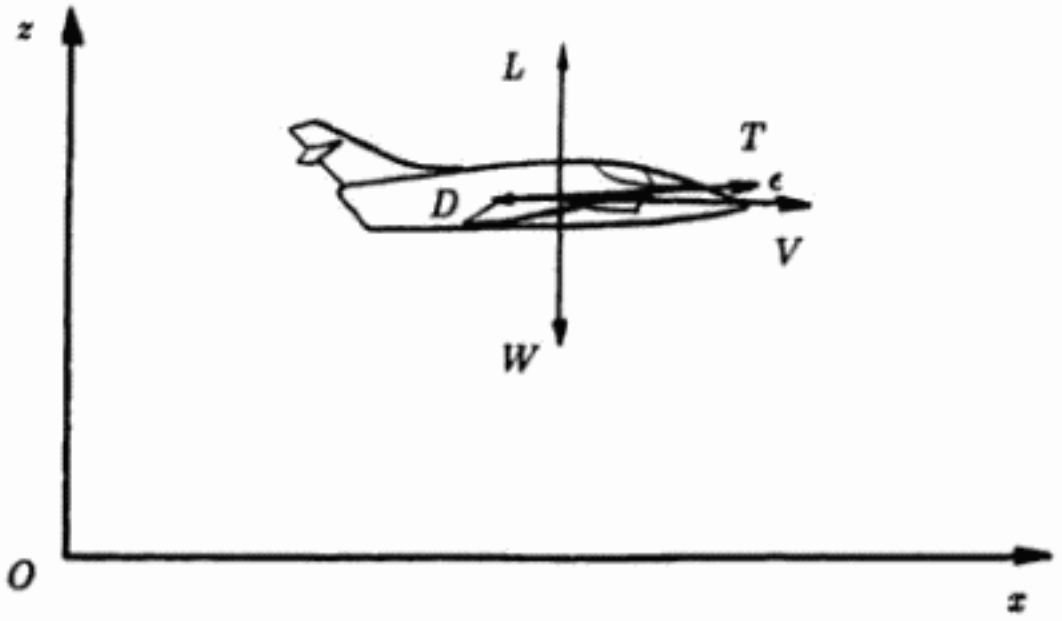

Figure 6.1: Flight at constant altitude.

The thrust T is a function of the Mach number M, altitude z and engine throttle setting N. The thrust specific fuel consumption, c, is a function of the same parameters. Hence, in general, we have

$$\begin{aligned} T &= T(M, z, N) \\ c &= c(M, z, N) \end{aligned} \tag{6.2}$$

On the other hand, we have the usual relationships for the drag and the lift force

$$\begin{aligned} D &= \frac{1}{2}\rho S C_D V^2 \\ L &= \frac{1}{2}\rho S C_L V^2 \end{aligned} \tag{6.3}$$

where ρ is the atmospheric density and S a reference area selected for evaluating the drag coefficient C_D and the lift coefficient C_L. The analysis will be simplified and the results obtained are more explicit if we use the usual parabolic drag polar

$$C_D = C_{D_0}(M) + K(M)C_L^2 \tag{6.4}$$

where the zero-lift drag coefficient C_{D_0} and the induced drag factor K are functions of the Mach number. Parabolic drag polar is a good approximation for cruise performance analysis since during the cruise the angle-of-attack is in the range where Eq. (6.4) is essentially valid. Special attention should be given to the case of flight near the stall speed where this formula is no longer valid.

Equations (6.1) through (6.4) provide the relations necessary for determining cruise performance at constant altitude. Typical cruise performance problems involve the derivation of the solutions for the aerodynamic and engine controls for maximum range and maximum endurance.

6.2 Aerodynamic and engine controls for steady cruise

Two assumptions will be introduced to simplify the analysis. The first one is that the thrust vector is nearly aligned with the velocity vector so that the thrust angle ε is negligibly small. That is to say, in the equations (6.1) we shall take approximately

$$\begin{aligned} T\cos\varepsilon &\approx T \\ T\sin\varepsilon &\approx 0 \end{aligned} \tag{6.5}$$

This assumption has to be used with care. During an approach before landing, an aircraft of the delta-wing type can fly at high angle-of-attack such that ε can reach say 15° or higher. Then, the contribution of the term $T\sin\varepsilon$ in the lift direction is about 25% of the thrust. Since, in such a case, high thrust setting is generally used, the component $T\sin\varepsilon$ cannot be neglected. (See Exercises 6-1 and 6-2.)

The second assumption introduced is that the variation of speed is small so that the inertia term mdV/dt can be neglected. This assumption, called the assumption of steady state cruise, is especially true for the problem of long-range cruise to be analyzed in this chapter. We shall discuss the special case of accelerated or decelerated flight in the last section.

With these two assumptions, we obtain from the general equations (6.1)

$$mg = \frac{1}{2}\rho SV^2 C_L \tag{6.6}$$

$$T = \frac{1}{2}\rho S V^2 C_D \tag{6.7}$$

The first equation will be referred to as the lift equation and the second one, the thrust equation. They are so named after the two main controls, namely the lift control and the thrust control as discussed below.

At a given altitude, characterized by the atmospheric density ρ, and for a certain weight $W = mg$, for each stabilized speed V, the lift coefficient C_L is uniquely determined from Eq. (6.6). The Mach number M, being a function of z and V, is known, and hence we obtain the drag coefficient C_D from the parabolic drag polar (6.4). Then, from Eq. (6.7), we have the necessary thrust magnitude T. From Eq. (6.2), this thrust magnitude is obtained by using the appropriate engine throttle setting N. The corresponding thrust specific fuel consumption c, is deduced and subsequently the variation of the weight is obtained from the last of the equations (6.1), reproduced here for convenience

$$\frac{d(mg)}{dt} = -cT \tag{6.8}$$

The cycle of control is then repeated with Eq. (6.6).

The equations for steady flight are now analyzed, first for static performance and then for integral performance.

The static performance of an aircraft is defined as its behavior under steady state flight condition. For level flight, the static performance is governed by the two basic equations (6.6) and (6.7). It will be shown that performance characteristics such as the stalling speed, the maximum speed, the minimum mass flow rate, the aerodynamic ceiling and the propulsive ceiling can all be deduced from the analysis of these two equations.

In integral performance, we are interested in the distance travelled and the time of flight. These quantities are obtained by integrating the equation for the range. Of special interest are the maximum distance travelled for a given amount of fuel, and the time of flight as functions of the altitude and the speed selected for cruise.

6.3 The lift equation

The lift equation, Eq. (6.6), shows that the lift is used to balance the weight in level flight. High-performance aircraft generally cruise at high altitude and in the speed regime where the effect of compressible fluid is being felt. If a is the speed of sound, p the ambient pressure and k the ratio of the specific heats, with the value $k = 1.4$ for air, we have the classical relations

$$\frac{V}{a} = M \tag{6.9}$$

and

$$a^2 = \frac{kp}{\rho} \tag{6.10}$$

With these relations, we easily transform the lift equation into

$$\omega = C_L M^2 \tag{6.11}$$

where we define the dimensionless wing loading

$$\omega = \frac{2W}{kpS} \tag{6.12}$$

At each flight altitude, specified by the ambient pressure p, and with the current weight $W = mg$, the dimensionless wing loading ω is known. Then Eq. (6.11) shows that each value of the lift coefficient C_L, selected as the control for the flight , corresponds to a flight Mach number M. As has been discussed in Chapter 3, the lift coefficient C_L is bounded by its maximum value $C_{L_{max}}(M)$. Then, in the (ω, M) space which is physically the altitude–speed space, the domain of flight is bounded by the curve

$$\omega = C_{L_{max}}(M) M^2 \tag{6.13}$$

Since $C_{L_{max}}$ is a function of the Mach number we can plot this curve for each aircraft aerodynamic characteristic $C_{L_{max}}(M)$ (Fig. 6.2). The curve, called the flight envelope, delimits the domain of flight inside which level flight is possible. As characterized by the function $C_{L_{max}}$, the limitation is due to the aerodynamic characteristics of the aircraft considered. At low Mach number, $C_{L_{max}}$ is nearly constant and the flight envelope is nearly a parabola. As the speed approaches the speed of sound, $M \to 1$, for a subsonic aerodynamic configuration, the value

$C_{L_{max}}$ drops drastically to near zero and the flight envelope behaves as shown in Fig. 6.2. On the other hand, if the aircraft is aerodynamically shaped to operate in the supersonic flight speed regime, $C_{L_{max}}$ drops in the transonic region and then tends to a near constant value for moderate supersonic speeds. This near constant value is lower than the constant value at low subsonic speeds. Nevertheless, from Eq. (6.13), it is seen that, as M increases, ω again increases and the flight envelope again becomes nearly parabolic in the supersonic speed regime. The flight domain in Fig. 6.2 shows clearly the influence of altitude and weight on the permissible flight Mach number. This domain can be further restricted on the right side by the maximum Mach number which the engines can deliver at any given altitude.

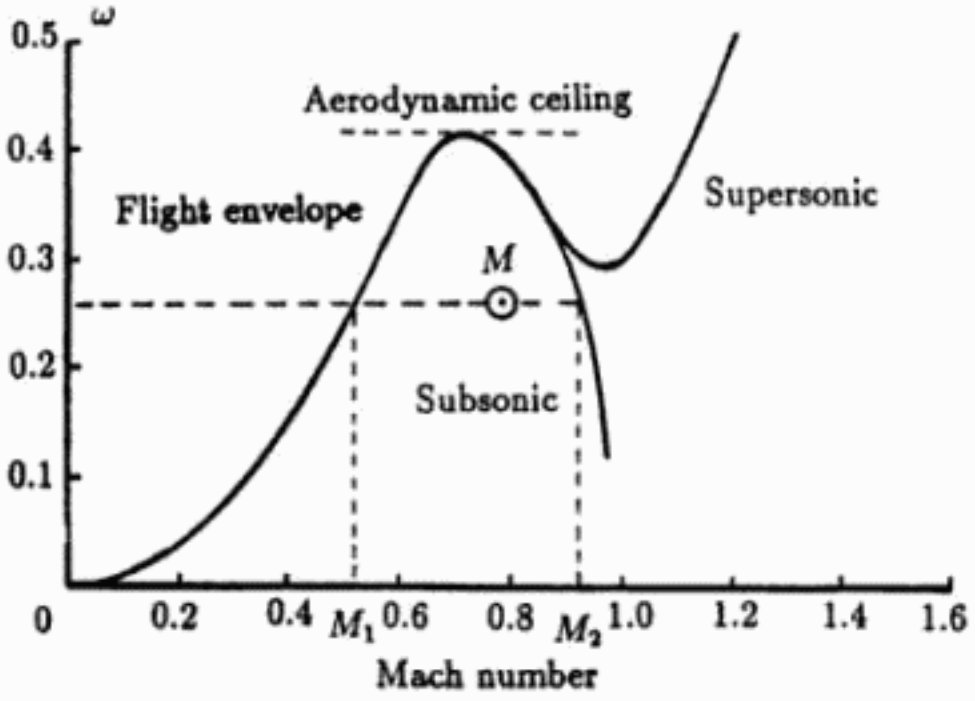

Figure 6.2: Domain of flight for subsonic aircraft and supersonic aircraft.

For each weight, the ordinate in the figure is a measure of the altitude z through the ambient pressure p. At the cruise altitude, because of the flight envelope, the Mach number can only be selected between the two values M_1 and M_2. The smaller value M_1, is the stalling Mach

number. At that point, because of the low speed flight selected, the value of C_L has reached its stalling value $C_{L_{max}}$ and level flight at lower Mach number is not possible. The higher value M_2, is the critical stall Mach number. At that point, again we have $C_L = C_{L_{max}}$, but this is because at high Mach number, the maximum value $C_{L_{max}}$ has decreased to the point that it is not possible to maintain level flight at higher Mach number.

Now, if we increase the cruise altitude, for the same value of the weight, ω increases and the interval for permissible Mach number $[M_1, M_2]$ decreases. At the point of maximum value of ω, we have $M_1 = M_2$. The flight level at this point is called the aerodynamic ceiling. Above this altitude, level flight is not possible no matter how powerful a propulsion system is used to sustain the flight. This limitation is due to the aerodynamic characteristics of the aircraft. The Mach number at the aerodynamic ceiling is obtained by solving the equation

$$\frac{d}{dM}(C_{L_{max}} M^2) = 0 \tag{6.14}$$

It is convenient for the notation to follow Miele by using the logarithmic derivative which is defined as (Miele, 1962)

$$y_x = \frac{d(\operatorname{Log} y)}{d(\operatorname{Log} x)} = \frac{x}{y}\frac{dy}{dx} \tag{6.15}$$

In terms of the logarithmic derivative, we have the equation

$$(C_{L_{max}})_M + 2 = 0 \tag{6.16}$$

which shows that this Mach number depends solely on the function $C_{L_{max}}(M)$. Once the Mach number at the ceiling has been obtained from Eq. (6.16), the maximum value of ω at the ceiling can be evaluated from Eq. (6.13). Then from the definition (6.12) of ω, it is seen that, although the value of ω_{max} is unique for each aircraft aerodynamic configuration, that is for each function $C_{L_{max}}(M)$, the aerodynamic ceiling varies with the corresponding weight. More specifically, it is higher for smaller weights and lower for larger values. For a supersonic aircraft, although the aerodynamic ceiling exists at subsonic speed, with a sufficiently high thrust we can cruise at supersonic speed. The ceiling is higher and depends on the propulsive thrust. Finally we

notice that, based on aerodynamic data, the function $C_{L_{max}}(M)$ can always be modeled as a polynomial for the analysis.

6.4 The thrust equation

We have discussed the static performance using solely the lift equation but in level flight the thrust equation, Eq. (6.7), must also be satisfied. The analysis of this equation will be conducted separately for the case of a propeller driven aircraft and the case of a jet powered aircraft.

6.4.1 Propeller driven aircraft

For aircraft, equiped with propellers driven by reciprocating engines, these engines are characterized by their power. We express the thrust equation in terms of powers by multiplying both sides of Eq. (6.7) by the speed V,

$$\underset{\text{power available}}{TV} = \underset{\text{power required}}{\frac{1}{2}\rho S C_D V^3} \tag{6.17}$$

The left-hand side of this equation, which is the product of the speed and the thrust produced by the propulsion system (engines+propellers) is the power available. The right-hand side can be seen as the power required to overcome the drag force. These two powers must be equal to maintain steady state level flight.

The function for the power available

$$P_a = TV \tag{6.18}$$

is plotted versus the speed in Fig. 6.3. Since the speed of sound is constant in level flight, the abcissa can be considered as representing the Mach number. At $V = 0$, $P_a = 0$, and the curve starts at the origin. Then, as the speed is increased, P_a increases rapidly and becomes nearly constant at the speed range corresponding to the power setting effectively used for cruise. At high speed, the tips of the propellers, acting as aerodynamic lifting airfoils, stall and the corresponding thrust

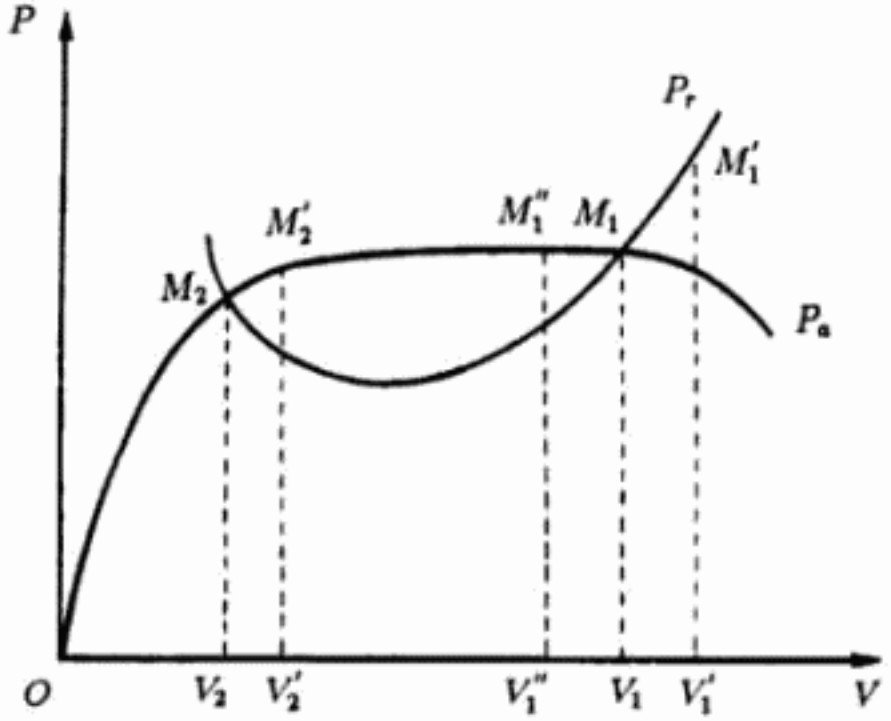

Figure 6.3: Variation of power available and power required as functions of speed.

T decreases drastically. This makes the product $P_a = TV$ decrease as the speed increases.

The variation of the power required, P_r, as a function of the speed is more explicit. First, we have

$$P_r = \frac{1}{2}\rho S C_D V^3 \tag{6.19}$$

On the other hand, from Eq. (6.6) we obtain the speed

$$V = \sqrt{\frac{2W}{\rho S C_L}} \tag{6.20}$$

By substituting into Eq. (6.19), we have

$$P_r = \sqrt{\frac{2W^3}{S}} \frac{1}{\sqrt{\rho}} \frac{C_D}{C_L^{3/2}} \tag{6.21}$$

This equation is written in the form of three factors to show separately the effects of weight, of altitude and of aerodynamic characteristics.

For a given weight, and cruise altitude, we first discuss the behavior of the power required as a function of the speed for a perfectly general drag polar. For a propeller driven aircraft, the cruise speed is generally low enough for us to neglect the effect of the Mach number and consider a general lift–drag relationship

$$f(C_D, C_L) = 0 \tag{6.22}$$

A typical plot of this function is shown in Fig. 6.4(b). Theoretically, at any speed selected, we have the value C_L from the lift equation (6.20), and then the drag coefficient C_D from the drag polar (6.22). Then, we calculate the corresponding value for P_r from Eq. (6.21). At very high speed, C_L is small and C_D is practically constant. From Eq. (6.19), P_r varies as V^3. We are in the zone 1 in Fig. 6.4. On the other hand, at low speed, the value of C_L is near to its maximum value. A small variation of C_L leads to a large variation of C_D and, as a consequence of Eq. (6.19), this provides a large variation of P_r even for a small variation of the speed V. We are in the zone 2 in Fig. 6.4. In this zone, for a variation $\Delta V > 0$, we have $\Delta C_L < 0$ with a large and negative $\Delta C_D < 0$. Hence we have a steep decrease in P_r. Thus, between these two high variations for P_r, first a steep decrease and later on a steep increase, we have a minimum for the curve $P_r = F(V)$. This occurs at the minimum of $C_D/C_L^{3/2}$ subject to the lift–drag relation (6.22).

To obtain an accurate assessment of the behavior of the function P_r, near to the stall speed where $C_L = C_{L_{max}}$, we take the derivative of Eq. (6.19) with respect to V to obtain

$$\frac{dP_r}{dV} = \frac{1}{2}\rho S\left(3V^2 C_D + V^3 \frac{dC_D}{dV}\right)$$

But, with the aid of Eq. (6.20), we have

$$\frac{dC_D}{dV} = \frac{dC_D}{dC_L}\frac{dC_L}{dV} = -\frac{2C_L}{V}\frac{dC_D}{dC_L}$$

Therefore, we have

$$\frac{dP_r}{dV} = \frac{1}{2}\rho S V^2\left(3C_D - 2C_L \frac{dC_D}{dC_L}\right) \tag{6.23}$$

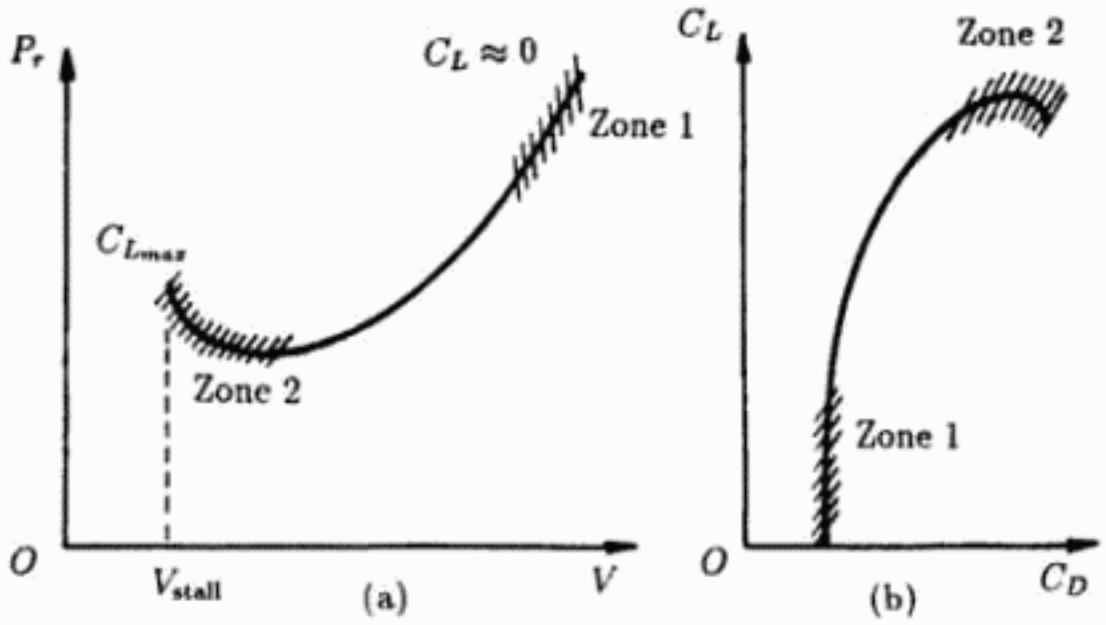

Figure 6.4: Plots of (a) P_r versus V and (b) C_L versus C_D.

At the stall speed, $C_L = C_{L_{max}}$, the value of C_D is finite while $dC_L/dC_D = 0$. Hence, $dC_D/dC_L = \infty$ and the slope of the curve P_r is infinite. Again, we emphasize the fact, already mentioned in Chapter 3, that a good modeling of the parabolic drag polar, as represented by Eq. (6.4), should include the lift coefficient beyond the value $C_L = \sqrt{3C_{D_0}/K}$, which is the lift coefficient for the minimum of $C_D/C_L^{3/2}$.

In summary, we conclude that by neglecting the effect of Mach number (either using an accurate modeling of the drag polar as represented by the general relationship (6.22), or an adequate parabolic representation as shown in Eq. (6.4) valid up to a sufficiently high lift coefficient) the plot of P_r versus V is such that it starts out at the stall speed and decreases rapidly to a minimum for a minimum of $C_D/C_L^{3/2}$ and then increases with higher speed (Fig. 6.4(a)). With a parabolic drag polar, the minimum of P_r occurs when $C_D/C_L^{3/2}$ is a minimum,

that is for

$$C_L = \sqrt{\frac{3C_{D_0}}{K}} = \sqrt{3}C_L^*, \qquad C_D = 4C_{D_0} = 2C_D^* \tag{6.24}$$

The corresponding speed is obtained from the lift equation (6.20), while from Eq. (6.21) we have the minimum power required.

$$P_r^* = \frac{2}{3^{3/4}E_{max}}\sqrt{\frac{2W^3}{\rho S C_L^*}} \tag{6.25}$$

Returning to Fig. 6.3, for steady cruise, we have the equality $P_a = P_r$. The two curves for the powers may intersect each other at two points M_1 and M_2 with two speed regimes V_1 and V_2 for cruise with the same power setting. The high speed V_1, with low lift coefficient, and hence low angle-of-attack, is stable. This is because with the same throttle setting if the flight is perturbed to a higher speed $V_1' > V_1$, we shall have $P_a < P_r$. With insufficient power, the aircraft decelerates and we return to the initial speed. If the perturbed speed is lower, that is with $V_1'' < V_1$, we shall have $P_a > P_r$ and hence with excess power, the aircraft accelerates to return to the initial speed V_1. A similar discussion shows that the high angle-of-attack, low speed regime V_2 is unstable. While with a higher perturbed speed $V_2' > V_2$, the aircraft tends to accelerate away to the stable high speed V_1, a smaller perturbed speed $V_2'' < V_2$ may decrease further to the stall speed.

From the diagram of the powers, at any flight altitude, we have a well determined curve for the power required. If we reduce the power available, the curve for P_a becomes lower and the two speed regimes V_1 and V_2 tend toward each other. The minimum power available P_a to sustain horizontal flight is attained when the two curves become tangential at the lowest point on the power required curve. For a parabolic drag polar, the solution has been given in Eqs. (6.24) and (6.25). From the lift equation, the dynamic pressure for flight with minimum power is

$$\frac{1}{2}\rho V^2 = \frac{W}{S\sqrt{3C_{D_0}/K}} \tag{6.26}$$

With regard to the angle-of-attack, for flight at minimum power, it is always the same at all altitudes and weights, being the one which minimizes $C_D/C_L^{3/2}$. If we use an average weight for the calculation,

Eq. (6.26) shows that the dynamic pressure is constant. Hence, from definition (3.58), flight at minimum power is always conducted at the same equivalent speed V_e, regardless of the flight altitude. As discussed in Chapter 3, at low subsonic speeds, V_e is the same as the calibrated speed V_c which we take as the indicated speed V_i for a perfect speed indicator.

From Eq. (6.21), it is clear that if we increase the weight, the power required increases as $W^{3/2}$. This leads to the same increase in the power available to sustain the cruise at the same angle-of-attack. As for the effect of the altitude, it is enlightening for a general discussion to change the abcissa in the power diagram from the true speed V to the equivalent speed V_i through the relation

$$V = \frac{V_i}{\sqrt{\sigma}} \tag{6.27}$$

where, as usual, $\sigma = \rho/\rho_0$ denotes the density ratio. For the discussion in this text, we emphasize the fact that the symbol V_i denotes the transformation (6.27). In general, it stands for the equivalent speed. Only in incompressible fluid is it the indicated speed. At the same time, we change the ordinate from P to $P\sqrt{\sigma}$. Then from the lift equation (6.20) we obtain

$$V_i = \sqrt{\frac{2W}{\rho_0 S C_L}} \tag{6.28}$$

while from Eq. (6.21), we have

$$P_r\sqrt{\sigma} = \sqrt{\frac{2W^3}{\rho_0 S}}\frac{C_D}{C_L^{3/2}} \tag{6.29}$$

Then, with a general drag polar, as given by Eq. (6.22), the plot of the modified power required $P_r\sqrt{\sigma}$ versus the equivalent speed V_i is independent of the altitude. This is because, for each V_i, we obtain a well defined value C_L from Eq. (6.28), with the corresponding C_D from the drag polar (6.22). The value $P_r\sqrt{\sigma}$ is obtained from Eq. (6.29) and the mapping from V_i to $P_r\sqrt{\sigma}$ is independent of the altitude. The explicit relationship using a parabolic drag polar is given in Exercise 6-3. The plots of $P_r\sqrt{\sigma}$ and $P_a\sqrt{\sigma}$ versus the equivalent speed V_i are shown in Fig. 6.5.

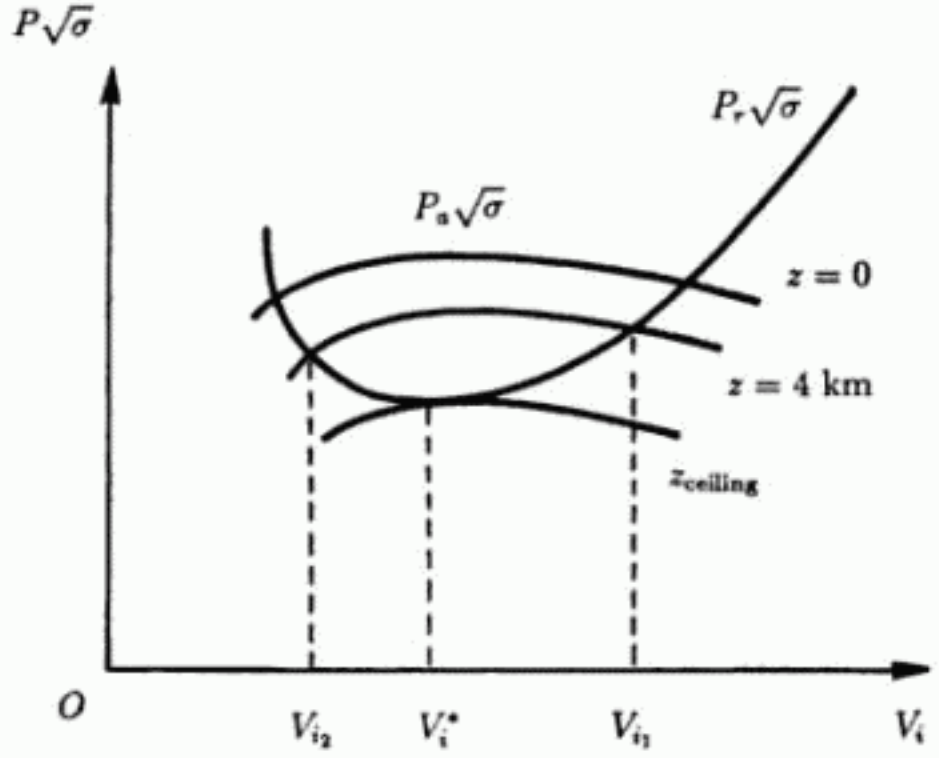

Figure 6.5: The influence of altitude on cruise speed.

For the plot of $P_a\sqrt{\sigma}$ versus V_i, we consider the case of a fixed throttle setting. Let P_0 be the power available at sea level. For an aspirated engine, P_a is proportional to the density and we have

$$P_a = P_0\sigma \tag{6.30}$$

Then $P_a\sqrt{\sigma}$ decreases as $\sigma^{3/2}$ when the altitude increases. With a supercharged engine, with a given throttle setting, the power available remains essentially constant up to a certain critical altitude. In this case $P_a\sqrt{\sigma} = P_0\sqrt{\sigma}$, and the modified power $P_a\sqrt{\sigma}$ decreases as $\sqrt{\sigma}$ when the altitude increases. Above the critical altitude, P_a is proportional to the density and we have the approximate law

$$P_a = P_c\left(\frac{\rho}{\rho_c}\right) \tag{6.31}$$

where subscript c denotes the condition at the critical altitude. Above the critical altitude, with supercharged engines $P_a\sqrt{\sigma}$ decreases as $\sigma^{3/2}$

when the altitude increases. In both cases, at a certain sufficiently high altitude, the two curves for $P_r\sqrt{\sigma}$ and $P_a\sqrt{\sigma}$ become tangential at the speed V_i^* which is the limit of the two speeds V_{i_1} and V_{i_2}. Since this is the speed at the lowest point on the P_r curve, for a parabolic drag polar, we use the solution (6.24) in Eq. (6.28) to obtain

$$V_i^* = \sqrt{\frac{2W}{\rho_0 S}}\left(\frac{K}{3C_{D_0}}\right)^{1/4} \tag{6.32}$$

When the two power curves become tangential, we have reached the highest altitude, called the ceiling, for the prescribed power throttle setting. To cruise at higher altitude it is necessary to increase the power available. The propulsive ceiling is attained when the tangency occurs with the maximum power available. The density at the ceiling can be calculated by setting this maximum power available equal to the minimum power required P_r^* as given by Eq. (6.25). Then, for aspirated engines, by using Eq. (6.30) with $P_0 = P_{max}$, we have the condition at the ceiling

$$\frac{\rho_{\text{ceiling}}}{\rho_0} = \left(\frac{P_{r_0}^*}{P_{max}}\right)^{2/3} \tag{6.33}$$

where P_{max} is the maximum power at sea level, and $P_{r_0}^*$ is the minimum power required at sea level, and it is calculated from Eq. (6.25) with $\rho = \rho_0$.

With supercharged engines, the value P_{max} is constant up to the critical altitude with density ρ_c. We first evaluate the minimum power required $P_{r_c}^*$ at this altitude by using $\rho = \rho_c$ in Eq. (6.25). If $P_{max} < P_{r_c}^*$, the ceiling is below the critical altitude. The density at the ceiling is calculated from

$$\frac{\rho_{\text{ceiling}}}{\rho_0} = \left(\frac{P_{r_0}^*}{P_{max}}\right)^2 \tag{6.34}$$

If $P_{max} > P_{r_c}^*$, as is usually the case with supercharged engines, to evaluate the density at the ceiling, we can use Eq. (6.33) but with subscript "o" replaced by subscript "c" as the reference point is now at the critical altitude, and not at sea level. We tacitly admit the fact that the maximum power P_{max} is evaluated at the critical altitude and it is essentially the same as the maximum power at sea level.

6.4.2 Turbojet aircraft at subsonic speeds

Turbojet engines and rockets are characterized by their thrust. Hence, for these propulsion systems, we consider directly the thrust equation

$$T = \frac{1}{2}\rho S C_D V^2 \tag{6.35}$$

Thrust available Thrust required

The left-hand side of this equation represents the thrust available, T_a, and the right-hand side is the thrust required, T_r. At low Mach number where we can neglect the effects of compressiblity, we can conduct a parallel discussion to that for the power equations for propeller driven aircraft. The plots of T_a and T_r versus speed are shown in Fig. 6.6. For rocket engines, the thrust produced is practically independent of the speed and the altitude. For turbojet engines (whose range of application varies between Mach number 0 and 3) at a prescribed altitude and in the subsonic range, the thrust increases slightly with speed at high speed, as shown in the graph.

For the thrust required, we have the expression

$$T_r = \frac{1}{2}\rho S C_D V^2 \tag{6.36}$$

Using the lift equation (6.20), we put it in the form

$$T_r = W\frac{C_D}{C_L} \tag{6.37}$$

Again, we consider a general drag polar as given in Eq. (6.22) to study the variation of T_r with respect to V at any flight altitude. At any speed, at the prescribed altitude, we have the value C_L from Eq. (6.20), and then the drag coefficient C_D from the drag polar (6.22). Then, we compute T_r from Eq. (6.37). From the plot of a realistic drag polar as shown in Fig. 6.4(b), at high speed, C_L is small and C_D is practically constant. From Eq. (6.36), T_r varies as V^2. On the other hand, at low speed, the value of C_L is near to its maximum value. A small variation of C_L leads to a large variation of C_D and as a consequence of Eq. (6.36), this provides a large variation of T_r even for a small variation of the speed V. Just as in the case of the variation of the power required,

near the stall speed, for a variation $\Delta V > 0$, we have $\Delta C_L < 0$ with a large and negative $\Delta C_D < 0$. Then, from Eq. (6.36) we have a steep decrease in T_r. Thus, between these two high variations for T_r, first a steep decrease and, later on, a steep increase, we have a minimum for the curve $T_r = F(V)$. This occurs at the minimum of C_D/C_L and hence, for an angle-of-attack providing the maximum lift-to-drag ratio.

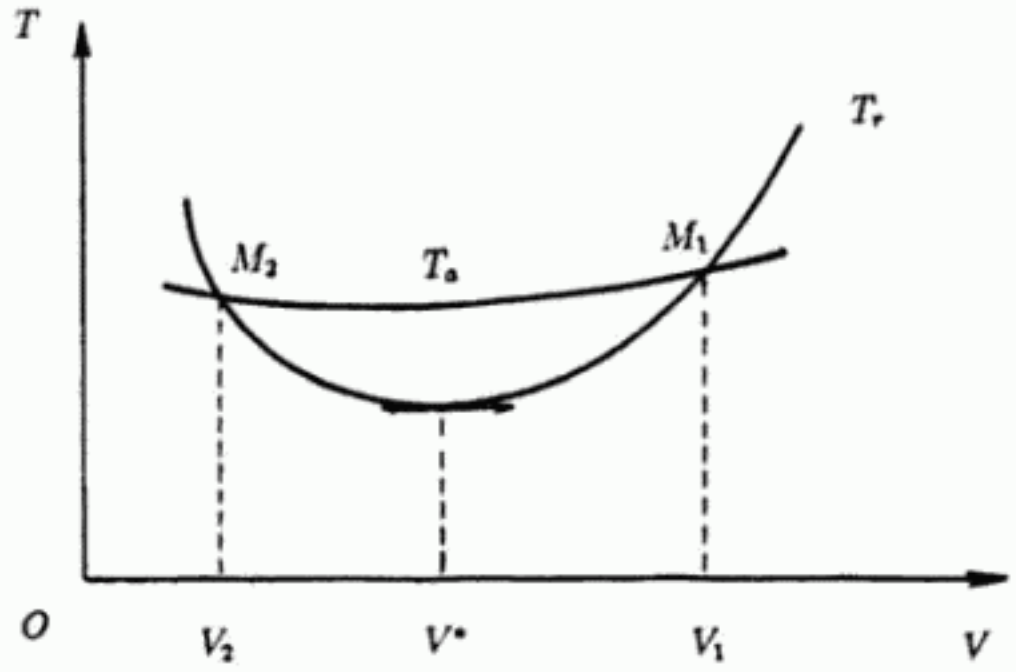

Figure 6.6: Variation of thrust available and thrust required as functions of speed.

As in the case of the power required we consider the slope of the thrust required curve near to the stall speed. By taking the derivative of Eq. (6.36) with respect to V and using Eq. (6.20), we have

$$\frac{dT_r}{dV} = \rho SV\left(C_D - C_L\frac{dC_D}{dC_L}\right) \tag{6.38}$$

At the stall speed, $C_L = C_{L_{max}}$, the value of C_D is finite while $dC_L/dC_D = 0$. Hence, $dC_D/dC_L = \infty$ and the slope of the curve T_r is infinite.

We conclude that the plot of T_r versus speed is such that is starts out at the stall speed and decreases to a minimum for a minimum of C_D/C_L and then increases with higher speed. With a parabolic drag polar, the minimum thrust required occurs at maximum lift-to-drag ratio, that is for

$$C_L = \sqrt{\frac{C_{D_0}}{K}} = C_L^*, \qquad C_D = 2C_{D_0} = C_D^* \tag{6.39}$$

From Eq. (6.37), we have the minimum value of T_r

$$T_r^* = \frac{W}{E_{max}} \tag{6.40}$$

For steady cruise, we have the equality $T_a = T_r$. The two curves for the thrusts may intersect each other at two points M_1 and M_2 with two speed regimes V_1 and V_2 for cruise with the same thrust setting. A similar discussion to that carried out for the power diagram leads to the same conclusion that the high speed regime V_1 is stable while the low speed regime V_2 is unstable.

At any flight altitude, if we reduce the thrust available, the curve for T_a becomes lower and the two speed regimes V_1 and V_2 tend toward each other. The minimum thrust available T_a to sustain horizontal flight is attained when the two curves become tangential at the lowest point on the thrust required curve. If the solution (6.39) is used in the lift equation (6.20), we obtain the dynamic pressure for flight with minimum thrust

$$\frac{1}{2}\rho V^{*2} = \frac{W}{S\sqrt{C_{D_0}/K}} \tag{6.41}$$

As for the angle-of-attack, for flight at minimum thrust, it is always the same at all altitudes and weights, being that for maximum lift-to-drag ratio. Since from Eq. (6.41) the corresponding speed increases as the altitude increases, with lower values of the density ρ, and since the speed of sound decreases with altitude in the troposphere and is constant in the stratosphere, the Mach number for cruise with minimum thrust increases with altitude. Therefore, the results in this section are restricted to the altitude range where the cruise Mach number is clearly subsonic so that the influence of Mach number on aerodynamic characteristics can be neglected. Within this assumption, with an average value for W, the dynamic pressure for minimum thrust is constant

and the corresponding equivalent speed V_i^* is the same regardless of the flight altitude.

From Eq. (6.37), it is clear that for the same angle-of-attack, the thrust is proportional to the weight.

To see the influence of altitude, in the thrust diagram, we change the abcissa from true speed V to equivalent speed V_i through the relation (6.27). But here, it is not necessary to change the ordinate as in the case of the diagram for powers. The mapping from V_i in Eq. (6.28) to T_r in Eq. (6.37) through the lift–drag relationship (6.22) is independent of the altitude. Then the plot of T_r versus V_i is the same for all altitudes (Fig. 6.7, also see Exercise 6-6).

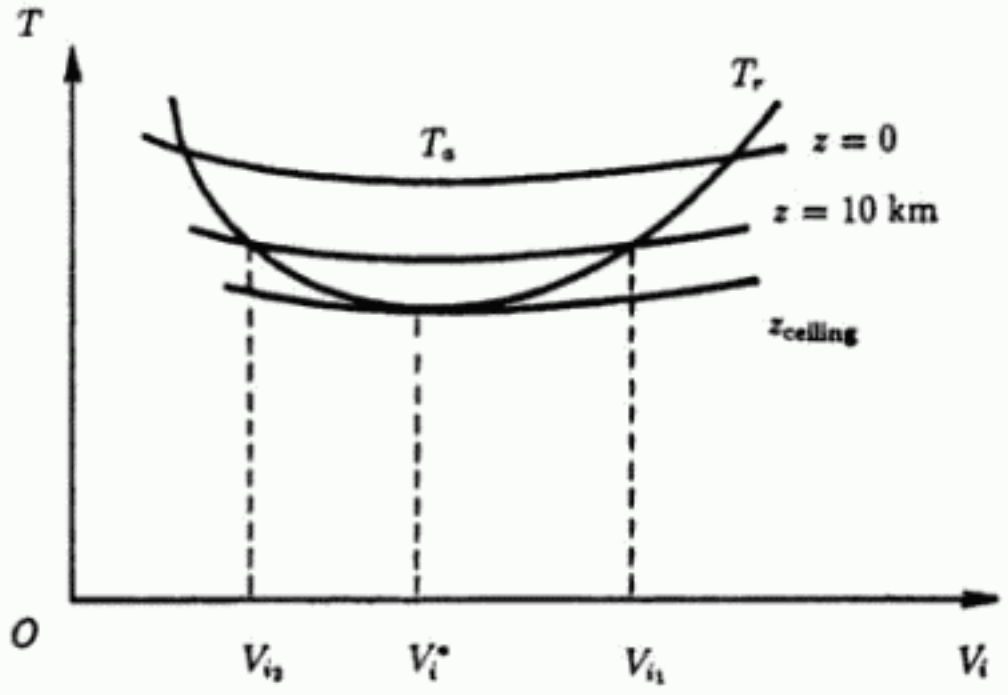

Figure 6.7: Variation of thrust available and thrust required as functions of V_i.

We first consider the case of constant thrust available. This is the case for rocket engines, or for turbojet engines with the necessary adjustment to keep constant thrust as the altitude increases. Then the equivalent speed V_i is the same at any two different altitudes and from

Eq. (6.28) the lift coefficient C_L, that is the angle-of-attack, is the same. But, from the transformation (6.27), with the same V_i, the true speed V is higher at higher altitude. As an example, for the same thrust available, if we fly at sea level with a true speed $V_0 = V_i$, at an altitude of 40,000 ft where the density is about one fourth the value at sea level, the true speed is twice the speed at sea level. This explains the fundamental characteristic of jet aircraft being faster at higher altitude with the same thrust available.

For the case of fixed throttle setting, let T_0 be the thrust available at sea level. We use the simple law

$$T_a = T_0\sigma \tag{6.42}$$

Then, T_a decreases as the altitude increases. From Fig. 6.7, we see that the cruise equivalent speed decreases and hence from Eq. (6.28) the angle-of-attack increases. But we cannot deduce any definite conclusion on the direction of variation of the true speed. When the two curves for T_r and T_a become tangential at the speed V_i^* which is the limit of the two speeds V_{i_1} and V_{i_2}, we reach the ceiling for the prescribed thrust throttle setting. To cruise at higher altitude, it is necessary to increase the thrust available. The propulsive ceiling is attained when the tangency occurs with the maximum thrust available. The density at the ceiling can be calculated by setting this maximum thrust available equal to the minimum thrust required as given in Eq. (6.40). We have

$$\frac{\rho_{\text{ceiling}}}{\rho_0} = \frac{W/E_{max}}{T_{max}} \tag{6.43}$$

where T_{max} is the maximum thrust at sea level. This propulsive ceiling is higher with lower weight and higher maximum lift-to-drag ratio.

6.4.3 Turbojet aircraft at supersonic speeds

We have seen above that, with a sufficiently high thrust available, flying at higher altitude leads to a higher true speed and, as a consequence, to a higher Mach number. Then, we may enter a speed regime where the effect of compressibility on the drag polar should be included in the analysis. The analysis can only be carried out with an accurate modeling of the drag polar and of the thrust available as functions of Mach number.

With the influence of Mach number, we consider the lift equation (6.11) for the analysis. If the relations (6.9) and (6.10) are used in Eq. (6.36), we obtain for the thrust required

$$\tau_r = M^2 C_D \tag{6.44}$$

where, by definition, τ_r is the dimensionless thrust required

$$\tau_r = \frac{2T_r}{kpS} \tag{6.45}$$

Similarly, we define the dimensionless thrust available

$$\tau_a = \frac{2T_a}{kpS} \tag{6.46}$$

Since T_a is a function of the engine throttle setting, of the altitude and the Mach number, for a prescribed throttle setting, and at a prescribed altitude, τ_a is a function of Mach number. While at subsonic speeds, τ_a is nearly constant, it increases with Mach number at supersonic speeds as shown in Fig. 6.8. On the other hand, if we use the Mach-dependent parabolic drag polar, as given by Eq. (6.4), in Eq. (6.44) and calculate the lift coefficient from the lift equation (6.11), we have, for the dimensionless thrust required at the flight altitude

$$\tau_r = M^2 \left[C_{D_0}(M) + \frac{\omega^2 K(M)}{M^4} \right] \tag{6.47}$$

where we recall the definition of the dimensionless weight, $\omega = 2W/kpS$. At low Mach number, we have the well known behavior of τ_r, namely that as the Mach number varies, τ_r first decreases to a minimum, then increases. In the transonic region, when M is approaching unity, we have a high increase in C_{D_0} in a very small interval ΔM. Therefore, in Eq. (6.47), in the transonic region, while the second term is nearly the same, we have a sharp increase in the first term. When the speed becomes clearly supersonic, after a steep rise near the sonic speed, $C_{D_0}(M)$ decreases to a near constant value. At very high Mach number, the lift coefficient C_L is small and therefore τ_r is nearly proportional to M^2. This gives a typical variation of τ_r as a function of M as seen in Fig. 6.8.

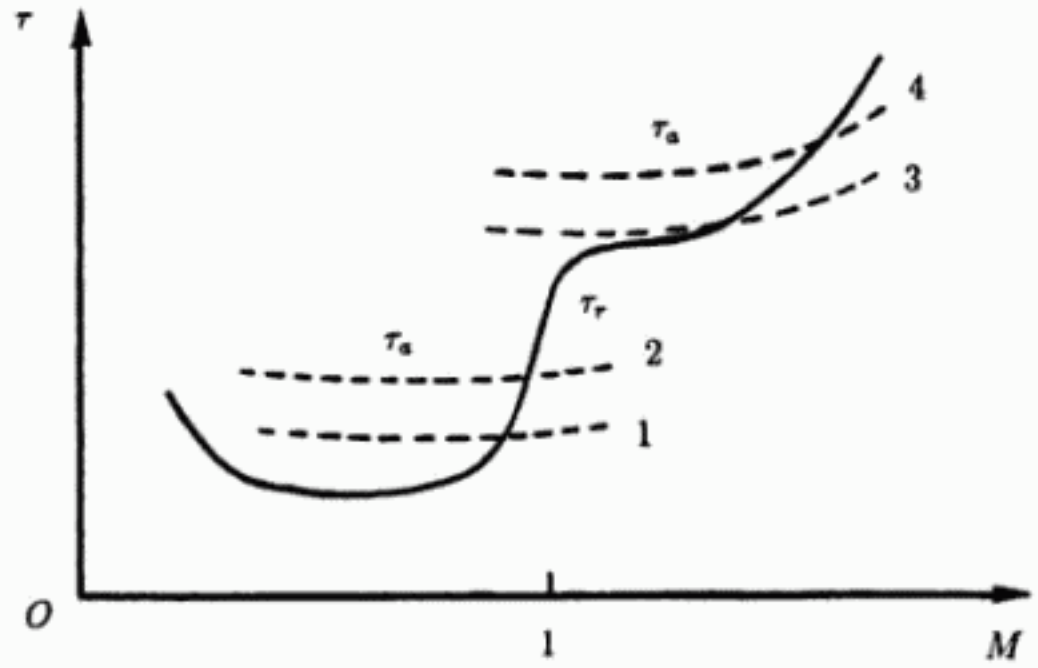

Figure 6.8: Variation of thrust available and thrust required as functions of Mach number.

Flight performance, in terms of the maximum speed depends, on the one hand, on the aerodynamic characteristics which govern the τ_r curve and, on the other hand, on the engine characteristics which govern the τ_a curve.

For a transonic aircraft the increase in the thrust required τ_r near to the sonic speed is very significant. A moderate increase in the thrust available τ_a provides only a small increase in the Mach number. This is shown as the thrust levels 1 and 2 in Fig. 6.8. This explains the phenomenon known as the sound barrier which restricted the speed of early jet aircraft to the subsonic regime.

For a supersonic aircraft, with improved aerodynamic characteristics, the sharp increase in the zero-lift drag coefficient, $C_{D_0}(M)$, in the transonic region is less severe. Then, with high-thrust engines, flight in the clearly supersonic region is accessible. In this region a small increase in the thrust available τ_a may lead to a significant increase in the Mach number. This is shown as the thrust levels 3 and 4 in Fig. 6.8.

In the supersonic region, depending on the aerodynamic and engine characteristics, the slopes of the curves τ_r and τ_a may be nearly equal and we may have up to three intersecting points for the two curves.

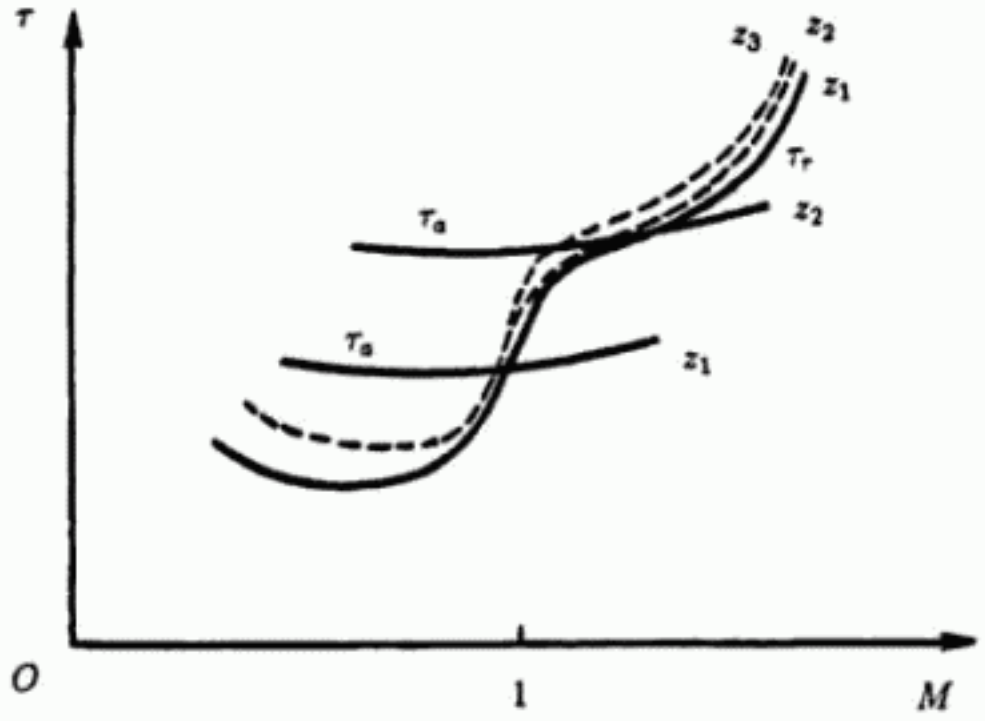

Figure 6.9: Variation of dimensionless thrust with altitude and Mach number.

Concerning the influence of altitude, again for a prescribed throttle setting, we assume that the thrust available is proportional to the density as given in Eq. (6.42). We recall from Chapter 3 the equation of state for a perfect gas

$$p = \rho R\theta \tag{6.48}$$

where here we use θ for the temperature in degrees Kelvin and R is the specific gas constant, $R = 287$ joules/kg°K. By using the thrust law (6.42) and the relation (6.48) in Eq. (6.46), we obtain

$$\tau_a = \frac{2T_0}{kR\rho_0 S\theta} \tag{6.49}$$

where T_0 is the thrust available at sea level, and at any throttle setting, it is a function of Mach number. Then, in the troposphere, up to an

altitude of 11 km, when the altitude increases the temperature of the air decreases and the dimensionless thrust available τ_a increases. As for the dimensionless thrust required τ_r, from Eq. (6.47), the second term $\omega^2 K/M^4$ increases with altitude since ω increases when the ambient pressure decreases. But this term, which is equal to KC_L^2 remains small at high speeds. We can consider the plot of τ_r as nearly fixed and hence, as seen in Fig. 6.9, the stabilized cruise Mach number increases as the altitude increases. This is shown at altitude levels $z_1 < z_2 < 11$ km.

In the stratosphere, $z > 11$ km, according to the standard atmosphere, the temperature remains constant. The plot of τ_a is fixed. In the same figure, we assume that it is now at the altitude $z_2 > 11$ km. If we fly at a higher altitude $z_3 > z_2$, and want to keep the same Mach number, by the lift equation (6.11), with a higher value of ω the lift coefficient C_L is higher, and consequently the drag coefficient C_D is higher. From Eq. (6.44) the dimensionless thrust required τ_r is higher, and to maintain steady cruise, it would require a higher value of τ_a. If the throttle setting is kept the same, the cruise Mach number will be smaller.

As a result of the discussion, with maximum throttle setting, the maximum stabilized Mach number of a turbojet aircraft is attained in the vicinity of the tropopause, at an altitude of 11 km.

6.4.4 The thrust coefficient

From engine and aerodynamic data, if sufficient knowledge of the influence of Mach number is available, we can consider the thrust equation (6.35) in the form

$$C_T = C_D \tag{6.50}$$

where by definition

$$C_T = \frac{2T_a}{\rho S V^2} = \frac{\tau_a}{M^2} \tag{6.51}$$

We shall refer to this dimensionless quantity as the thrust coefficient. At any given altitude, and for each throttle setting, τ_a is a function of Mach number. Hence C_T is also a function of Mach number and since τ_a only increases moderately with M , C_T decreases as Mach number increases. For a transonic aircraft, in the sonic region, the zero lift drag

coefficient $C_{D_0}(M)$ shows sharp increase. Since these aircraft can only attain a near sonic speed with a very small lift coefficient, the drag coefficient C_D is close to $C_{D_0}(M)$ as shown in Fig. 6.10.

It is seen from the figure that even for a 50% increase in the thrust available from level 1 to level 2, the maximum Mach number attained for these aircraft is nearly constant in the range 0.94 to 0.96. Since for any Mach number, the true speed is proportional to the speed of sound which, in turn, is proportional to the square root of the temperature, early speed records for jet aircraft which were essentially transonic were obtained during the summer in tropical countries.

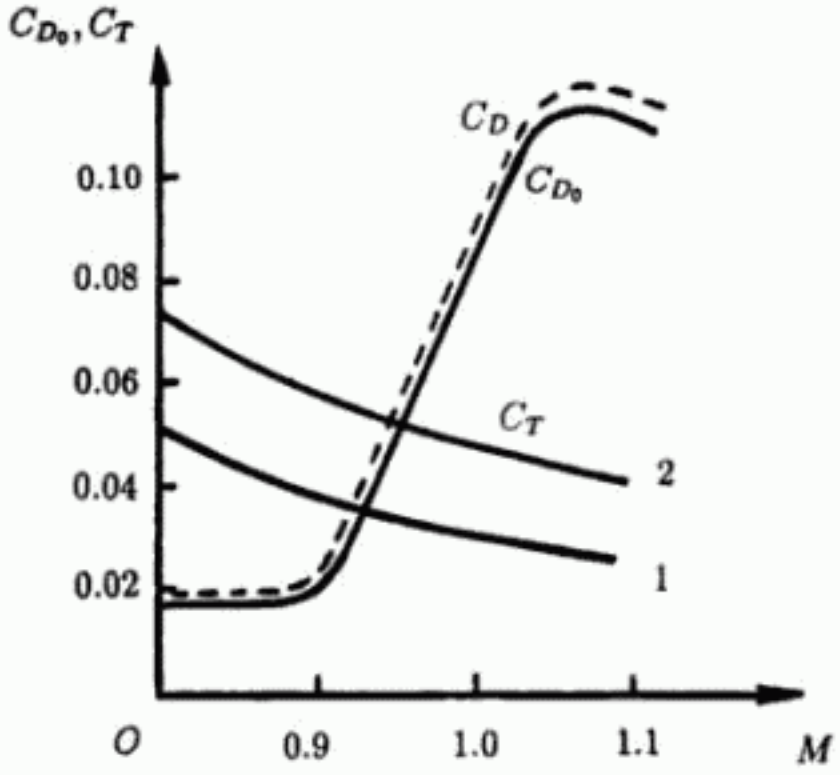

Figure 6.10: The variations of C_T and $C_{D_0}(M)$ for a transonic aircraft.

For supersonic aircraft, the sharp increase in $C_{D_0}(M)$ in the sonic region is less pronounced. A typical plot of the drag coefficient

$$C_D = C_{D_0}(M) + \frac{K(M)\omega^2}{M^2} \tag{6.52}$$

for a typical supersonic aircraft is shown in Fig. 6.11. On the same figure, we have plotted the thrust coefficient C_T at two levels, one slightly larger than the other.

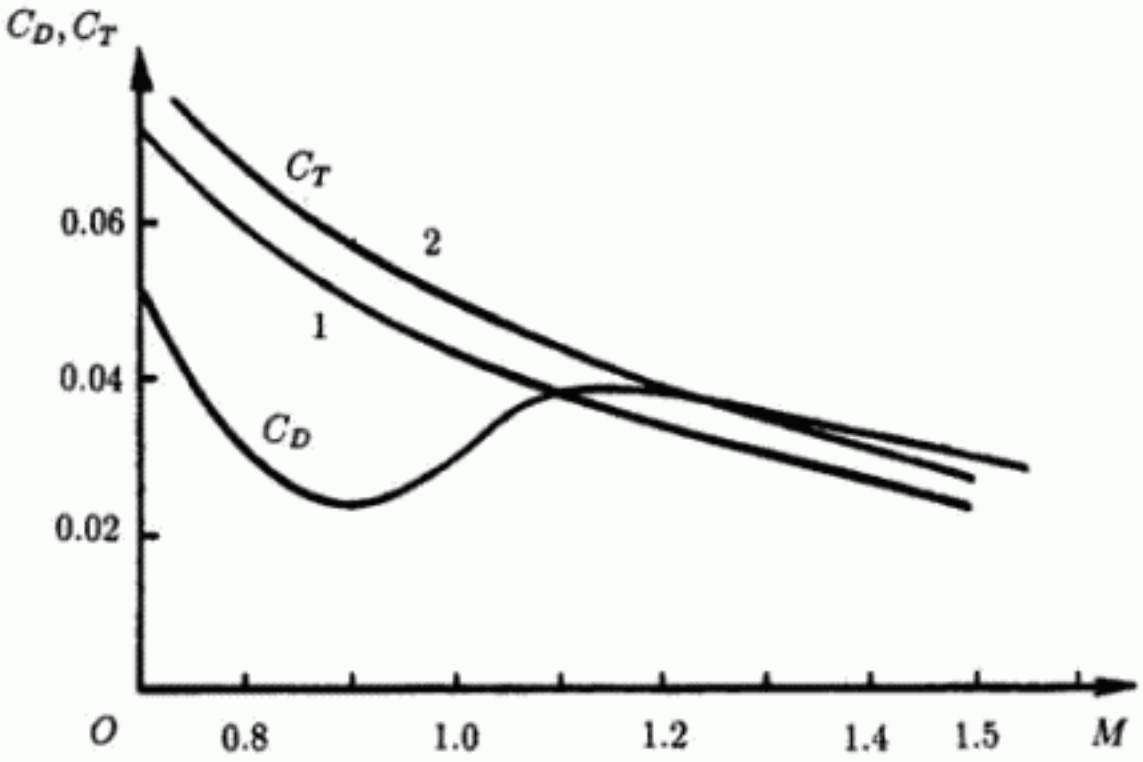

Figure 6.11: The variations of C_T and C_D for a supersonic aircraft.

The behavior of the thrust coefficient C_T is as before, but now at a higher level. It is seen from the thrust diagram that, at supersonic cruise Mach number, the curves C_D and C_T have nearly the same slope. A large increase in Mach number can be achieved with a moderate increase in thrust and a refinement of the aerodynamic characteristics to reduce the zero-lift drag coefficient $C_{D_0}(M)$.

6.5 Range and endurance of propeller driven aircraft

In static performance, we have evaluated the power required and the thrust required and their minima, the cruise speed, the aerodynamic ceiling and the propulsive ceiling. Performance characteristics

such as the fuel consumption to cover a prescribed distance, the distance travelled and the time of flight for a given amount of fuel, are obtained by integrating the equations of motion for a specific flight program. The analysis of these characteristics is within the domain of flight integral performance.

It is appropriate to prescribe the weight of the fuel and calculate the time of flight, or endurance, and the distance covered, or the range. Theoretically, we should specify a flight program in angle-of-attack, and in thrust as a function of time, and perform a numerical integration of the exact equations of motion in the vertical plane from the initial weight W_1 to the final weight W_2 to obtain the range x and the flying time t. For an analytical study, it is appropriate to neglect the inertia terms during the cruise and use the small angle approximation for the flight path to consider the equations for the equilibrium of the forces reproduced here for convenience. We have

$$T = \frac{1}{2}\rho S V^2 C_D \tag{6.53}$$

and

$$mg = \frac{1}{2}\rho S V^2 C_L \tag{6.54}$$

In addition, we have a general lift–drag relationship

$$f(C_D, C_L, M) = 0 \tag{6.55}$$

which is dependent on Mach number. When the drag polar is parabolic, we have the explicit relation (6.4).

The cruise is usually performed at constant altitude, or with a small variation, so that we have the equation for the distance travelled

$$\frac{dx}{dt} = V \tag{6.56}$$

Finally, we have the equation for the mass flow

$$\frac{dm}{dt} = -\frac{C_H}{g} \tag{6.57}$$

where C_H is the time rate of fuel consumption, to be made more explicit later with the propulsion system in use.

6.5.1 Practical flight programs

For cruise, we generally consider the following flight programs:

1. Flight at constant altitude and constant speed.
2. Flight at constant speed and constant angle-of-attack.
3. Flight at constant altitude and constant angle-of-attack.

Although Eq. (6.55) for the drag polar, and Eq. (6.57) for the mass flow rate are in the general form, Eqs. (6.53), (6.54) and (6.56) were derived with the conditions $dz/dt = 0$ and $dV/dt = 0$. Therefore, if these equations are used for integration to obtain range and endurance, the results are only strictly correct for the case of constant altitude–constant speed flight. Nevertheless, we propose to show that they are sufficiently accurate for use in the other two cases.

For the case of constant speed–constant angle-of-attack flight, we first have $dV/dt = 0$, and the thrust equation has the form

$$T = \frac{1}{2}\rho S V^2 C_D + W \sin\gamma \tag{6.58}$$

As for the lift equation, although here $\gamma \neq 0$, we can assume that its variation is infinitesimally small, that is $d\gamma/dt \approx 0$, and we have

$$\frac{1}{2}\rho S V^2 C_L = W \cos\gamma \tag{6.59}$$

With constant values for V and C_L and with the same value for γ, we have between the initial weight W_1 and the final weight W_2, the ratio

$$\frac{\rho_1}{\rho_2} = \frac{W_1}{W_2} \tag{6.60}$$

By Eq. (6.59), as W decreases during the cruise, the altitude slowly increases and this program is commonly referred to as the cruise-climb flight. We define the fuel weight fraction as the ratio of the fuel weight ΔW to the initial weight W_1

$$\zeta = \frac{\Delta W}{W_1} \tag{6.61}$$

The value of ζ is of the order of 10^{-1}. Then, by using an exponential atmosphere in Eq. (6.60), we have the gain in altitude, $\Delta z = z_2 - z_1$, as (see Exercise 6-8)

$$\beta \Delta z = \text{Log} \frac{1}{1-\zeta} = \zeta + \frac{1}{2}\zeta^2 + \frac{1}{3}\zeta^3 + \cdots \tag{6.62}$$

Over a total range x, the slope of the cruise-climb flight path is

$$\tan \gamma = \frac{\Delta z}{x} \tag{6.63}$$

Since $1/\beta = 7.163$ km, and x is of the order of 10^3 km, for any realistic value for the fuel weight fraction ζ, this flight path angle is indeed small. Then, we can set $\gamma = 0$ in Eqs. (6.58) and (6.59) for the calculation of range and endurance.

For the case of constant altitude–constant angle-of-attack flight, Eq. (6.54) is constantly satisfied, and the speed decreases as the square root of the weight. Since the speed decreases, $dV/dt \neq 0$, and theoretically we have an inertia force in the thrust equation

$$T = \frac{1}{2}\rho S V^2 C_D + m\frac{dV}{dt} \tag{6.64}$$

By assuming a constant deceleration we evaluate the average value from the initial speed V_1 to the final speed V_2

$$m\frac{dV}{dt} = m\frac{\Delta V}{\Delta t} = -m\frac{V_1 - V_2}{\Delta t}$$

On the other hand, if in Eq. (6.56) we use an average speed as the arithmetic mean for the integration, we have

$$x = \frac{1}{2}(V_1 + V_2)\Delta t$$

Then the mean value for the inertia force is

$$m\frac{dV}{dt} = -\frac{m}{2x}(V_1^2 - V_2^2) \tag{6.65}$$

From Eq. (6.54), we evaluate the ratio of the squares of the speed for constant values of ρ and C_L

$$\frac{V_1^2}{V_2^2} = \frac{W_1}{W_2} = \frac{1}{1-\zeta} \tag{6.66}$$

Therefore, we have

$$m\frac{dV}{dt} = -\frac{\zeta}{x(1-\zeta)}\left(\frac{1}{2}mV_2^2\right) \tag{6.67}$$

We express the kinetic energy in terms of the equivalent potential energy by the relation

$$\frac{1}{2}mV_2^2 = mg\Delta z \tag{6.68}$$

Then, the additional inertia force is

$$m\frac{dV}{dt} = -\frac{\Delta z\zeta W}{x(1-\zeta)} \tag{6.69}$$

From Eq. (6.68), with a speed of 150 m/s, the equivalent change in the altitude is 1.147 km. Therefore in Eq. (6.69), the coefficient of W is of the same order of magnitude as, or even less than, the value of $\tan\gamma$ from Eq. (6.63). We can then neglect the inertia term in the thrust equation with the same accuracy.

6.5.2 General considerations for range and endurance

For propeller driven aircraft, the variation of weight is proportional to the power, and we can write Eq. (6.57) as

$$\frac{dW}{dt} = -C_H = -\frac{c_p}{\eta_p}P_a \tag{6.70}$$

where $P_a = TV$ is the thrust power available, c_p is the power specific fuel consumption and η_p is a factor called the propeller efficiency. While c_p can be considered as constant, the propeller efficiency varies with the airspeed. With a variable pitch, constant-speed propeller, the value for η_p can be assumed to be constant over the practical range of cruise speed. Its value is in the range 0.80 to 0.90.

From Eq. (6.70), at each value of W, to maximize the time of flight, we must use the minimum P_a. Since for cruise, $P_a = P_r$, from Eq. (6.21), we must select the angle-of-attack to minimize the ratio $C_D/C_L^{3/2}$. For a parabolic drag polar, the solution is given in Eq. (6.24) with the minimum power from Eq. (6.25). Furthermore, since P_r^* is inversely proportional to $\sqrt{\sigma}$, maximum endurance is achieved at the lowest altitude.

We obtain the equation for the range by dividing Eq. (6.70) by Eq. (6.56). Then, we have

$$\frac{dW}{dx} = -\frac{c_p P_a}{\eta_p V_g} \tag{6.71}$$

The subscript g, introduced here for V_g , points to the fact that in Eq. (6.56), to find the actual distance by integration, the speed used must be the ground speed V_g with respect to the fixed earth used as the reference frame. If there is no wind, $V_g = V$. We first consider this case and, at each value of W, to maximize the range, we must use the minimum of the ratio P_a/V. By using the equations for equilibrium of force, we have simply

$$\frac{P_a}{V} = T = D = W\frac{D}{L} = \frac{W}{C_L/C_D} \tag{6.72}$$

Hence, the minimum of P_a/V is obtained by using the maximum lift-to-drag ratio. Furthermore, since altitude is not involved in the last two equations, range is independent of altitude. In practice, a flight at higher altitude decreases the flying time. Also, the power specific fuel consumption c_p is actually smaller at altitude and, in theory, the maximum range is largest at the critical altitude where we obtain the best engine performance.

To show the influence of wind on the angle-of-attack, we consider the case of a head wind of magnitude V_w. Then $V_g = V - V_w$, and we can write,

$$\frac{P_a}{V_g} = \frac{P_r\sqrt{\sigma}}{V_g\sqrt{\sigma}} = \frac{P_r\sqrt{\sigma}}{V_i - V_{iw}} \tag{6.73}$$

In this equation, V_i is the equivalent of the airspeed which we consider as the indicated speed and $V_{iw} = V_w\sqrt{\sigma}$ is the equivalent wind speed. We have shown in Fig. 6.5 that the plot of $P_r\sqrt{\sigma}$ versus V_i is independent of altitude. The plot is reproduced in Fig. 6.12.

Let I be the point on the V_i axis with abcissa V_{iw}. From Eq. (6.73), the minimum of P_a/V_g is at the point B obtained by drawing the tangent from the point I to the $P_r\sqrt{\sigma}$ curve. It is to the right of point A which corresponds to the case where $V_w = 0$. Since at A we have the angle-of-attack for maximum lift-to-drag ratio, for a head wind we are at the point B and with higher equivalent speed, the corresponding angle-of-attack is slightly smaller.

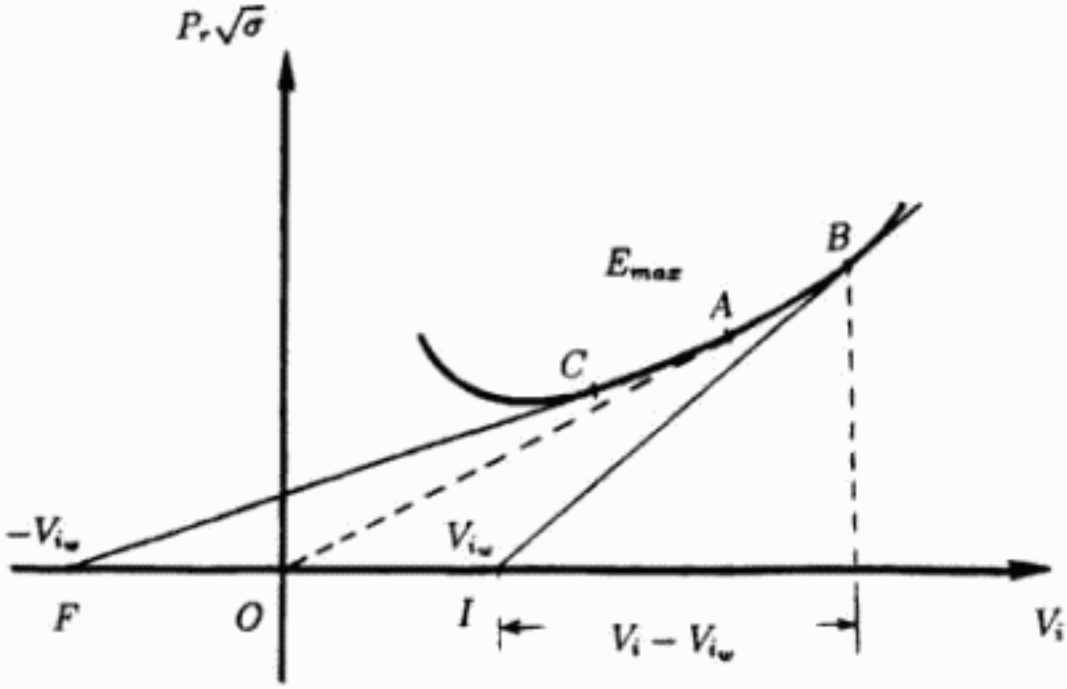

Figure 6.12: Influence of wind on the optimum angle-of-attack for maximum range.

By a similar discussion for a tail wind, we use the point F with abcissa, $-V_{iw}$, to obtain the optimum point C with lower equivalent speed and slightly higher angle-of-attack.

We should notice that although the curve $P_r\sqrt{\sigma}$ is the same for all altitudes, with the same wind speed V_w with respect to the ground, the equivalent value $V_w\sqrt{\sigma}$ is smaller at higher altitude and, as a consequence, the effect of the wind on the optimum angle-of-attack is smaller.

6.5.3 Calculation of range

Using Eq. (6.72) in Eq. (6.71) for the integration, we obtain for the range

$$x = -\frac{\eta_p}{c_p}\int_1^2 \frac{E}{W}\,dW \tag{6.74}$$

where $E = C_L/C_D$ is the lift-to-drag ratio. Since we have validated the use of the steady-state equations for the evaluation of cruise performance, if E is held constant, the quadrature can be performed to give

$$x = \frac{\eta_p}{c_p} E \operatorname{Log} \frac{W_1}{W_2} = \frac{\eta_p}{c_p} E \operatorname{Log} \frac{1}{1-\zeta} \tag{6.75}$$

This equation is commonly referred to as the Breguet range equation and it is valid for both the constant speed–constant angle-of-attack flight and the constant altitude–constant angle-of-attack flight. The maximum range is obtained by using the maximum lift-to-drag ratio, $E = E_{max}$ and, as discussed above, it is independent of altitude. The difference in the conduct of the two flight programs is that, for constant altitude flight the speed decreases as the square root of the weight and the power has to be adjusted accordingly, and for the case of constant speed flight, the aircraft enters a cruise-climb. In both cases the range is the same.

For the case of constant altitude–constant speed flight, since $E = L/D = W/D$, the integral (6.74) has the form

$$x = -\frac{\eta_p}{c_p} \int_1^2 \frac{dW}{D} \tag{6.76}$$

Now, since with a parabolic drag polar

$$\begin{aligned} W &= qSC_L \\ D &= qS(C_{D_0} + KC_L^2) \end{aligned} \tag{6.77}$$

with constant dynamic pressure $q = \rho V^2/2$, we can use C_L, which is varying proportionally with W, as a variable for integration to obtain

$$x = \frac{\eta_p}{c_p} \int_2^1 \frac{dC_L}{C_{D_0} + KC_L^2} \tag{6.78}$$

The integration of this equation can be easily performed and we obtained the solution (see Exercise 6-9),

$$x = \frac{2\eta_p E_{max}}{c_p} \operatorname{Arc\,tan} \frac{\lambda_1 - \lambda_2}{1 + \lambda_1 \lambda_2} \tag{6.79}$$

where by definition, λ is the normalized lift coefficient

$$\lambda = \frac{C_L}{\sqrt{C_{D_0}/K}} = \frac{C_L}{C_L^*} \tag{6.80}$$

We notice that the ratio of the lift coefficients is the same as the ratio of the weights

$$\frac{\lambda_2}{\lambda_1} = \frac{W_2}{W_1} = w \tag{6.81}$$

Hence, using λ_1 as the unknown parameter, to maximize the range, we must select the initial lift coefficient to maximize the argument of the arc tangent, namely the function

$$\frac{\lambda_1 - \lambda_2}{1 + \lambda_1\lambda_2} = \frac{(1-w)\lambda_1}{1 + w\lambda_1^2} = f(\lambda_1) \tag{6.82}$$

Upon performing the optimization, we obtain the solution $w\lambda_1^2 = 1$, and upon substituting into Eq. (6.79), we have the maximized range in the case of constant altitude–constant speed flight

$$x = \frac{2\eta_p E_{max}}{c_p} \text{Arc tan}\left[\frac{1}{2}\left(\sqrt{\frac{W_1}{W_2}} - \sqrt{\frac{W_2}{W_1}}\right)\right] \tag{6.83}$$

We notice that this formula depends only on the weight ratio. An alternate form, in terms of the fuel weight fraction, is

$$x = \frac{2\eta_p E_{max}}{c_p} \text{Arc tan}\left(\frac{\zeta}{2\sqrt{1-\zeta}}\right) \tag{6.84}$$

If we compare this solution with the solution (6.75) using $E = E_{max}$ for the maximum range in the case of constant angle-of-attack cruise, we can detect that the range with constant angle-of-attack is slightly superior (see Exercise 6-10). In all the flight programs, aircraft with high maximum lift-to-drag ratio, E_{max}, high values of propeller efficiency, η_p, and low values of specific fuel consumption, c_p, will have better range performance.

6.5.4 Calculation of endurance

By inverting Eq. (6.70), setting $P_a = P_r$, with P_r as given by Eq. (6.21), we have the equation for evaluating the time of flight

$$\frac{dt}{dW} = -\frac{\eta_p}{c_p}\sqrt{\frac{\rho S}{2W^3}}\frac{C_L^{3/2}}{C_D} \tag{6.85}$$

We first consider the case of constant speed–constant angle-of-attack flight. Let V_1 be the speed selected for cruise. We have shown from the lift equation (6.54) that the density decreases as the weight decreases and since the range for this cruise-climb has been obtained in Eq. (6.75) we simply divide it by the constant speed to have the endurance

$$t = \frac{\eta_p E}{c_p V_1} \operatorname{Log} \frac{1}{1-\zeta} \tag{6.86}$$

With V_1 computed from the lift equation, we have the alternate form

$$t = \frac{\eta_p}{c_p} \sqrt{\frac{\rho_1 S}{2W_1}} \frac{C_L^{3/2}}{C_D} \operatorname{Log} \frac{1}{1-\zeta} \tag{6.87}$$

The maximum endurance is obtained with the lowest starting flight altitude and the angle-of-attack which minimizes $C_D/C_L^{3/2}$. Using the solution (6.24), we have the maximum endurance for this case

$$\max t_{V,\alpha} = \frac{3^{3/4} E_{max}}{2} \frac{\eta_p}{c_p} \sqrt{\frac{\rho_1 S C_L^*}{2W_1}} \operatorname{Log} \frac{1}{1-\zeta} \tag{6.88}$$

We have used the subscript (V, α) to emphasize the fact that this formula concerns the case of constant speed–constant angle-of-attack flight.

We next consider the case of constant altitude–constant angle-of-attack flight. The time of flight is obtained by integrating Eq. (6.85) with respect to W. We have, for any altitude and angle-of-attack selected

$$t = \frac{\eta_p}{c_p} \sqrt{2\rho S} \frac{C_L^{3/2}}{C_D} \left(\frac{1}{\sqrt{W_2}} - \frac{1}{\sqrt{W_1}} \right) \tag{6.89}$$

This equation is known as the Breguet endurance equation. Again, it appears that to maximize endurance, we must fly at the lowest altitude with a minimum of $C_D/C_L^{3/2}$. In terms of the fuel weight fraction, we have maximum endurance for the case of constant altitude–constant angle-of-attack flight in the form

$$\max t_{z,\alpha} = 3^{3/4} E_{max} \frac{\eta_p}{c_p} \sqrt{\frac{\rho_1 S C_L^*}{2W_1}} \left(\frac{1}{\sqrt{1-\zeta}} - 1 \right) \tag{6.90}$$

Finally, for the usual practical flight program at constant altitude and constant speed, we can use Eq. (6.77) in Eq. (6.85) to obtain the integration with respect to C_L which is varying as

$$t = \frac{\eta_p}{c_p V_1} \int_2^1 \frac{dC_L}{C_{D_0} + KC_L^2} \tag{6.91}$$

where V_1 is the constant speed selected for cruise. This quadrature has been performed in the solution (6.79), and by using the lift equation to evaluate V_1, we obtain the time of flight in the form

$$t = \frac{2\eta_p E_{max}}{c_p} \sqrt{\frac{\rho_1 S C_L^*}{2W_1}} \sqrt{\lambda_1}\, \text{Arc tan} \left[\frac{(1-w)\lambda_1}{1 + w\lambda_1^2} \right] \tag{6.92}$$

where as defined in Eqs. (6.80) and (6.81) λ_1 is the initial normalized lift coefficient and w is the weight ratio. Again, in this flight program, the maximum endurance is achieved at the lowest flight altitude. For any weight ratio, the selected constant speed for cruise is optimum for the corresponding lift coefficient which maximizes the function

$$f(\lambda_1) = \sqrt{\lambda_1}\, \text{Arc tan} \left[\frac{(1-w)\lambda_1}{1 + w\lambda_1^2} \right] \tag{6.93}$$

By writing the equation $df/d\lambda_1 = 0$, we have a transcendental equation for evaluating the optimum value of λ_1 in terms of the fuel weight fraction $\zeta = 1 - w$. Although it is possible to find the solution as a power series in ζ, since ζ is small, the argument of the arc tangent is small and we can consider an approximation for the function

$$f(\lambda_1) = \frac{\zeta \lambda_1^{3/2}}{1 + \lambda_1^2} \tag{6.94}$$

This function is a maximum for $\lambda_1 = \sqrt{3}$ as expected and we obtain the maximum endurance for the case of constant altitude–constant speed flight in the form

$$\max t_{z,V} = 2(3)^{1/4} E_{max} \frac{\eta_p}{c_p} \sqrt{\frac{\rho_1 S C_L^*}{2W_1}}\, \text{Arc tan} \left(\frac{\sqrt{3}\zeta}{4 - 3\zeta} \right) \tag{6.95}$$

The three formulas (6.88), (6.90) and (6.95) for the maximum endurance in the three flight programs contain the same factor which

makes explicit the influence of E_{max}, W_1/S, ρ_1, η_p and c_p. It is clear that for aircraft with high values of maximum lift-to-drag ratio, E_{max}, high propeller efficiency, η_p, low wing loading, W_1/S, and low power specific fuel consumption, c_p, the endurance is longer. Also, flying at low altitude with a high value of the density ρ_1 extends the endurance. As for the flight programs, it can be shown analytically, or at least verified numerically that the flight at constant altitude–constant angle-of-attack gives the best endurance while the flight at constant speed–constant angle-of-attack gives the least endurance (see Exercise 6-11).

6.6 Range and endurance of turbojet aircraft

For turbojet aircraft flying at higher altitude and with a higher speed range, the equations for the equilibrium of the forces, at negligible flight path angle, reported in the previous section are still valid for the evaluation of cruise performance. The difference here is that the time rate of fuel consumption, C_H, is proportional to the thrust produced, and we write Eq. (6.57) for the mass flow as

$$\frac{dW}{dt} = -cT \tag{6.96}$$

where c is the thrust specific fuel consumption. It has been shown in Eq. (6.2) that c depends on the flight altitude z, the Mach number M, and engine control N. While at low Mach number, c is practically constant, at supersonic speeds the value of c depends strongly on engine control in terms of the rotor speed N. For good performance, it is necessary to have a low value for c and typically if N_{max} is the maximum permissible value for the rotor speed, c is a minimum when the ratio N/N_{max} is in the range 0.80 to 0.85.

Another factor to be considered in the evaluation of the performance in range and endurance of turbojet aircraft is the influence of Mach number. While an accurate assessment of the performance requires a careful analysis of detailed aerodynamic and propulsive data, the discussion of the static performance presented in Sections 6.3 and 6.4 has provided us with sufficient information for a qualitative and even quantitative evaluation of integral performance.

6.6.1 General considerations for range and endurance

By dividing Eq. (6.96) by Eq. (6.56), we have the equation for range

$$\frac{dW}{dx} = -c\frac{T_a}{V} \tag{6.97}$$

Since we have validated the equations (6.53) and (6.54) for use in cruise integral performance, even in the case of slow variations in altitude and speed, we can use these equations to rewrite Eq. (6.97) in the form

$$\frac{dW}{dx} = -c\sqrt{\frac{\rho S W}{2}}\frac{C_D}{C_L^{1/2}} \tag{6.98}$$

At any altitude, as specified by the value of the density ρ, and with the current weight W, to maximize the range instantaneously, it is necessary to minimize the function $c(C_D/C_L^{1/2})$. Depending on the type of aircraft, we have the following optimum cruise conditions.

a) Subsonic aircraft

At clearly subsonic speed, that is for a Mach number below the critical Mach number for a sharp increase in the zero-lift drag coefficient $C_{D_0}(M)$, we neglect the effect of compressibility of air. For a constant value of c, the angle-of-attack selected for cruise is the angle-of-attack α_1 which minimizes the function $C_D/C_L^{1/2}$. For a parabolic drag polar, we have the solution

$$\begin{aligned} C_L &= \sqrt{\frac{C_{D_0}}{3K}} = \frac{\sqrt{3}}{3}C_L^* \\ C_D &= \frac{4}{3}C_{D_0} = \frac{2}{3}C_D^* \end{aligned} \tag{6.99}$$

With this optimum lift control, the right-hand side of Eq. (6.98) is further minimized with the lowest possible value for the density ρ. Then, to maximize the range we must fly at the highest possible altitude. But, since $T_a = T_r$ for cruise, by considering Eq. (6.37) for T_r and the law of variation of thrust (6.42) for T_a, we have, upon using the lift control (6.99), the equality for cruise at optimum angle of attack α_1,

$$T_a = T_0\frac{\rho}{\rho_0} = \frac{2}{\sqrt{3}}\frac{W}{E_{max}} \tag{6.100}$$

From this equation, we can see that before reaching the propulsive ceiling where at its maximum value $T_a = W/E_{max}$, there is an altitude, above which, the thrust is not sufficient to cruise at the angle-of-attack α_1. Therefore, for subsonic aircraft, if by operational consideration the cruise altitude is prescribed, and if it is low enough, the optimum angle-of-attack is α_1, and higher cruise altitude provides longer range. If the altitude is sufficiently high, close to the propulsive ceiling, we write the cruise condition $T_a = T_r$ as

$$T_0 \frac{\rho}{\rho_0} = \frac{W}{C_L/C_D} \tag{6.101}$$

By solving for ρ and upon substituting in Eq. (6.98), we obtain

$$\frac{dW}{dx} = -c\sqrt{\frac{\rho_0 S}{2T_0}} W \frac{C_D^{3/2}}{C_L} \tag{6.102}$$

To maximize the range, we minimize the right-hand side of this equation. Since T_0 is the thrust at sea level, it is benificial to use the maximum possible thrust. In cruise, it is usually set at 83% of the maximum thrust. The optimum angle-of-attack to be selected is the angle α_2 which minimizes the function $C_D/C_L^{2/3}$. For a parabolic drag polar, we have the solution

$$\begin{aligned} C_L &= \sqrt{\frac{C_{D_0}}{2K}} = \frac{\sqrt{2}}{2} C_L^* \\ C_D &= \frac{3}{2} C_{D_0} = \frac{3}{4} C_D^* \end{aligned} \tag{6.103}$$

The corresponding angle-of-attack α_2 is higher than α_1 but is less than the value α^* for maximum lift-to-drag ratio. The optimum altitude is given by Eq. (6.101) with the lift-to-drag ratio evaluated with the solution (6.103).

b) Transonic aircraft

The equation (6.102) is valid for subsonic speed, and to maximize the range, the so-called installed thrust T_0 must be used at the maximum allowable value. For transonic aircraft, with sufficient thrust, the corresponding cruise speed is high and the Mach number is near to the

critical Mach number for a sharp increase in $C_{D_0}(M)$. By considering a typical variation of $C_{D_0}(M)$ as shown in Fig. 6.10, we may assume that the cruise Mach number is restricted to a narrow range where we have a sudden rise in $C_{D_0}(M)$. If in Eq. (6.97), we put $T_a = T_r = W/E$, and change V into Mach number, we have

$$\frac{dW}{dx} = -\frac{cW}{a(ME)} \tag{6.104}$$

where a is the speed of sound at the flight altitude. If we assume that the optimum cruise is in the stratosphere where the speed of sound is constant, then since the Mach number is nearly stationary, the minimization of the right hand side of this equation leads to selecting the angle-of-attack α^* for maximum lift-to-drag ratio, $E = E_{max}$. Then, a practical approximation for maximum range of transonic aircraft is that the flight is at maximum lift-to-drag ratio, with $\alpha = \alpha^*$, using the Mach number which starts a sharp increase in $C_{D_0}(M)$ and at the altitude which allows steady cruise under these conditions.

c) Supersonic aircraft

For supersonic aircraft, the aerodynamic and propulsive characteristics are such that the equilibrium of forces allows the selection of the cruise altitude and the cruise Mach number over a wider range. If we use the Mach dependent parabolic drag polar as given in Eq. (6.4), and Eq. (6.11) for the lift equation, the negative of the right-hand side of Eq. (6.104) has the form

$$F(p, M) = \frac{kpS}{2a}\, c(p, M) M \left[C_{D_0}(M) + \frac{K(M)\omega^2}{M^4} \right] \tag{6.105}$$

where we recall the definition of the dimensionless wing loading

$$\omega = \frac{2W}{kpS} = \omega(p) \tag{6.106}$$

Supersonic cruise is generally in the stratosphere so that we can consider constant speed of sound. Still, the function $F(p, M)$ depends on the ambient pressure, that is on the altitude, and on the Mach number. We have a parametric optimization problem, namely to find the

altitude pressure p, and the Mach number M to minimize this function. For any current weight, there exist a cruise Mach number, and a corresponding cruise altitude which minimize the function F. If this solution is used, the cruise range is maximized.

Concerning the time of flight, we invert the equation (6.96) and set $T_a = T_r$, with T_r as given in Eq. (6.37) to obtain

$$\frac{dt}{dW} = -\frac{E}{cW} \tag{6.107}$$

From this equation, to maximize the endurance instantaneously, the use of maximum lift-to-drag ratio, $E = E_{max}$ is dictated. To a first order of approximation, at low speed where the effect of Mach number on the drag polar can be neglected, since the altitude is not involved in Eq. (6.107), endurance is independent of altitude. But, from the lift equation (6.54), at any lift coefficient selected for cruise, flight at higher altitude leads to higher speed, so that there exists an altitude where the cruise Mach number reaches the critical Mach number which affects the drag polar. Above this altitude, the cruise Mach number keeps increasing and $E_{max}(M)$, as a function of the Mach number, decreases. The endurance decreases.

6.6.2 Calculation of endurance

We first evaluate the time of flight since its discussion is simpler. This is obtained by integrating Eq. (6.107) under a specific flight program.

For constant angle-of-attack cruise, E is constant and with a constant c, we have the solution

$$t = \frac{E}{c} \operatorname{Log} \frac{W_1}{W_2} = \frac{E}{c} \operatorname{Log} \frac{1}{1-\zeta} \tag{6.108}$$

The formula is valid for both the constant speed–constant angle-of-attack flight and the constant altitude–constant angle-of-attack flight. The only difference is that with constant speed, from the lift equation (6.54) as the weight decreases, the density decreases and the aircraft enters a cruise-climb mode, and with constant altitude, the speed decreases as the square root of the weight. The maximum endurance is

obtained by using $E = E_{max}$ in Eq. (6.108), and at low speed it is independent of altitude. If we use the lift equation (6.11), we have for the cruise Mach number, with the lift coefficient at maximum lift-to-drag ratio.

$$M = \sqrt{\frac{\omega}{C_L^*}} \tag{6.109}$$

At a certain altitude, where ω is sufficiently large, this Mach number attains the critical Mach number which starts to decrease $E_{max}(M)$. Above this altitude, the maximum endurance decreases as the altitude increases.

The maximum endurance flight is only of interest for missions requiring the longest stay of the aircraft in the air. Also, it is used in holding patterns. Therefore, in practice, the flight is at low altitude, with low Mach number as given by Eq. (6.109), with the angle-of-attack α^* and the corresponding thrust to satisfy the thrust equation.

Since in practice, the flight is at constant altitude and constant speed, we now integrate Eq. (6.107) under these conditions. We use Eq. (6.77) with constant q to change the variable of integration from W to C_L. Then, we have with a constant value for the thrust specific fuel consumption

$$t = \frac{1}{c}\int_2^1 \frac{dC_L}{C_{D_0} + KC_L^2} \tag{6.110}$$

This integral is the same as the integral in Eq. (6.78) and we obtain with constant C_{D_0} and K

$$t = \frac{2E_{max}}{c} \text{Arc tan}\left[\frac{(1-w)\lambda_1}{1+w\lambda_1^2}\right] \tag{6.111}$$

where $w = W_2/W_1$ is the weight ratio and $\lambda_1 = C_{L_1}/C_L^*$ is the starting normalized lift coefficient. Since, in terms of the equivalent speed, which we may take as the indicated speed in incompressible fluid

$$C_{L_1} = \frac{2W_1}{\rho_0 S V_{i_1}^2} \tag{6.112}$$

for any constant speed V_{i_1} selected for cruise we have a well determined value for λ_1, with this same V_{i_1} the endurance is the same at all altitudes, provided that the cruise Mach number is less than the critical

Mach number. We have seen above that the maximum of the arc tangent in Eq. (6.111) is attained when $w\lambda_1^2 = 1$. Then, for cruise with constant altitude and constant speed, the maximum endurance is

$$t = \frac{2E_{max}}{c} \text{Arc tan}\left(\frac{\zeta}{2\sqrt{1-\zeta}}\right) \tag{6.113}$$

This is slightly less than the endurance calculated from Eq. (6.108) with $E = E_{max}$ (see Exercise 6-12).

In the case of constant altitude–constant speed cruise, the dynamic pressure is constant and the lift coefficient, being proportional to the weight, slowly decreases. At any altitude, the optimum speed for cruise is calculated from

$$\frac{1}{2}\rho V^2 = \frac{\sqrt{W_1 W_2}}{S C_L^*} \tag{6.114}$$

During the optimum cruise, the lift coefficient decreases according to the relation

$$\frac{C_L}{C_L^*} = \frac{W}{\sqrt{W_1 W_2}} \tag{6.115}$$

Hence, it is near the value at maximum lift-to-drag ratio.

6.6.3 Calculation of range

For the range, we integrate Eq. (6.98) or its equivalent. For the moment, we restrict the analysis to a fixed drag polar. We first consider the case of constant altitude–constant angle-of-attack flight. Equation (6.98) can be integrated with respect to weight to give

$$x = \frac{2}{c}\sqrt{\frac{2W_1}{\rho_1 S}} \frac{C_L^{1/2}}{C_D}(1 - \sqrt{1-\zeta}) \tag{6.116}$$

At any flight altitude, as specified by the air density ρ_1, the optimum angle-of-attack is α_1 which minimizes $C_D/C_L^{1/2}$. If solution (6.99) is used, we have the maximized range.

$$\max x_{z,\alpha} = \frac{3^{3/4} E_{max}}{c}\sqrt{\frac{2W_1}{\rho_1 S C_L^*}}(1 - \sqrt{1-\zeta}) \tag{6.117}$$

This range increases with altitude, provided that the corresponding Mach number remains subsonic. The cruise speed, and consequently the cruise Mach number, decreases as the square root of the weight.

For the case of constant speed–constant angle-of-attack flight, the integration of Eq. (6.104) with constant $V = Ma$ and constant E leads to the Breguet-Leduc formula

$$x = \frac{VE}{c} \operatorname{Log} \frac{1}{1-\zeta} \tag{6.118}$$

From the lift equation (6.54), since V and C_L are constant, the density decreases with the weight and the aircraft enters a cruise-climb mode. By evaluating the constant speed at the initial point, we obtain the equivalent formula

$$x = \frac{1}{c}\sqrt{\frac{2W_1}{\rho_1 S}} \frac{C_L^{1/2}}{C_D} \operatorname{Log} \frac{1}{1-\zeta} \tag{6.119}$$

Again, the optimum constant angle-of-attack selected is α_1, and at any starting altitude, the maximized range is

$$\max x_{V,\alpha} = \frac{3^{3/4} E_{max}}{2c} \sqrt{\frac{2W_1}{\rho_1 S C_L^*}} \operatorname{Log} \frac{1}{1-\zeta} \tag{6.120}$$

This range increases with altitude, provided that the corresponding cruise Mach number does not change the aerodynamic characteristics. The optimum operating altitude is near to the propulsive ceiling.

For the usual case of constant altitude–constant speed flight, if V is the speed selected for cruise, the range is simply proportional to the time of flight. This time is given in Eq. (6.111), and by using the lift equation (6.54) to express the constant speed in terms of the initial weight and the initial lift coefficient, we obtain for the range

$$x = \frac{2E_{max}}{c}\sqrt{\frac{2W_1}{\rho_1 S C_L^*}} \frac{1}{\sqrt{\lambda_1}} \operatorname{Arc\,tan}\left[\frac{(1-w)\lambda_1}{1+w\lambda_1^2}\right] \tag{6.121}$$

To maximize the range, we must fly at the highest possible altitude. At any flight altitude the initial normalized lift coefficient λ_1 selected must be such that it maximizes the function

$$f(\lambda_1) = \frac{1}{\sqrt{\lambda_1}} \operatorname{Arc\,tan}\left[\frac{(1-w)\lambda_1}{1+w\lambda_1^2}\right] \tag{6.122}$$

By writing the equation $df/d\lambda_1 = 0$, we have a transcendental equation for evaluating the optimum value of λ_1 in terms of the fuel weight fraction $1 - w = \zeta$. The solution can be found analytically as a power series in ζ. But since ζ is small we can consider an approximation for the function

$$f(\lambda_1) = \frac{\zeta\sqrt{\lambda_1}}{1+\lambda_1^2} \tag{6.123}$$

This function is a maximum for $\lambda_1^2 = 1/3$ as expected and we obtain the maximum range for the case of constant altitude–constant speed flight in the form

$$\max x_{s,V} = \frac{2(3)^{1/4}E_{max}}{c}\sqrt{\frac{2W_1}{\rho_1 S C_L^*}}\ \text{Arc tan}\left(\frac{\sqrt{3}\zeta}{4-\zeta}\right) \tag{6.124}$$

The three formulas (6.117), (6.120) and (6.124) for maximum range in the three flight programs contain the same factor which makes explicit the influence of E_{max}, W_1/S, ρ_1 and c. It is clear that for aircraft with high values of maximum lift-to-drag ratio, E_{max}, high wing loading W_1/S, low thrust specific fuel consumption, c, the range is longer. Also, flying at high altitude with a low value of air density ρ_1, extends the range. As for the flight programs, it can be shown analytically, or at least verified numerically that flight at constant speed–constant angle-of-attack gives the best range and flight at constant altitude–constant speed gives the least range (see Exercise 6-13).

6.7 Supersonic cruise

The formulas for range derived previously have shown that, for turbojet aircraft, flying at higher altitude extends the range considerably. But even with very high thrust and high aerodynamic ceiling we cannot use these formulas with ρ_1 approaching zero for infinite range since at a particular high altitude, the corresponding cruise Mach number would exceed the critical Mach number. The maximum lift-to-drag ratio decreases and the range decreases. We have shown in Subsection 6.6.1 that there exist a cruise Mach number and a cruise altitude for best range in the case where the propulsion system is adequate for flight at high altitude and high speed.

Under the assumption that the equations for nearly steady cruise can be used for the analysis, we consider the two formulas most appropriate for the discussion of the influence of Mach number, namely the Breguet-Leduc formula (6.118) for constant speed–constant angle-of-attack flight, and the expression (6.121) for constant altitude–constant speed flight.

6.7.1 Cruise at constant speed and constant angle-of-attack

We recall that to obtain Eq. (6.118), we integrate Eq. (6.104) with constant speed and constant angle-of-attack. Furthermore, we recall the lift equation written in terms of Mach number

$$\omega = M^2 C_L \tag{6.125}$$

where $\omega = 2W/kpS$. We assume that the flight is in the stratosphere, and hence the speed of sound is constant. This leads to constant Mach number. At fixed Mach number, with the selected constant angle-of-attack, the lift-to-drag ratio ($E = C_L/C_D$) is fixed. This validates Eq. (6.118). The range is expressed as the product of a function which depends solely on the fuel weight fraction and a factor $F = VE/c$, most appropriately called the range factor. If we use the drag polar (6.4), and the lift equation (6.125), we have the range factor in the form

$$F(\omega, M) = \frac{a\,\omega}{c[MC_{D_0}(M) + K\omega^2 M^{-3}]} \tag{6.126}$$

At any current weight, ω, which is inversely proportional to the ambient pressure, represents the altitude. Since the range factor depends on the altitude, and the Mach number, we have the optimum conditions for maximum range

$$\begin{aligned} \frac{\partial F}{\partial \omega} &= 0 \\ \frac{\partial F}{\partial M} &= 0 \end{aligned} \tag{6.127}$$

If the thrust specific fuel consumption c depends only on the Mach number, the first equation leads to the relation

$$\omega = M^2 \sqrt{\frac{C_{D_0}}{K}} \tag{6.128}$$

Upon substituting into Eq. (6.126), we are led to the maximization with respect to M of the function

$$F(M) = \frac{aM}{2c\sqrt{C_{D_0}(M)K(M)}} = \frac{aME_{max}(M)}{c(M)} \tag{6.129}$$

The optimum Mach number for cruise is obtained by solving the equation

$$\frac{d}{dM}\left(\frac{ME_{max}}{c}\right) = 0 \tag{6.130}$$

We have exactly the same equation by combining the two equations (6.127). If this Mach number is used in Eq. (6.128) we see that since ω is constant, the aircraft enters a cruise-climb mode. In practice, if flight is restrained at constant altitude, we can divide the flight trajectory into segments and in each segment adopt an average altitude near to the optimum which increases as the weight decreases. Since the drag polar is fixed at a fixed value of Mach number, the optimum relation (6.128) shows that flight is continuously at maximum lift-to-drag ratio.

By using the optimum Mach number, as calculated from Eq. (6.130), in Eq. (6.129) for the range factor, we obtain upon substituting into Eq. (6.118), the maximum range for constant speed–constant angle-of-attack cruise climb in the stratosphere

$$x = \frac{a_* ME_{max}}{c} \operatorname{Log} \frac{1}{1-\zeta} \tag{6.131}$$

For flight in the troposphere, we have a similar but approximate formula for the range (see Exercises 6-19 and 6-20).

6.7.2 Cruise at constant altitude and constant speed

In this flight program at constant altitude, the speed of sound is constant, and at constant speed we have constant Mach number. Hence, the use of Eq. (6.121) for range is justified. We first transform this equation by noticing that

$$\sqrt{\frac{2W_1}{\rho_1 S C_L^*}} \frac{1}{\sqrt{\lambda_1}} = V_1 = aM \tag{6.132}$$

where M is the constant Mach number used for cruise. Furthermore, using the lift equation (6.125), we have

$$\lambda_1 = \frac{C_{L_1}}{C_L^*} = \frac{\omega_1}{C_L^* M^2} \tag{6.133}$$

Therefore, in terms of the Mach number, the range for cruise, has the form

$$x = \frac{2aME_{max}}{c} \text{Arc tan}\left[\frac{C_L^* M^2(1-w)\omega_1}{C_L^{*2} M^4 + w\omega_1^2}\right] \tag{6.134}$$

where, for convenience, we recall the definition

$$\begin{aligned} w &= \frac{W_2}{W_1}, \qquad & \omega_1(p) &= \frac{2W_1}{kpS} \\ E_{max}(M) &= \frac{1}{2\sqrt{KC_{D_0}}}, & C_L^*(M) &= \sqrt{\frac{C_{D_0}}{K}} \end{aligned} \tag{6.135}$$

Since the thrust specific fuel consumption, c, is a function of altitude and Mach number, and the speed of sound a, is a function of altitude when expressed in terms of the altitude pressure, the range is clearly a function of altitude and Mach number. We shall assume that c is a function of Mach number only and for generality we include the case where the optimum flight altitude may be in the troposphere.

Let δ be the ratio of the ambient pressure to the pressure at the tropopause (subscript $*$),

$$\delta = \frac{p}{p_*} \tag{6.136}$$

Then, as has been shown in Chapter 3, for a standard atmosphere, we have the simple law

$$\frac{p}{p_*} = \left(\frac{\rho}{\rho_*}\right)^b \tag{6.137}$$

with the constant exponent $b = 1.235$ in the troposphere and $b = 1$ in the stratosphere. Then, using Eq. (6.10), we have the ratio for the speed of sound

$$\frac{a}{a_*} = \left(\frac{p}{p_*}\right)^{(b-1)/2b} = \delta^{(b-1)/2b} \tag{6.138}$$

With this law, Eq. (6.134), in terms of δ and M, has the new form

$$x = 2a_* \frac{ME_{max}}{c} \delta^{(b-1)/2b} \text{Arc tan}\left[\frac{C_L^* M^2(\omega_{1*} - \omega_{2*})\delta}{C_L^{*2} M^4 \delta^2 + \omega_{1*}\omega_{2*}}\right] \tag{6.139}$$

where ω_{1*} and ω_{2*} are constants defined as

$$\omega_{1*} = \frac{2W_1}{kp_*S}, \qquad \omega_{2*} = \frac{2W_2}{kp_*S} \tag{6.140}$$

At each cruise altitude, as specified by the pressure ratio δ, the optimum Mach number is obtained from the equation $\partial x/\partial M = 0$, written explicitly as

$$\left(\frac{ME_{max}}{c}\right)' \text{Arc tan}\left[\frac{C_L^* M^2(\omega_{1*} - \omega_{2*})\delta}{C_L^{*2} M^4 \delta^2 + \omega_{1*}\omega_{2*}}\right] + \frac{ME_{max}}{c} \frac{(\omega_{1*} - \omega_{2*})\delta(C_L^* M^2)'(\omega_{1*}\omega_{2*} - \delta^2 C_L^{*2} M^4)}{[C_L^* M^2 \delta(\omega_{1*} - \omega_{2*})]^2 + [\delta^2 C_L^{*2} M^4 + \omega_{1*}\omega_{2*}]^2} = 0 \tag{6.141}$$

where the prime denotes the derivative with respect to M. If the optimum cruise altitude is to be evaluated, we add the equation $\partial x/\partial \delta = 0$, written as

$$\frac{b-1}{2b} \text{Arc tan}\left[\frac{C_L^* M^2(\omega_{1*} - \omega_{2*})\delta}{C_L^{*2} M^4 \delta^2 + \omega_{1*}\omega_{2*}}\right] + \frac{(\omega_{1*} - \omega_{2*})\delta(C_L^* M^2)(\omega_{1*}\omega_{2*} - \delta^2 C_L^{*2} M^4)}{[C_L^* M^2 \delta(\omega_{1*} - \omega_{2*})]^2 + [\delta^2 C_L^{*2} M^4 + \omega_{1*}\omega_{2*}]^2} = 0 \tag{6.142}$$

By eliminating the arc tangent between the last two equations we obtain a resulting formula for evaluating the optimal Mach number

$$\left(\frac{ME_{max}}{c}\right)' (C_L^* M^2) = \frac{b-1}{2b} \frac{ME_{max}}{c} (C_L^* M^2)' \tag{6.143}$$

We can write this equation as

$$\frac{d}{dM}\left[\frac{M^{1/b} E_{max}(M)}{c(M) C_L^{*(b-1)/2b}}\right] = 0 \tag{6.144}$$

We obtain the following interesting result. With an adequate propulsion system, for given aerodynamic characteristics as specified by the functions $C_{D_0}(M)$ and $K(M)$, and for a thrust specific fuel consumption dependent on Mach number, $c = c(M)$, the optimum Mach number for cruise with maximum range is the one that maximizes the function

$$G(M) = \frac{M^{1/b} E_{max}(M)}{c(M)[C_L^*(M)]^{(b-1)/2b}} \tag{6.145}$$

This function G, which is inversely proportional to c, has the dimensions of time. For constant c, we can omit this factor and the optimum cruise Mach number is purely a function of the aerodynamic characteristics. For flight in the stratosphere, $b = 1$, and Eq. (6.144) is reduced to Eq. (6.130).

For a transonic aircraft, if we follow the variation of the function $G(M)$, then at low Mach number, it is proportional to $M^{1/b}$ and we are led to fly at high Mach number. But beyond the critical Mach number, if we assume a sudden rise in $C_{D_0}(M)$ during a small variation ΔM, then within this interval $G(M)$ is inversely proportional to $C_{D_0}^{(3b-1)/4b}$. The function starts to decrease. Hence, it is expected that for this type of aircraft the optimum Mach number is subsonic, at the point where there is a sharp increase in the function $C_{D_0}(M)$.

For a supersonic aircraft, there exists another optimum Mach number in the supersonic range. Although the value E_{max} is lower at this Mach number, the optimum condition (6.142) has to be satisfied and it generally leads to selecting the high altitude–high Mach number program for cruise.

In summary, when sufficient data for aerodynamic and engine characteristics are available, the optimum Mach numbers which locally maximize the function $G(M)$ as defined in Eq. (6.145) can be evaluated numerically, or graphically for flight in the troposphere with $b = 1.235$ and in the stratosphere with $b = 1$. Then, Eq. (6.142) can be solved for the optimum cruise altitude, in terms of the pressure ratio $\delta = p/p_s$. In particular, for flight in the stratosphere, we immediately have the solution

$$\delta = \frac{2\sqrt{W_1 W_2}}{k p_s S} \frac{1}{M^2 C_L^*} \tag{6.146}$$

For this altitude to exist, we must have the condition $\delta < 1$ and hence, in general, the cruise corresponds to high Mach number, that is at supersonic speed.

As an example, we have plotted in Fig. 6.13, the variation of the function $G(M)$ for a light-weight, supersonic cruiser. For this aircraft, in the troposphere we have two optimum Mach numbers, $M = 0.831$ and $M = 1.393$, and in the stratosphere, we also have two optimum Mach numbers, $M = 0.859$ and $M = 1.420$. By using the optimum Mach numbers for the case of $b = 1$ in Eq. (6.146) for the optimum cruise altitude, we would generally find that only the high Mach number

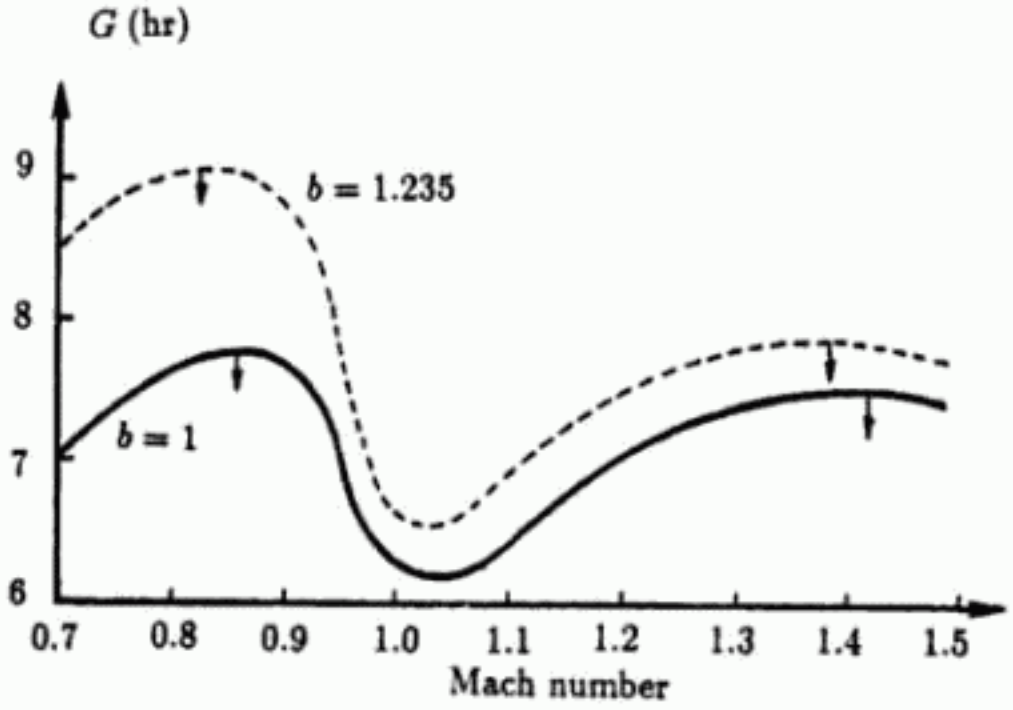

Figure 6.13: Variation of the function G for a supersonic aircraft.

leads to the physical condition $\delta < 1$ for flight in the stratosphere. If this is true, then using this solution for δ in Eq. (6.139) we obtain the maximized range in the stratosphere

$$x = 2a_* \frac{ME_{max}}{c} \text{ Arc tan}\left(\frac{\zeta}{2\sqrt{1-\zeta}}\right) \tag{6.147}$$

As compared to the solution (6.131) for cruise-climb, the range with constant altitude cruise is slightly shorter.

For cruise in the troposphere, where $b = 1.235$, Eq. (6.142) for the optimum pressure ratio has to be solved numerically. But an approximate solution can be obtained as follows. Let

$$\delta = \frac{\sqrt{\omega_{1*}\omega_{2*}}}{M^2 C_L^*} d = \frac{2\sqrt{W_1 W_2}}{k p_* S} \frac{d}{M^2 C_L^*} \tag{6.148}$$

where d is the new unknown. With this transformation we can write

Eq. (6.142) in the form

$$d^2 = 1 + \frac{b-1}{2b}\frac{(1+d^2)^2 + B^2 d^2}{Bd} \text{ Arc tan}\left(\frac{Bd}{1+d^2}\right) \tag{6.149}$$

where

$$B = \frac{\omega_{1*} - \omega_{2*}}{\sqrt{\omega_{1*}\omega_{2*}}} = \frac{\zeta}{\sqrt{1-\zeta}} \tag{6.150}$$

Hence, the modifying factor d in Eq. (6.148) is a function of B, that is of the fuel weight fraction ζ. For all realistic values of B between 0 and 0.6, which corresponds to $\zeta = 0.446$, the value of d as calculated from Eq. (6.149) is nearly stationary. It slowly increases from the limiting value $d = \sqrt{(3b-1)/(b+1)} = 1.100132$, when $B = 0$, to $d = 1.106318$ when $B = 0.6$. Therefore, for all practical applications, we can use Eq. (6.148) to evaluate the optimum cruise altitude, using the value $d = 1$ for flight in the stratosphere and $d = 1.1$ for flight in the troposphere. For cruise in the troposphere, since from Eq. (6.148) with $d = 1.1$, the condition $\delta > 1$ must be satisfied, it leads to selecting the low Mach number. The corresponding range is

$$x = 2a_* \frac{ME_{max}}{c}\, \delta^{(b-1)/2b} \text{ Arc tan}\left[\frac{d\zeta}{(1+d^2)\sqrt{1-\zeta}}\right] \tag{6.151}$$

with δ as given by Eq. (6.148). By comparing this equation with the lift equation (6.125), it is seen that the optimum lift coefficient varies as

$$\frac{C_L}{C_L^*} = \frac{W}{d\sqrt{W_1 W_2}} \tag{6.152}$$

Hence, it decreases during the cruise while staying near the value for maximum lift-to-drag ratio.

In summary, the optimum Mach numbers, as calculated by maximizing the function $G(M)$ are well determined once the functions $C_{D_0}(M)$, $K(M)$ and $c(M)$ are specified. One of these Mach numbers will give the maximum range if the corresponding optimum altitude exists. This is assessed by the test $\delta > 1$ in the troposphere and $\delta < 1$ in the stratosphere. From Eq. (6.148) for the optimum altitude, it is clear that, for any prescribed aerodynamic and engine characteristics providing a specific optimum value for $M^2 C_L^*$, it suffices to modify the wing loading $\sqrt{W_1 W_2}/S$ to change the optimum cruise altitude. In

general, there are four possibilities for the optimum altitudes as shown in Fig. 6.14.

In case (a), both layers of the atmosphere have optimum altitude. The global best altitude corresponds to the one with greater range. But flying in the stratosphere at higher speed has the advantage of shorter flying time. Only one optimum altitude exists for the cases (b) and (c). Case (b) is usually the case of a supersonic transport and case (c) corresponds to a subsonic transport. In case (d), the solution (6.148) fails to provide a solution for the altitude. The optimum altitude in this case is the tropopause. The cruise optimum Mach number is obtained by solving Eq. (6.141) with $\delta = 1$.

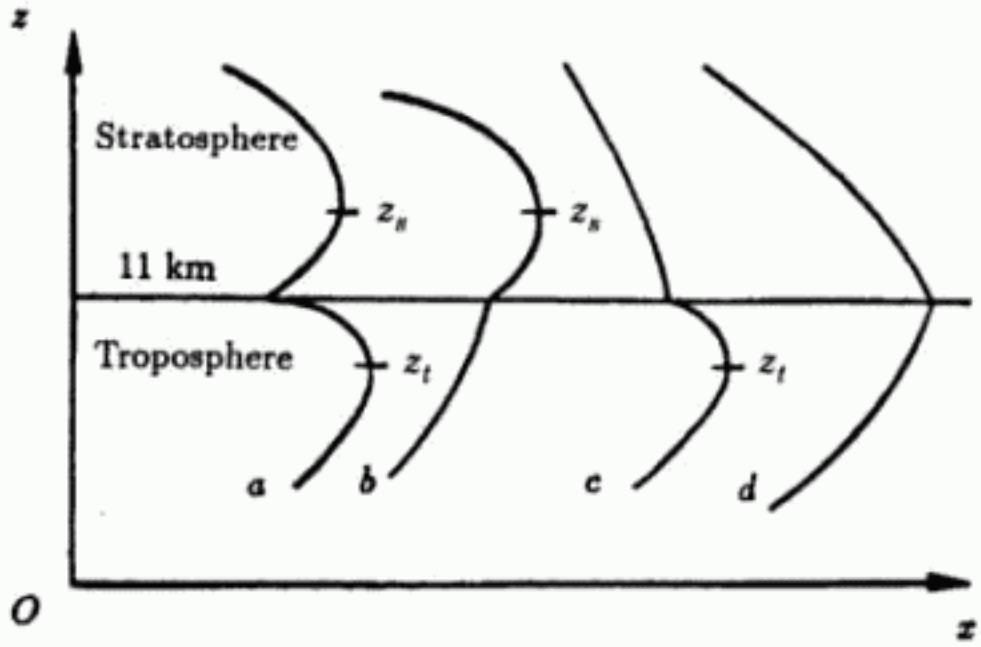

Figure 6.14: Optimum cruise altitude.

6.8 Range of turboprop and turbofan aircraft

As has been discussed in Chapter 4, in consideration of fuel economy, speed and range, the turboprops and the turbofans combine

the good propulsive efficiency and high thrust at low speeds of the piston-prop with the near constant thrust advantage at high speeds of the turbojet. Consequently, their performance is between that of the piston-prop and the turbojet.

For the evaluation of the range of aircraft equipped with these gas turbine engines, we recall the relevant equations. The total thrust available for the propulsion is

$$T = \frac{\eta_p P_s}{V} + T_j \tag{6.153}$$

In this equation, P_s is the shaft power which is converted into thrust power by the coefficient η_p which is the propeller efficiency for a turboprop and the fan efficiency for a turbofan. In addition, T_j is the additional jet thrust. By multiplying the equation by the speed, we have the total power available

$$P = \eta_p P_s + T_j V \tag{6.154}$$

In evaluating the airspeed, for a turboprop we consider the power diagram similar to that in Fig. 6.3, while for a turbofan we consider the thrust diagram such as that in Fig. 6.6. The plots for the power required and the thrust required are the same. We assume that at the flight altitude, for each throttle setting, the shaft power P_s and the jet thrust T_j are constant in the speed range appropriate for cruise. Then, according to Eq. (6.154), with the value of T_j typically at about 10 per cent of the total thrust, the power available for a turboprop is not nearly constant but it increases linearly with the speed. From Fig. 6.3, with this modification, we expect the cruise speed V_1 to be higher than that for a piston-prop. At the limit, when V_1 tends toward V_2, the speed for flight with minimum power (maximum endurance) is also higher than the value given in Eq. (6.26) for a piston-prop.

For a turbofan, we consider the thrust diagram. Then, according to Eq. (6.153), the thrust available is not nearly constant but it decreases as the speed increases. From Fig. 6.6, with this modification, we expect the cruise speed V_1 to be less than that for a pure turbojet. At the limit, when V_1 tends toward V_2, the speed for flight with minimum thrust (maximum endurance) is also lower than the value given in Eq. (6.41) for a turbojet. We refer back to the Exercises 4-6 to 4-10 for an analytical derivation of the pertinent relations.

The simplest way to calculate the range is to treat the turboprop as a power generator and the turbofan as a thrust generator. In subsonic flight at constant speed and constant angle-of-attack, we can use the Breguet range equation (6.75) for the turboprop and the Breguet-Leduc equation (6.118) for the turbofan. In these equations, the parameter c is called the equivalent thrust specific fuel consumption and the parameter c_p is the equivalent power specific fuel consumption. Although with good engine data, we may come up with values for c or c_p which give a fairly accurate evaluation of the range, the straight application of the Breguet equations leads to the conclusion that the optimum speed for maximum range of the turboprop is the same as that for the piston-prop and the optimum speed of the turbofan is the same as that for the turbojet with the same wing loading and aerodynamic characteristics. We have shown above that for the case of maximum endurance there are some modifications on the optimum speeds which also reflect on the optimum angles-of-attack.

To obtain an improved formula, we follow Hale (Hale, 1984) and identify Eq. (6.153) with the fractionizing of the total thrust

$$T = (1-k)T + kT = (1-k)\frac{P}{V} + kT \tag{6.155}$$

Then, for example if at the cruise altitude, with the required throttle setting to maintain the selected cruise speed, from engine data the jet thrust accounts for 10% of the total thrust, we take $k = 0.1$ for the analysis. We recall Eqs. (6.71) and (6.97) for the power part and the thrust part, respectively

$$\begin{aligned} \frac{dx}{dW} &= -\frac{\eta_p}{c_p}\frac{V}{P} = -\frac{\eta_p}{c_p}\frac{E}{W} \\ \frac{dx}{dW} &= -\frac{V}{cT} = -\frac{VE}{cW} \end{aligned} \tag{6.156}$$

Then, by using the same fractionizing and treating the power part and the thrust part separately, we obtain

$$x = (1-k)x + kx = -\frac{\eta_p}{c_p}(1-k)\int \frac{E\,dW}{W} - \frac{k}{c}\int \frac{VE\,dW}{W} \tag{6.157}$$

By integrating this equation for the case of constant speed–constant angle-of-attack cruise we obtain the combined Breguet range equation

valid for both the turboprop and the turbofan

$$x = E\left[(1-k)\frac{\eta_p}{c_p} + k\frac{V}{c}\right] \text{Log}\,\frac{1}{1-\zeta} \tag{6.158}$$

The parameter k varies between 0 and 1 with $k = 0$ for a pure piston-prop and $k = 1$ for a pure turbojet. By using the lift equation (6.20) for V, a parabolic drag polar and the normalized lift coefficient $\lambda = C_L/C_L^*$ as a control for the flight, we rewrite Eq. (6.158) in the form

$$x = 2E_{max}\frac{\lambda}{(1+\lambda^2)}\left[(1-k)\frac{\eta_p}{c_p} + \frac{kV^*}{c\lambda^{1/2}}\right] \text{Log}\,\frac{1}{1-\zeta} \tag{6.159}$$

where

$$V^* = \sqrt{\frac{2W_1}{\rho_1 S C_L^*}} \tag{6.160}$$

is a reference speed which is the speed sufficient to generate a lift to balance the weight at the initial time using the lift coefficient for maximum lift-to-drag ratio. In the combined range equation, the values for c, c_p, η_p and k are known from engine data. From the aerodynamic characteristics C_{D_0} and K, we calculate E_{max} and C_L^*. The initial wing loading W_1/S and the initial flight altitude, in terms of ρ_1, are also given. For each prescribed fuel weight fraction ζ, the range can be calculated if the cruise lift coefficient (or equivalently the cruise speed) is specified. The optimum lift coefficient λ is given by the equation $dx/d\lambda = 0$. This is

$$(1-\lambda^2)\lambda^{1/2} = M(3\lambda^2 - 1) \tag{6.161}$$

where, by definition

$$M = \frac{kV^*c_p}{2(1-k)c\eta_p} \tag{6.162}$$

It can be easily seen that when k varies from 0 to 1, the optimum normalized lift coefficient varies form 1 to $1/\sqrt{3}$ as expected.

As a numerical example, we consider the cruise of a turboprop such that $V^* = 380$ mph at the flight altitude. For the engine characteristics at the flight altitude and in the speed regime near to this reference speed we take $k = 0.1$, $c = 0.96$ lb/hr/lb for the jet part. We consider a propeller efficiency of $\eta_p = 0.85$ and an average value

of $c_p = 0.45$ lb/h/hp for the power part. This characteristic has the dimensions of inverse of length and when converted into statute miles we have the numerical value $c_p = 0.45/375$. With these values we calculate $M = 0.031046$. The optimum normalized lift coefficient from Eq. (6.161) is $\lambda = 0.970785$. Hence the optimum angle-of-attack is less than that for a pure piston-prop. By observing that $V = V^*/\lambda^{1/2}$, we obtain an optimum cruise speed of $V = 385.676$ mph. Finally by considering a maximum lift-to-drag ratio of $E_{max} = 15$ and a fuel weight fraction of $\zeta = 0.2$, the maximum range from Eq. (6.159) is $x = 2267.28$ mi. The flight time is 5.88 hours.

It should be noticed that, by changing the cruise altitude we have a new value for the reference speed V^*. A new set of values for the parameters k, c, η_p and c_p have to be generated from engine data for the calculation of the range.

6.9 Non-steady flight

To change the speed regime or in a test flight to evaluate the aerodynamic and engine characteristics of the aircraft, we may engage a large difference between the thrust available and the thrust required. In this case we consider the equation for the variation of speed

$$m\frac{dV}{dt} = T - \frac{1}{2}\rho S V^2 (C_{D_0} + K C_L^2) \tag{6.163}$$

By maintaining a constant thrust, and using the lift equation (6.54), we rewrite this equation as

$$\frac{\rho S C_{D_0}}{m} dt = -\frac{2V^2\, dV}{V^4 - \dfrac{2T}{\rho S C_{D_0}} V^2 + \dfrac{4KW^2}{(\rho S)^2 C_{D_0}}} \tag{6.164}$$

By neglecting the variation of mass, this equation can be integrated analytically for constant T, C_{D_0} and K. We consider the equation

$$V^4 - \frac{2T}{\rho S C_{D_0}} V^2 + \frac{4KW^2}{(\rho S)^2 C_{D_0}} = 0 \tag{6.165}$$

This equation has two positive roots if the thrust is higher than the minimum thrust for steady cruise at constant altitude.

$$V_1 = \frac{1}{\sqrt{\rho S C_{D_0}}}\sqrt{T + \sqrt{T^2 - (W/E_{max})^2}}$$
$$V_2 = \frac{1}{\sqrt{\rho S C_{D_0}}}\sqrt{T - \sqrt{T^2 - (W/E_{max})^2}} \tag{6.166}$$

With these definitions for V_1 and V_2, equation (6.164) becomes

$$\frac{\rho S C_{D_0}}{m} dt = -\frac{2V^2\, dV}{(V^2 - V_1^2)(V^2 - V_2^2)} \tag{6.167}$$

By integrating from a certain initial speed V_0, we have the time of flight

$$t = \frac{m}{\rho S C_{D_0}(V_1^2 - V_2^2)} \left[V_1 \operatorname{Log} \frac{(V_1 + V)(V_1 - V_0)}{(V_1 - V)(V_1 + V_0)} + V_2 \operatorname{Log} \frac{(V - V_2)(V_0 + V_2)}{(V + V_2)(V_0 - V_2)}\right] \tag{6.168}$$

This formula is valid for both the accelerating flight from V_0 to a higher V_1 or decelerating flight from V_0 to a lower V_1. We notice that the speed reaches V_1 asymptotically in infinite time. This is because the speed V_1 is the steady cruise speed, and when V is near V_1, we nearly have $T_a = T_r$. The acceleration or the deceleration is infinitesimally small and the speed becomes nearly constant.

When $T < W/E_{max}$, or in the case of pure coasting flight where $T = 0$, the roots of Eq. (6.165) become complex. In this case the flight is decelerating. Let

$$k_1^2 = \frac{1}{2\rho S C_{D_0}}\left(\frac{W}{E_{max}} + T\right)$$
$$k_2^2 = \frac{1}{2\rho S C_{D_0}}\left(\frac{W}{E_{max}} - T\right) \tag{6.169}$$

where the constants k_1 and k_2 have the dimension of a speed. In this case, Eq. (6.164) becomes

$$\frac{\rho S C_{D_0}}{m} dt = \left[\frac{V}{(V + k_1)^2 + k_2^2} - \frac{V}{(V - k_1)^2 + k_2^2}\right]\frac{dV}{2k_1} \tag{6.170}$$

By integrating from a certain initial speed V_0, we obtain the time of flight

$$t = \frac{m}{4\rho S C_{D_0}} \left\{ \frac{1}{k_1} \operatorname{Log} \left[\frac{(V_0 - k_1)^2 + k_2^2}{(V_0 + k_1)^2 + k_2^2} \frac{(V + k_1)^2 + k_2^2}{(V - k_1)^2 + k_2^2} \right] + \frac{2}{k_2} \operatorname{Arc\,tan} \left[\frac{2k_2(V_0 - V)(V_0 V + k_1^2 + k_2^2)}{[V_0^2 - (k_1^2 + k_2^2)][V^2 - (k_1^2 + k_2^2)] + 4k_2^2 V_0 V} \right] \right\} \tag{6.171}$$

With insufficient thrust to sustain a prolonged level flight, the speed decreases continuously to any final speed V_f in finite time.

Exercises

6-1. a) Show that if the thrust angle-of-attack ε is not small, under the condition of steady state level flight, the flight speed is given by

$$V = \sqrt{\frac{2W}{\rho S(C_L + C_D \tan \varepsilon)}}$$

In general, the thrust line is fixed in the aircraft. If this line is used as a reference line to measure the angle-of-attack α, then $\varepsilon = \alpha$. Show that the stall speed is attained when $\varepsilon = \varepsilon_{max}$, $C_L = C_{L_{max}}$, $C_D = C_{D_{max}}$ and it is lower as compared to the case where the thrust component is not included in the lift direction.

b) Show that the thrust required is

$$T_r = \frac{WC_D}{C_L \cos \varepsilon + C_D \sin \varepsilon} = \frac{W}{E \cos \varepsilon + \sin \varepsilon}$$

Again, use ε as the angle-of-attack. The thrust required is minimized by maximizing the function

$$f(\alpha) = E(\alpha) \cos \alpha + \sin \alpha$$

Show that the solution is

$$\tan \alpha = \frac{1 + (dE/d\alpha)}{E} \approx \frac{1}{E_{max}}$$

The approximation is due to the fact that E should be near its maximum value and hence $dE/d\alpha \approx 0$. Then, show that the minimum thrust required is

$$T_{min} = \frac{W}{\sqrt{E_{max}^2 + 1}}$$

6-2. Under the condition in Exercise 6-1, show that the power required, defined as $P_r = T_r V$, is

$$P_r = \sqrt{\frac{2W^3}{S}} \frac{1}{\sqrt{\rho}} \frac{\sqrt{\cos\varepsilon}\, C_D}{(C_L \cos\varepsilon + C_D \sin\varepsilon)^{3/2}}$$

which obviously reduces to Eq. (6.21) for $\varepsilon = 0$.

6-3. By using a parabolic drag polar in Eq. (6.29), with the lift coefficient evaluated from Eq. (6.28), show that

$$P_r\sqrt{\sigma} = \frac{1}{2}\rho_0 S C_{D_0} V_i^3 + \frac{2KW^2}{\rho_0 S V_i}$$

Therefore, the plot of $P_r\sqrt{\sigma}$ versus V_i is independent of altitude. By minimizing this function with respect to V_i, show that the equivalent speed for minimum power required is given by

$$\frac{1}{2}\rho_0 V_i^2 = \frac{W}{S}\sqrt{\frac{K}{3C_{D_0}}}$$

From this, deduce Eq. (6.25) for P_r^*.

6-4. From the definition (6.15), show that the following properties of the logarithmic derivative hold

$$x_M + y_M = (xy)_M$$
$$x_M - y_M = (x/y)_M$$
$$(x^n)_M = n x_M$$
$$\frac{x_M}{y_M} = x_y = \frac{1}{y_x}$$

6-5. Show that the condition

$$(C_{L_{max}})_M + 2 = 0$$

is the same as the condition for the maximum of $(C_{L_{max}} M^2)$. A property of the function $C_{L_{max}}(M)$ is that it is constant at low Mach number and, after a certain critical subsonic Mach number, it starts to decrease continuously. Then, show that if a solution to the equation above exists, it must occur before $C_{L_{max}}$ starts to increase.

6-6. By using a parabolic drag polar in Eq. (6.37) and using Eq. (6.28) to evaluate the lift coefficient, show that

$$T_r = \frac{1}{2}\rho_0 S C_{D_0} V_i^2 + \frac{2KW^2}{\rho_0 S V_i^2}$$

Therefore, the plot of T_r versus V_i is independent of the altitude. By minimizing this function with respect to V_i, show that the equivalent speed for minimum thrust required is given by

$$\frac{1}{2}\rho_0 V_i^2 = \frac{W}{S}\sqrt{\frac{K}{C_{D_0}}}$$

From this, deduce Eq. (6.40) for T_r^*.

6-7. Consider Eq. (6.47) for the dimensionless thrust required,

$$\tau_r = M^2\left[C_{D_0}(M) + \frac{\omega^2 K(M)}{M^4}\right].$$

Show that the Mach number which minimizes this function is given by the equation

$$\omega = M^2\sqrt{\frac{C_{D_0}}{K}}\sqrt{\frac{2 + C_{D_0 M}}{2 - K_M}}$$

where subscript M denotes the logarithmic derivative. For a given value of ω, at a low value of M, C_{D_0} and K are constant and the right-hand side of this equation is small and is less than ω. Near the transonic region, C_{D_0} has a sharp increase and dC_{D_0}/dM is positive and very large. Hence, the right-hand side is large and it exceeds the value ω. We conclude that the optimum Mach number which minimizes τ_r is subsonic.

6-8. Let W_1 be the initial weight and W_2 the final weight. If $\Delta W = W_1 - W_2$ is the weight of the fuel, we have defined the fuel weight fraction

$$\zeta = \frac{\Delta W}{W_1}$$

a) Verify the following relations

$$\frac{W_1}{W_2} = \frac{1}{1-\zeta}$$

$$\sqrt{\frac{W_1}{W_2}} - \sqrt{\frac{W_2}{W_1}} = \frac{\zeta}{\sqrt{1-\zeta}}$$

$$\frac{1}{\sqrt{W_2}} - \frac{1}{\sqrt{W_1}} = \frac{1}{\sqrt{W_1}}\left(\frac{1}{\sqrt{1-\zeta}} - 1\right)$$

$$\sqrt{W_1} - \sqrt{W_2} = \sqrt{W_1}(1 - \sqrt{1-\zeta})$$

b) From Eq. (6.60) for the density ratio, show that if an exponential atmosphere of the form $\rho = \rho_0 \exp(-\beta z)$ is used, we have

$$\exp(\beta \Delta z) = \frac{1}{1-\zeta}$$

Therefore, we have Eq. (6.62).

6-9. Consider the integral in Eq. (6.78)

$$I = \int_2^1 \frac{dC_L}{C_{D_0} + KC_L^2}$$

By using a rescaled lift coefficient $\lambda = C_L / \sqrt{C_{D_0}/K}$, and noticing that $E_{max} = 1/2\sqrt{KC_{D_0}}$, show that

$$I = 2E_{max} \int_2^1 \frac{d\lambda}{1+\lambda^2} = 2E_{max}(\text{ Arc tan } \lambda_1 - \text{ Arc tan } \lambda_2)$$

Let

$$\lambda_1 = \tan \beta_1, \qquad \lambda_2 = \tan \beta_2$$

Then

$$I = 2E_{max}(\beta_1 - \beta_2)$$

On the other hand

$$\tan(\beta_1 - \beta_2) = \frac{\tan \beta_1 - \tan \beta_2}{1 + \tan \beta_1 \tan \beta_2} = \frac{\lambda_1 - \lambda_2}{1 + \lambda_1 \lambda_2}$$

Deduce Eq. (6.79).

6-10. Define the range factor for propeller driven aircraft

$$F_R = \frac{\eta_p}{c_p} E_{max}$$

Then, from Eq. (6.75) for constant angle-of-attack flight, and Eq. (6.84) for constant altitude–constant speed flight, we have the respective maximum ranges

$$x_\alpha = F_R A(\zeta)$$
$$x_{s,V} = F_R B(\zeta)$$

where A are B are functions of the fuel weight fraction ζ

$$A = \text{Log}\left(\frac{1}{1-\zeta}\right)$$
$$B = 2\,\text{Arc tan}\left(\frac{\zeta}{2\sqrt{1-\zeta}}\right)$$

Show that we have the following series expansions

$$A = \zeta + \frac{1}{2}\zeta^2 + \frac{1}{3}\zeta^3 + \frac{1}{4}\zeta^4 + \frac{1}{5}\zeta^5 + \cdots$$

$$B = \frac{\zeta}{\sqrt{1-\zeta}}\left[1 - \frac{\zeta^2}{12(1-\zeta)} + \frac{\zeta^4}{80(1-\zeta)^2} - \cdots\right]$$

$$= \zeta + \frac{1}{2}\zeta^2 + \frac{7}{24}\zeta^3 + \frac{3}{16}\zeta^4 + \frac{83}{640}\zeta^5 + \cdots$$

Hence, we have the difference

$$A - B = \frac{1}{24}\zeta^3 + \frac{1}{16}\zeta^4 + O(\zeta^5)$$

and the ratio

$$\frac{A}{B} = 1 + \frac{1}{24}\zeta^2 + \frac{1}{24}\zeta^3 + \frac{43}{1152}\zeta^4 + O(\zeta^5)$$

These formulas show that $x_\alpha > x_{z,V}$ and at the same time give an estimate of the ratio of the two ranges. To complete the proof, show that the function $(A - B)$ increases as ζ increases in the interval $\zeta \in (0,1)$, that is

$$\frac{d}{d\zeta}(A - B) = \frac{(1 - \sqrt{1-\zeta})^2}{(1-\zeta)(2-\zeta)} > 0$$

6-11. Define the endurance factor for propeller driven aircraft as

$$F_E = \frac{3^{3/4} E_{max}}{2} \frac{\eta_p}{c_p} \sqrt{\frac{\rho_1 S C_L^*}{2W_1}}$$

Then from Eqs. (6.88), (6.90) and (6.95), with the subscripts denoting the respective constant parameters, we have the following maximum endurances

$$t_{z,\alpha} = F_E\, C(\zeta)$$
$$t_{z,V} = F_E\, D(\zeta)$$
$$t_{V,\alpha} = F_E\, A(\zeta)$$

where the function $A(\zeta)$ is the same as in Exercise 6-10, while

$$C(\zeta) = 2\left(\frac{1}{\sqrt{1-\zeta}} - 1\right)$$
$$D(\zeta) = \frac{4}{\sqrt{3}} \text{ Arc tan } \frac{\sqrt{3}\zeta}{4 - 3\zeta}$$

Show that we have the following series expansions

$$C = \zeta + \frac{3}{4}\zeta^2 + \frac{5}{8}\zeta^3 + \frac{35}{64}\zeta^4 + \frac{63}{128}\zeta^5 + \cdots$$

$$D = \zeta + \frac{3}{4}\zeta^2 + \frac{1}{2}\zeta^3 + \frac{9}{32}\zeta^4 + \frac{9}{80}\zeta^5 + \cdots$$

Therefore, we have the differences

$$C - D = \frac{1}{8}\zeta^3 + \frac{17}{64}\zeta^4 + \frac{243}{640}\zeta^5 + \cdots$$

$$D - A = \frac{1}{4}\zeta^2 + \frac{1}{6}\zeta^3 + \frac{1}{32}\zeta^4 - \frac{7}{80}\zeta^5 + \cdots$$

These formulas clearly show that for small ζ, $t_{z,\alpha} > t_{z,V} > t_{V,\alpha}$ and that $t_{z,\alpha}$ and $t_{z,V}$ are nearly the same. To enforce the assessment for larger values of the fuel weight fraction ζ, show that

$$\frac{d}{d\zeta}(C - D) = \frac{\zeta^2 + 2(1-\zeta)(1-\sqrt{1-\zeta})^2}{(1-\zeta)\sqrt{1-\zeta}[3(1-\zeta)^2+1]} > 0$$

in the interval $\zeta \in (0,1)$, and

$$\frac{d}{d\zeta}(D - A) = \frac{\zeta(2-3\zeta)}{(1-\zeta)[3(1-\zeta)^2+1]} > 0$$

in the interval $\zeta \in (0,2/3)$.

6-12. For a turbojet aircraft, define the endurance factor as

$$F_E = \frac{E_{max}}{c}$$

Then, from Eq.(6.108) for constant angle-of-attack flight, and Eq. (6.113) for constant altitude–constant speed flight, we have

$$t_\alpha = F_E\, A(\zeta)$$
$$t_{z,V} = F_E\, B(\zeta)$$

where the functions A and B are the same as in Exercise 6-10.

Then, conclude that at low altitude, the endurance is independent of the altitude, and above a critical altitude where the cruise Mach number exceeds the critical Mach number M_{cr} for the effect of the compressibility of the air to be taken into account, the endurance decreases as the altitude increases. Show that this critical altitude is evaluated from

$$\frac{2W}{kp_{cr}S} = M_{cr}\left[\frac{C_{D_0}(M_{cr})}{K(M_{cr})}\right]^{1/2}$$

Also, use the results in Exercise 6-10 to conclude that $t_a > t_{z,V}$.

6-13. For a turbojet aircraft cruising at subsonic speeds, define the range factor as

$$F_R = \frac{3^{3/4} E_{max}}{2c} \sqrt{\frac{2W_1}{\rho_1 S C_L^*}}$$

From Eqs. (6.117), (6.120) and (6.124), with the subscripts denoting the respective constant parameters, we have the following maximum ranges

$$x_{V,a} = F_R A(\zeta)$$
$$x_{z,a} = F_R G(\zeta)$$
$$x_{z,V} = F_R H(\zeta)$$

where the function $A(\zeta)$ is the same as in Exercise 6-10, while

$$G(\zeta) = 2(1 - \sqrt{1-\zeta})$$

$$H(\zeta) = \frac{4}{\sqrt{3}} \text{Arc tan} \frac{\sqrt{3}\zeta}{4-\zeta}$$

Show that we have the following series expansions

$$G = \zeta + \frac{1}{4}\zeta^2 + \frac{1}{8}\zeta^3 + \frac{5}{64}\zeta^4 + \frac{7}{128}\zeta^5 + \cdots$$

$$H = \zeta + \frac{1}{4}\zeta^2 - \frac{1}{32}\zeta^4 - \frac{1}{80}\zeta^5 - \cdots$$

Therefore, we have the differences

$$A - G = \frac{1}{4}\zeta^2 + \frac{5}{24}\zeta^3 + \frac{11}{64}\zeta^4 + \frac{93}{640}\zeta^5 + \cdots$$

$$G - H = \frac{1}{8}\zeta^3 + \frac{7}{64}\zeta^4 + \frac{43}{640}\zeta^5 + \cdots$$

Therefore, for small ζ, $x_{V,\alpha} > x_{s,\alpha} > x_{s,V}$ and $x_{s,\alpha}$ and $x_{s,V}$ are nearly the same. To complete the assessment for large values of ζ, show that the derivatives of the differences $(A - G)$ and $(G - H)$ with respect to ζ remain positive in the interval $(0, 1)$.

6-14. For a standard atmosphere, we have used the simple law

$$\frac{p}{p_*} = \left(\frac{\rho}{\rho_*}\right)^b$$

where subscript $(*)$ denotes the condition at the tropopause and $b = 1$ in the stratosphere and $b = 1.235$ in the troposphere. The Table in Appendix 1 gives the ratio p/p_0 and ρ/ρ_0 with respect to the condition at sea level.

a) Show that we have

$$\frac{p}{p_0} = \left(\frac{\rho}{\rho_0}\right)^{1.235}$$

in the troposphere and use the Appendix to verify the accuracy of this formula.

b) Show that in the stratosphere, we have

$$\frac{p}{p_0} = \left(\frac{\rho_*}{\rho_0}\right)^{0.235} \frac{\rho}{\rho_0}$$

and use the Appendix to verify the accuracy of this formula.

c) From Eq. (6.138) show that in the troposphere with $b = 1.235$, we have the relationship

$$\frac{a}{a_0} = \left(\frac{\rho}{\rho_0}\right)^{(b-1)/2}$$

and use the Appendix to verify the accuracy of this formula.

6-15. Show that the function G as defined in Eq. (6.145) can be written as

$$G = (M^2 C_L^*)^{(1-b)/2b} \frac{M E_{max}}{c}$$

Hence, by taking logarithms, we have

$$\text{Log}\, G = \frac{1-b}{2b}\,\text{Log}\,(M^2 C_L^*) + \text{Log}\left(\frac{M E_{max}}{c}\right)$$

Then, show that the equation $d(\text{Log}\, G)/dM = 0$ is precisely Eq. (6.143).

6-16. Show that the function G can be put in the form

$$G(M) = \frac{M^{1/b}}{2c\, C_{D_0}^{(3b-1)/4b} K^{(b+1)/4b}}$$

The optimum Mach number is the one which maximizes this function. At low Mach number where C_{D_0} and K are constant G increases proportionally to $M^{1/b}$. Near the sonic speed where $C_{D_0}(M)$ has a sudden increase, it is clear that G decreases. This explains the behavior of G as shown in Fig. 6.13.

6-17. We have shown in Fig. 6.14 for constant altitude–constant speed flight that there are four types of aircraft for cruise with maximum range:

1. Aircraft of type (a) with optimum cruise altitude in both the two lower layers of the atmosphere.
2. Aircraft of type (b) specifically designed for supersonic cruise in the stratosphere.
3. Aircraft of type (c) for subsonic cruise in the troposphere.
4. Aircraft of type (d) for subsonic cruise in the tropopause.

It is proposed to compare the two maximized ranges for aircraft of type (a).

First show that the general formula for maximum range is

$$x = 2a_* \left(\frac{2\sqrt{W_1 W_2}}{k p_* S}\right)^{(b-1)/2b} G d^{(b-1)/2b}\, \text{Arc tan}\left(\frac{Bd}{1+d^2}\right) \qquad (1)$$

where as usual, $b = 1$, $d = 1$ in the stratosphere and $b = 1.235$, $d \approx 1.1$ in the troposphere. Furthermore, here B is defined in Eq. (6.150) as

$B = \zeta/\sqrt{1-\zeta}$ and G is evaluated at its maximum value, $G = C_s$ in the stratosphere and $G = G_t$ in the troposphere. Deduce that the ratio of the two ranges is

$$\frac{x_t}{x_s} = \frac{G_t}{G_s}\left(\frac{2\sqrt{W_1 W_2}}{k p_s S}\right)^{(b-1)/2b} d_1 \tag{2}$$

where

$$d_1 = d^{(b-1)/2b}\,\text{Arc tan}\left(\frac{Bd}{1+d^2}\right)\Big/\,\text{Arc tan}\left(\frac{B}{2}\right)$$

For small values of B, show that we have approximately

$$d_1 = \frac{2d^{(3b-1)/2b}}{1+d^2} = 1.005$$

From Eq. (2), it is clear that to favor supersonic cruise in the stratosphere which gives better range and shorter flying time, we must have aircraft with low wing loading W/S and high value of $G_s = M E_{max}/c$.

6-18. For cruise with constant Mach number and constant angle-of-attack, show that

$$\frac{p_1}{p_2} = \frac{W_1}{W_2}$$

By using the results of Exercise 6-14, show that although during this cruise-climb, the speed of sound is constant in the stratophere, in the troposphere we have

$$\frac{a_2}{a_1} = (1-\zeta)^{(b-1)/2b} = 1 - \frac{b-1}{2b}\zeta - \frac{b^2-1}{8b^2}\zeta^2 - \cdots$$

Then, the relative decrease in the speed of sound is

$$\frac{\Delta a}{a_1} = \frac{b-1}{2b}\zeta\left[1 + \frac{b+1}{4b}\zeta + \cdots\right]$$

and it is of the order of ζ^2.

6-19. We recall that the Breguet-Leduc equation (6.131) has been obtained with the assumption of constant speed–constant angle-of-attack flight in the stratosphere. To obtain a similar equation for flight

in the troposphere, in the basic equation (6.104), we may assume constant Mach number and constant angle-of-atttack flight, hence a constant value for ME/c, and also constant average value for the speed of sound. Then the range is obtained by quadrature as

$$x = F \operatorname{Log} \frac{1}{1-\zeta} \tag{1}$$

with the range factor as given in Eq. (6.126) reproduced here for convenience

$$F(\omega, M) = \frac{a\,\omega}{c[MC_{D_0}(M) + (K\omega^2/M^3)]} \tag{2}$$

The range as given by Eq. (1) for flight in the troposphere with constant M and ω is only approximate. Since the speed of sound decreases during the cruise climb, the range factor F also decreases.

a) To maximize this factor with respect to the constant parameters M and ω, use Eq. (6.138) to show that with respect to the reference level at the tropopause

$$\frac{a}{a_*} = \left(\frac{\omega}{\omega_*}\right)^{(1-b)/2b}$$

where $\omega_* = 2W/kp_*S$ is the value of ω evaluated at the tropopause. If, it is used as an average value we are led to maximizing

$$F(\omega, M) = a_* \left(\frac{\omega}{\omega_*}\right)^{(1-b)/2b} \frac{\omega}{c[MC_{D_0}(M) + (K\omega^2/M^3)]}$$

with respect to M and ω. Show that the solution is obtained by solving the system of equations

$$\omega = M^2 \sqrt{\frac{C_{D_0}}{K}} \sqrt{\frac{b+1}{3b-1}} \tag{3}$$

and

$$\omega = M^2 \sqrt{\frac{C_{D_0}}{K}} \left[\frac{1 + (C_{D_0}c)_M}{3 - (Kc)_M}\right]^{1/2} \tag{4}$$

where subscript M denotes the logarithmic derivative.

b) Show that the optimum Mach number is calculated from

$$(b+1)(Kc)_M + (3b-1)(C_{D_0}c)_M = 4 \tag{5}$$

On the other hand, from Exercise 6-16, show that

$$(2G)^b = \frac{M}{(C_{D_0}c)^{(3b-1)/4}(Kc)^{(b+1)/4}}$$

Deduce that the optimum Mach number from Eq. (5) is precisely the one which maximizes the function $G(M)$.

c) Show that the constant lift coefficient during the cruise-climb in the troposphere at the optimum altitude is

$$C_L = C_L^* \sqrt{\frac{b+1}{3b-1}}$$

6-20. a) Continuing the previous Exercise, show that the maximum range for cruise-climb in the troposphere is

$$x = \frac{\sqrt{(b+1)(3b-1)}}{2b} a_* \left(\frac{ME_{max}}{c}\right) \delta^{(b-1)/2b} \operatorname{Log} \frac{1}{1-\zeta}$$

where $ME_{max}(M)/c(M)$ is evaluated with the optimum Mach number.

b) When compared to Eq. (6.151), the difference here is that since $\delta = p/p_*$, it is constant for the constant altitude cruise, but it slowly decreases during the cruise-climb. By using the same average constant value for δ, we compare

$$x_{M,\alpha} = FA(\zeta), \quad \text{from the equation above}$$

with

$$x_{z,V} = FB(\zeta), \quad \text{from Eq. (6.151)},$$

where F is the common constant factor with the functions A and B defined here as

$$A = \frac{\sqrt{(b+1)(3b-1)}}{2b} \operatorname{Log} \frac{1}{1-\zeta}$$

$$B = 2 \operatorname{Arc\,tan}\left[\frac{d\zeta}{(1+d^2)\sqrt{1-\zeta}}\right]$$

where $b = 1.235$ and $d \approx 1.1$.

Recall that we have used the limiting value for d computed from

$$d = \sqrt{\frac{3b-1}{b+1}}$$

Hence, show that

$$\frac{d}{1+d^2} = \frac{\sqrt{(b+1)(3b-1)}}{4b} = k = 0.4977$$

By using four terms of the series expansions for A and B, show that

$$A = 2k\left(\zeta + \frac{1}{2}\zeta^2 + \frac{1}{3}\zeta^3 + \frac{1}{4}\zeta^4 + \cdots\right)$$

$$B = 2k\left(\zeta + \frac{1}{2}\zeta^2 + \frac{9-8k^2}{24}\zeta^3 + \frac{5-8k^2}{16}\zeta^4 + \cdots\right)$$

Therefore, we have the difference

$$A - B = \frac{k}{12}(8k^2-1)\zeta^3 + \frac{k}{8}(8k^2-1)\zeta^4 + \cdots$$

We deduce the ratio of the ranges

$$\frac{x_{M,\alpha}}{x_{z,V}} = \frac{A}{B} = 1 + \frac{8k^2-1}{24}\zeta^2 + \frac{8k^2-1}{24}\zeta^3 + \cdots$$

As compared to the case of flight in the stratosphere with $k = 0.5$, the increase in range for cruise climb is slightly less when flight is in the troposphere.

7

Climb performance

7.1 Introduction

In this chapter, we consider the case of climbing flight when the thrust is sufficiently high at a relatively low speed so that the excess power allows the aircraft to gain altitude. In general, climb is performed in a vertical plane. The problem of climb with change in the heading will be discussed in Chapter 9, on turning performance. For flight in the vertical plane, we have the equations as derived in Chapter 2,

$$\begin{aligned}
\frac{dx}{dt} &= V\cos\gamma \\
\frac{dz}{dt} &= V\sin\gamma \\
\frac{dV}{dt} &= \frac{g}{W}(T\cos\epsilon - D) - g\sin\gamma \\
V\frac{d\gamma}{dt} &= \frac{g}{W}(T\sin\epsilon + L) - g\cos\gamma
\end{aligned} \tag{7.1}$$

Again, we use standard notation as shown in Fig. 7.1. The performance parameters of interest in climbing are the rate of climb, the climb angle, the time to climb and the fuel consumption for the climb. For fighter aircraft we are interested in the maximum rate of climb. This is vital to reach the operational altitude in the shortest time. On the other hand, after a take-off, it may be necessary to clear an obstacle in a short distance. In this case, we shall adopt a flight program for maximum

climb angle. In general, the climb portion involves only a small fraction of the total flying time. Hence, to ease the analysis, except for the case of calculating the fuel consumption for the climb, we treat the weight, $W = mg$, as constant, being its average value during the climb.

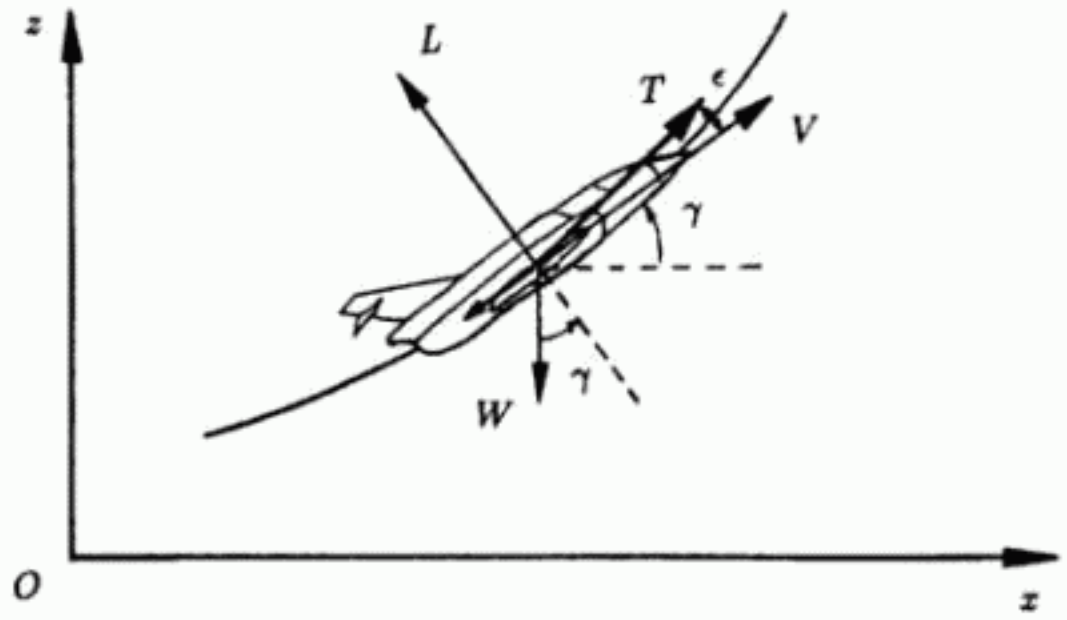

Figure 7.1: Climbing flight.

7.2 Steady climb

In static performance, we consider the behavior of the trajectory under steady state flight conditions. We shall assume that the variations in speed and flight path angle are small and neglect the inertia forces. Furthermore, we shall assume that the thrust is nearly aligned with the velocity vector, and hence $\epsilon \approx 0$. Then, from the last two equations in Eqs. (7.1), we have the thrust and the lift equations

$$T = \frac{1}{2}\rho S V^2 C_D + W \sin\gamma \tag{7.2}$$

and

$$W \cos\gamma = \frac{1}{2}\rho S V^2 C_L \tag{7.3}$$

As usual, the drag and the lift coefficients are related by a drag polar relationship

$$f(C_D, C_L, M) = 0 \tag{7.4}$$

which is dependent on the Mach number M. For a given throttle setting, we assume that the thrust $T = T(V, z)$ is a known function of the speed and the altitude. Since $M = V/a(z)$, while the speed of sound $a(z)$ is, on the assumption of a standard atmosphere, a known function of altitude, at each altitude z, we have three equations for the four unknowns, V, γ, C_D and C_L. This leads to an infinity of trajectories and we have the option to use one variable, say the lift coefficient C_L, as a control to achieve the desired optimum trajectory.

We first consider the rate of climb, which is defined as the vertical component of the velocity vector

$$V_z = V \sin \gamma \tag{7.5}$$

The starting equation to be considered here is the thrust equation (7.2). It is more enlightening for the discussion to express it in terms of the power by multiplying the equation by the speed V. We have

$$TV = \frac{1}{2}\rho S V^3 C_D + WV \sin \gamma \tag{7.6}$$

We identify the different terms in this equation as

$TV = P_a$, power available for climb.

$\frac{1}{2}\rho S V^3 C_D = P_r$, power required for level flight at the same speed.

Then, with the definition (7.5), we have for the rate of climb

$$V_z = \frac{P_a - P_r}{W} \tag{7.7}$$

This equation clearly shows that the excess in power, compared to level flight, is used to produce proportionally a rate of climb.

From this equation, we deduce the climb angle

$$\sin \gamma = \frac{V_z}{V} = \frac{P_a - P_r}{VW} \tag{7.8}$$

Climb performance is most sensitive to the power produced by the propulsion system. Therefore, we analyze separately the performance,

first of propeller driven aircraft, and next of jet and a rocket powered aircraft.

7.3 Climb of a propeller driven aircraft

As discussed in Chapter 6, for a given throttle setting, at each altitude and in the speed range of interest, the power available is nearly constant. Furthermore, for this type of aircraft, the climb angle is usually less than 20° and we can use the approximation $\cos\gamma \approx 1$ to write the lift equation

$$W = \frac{1}{2}\rho S V^2 C_L \tag{7.9}$$

7.3.1 Rate of climb

According to Eq. (7.7), at each altitude with the corresponding nearly constant value for P_a, the rate of climb V_z is maximized when the power required is minimized. Since for small climb angles, the lift equation (7.9) is the same as for the case of level flight, we can use the same plot for power versus speed as in Chapter 6. In Fig. 7.2, we have added the plot of the rate of climb V_z which is proportional to the excess power $\Delta P = P_a - P_r$. When $P_a = P_r$, we have the condition for steady level flight, and $V_z = 0$. For a given throttle setting, it is seen that there exists an optimum speed for maximum rate of climb. This speed corresponds to the lowest point on the power required curve. We recall that if the approximate relation (7.9) is used, then

$$P_r = \sqrt{\frac{2W^3}{\rho S}}\frac{C_D}{C_L^{3/2}} \tag{7.10}$$

The angle-of-attack used for maximum rate of climb is the one that minimizes the ratio $C_D/C_L^{3/2}$. For a parabolic drag polar of the form

$$C_D = C_{D_0} + KC_L^2 \tag{7.11}$$

we have obtained in Chapter 6 the solution

$$C_L = \sqrt{\frac{3C_{D_0}}{K}}, \quad C_D = 4C_{D_0} \tag{7.12}$$

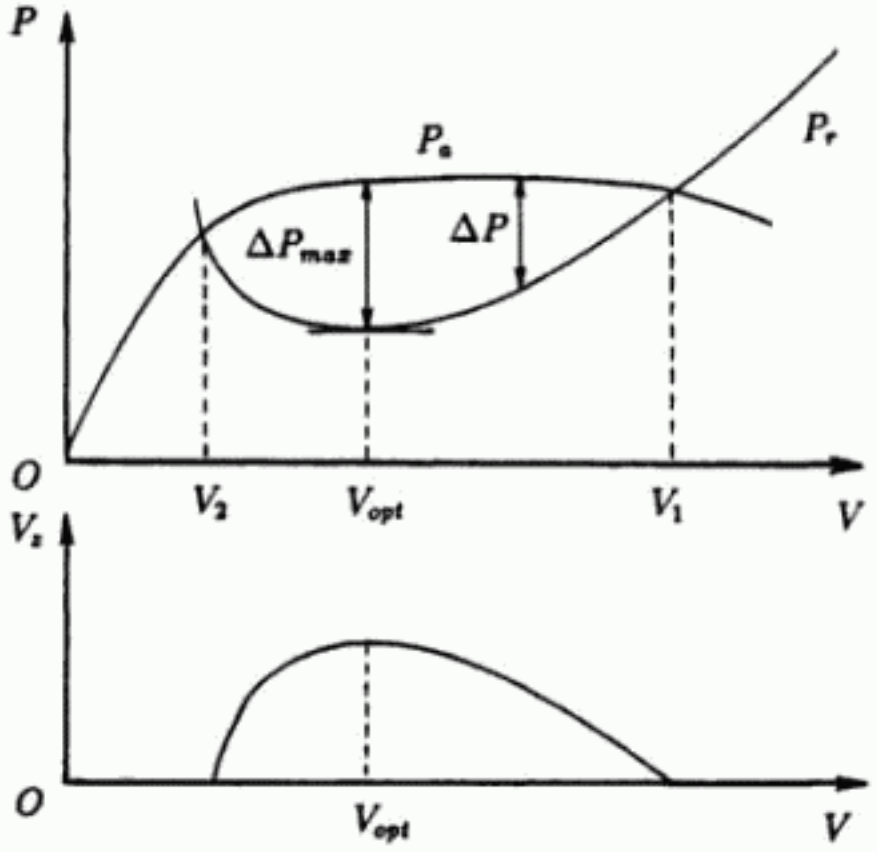

Figure 7.2: Power diagrams and rate of climb for propeller driven aircraft.

Using this solution to calculate P_r and on substituting into Eq. (7.7), we have the maximum rate of climb (see Exercise 7.1). Again, as discussed in the previous chapter, from the lift equation, the optimum dynamic pressure is

$$\frac{1}{2}\rho V^2 = \frac{W}{S}\sqrt{\frac{K}{3C_{D_0}}} \tag{7.13}$$

For an average constant weight, it is constant. Consequently, during the climb, as the density ρ decreases the true airspeed increases, but the equivalent speed V_i remains constant.

With the definition (7.5), we write the second equation in system (7.1)

$$\frac{dt}{dz} = \frac{1}{V_z} \tag{7.14}$$

Then, the time to climb from the initial altitude z_1 to the final altitude z_f is

$$t = \int_{z_1}^{z_f} \frac{dz}{V_z} \tag{7.15}$$

This integral is minimized if we constantly use the maximum rate of climb. The climb is then the fastest climb. In order to perform the integration, we have to examine the influence of various parameters on the rate of climb.

We recall the definition of the equivalent airspeed which can be considered as the same as the indicated airspeed for low speed when the influence of Mach number is neglected

$$q = \frac{1}{2}\rho V^2 = \frac{1}{2}\rho_0 V_i^2 \tag{7.16}$$

Here ρ_0 is the value of the standard atmospheric density at sea level. If the dynamic pressure is kept constant at its optimum value according to Eq. (7.13), then the equivalent speed is constant.

To examine the influence of the power available on the rate of climb, we multiply Eq. (7.7) by $\sqrt{\sigma}$ where $\sigma = \rho/\rho_0$ is the ratio of the current density to the density at sea level. Then, we have

$$V_z\sqrt{\sigma} = \frac{1}{W}(P_a\sqrt{\sigma} - \frac{1}{2}\rho_0 S V_i^3 C_D) \tag{7.17}$$

This expression is general and, as long as we use constant equivalent speed for climbing, the second term on the right-hand side is constant. Of course, for maximum rate of climb we use the optimum relation (7.13) for q to calculate V_i from Eq. (7.16). Then, it is clear that at any altitude, as specified by the ratio σ, if we increase the power available P_a, the rate of climb increases.

As discussed in Chapter 4, with a constant throttle setting, the power available decreases as the air density decreases during the climb. With supercharged engines the loss in power is delayed and P_a remains constant until a certain critical altitude. Above this altitude, the power available, as a first order approximation, is proportional to the air density ρ. With this in mind, we can use Eq. (7.17) to see the effect of the density ratio σ on the rate of climb. Up to the critical altitude, since P_a is constant, V_z decreases because the second term on the right-hand side of Eq. (7.17), when divided by $\sqrt{\sigma}$, increases. Above the critical

altitude, we have the added effect of a decrease in the power available and the rate of climb is further reduced until it becomes zero. At that point, we reach the propulsive ceiling for the prescribed throttle setting. To continue the climb, it is necessary to increase the power available. The absolute propulsive ceiling is reached when maximum power is used in conjunction with the optimum climb speed and this results in $V_z = 0$ (see Exercise 7-2).

Finally, to see the effect of weight on the rate of climb, we return to Eq. (7.7), with the power required, P_r, as given by Eq. (7.10). For a fixed throttle setting, at each altitude, since V_z is first inversely proportional to W, with a heavier aircraft, the rate of climb is smaller. Furthermore, the excess power, $\Delta P = P_a - P_r$, is smaller since P_r is proportional to $W^{3/2}$ and thus increases with larger W. In climb performance, the weight of the aircraft is definitely a major factor.

We now evaluate the time to climb by first performing the integration in Eq. (7.15) in the altitude range where P_a is constant. Using Eq. (7.7) for V_z with Eq. (7.10) for P_r, we have

$$t = \frac{W}{P_a} \int_{z_1}^{z_f} \frac{\sqrt{\sigma}\, dz}{\sqrt{\sigma} - A} \tag{7.18}$$

where, by definition

$$A = \frac{1}{P_a} \sqrt{\frac{2W^3}{\rho_0 S}} \left(\frac{C_D}{C_L^{3/2}} \right) \tag{7.19}$$

Notice that A is constant if the climb is performed at constant equivalent speed which, from the lift equation (7.9) leads to constant angle-of-attack. For fastest climb, we use the solution (7.12). By using an exponential atmosphere with the independent variable

$$\xi = \sqrt{\sigma} = e^{-\beta z/2} \tag{7.20}$$

we transform the integral (7.18) into

$$t = -\frac{2W}{\beta P_a} \int_{\xi_1}^{\xi_f} \frac{d\xi}{\xi - A} \tag{7.21}$$

On performing the integration, we have the solution

$$t = \frac{2W}{\beta P_a} \operatorname{Log} \frac{\sqrt{\sigma_1} - A}{\sqrt{\sigma_f} - A} \tag{7.22}$$

If the final altitude is near the ceiling $\sqrt{\sigma_f} - A \approx 0$ and the time of climb is asymptotically infinite. In practice, we consider that the ceiling is reached when the rate of climb falls below a conventional small value. For example, using maximum power, when the rate of climb has reduced to 100 fpm, we reach the so called service ceiling.

For climb above the critical altitude, we assume that for fixed throttle setting, the power available is proportional to the density, that is

$$P_a = P_0\left(\frac{\rho}{\rho_c}\right) = P_0\sigma \tag{7.23}$$

where P_0 is the constant power available at the critical altitude with the prescribed throttle setting. We notice the new definition of σ as the ratio of the ambient density ρ to the density ρ_c at the critical altitude where the power available starts to decrease. Then, using the same transformation (7.20) with the new definition of σ, we have the integral for the time to climb,

$$t = -\frac{2W}{\beta P_0}\int_{\xi_1}^{\xi_f} \frac{d\xi}{\xi^3 - a^3} \tag{7.24}$$

where, by definition

$$a^3 = \frac{1}{P_0}\sqrt{\frac{2W^3}{\rho_c S}}\left(\frac{C_D}{C_L^{3/2}}\right) \tag{7.25}$$

By carrying out the integration, we have the explicit solution

$$\begin{aligned} t = \frac{2W}{3a^2\beta P_0}\Bigg[&\operatorname{Log}\frac{\sqrt{\sigma_1} - a}{\sqrt{\sigma_f} - a} - \frac{1}{2}\operatorname{Log}\frac{\sigma_1 + a\sqrt{\sigma_1} + a^2}{\sigma_f + a\sqrt{\sigma_f} + a^2} \\ &-\sqrt{3}\operatorname{Arc\,tan}\frac{a\sqrt{3}(\sqrt{\sigma_1} - \sqrt{\sigma_f})}{2\sqrt{\sigma_1\sigma_f} + a(\sqrt{\sigma_1} + \sqrt{\sigma_f}) + 2a^2}\Bigg] \end{aligned} \tag{7.26}$$

The formula is general for fixed throttle setting and constant equivalent speed climb above the critical altitude. For fastest climb, the solution (7.12) should be used in the definition (7.25).

7.3.2 Climb angle

The climb angle is given by Eq. (7.8). In practice, for propeller driven aircraft, climb is performed at constant equivalent speed $V_i = \sqrt{\sigma}V$. It is then appropriate to rewrite this equation as

$$\sin\gamma = \frac{V_z\sqrt{\sigma}}{V_i} \tag{7.27}$$

As mentioned earlier, to clear an obstacle at a short distance, it is advisable to use the steepest climb with maximum climb angle. To see the difference between this flight program and the fastest climb, we consider the plot of $V_z\sqrt{\sigma}$ versus V_i. For this purpose, we rewrite the lift equation (7.9) as

$$W = \frac{1}{2}\rho_0 S V_i^2 C_L \tag{7.28}$$

Then, with a parabolic drag polar, Eq. (7.17) becomes

$$V_z\sqrt{\sigma} = \frac{P_a\sqrt{\sigma}}{W} - \frac{\rho_0 S C_{D_0}}{2W}V_i^3 - \frac{2KW}{\rho_0 S V_i} \tag{7.29}$$

For fixed throttle setting, and at each altitude as specified by the density ratio, we can plot $V_z\sqrt{\sigma}$ versus V_i as shown in Fig. 7.3. It is clear that the optimum equivalent speed which maximizes the rate of climb V_z is such that

$$\frac{1}{2}\rho_0 V_i^2 = \frac{W}{S}\sqrt{\frac{K}{3C_{D_0}}} \tag{7.30}$$

Its equivalent form in terms of the true speed is given by Eq. (7.13).

At any altitude the equivalent speed and hence the angle-of-attack for maximum rate of climb remains the same, being the one that minimizes the ratio $C_D/C_L^{3/2}$. But for maximum climb angle, we maximize the ratio $V_z\sqrt{\sigma}/V_i$. The operating point is obtained by drawing the tangent from the origin to the curve plotting $V_z\sqrt{\sigma}$ versus V_i. From the graph, it is clear that the equivalent speed for maximum climb angle increases with the altitude, reaching the value for maximum rate of climb at the propulsive ceiling. Hence, climb with maximum angle is performed at an angle-of-attack higher than the angle-of-attack for minimum power required. This angle-of-attack easily exceeds the stall angle of attack at low altitude. In practice, after a take-off, even

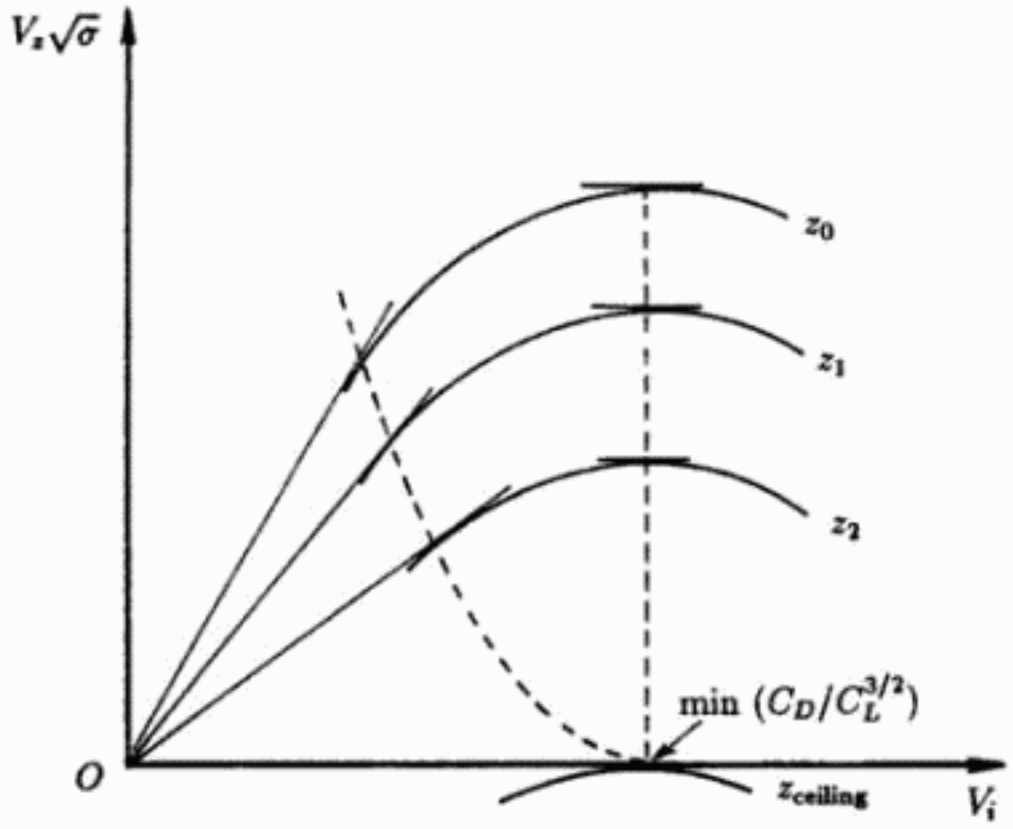

Figure 7.3: Plot of $V_s\sigma^{1/2}$ versus V_i.

with the intention of having maximum climb angle, we use a speed greater than the optimum speed. To obtain an analytical formula for this optimum speed, we use Eq. (7.29) to rewrite Eq. (7.27)

$$\sin\gamma = \frac{P_a\sqrt{\sigma}}{WV_i} - \frac{\rho_0 S C_{D_0} V_i^2}{2W} - \frac{2KW}{\rho_0 S V_i^2} \tag{7.31}$$

By taking the derivative of the right-hand side of this equation with respect to V_i and setting it equal to zero, we have the equation for the optimum speed for maximum climb angle

$$f(V_i) = V_i^4 + \frac{P_a\sqrt{\sigma}}{\rho_0 S C_{D_0}} V_i - \frac{4KW^2}{\rho_0^2 S^2 C_{D_0}} = 0 \tag{7.32}$$

The solution for this quartic equation does not have a simple form, but it is easy to locate the root. First, because of the factor $P_a\sqrt{\sigma}$, the

optimum equivalent speed varies with the altitude. Next, we observe that putting $V_i = 0$, we have $f(0) < 0$ while using the solution (7.30) for the maximum rate of climb, we have

$$f(V_i) = \frac{V_i}{\rho_0 S C_{D_0}} [P_a \sqrt{\sigma} - 2\rho_0 S V_i^3 C_{D_0}] \geq 0 \tag{7.33}$$

We have the inequality because inside the square brackets the second term is the modified power required $P_r \sqrt{\sigma} = \rho_0 S V_i^3 C_D/2$ evaluated at maximum rate of climb with $C_D = 4C_{D_0}$, while during the climb, before reaching the ceiling, we have $P_a > P_r$. The speed for maximum climb angle is smaller than the speed for maximum rate of climb as predicted by the graphical solution. Furthermore, by inspecting Eq. (7.32), we see that the root V_i is smaller, when $P_a \sqrt{\sigma}$ is higher at lower altitude (see Exercise 7-4).

If we use the optimum relation (7.32) to solve for $P_a \sqrt{\sigma}$, then upon substitution into Eq. (7.31), we obtain

$$\sin \gamma = \frac{\rho_0 S C_{D_0}}{W V_i^2} \left(\frac{2KW^2}{\rho_0^2 S^2 C_{D_0}} - \frac{3}{2} V_i^4 \right) \tag{7.34}$$

In this form, it is seen that the climb angle is high at low altitude where V_i is small. This maximum climb angle is zero at the ceiling when the condition (7.30) is realized.

In practice, we can use the fastest climb to have at the same time a relatively high climb angle (see Exercise 7-8).

7.4 Climb of a jet or rocket powered aircraft

For a turbojet or rocket powered aircraft, because of Eq. (7.7) for the rate of climb, it is still convenient for the analysis to use the curves plotting the powers versus the speed as shown in Fig. 7.4. The curve for the power required P_r is the same. For the power available, we have here

$$P_a = TV \tag{7.35}$$

For a rocket engine the thrust T is strictly constant. For a jet aircraft at relatively low speed for climb, T is nearly constant and the variation of P_a as a function of the speed V is linear. Again, we add below the

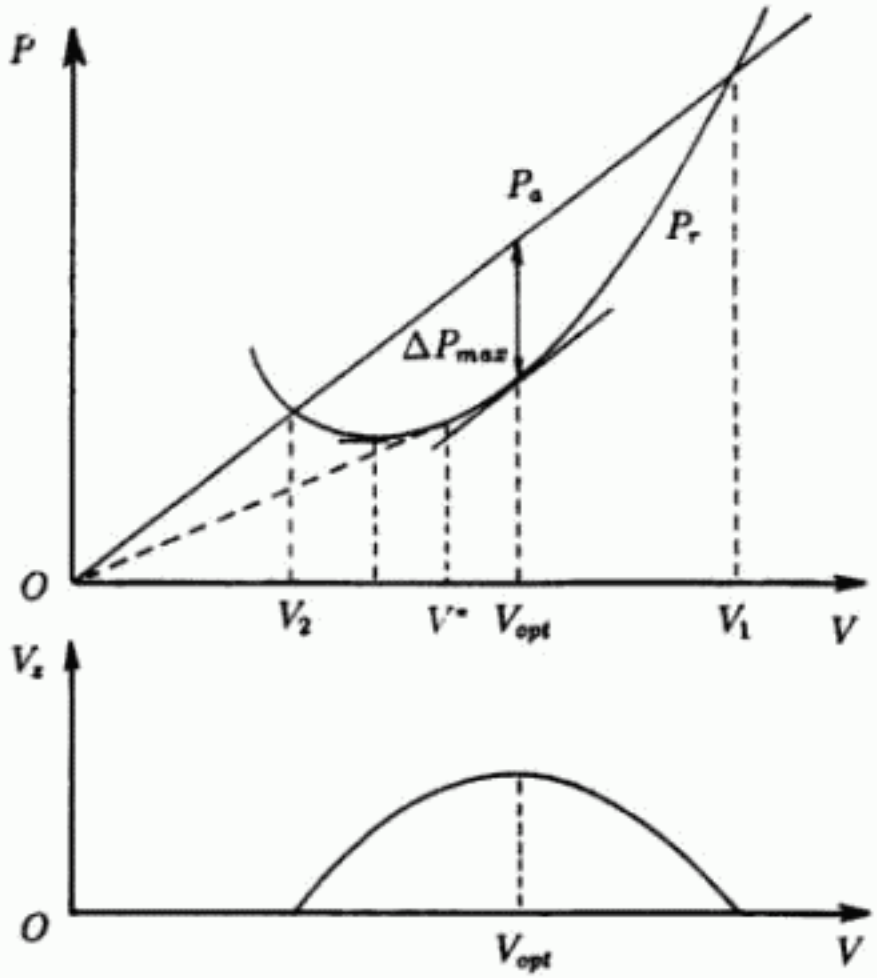

Figure 7.4: Power diagrams and rate of climb for jet aircraft.

graph for the powers the plot showing the variation of the rate of climb V_z which is proportional to the excess power $\Delta P = P_a - P_r$.

7.4.1 *Rate of climb*

First we notice that the optimum speed for maximum rate of climb, which corresponds to the maximum value of ΔP is not at the point of minimum P_r as for a propeller driven aircraft, but it is at the point where the tangent to the curve P_r is parallel to the linear plot for P_a. Since the thrust T is the slope of this line, the optimum speed is higher with higher values of the thrust. The optimum speed for maximum rate of climb is a minimum when the thrust is a minimum. In this case, the line P_a is tangent to the P_r curve and we have seen in Chapter 6 that for the case when $\cos\gamma \approx 1$, as will be considered first

here, the speed for minimum thrust corresponds to flight at maximum lift-to-drag ratio.

It is possible to discuss the influence of thrust available T_a, of altitude through the density ρ, and of weight W, on the maximum rate of climb and on the optimum speed for climb for a perfectly general lift-drag relationship independent of Mach number as has been done in the case of a propeller driven aircraft. To have explicit formulas for the discussion, we use a parabolic drag polar and the assumption of small climb angle as depicted in Eq. (7.9) to write Eq. (7.7) in the form

$$V_z = \frac{1}{W}\left(TV - \frac{1}{2}\rho S C_{D_0} V^3 - \frac{2KW^2}{\rho S V}\right) \tag{7.36}$$

The maximum rate of climb corresponds to the solution of the equation $\partial V_z/\partial V = 0$, written explicitly as

$$\frac{3\rho S C_{D_0}}{W} V^4 - 2\frac{T}{W} V^2 - \frac{4KW}{\rho S} = 0 \tag{7.37}$$

We consider the positive root for V^2,

$$V^2 = \frac{W}{3\rho S C_{D_0}}\left(\frac{T}{W} + \sqrt{\frac{T^2}{W^2} + \frac{3}{E_{max}^2}}\right) \tag{7.38}$$

It is clear that this optimum speed, which is now a function of the thrust, increases as the thrust-to-weight ratio increases. This has been predicted by the inspection of Fig. 7.4. This optimum speed is lowest for the minimum thrust which is

$$\frac{T}{W} = \frac{1}{E_{max}} \tag{7.39}$$

Using this value in Eq. (7.38), we have for the corresponding minimum speed

$$\frac{1}{2}\rho V^2 = \frac{W}{S}\sqrt{\frac{K}{C_{D_0}}} \tag{7.40}$$

which is indeed the value for maximum lift-to-drag ratio.

If we neglect the influence of Mach number, and write Eq. (7.38) in terms of equivalent speed through the transformation (7.16), we shall have

$$V_i^2 = \frac{W}{3\rho_0 S C_{D_0}}\left(\frac{T}{W} + \sqrt{\frac{T^2}{W^2} + \frac{3}{E_{max}^2}}\right) \tag{7.41}$$

Then, for a rocket engine, the thrust T is independent of the altitude and the optimum equivalent speed is constant during the climb. For a jet aircraft, with fixed throttle setting, the thrust decreases as the altitude increases. The equivalent speed decreases. Consequently, from the lift-equation (7.28), the lift coefficient C_L increases until the final value $C_L = C_L^* = \sqrt{C_{D_0}/K}$ at the propulsive ceiling.

The performance parameter of interest in climb is actually the rate of climb. Using the solution (7.38) in Eq. (7.36) and with the aid of Eq. (7.37), we have the maximum rate of climb in the form

$$\frac{V_z}{V} = \frac{1}{3E_{max}}(\tau + \sqrt{\tau^2 + 3}) - \frac{3}{E_{max}(\tau + \sqrt{\tau^2 + 3})} \tag{7.42}$$

where we have defined the magnified thrust-to-weight ratio

$$\tau = E_{max}\left(\frac{T}{W}\right) \tag{7.43}$$

This maximum rate of climb is zero, when $\tau = 1$ at the ceiling, as expected. Notice that we can use Eq. (7.42) to calculate $\sin\gamma$ for the climb angle in connection with the maximum rate of climb.

In terms of the magnified thrust-to-weight ratio, τ, we put Eq. (7.38) in the form

$$V^2 = \frac{2W}{3\rho S C_L^*}(\tau + \sqrt{\tau^2 + 3}) \tag{7.44}$$

The parameters which influence the maximum rate of climb V_z are the thrust available, the weight and the altitude.

In terms of τ, when the thrust increases, the right-hand side of Eq. (7.42) increases. Furthermore, since V_z is proportional to V, and from Eq. (7.44) the speed increases with τ, a higher thrust level definitely produces a higher rate of climb. Since τ is of the order of unity, the dependence of V_z on τ is clearly non-linear (see Exercise 7-9).

Concerning the influence of the weight W, with all the other parameters being the same, we examine the basic equation (7.7), with P_r given in Eq. (7.10). Then if W increases, V_z decreases as seen in Eq. (7.7). But compared to the case of climb of a propeller driven aircraft, in which while P_r is proportional to $W^{3/2}$, the ratio $C_D/C_L^{3/2}$

remains constant in optimum climb; for a jet aircraft this ratio decreases. Hence, the penalty of greater weight on the maximum rate of climb for a jet aircraft is less severe. Another way of looking at this is by inspecting Eqs. (7.42) and (7.44). First, since τ is inversely proportional to W, if W increases, τ decreases and from Eq. (7.42), V_z/V decreases. But then, V_z is proportional to the climb speed V, and from Eq. (7.44) this true speed increases with W and this partially compensates for the decrease in $V_z/V = \sin\gamma$. We refer to Exercise 7-11 for a quantitative analysis of the influence of weight on maximum rate of climb.

Concerning the influence of altitude, for the discussion and to prepare for the calculation of the time to climb, let

$$u = \tau + \sqrt{\tau^2 + 3} \tag{7.45}$$

In terms of u, we rewrite Eq. (7.42)

$$\frac{V_z}{V} = \frac{u^2 - 9}{3E_{max}u} \tag{7.46}$$

Equation (7.44) for the climb speed is simply

$$V^2 = \frac{2Wu}{3\rho S C_L^*} \tag{7.47}$$

Then, we have for the rate of climb

$$V_z = \frac{1}{3E_{max}}\sqrt{\frac{2W}{3\rho_0 S C_L^*}}\frac{u^2 - 9}{\sigma^{1/2}u^{1/2}} \tag{7.48}$$

If the aircraft is equipped with rocket engines, τ is constant and u is constant. Both the climb speed V and the rate of climb V_z, which are proportional to $\sigma^{-1/2}$, increase during the climb. As a consequence, rocket powered aircraft have remarkable climb performance. For a jet aircraft, we assume that the thrust available is proportional to the density ratio. Hence, we put

$$\tau = \tau_0\sigma \tag{7.49}$$

where τ_0 is the value of τ at sea level for the prescribed throttle setting. Notice that from the definition (7.45), we have the relation

$$\tau = \frac{u^2 - 3}{2u} \tag{7.50}$$

On using the last two equations in Eq. (7.48), we obtain

$$V_z = \frac{2}{3E_{max}}\sqrt{\frac{W\tau_0}{3\rho_0 SC_L^*}}\frac{u^2-9}{(u^2-3)^{1/2}} \tag{7.51}$$

Now, we can see that as σ decreases, τ decreases and u decreases. From Eq. (7.51), when we consider V_z as a function of u^2, when u^2 decreases from its large value at sea level to the limiting value $u^2 = 9$ at the ceiling, V_z is monotonically decreasing from an initial high value to zero at the propulsive ceiling.

As in the case of a propeller driven aircraft, for performance analysis, it is handy to have an analytical solution for the time to climb. Here, the solution is more complicated, and we first present some simple and approximate solutions. Again, we start with the basic integral (7.15) and use the maximum rate of climb to have the minimum time to climb.

For the case of constant thrust to climb, that is for the case of rocket engines or for jet engines which are constantly adjusted to maintain constant thrust, the solution is easily obtained. We use V_z as given by Eq. (7.48) with a constant value for u, and if an exponential atmosphere as given in Eq. (7.20) is used, we have the integral,

$$t = -\frac{6E_{max}}{\beta}\sqrt{\frac{3\rho_0 SC_L^*}{2W}}\frac{u^{1/2}}{u^2-9}\int_{\sigma_1}^{\sigma_f}\frac{d\sigma}{2\sqrt{\sigma}} \tag{7.52}$$

Upon integrating, we have the solution for the time to climb from the initial altitude (density ratio), to the final altitude,

$$t = \frac{6E_{max}}{\beta}\sqrt{\frac{3\rho_0 SC_L^*}{2W}}\frac{u^{1/2}}{u^2-9}(\sqrt{\sigma_1}-\sqrt{\sigma_f}) \tag{7.53}$$

We have a shorter time with large wing loading W/S and a high value of u , that is a high value of the thrust-to-weight ratio. We should not be misled by the factor E_{max} into thinking that a high value of E_{max} leads to longer time to climb. To explain this, we introduce the maximum rate of climb at sea level, using Eq. (7.48) with $\sigma = 1$.

$$V_{z_0} = \frac{1}{3E_{max}}\sqrt{\frac{2W}{3\rho_0 SC_L^*}}\frac{u_0^2-9}{u_0^{1/2}} \tag{7.54}$$

Then, since for constant thrust to climb, $u = u_0$, the time to climb is simply

$$t = \frac{2}{\beta V_{z_0}}(\sqrt{\sigma_1} - \sqrt{\sigma_f}) \tag{7.55}$$

The influences of W/S and T/W on V_{z_0} have the beneficial effects on the time to climb. That is to say that a high wing loading and a high thrust-to-weight ratio will decrease the time to climb. As for the effect of the maximum lift-to-drag ratio, since T_0/W is constant, E_{max} is simply proportional to τ_0. Furthermore, we notice that $C_L^* = 2C_{D_0}E_{max}$. Then, with the aid of Eq. (7.50), it is seen from Eq. (7.54) that V_{z_0} is proportional to the factor

$$F = \frac{u_0(u_0^2 - 9)}{\sqrt{C_{D_0}}(u_0^2 - 3)^{3/2}} \tag{7.56}$$

Then, in terms of the aerodynamic characteristics, a low value of the zero-lift drag coefficient, C_{D_0}, increases the rate of climb. As for the effect of E_{max}, which varies in the same direction as u_0, we easily find that

$$\frac{dF}{du_0} = \frac{9(u_0^2 + 3)}{\sqrt{C_{D_0}}(u_0^2 - 3)^{5/2}} > 0 \tag{7.57}$$

Hence if u_0 (that is E_{max}) increases, F increases and the maximum rate of climb increases.

The climb is generally performed to reach a certain altitude for cruise. Hence, it is of interest to also calculate the ground distance travelled during the climb. We assume that the atmosphere is at rest. For the case of constant-thrust to climb, the solution is simple. First, from Eq. (7.46), we have for the climb angle

$$\sin\gamma = \frac{u^2 - 9}{3E_{max}u} \tag{7.58}$$

For a constant value of u, the climb angle is constant. On evaluating this angle, the distance travelled is simply

$$x = \frac{\Delta z}{\tan\gamma} \tag{7.59}$$

where $\Delta z = z_f - z_1$ is the altitude difference.

The various effects on the rate of climb and the time to climb can be made more explicit by considering the case of high thrust-to-weight ratio and high value of maximum lift-to-drag ratio. This obviously implies that the range of altitude involved is relatively low. Then, for a large value of τ, from Eq. (7.45) we have the approximation

$$u \approx 2\tau \tag{7.60}$$

From Eq. (7.46) the climb angle for maximum rate of climb is

$$\sin\gamma = \frac{4\tau^2 - 9}{6E_{max}\tau} \tag{7.61}$$

Equation (7.47) for the climb speed is

$$V^2 = \frac{4W\tau}{3\rho S C_L^*} \tag{7.62}$$

From these expressions we obtain the maximum rate of climb for high thrust-to-weight ratio

$$V_z = \frac{1}{3E_{max}}\sqrt{\frac{W}{3\rho_0 S C_L^*}}\frac{4\tau^2 - 9}{\sigma^{1/2}\tau^{1/2}} \tag{7.63}$$

This equation can be obtained directly from Eq. (7.48) with the approximation (7.60). For fixed throttle setting, with the law of variation of thrust as given in Eq. (7.49) we obtain

$$V_z = \frac{1}{3E_{max}}\sqrt{\frac{W}{3\rho_0 S C_L^* \tau_0}}\frac{4\tau_0^2\sigma^2 - 9}{\sigma} \tag{7.64}$$

We introduce the maximum rate of climb at sea level

$$V_{z_0} = \frac{1}{3E_{max}}\sqrt{\frac{W}{3\rho_0 S C_L^* \tau_0}}(4\tau_0^2 - 9) \tag{7.65}$$

Then

$$\frac{V_z}{V_{z_0}} = \frac{4\tau_0^2\sigma^2 - 9}{(4\tau_0^2 - 9)\sigma} \tag{7.66}$$

With this simplified expression for the maximum rate of climb and an exponential atmosphere, the time-to-climb equation (7.15) leads to the integral

$$t = -\frac{4\tau_0^2 - 9}{\beta V_{z_0}}\int_{\sigma_1}^{\sigma_f}\frac{d\sigma}{4\tau_0^2\sigma^2 - 9} \tag{7.67}$$

By carrying out the quadrature, we have the time-to-climb on the assumption of high value for τ.

$$t = \frac{4\tau_0^2 - 9}{12\beta V_{z_0}\tau_0} \operatorname{Log} \frac{(2\tau_0\sigma_1 - 3)(2\tau_0\sigma_f + 3)}{(2\tau_0\sigma_1 + 3)(2\tau_0\sigma_f - 3)} \tag{7.68}$$

The approximate formulas (7.63) and (7.68) for the maximum rate of climb and the time to climb respectively were derived for simplicity in use. Since rigorously $\tau = 1$ at the ceiling, and in these formulas a value of $\tau = 1.5$ already results in $V_z = 0$ and $t = \infty$, the application of the approximate solutions at high altitude will give a rate of climb lower than the exact optimum value and a time to climb higher than the actual time. To see clearly the influence of various parameters, we can further use the approximation $4\tau^2 - 9 \approx 4\tau^2$ in Eq. (7.63) and, after some transformation, obtain the formula for the rate of climb for the case of fixed throttle setting

$$V_z = \frac{4}{3}\left[\frac{(T_0/W)^3(W/S)}{6\rho_0 C_{D_0}}\right]^{1/2}\sigma \tag{7.69}$$

With this simple formula, we can clearly see the beneficial effect of a high T_0/W, a high W/S and a low $\sqrt{C_{D_0}}$ on the rate of climb. Here, V_z is simply proportional to the density ratio and it tends exponentially to zero at very high altitude. By setting $\sigma = 1$, we have the maximum rate of climb V_{z_0} at sea level. If the expression (7.69) is used to integrate the time equation (7.15), we obtain the time to climb, from the initial altitude density σ_1 to the final density σ_f

$$t = \frac{1}{\beta V_{z_0}}\left(\frac{1}{\sigma_f} - \frac{1}{\sigma_1}\right) \tag{7.70}$$

This formula can also be deduced from Eq. (7.68) with the assumption of a large value for τ_0 (see Exercise 7-12).

We now consider the exact integration of the time equation for the case of fastest climb with fixed throttle setting. From Eq. (7.51) we calculate the rate of climb at sea level

$$V_{z_0} = \frac{2}{3E_{max}}\sqrt{\frac{W\tau_0}{3\rho_0 S C_L^*}}\frac{u_0^2 - 9}{(u_0^2 - 3)^{1/2}} \tag{7.71}$$

where to evaluate u_0 from Eq. (7.45) we use $\tau_0 = E_{max}(T_0/W)$ with T_0 being the thrust at sea level from the prescribed throttle setting. The time to climb is given by the integral

$$t = \frac{u_0^2 - 9}{(u_0^2 - 3)^{1/2} V_{z_0}} \int_{z_1}^{z_f} \frac{(u^2 - 3)^{1/2}}{u^2 - 9}\, dz \tag{7.72}$$

Let I be the integral in this equation. With Eq. (7.20) for the density ratio and using Eqs. (7.49) and (7.50), we have

$$d\tau = \tau_0\, d\sigma = -\beta\tau\, dz = \frac{u^2 + 3}{2u^2}\, du$$

Hence we have the change in the differentials

$$dz = -\frac{u^2 + 3}{\beta u(u^2 - 3)}\, du \tag{7.73}$$

The integral is then

$$I = \int_{z_1}^{z_f} \frac{(u^2 - 3)^{1/2}}{u^2 - 9}\, dz = -\frac{1}{\beta} \int_{u_1}^{u_f} \frac{(u^2 + 3)\, du}{u(u^2 - 9)(u^2 - 3)^{1/2}} \tag{7.74}$$

By using the new variable

$$u^2 - 3 = y^2 \tag{7.75}$$

we have the integral

$$I = -\frac{1}{\beta} \int_{y_1}^{y_f} \frac{(y^2 + 6)\, dy}{(y^2 + 3)(y^2 - 6)} \tag{7.76}$$

By carrying out the quadrature and using it in Eq. (7.72), we have the final expression for the fastest time to climb for the case of fixed throttle setting where the actual magnified thrust-to-weight ratio decreases from the initial value $\tau_1 = \tau_0\sigma_1$ at the initial altitude to the final value $\tau_f = \tau_0\sigma_f$ at the final altitude

$$t = \frac{u_0^2 - 9}{3\beta\sqrt{3(u_0^2 - 3)}\, V_{z_0}} \left[\sqrt{2}\, \mathrm{Log} \frac{(y_1 - \sqrt{6})(y_f + \sqrt{6})}{(y_1 + \sqrt{6})(y_f - \sqrt{6})} - \tan^{-1} \frac{\sqrt{3}(y_1 - y_f)}{3 + y_1 y_f}\right] \tag{7.77}$$

The formula is explicit and the integration is exact within the assumption that although the speed and the flight path angle are both slowly varying their inertial effects are negligible. Furthermore, we recall that the assumption that $\cos\gamma \approx 1$ has been used in deriving the basic formula for the maximum rate of climb. The application of this more rigorous formula for the fastest time to climb is straightforward. With the given data for aircraft and throttle setting, that is for given T_0/W, W/S, C_{D_0} and K, we can calculate C_L^* and E_{max}, and hence τ_0, u_0 and V_{x_0}. Actually, we can immediately calculate the coefficient in Eq. (7.77) as

$$\frac{u_0^2 - 9}{3\beta\sqrt{3(u_0^2 - 3)}V_{x_0}} = \frac{E_{max}}{2\beta}\sqrt{\frac{2\rho_0 C_{D_0}}{T_0/S}} \tag{7.78}$$

With this coefficient, it is seen that a high value of the so-called thrust loading $T_0/S = (T_0/W)(W/S)$ decreases the time to climb. Also a small value of the zero-lift drag coefficient reduces the time. As for the effect of the maximum lift-to-drag ratio, E_{max}, when we consider time as a function of E_{max}, it decreases as E_{max} increases. For any given pair of end-point altitudes, we have σ_1 and σ_f and calculate τ_1 and τ_f. Then we deduce u_1 and u_f and the corresponding y_1 and y_f for evaluating the two transcendental functions in Eq. (7.77).

For the distance travelled during the climb at constant throttle setting, we combine the first two equations in (7.1) to have

$$\frac{dx}{dx} = \tan\gamma \approx \sin\gamma \tag{7.79}$$

Using the general expression (7.58) for $\sin\gamma$ and the transformation (7.73), we obtain

$$x = -\frac{3E_{max}}{\beta}\int_{u_1}^{u_f} \frac{u^2 + 3}{(u^2 - 3)(u^2 - 9)}\,du \tag{7.80}$$

This gives the solution for the distance travelled

$$x = \frac{E_{max}}{\beta}\left[\operatorname{Log}\frac{(u_1 - 3)(u_f + 3)}{(u_1 + 3)(u_f - 3)} - \frac{\sqrt{3}}{2}\operatorname{Log}\frac{(u_1 - \sqrt{3})(u_f + \sqrt{3})}{(u_1 + \sqrt{3})(u_f - \sqrt{3})}\right] \tag{7.81}$$

7.4.2 Climb angle

For a jet aircraft, the climb angle is high, so that we return to the two basic steady state equations (7.2) and (7.3) and combine them to obtain

$$\sin\gamma = \frac{T}{W} - \frac{\cos\gamma}{E} \tag{7.82}$$

where $E = C_L/C_D$ is the lift-to-drag ratio. Using the half-tangent formula for $\sin\gamma$ and $\cos\gamma$, we have the equation

$$(\tau+1)\tan^2\frac{\gamma}{2} - 2E\tan\frac{\gamma}{2} + (\tau-1) = 0 \tag{7.83}$$

where temporarily we define $\tau = E(T/W)$ with an arbitrary value for E. The solution for the climb angle is then

$$\tan\frac{\gamma}{2} = \frac{1}{\tau+1}(E - \sqrt{E^2+1-\tau^2}) \tag{7.84}$$

Real solutions always exist since $E^2+1 > \tau^2$ for $T/W < 1$ regardless of the value of E, while when $T/W > 1$, the maximum climb angle is clearly $\gamma_{max} = 90°$. The negative sign is selected for the quadratic formula since the positive sign leads to $\gamma > 90°$.

From Eq. (7.84) it is seen that the climb angle is maximized when $E = E_{max}$. Hence, this formula for the maximum climb angle is used with $E = E_{max}$ and τ as defined in Eq. (7.43). Also, it is seen that when T/W decreases, the maximum climb angle decreases (see Exercises 7-14 and 7-15).

7.5 Non-steady climb

With the assumption of steady climb, we are led to the conclusion that in optimum climb the so-called stabilized speed varies with altitude. The assumption is made because, for a low rate of climb, the non-steady effect due to the tangential acceleration dV/dt is negligible. For fighter aircraft with high rates of climb, this term should be retained and we consider the thrust equation in the form

$$m\frac{dV}{dt} = T - D - mg\sin\gamma \tag{7.85}$$

By multiplying this equation by the speed V to express it in terms of powers and using the second equation in (7.1), we have the equation for non-steady climb

$$P_a - P_r = \frac{d}{dt}\left(\frac{1}{2}mV^2\right) + \frac{d}{dt}(mgz) \tag{7.86}$$

Compared to the simplified equation (7.6), we see that the excess power $\Delta P = P_a - P_r$ is used to produce a rate of change in altitude, or equivalently in potential energy $E_p = mgz$ and, in addition, a rate of change in kinetic energy $E_k = mV^2/2$. Since the change in the height $dz/dt = V_z$ is the rate of climb, to have the same dimension of a length, we introduce a new variable called the energy height, defined as

$$H = z + \frac{V^2}{2g} \tag{7.87}$$

The rate of change of energy height is

$$V_H = \frac{dH}{dt} = V_z + \frac{V}{g}\frac{dV}{dt} = V_z\left(1 + \frac{V}{g}\frac{dV}{dz}\right) \tag{7.88}$$

Equation (7.86) now has the form

$$V_H = \frac{P_a - P_r}{W} \tag{7.89}$$

which is similar to Eq. (7.7) for the rate of climb and we can use the plot of the powers to evaluate the variation of the rate of change of energy height as a function of the climb speed. From Eq. (7.88), we can see the non-steady effect on the rate of climb by rewriting it as

$$V_z = \frac{V_H}{1 + \dfrac{V}{g}\dfrac{dV}{dz}} \tag{7.90}$$

Since V_z is proportional to V_H it is benificial to maximize this rate of change of energy height. If the climb is performed at constant equivalent speed as in the case of a propeller driven aircraft, we consider

$$V_i = V\sqrt{\sigma} = Ve^{-\beta z/2} = \text{constant} \tag{7.91}$$

Hence

$$\frac{V}{g}\frac{dV}{dz} = \frac{\beta V_i^2}{2g\sigma} \tag{7.92}$$

At low altitude, and if the speed is low, the effect is negligible. But at high altitude where σ is small or at low altitude with high speed the non-steady effect is important.

The concept of energy height is particularly interesting in the case of optimum climb of fighter aircraft at high speed since this type of aircraft has high maneuverability and can easily transform its high kinetic energy into potential energy. From a practical point of view, in a minimum time to climb maneuver, it is not sufficient to reach the final altitude in the shortest time but also to have at this altitude a certain prescribed speed. Reaching the final altitude with a speed that is too low will require an additional long duration to accelerate in level flight to the required operational speed.

With the assumption of nearly constant weight, the problem of minimum time to climb is formulated as follows:

At the initial time t_1, the aircraft is at the initial altitude z_1, with speed V_1 and flight path angle γ_1. At the final time t_f, the aircraft is required to be at the final altitude z_f, with speed V_f and flight path angle γ_f. Find the thrust program $T(t)$ and the angle-of-attack program $\alpha(t)$ as functions of the time such that the time to climb $\Delta t = t_f - t_1$ is a minimum. This optimal control problem can only be solved by functional optimization (Vinh, 1981). We present here a simple solution using the energy concept and if it is correctly applied, it will lead to an acceptable sub-optimal solution.

The problem concerns high speed and high maneuverability aircraft and as such, it is assumed that the flight path angle can be changed instantaneously. Hence, we do not consider the requirements in γ_1 and γ_f. We consider Eq. (7.89) in the form

$$\frac{dH}{dt} = \frac{1}{W}(TV - DV) = V_H \tag{7.93}$$

where we recall that the energy height is defined in Eq. (7.87). The main assumption, called the energy state approximation is that $\Delta H = 0$ leads to $\Delta t = 0$, that is in keeping the energy height constant, we can instantaneously transform the high kinetic energy into the potential energy by a zoom climb, or conversely from a high altitude we can

perform a dive to quickly pick up the necessary high speed. Hence, the problem is to go from the initial energy height $H_1 = z_1 + (V_1^2/2g)$ to the final energy height $H_f = z_f + (V_f^2/2g)$ in minimum time. The time to climb is

$$t = \int_{H_1}^{H_f} \frac{dH}{V_H} \tag{7.94}$$

and it is necessary at each energy height to have the maximum rate V_H. We notice that this equation is a generalization of Eq. (7.15) with the non-steady effect included. Figure 7.5 plots the lines of constant energy height, and they are a family of parabolas in the (V, z) space with a vertical translation when we vary the constant parameter H. In this space, the point A is the initial point and the point G is the final point.

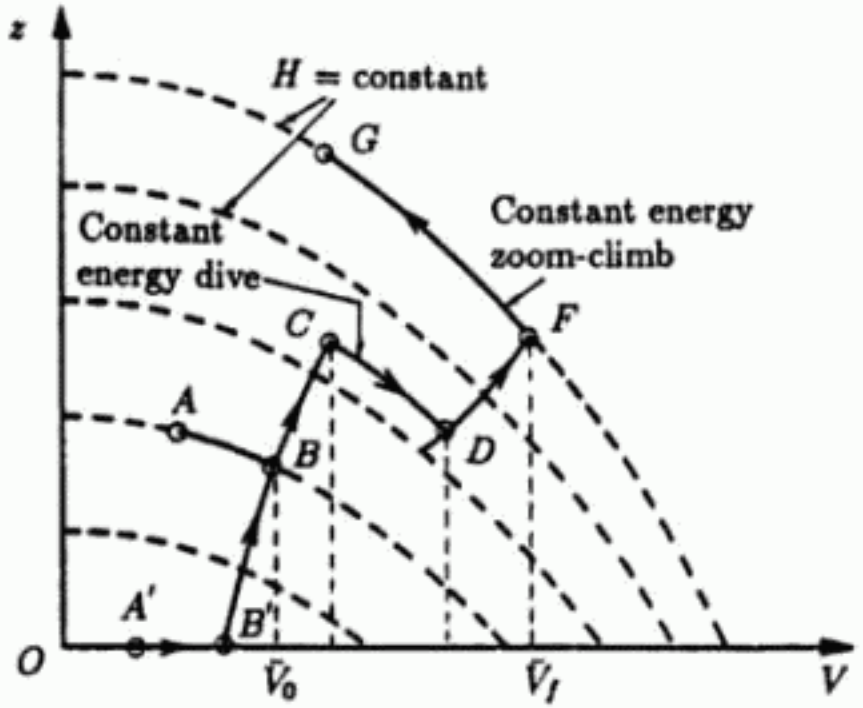

Figure 7.5: Lines of constant energy height and a typical minimum-time energy-climb flight path in (V, z) space.

From Eq. (7.93), since the fuel consumption is not imposed on the problem, to maximize V_H, at each instant, we use the maximum thrust available. Then

$$T = T_{max}(V, z) = T_{max}(V, H) \tag{7.95}$$

Now, we consider the expressions for the drag and the lift equation for nearly constant γ

$$D = \frac{1}{2}\rho(z)SV^2C_D \tag{7.96}$$

$$\frac{L}{W} = \frac{\rho(z)SV^2C_L}{2W} = \cos\gamma = n \tag{7.97}$$

In flight mechanics, we define the lift-to-weight ratio $n = L/W$ as the load factor. For flight in the vertical plane, n is the cosine of the flight path angle, with $n \approx 1$ when the flight path angle is small. If we use a parabolic drag polar, at high speed, the zero-lift drag coefficient C_{D_0}, and the induced drag factor K are functions of the Mach number $M = V/a(z)$. Hence they are functions of V and z, or equivalently of V and H. Therefore, we consider the drag polar in the form

$$C_D = C_{D_0}(V,z) + K(V,z)C_L^2 \tag{7.98}$$

Then, from the last three equations, it appears that we have the following functional dependence of the drag

$$D = D(V,z,n) = D(V,H,n) \tag{7.99}$$

If we use a constant average value for $n = \cos\gamma$, or simply put $n \approx 1$ the drag D is a function of V and H and, using H as a parameter, for constant H , we can plot the variation of V_H as function of the speed V as shown in Fig. 7.6. We constantly climb at maximum rate if at each value of the energy height we select the optimum climb speed V such that V_H is a maximum. The variation of the optimum speed is shown by the dashed line. Mathematically, V is obtained as a function of H from the equation $\partial V_H/\partial V = 0$, written explicitly as

$$T_{max}(V,H) - D + \left(\frac{\partial T_{max}}{\partial V} - \frac{\partial D}{\partial V}\right)V = 0 \tag{7.100}$$

Equation (7.100) is a generalization of Eq. (7.37). In deriving this equation previously, we have first neglected the non-steady effect by considering $V_z \approx V_H$. Furthermore, we have neglected the influence of Mach number on the thrust available. In the optimum climb of high-performance aircraft, it is important to consider the influence of altitude and speed on the maximum thrust available $T_{max}(V,z)$ and

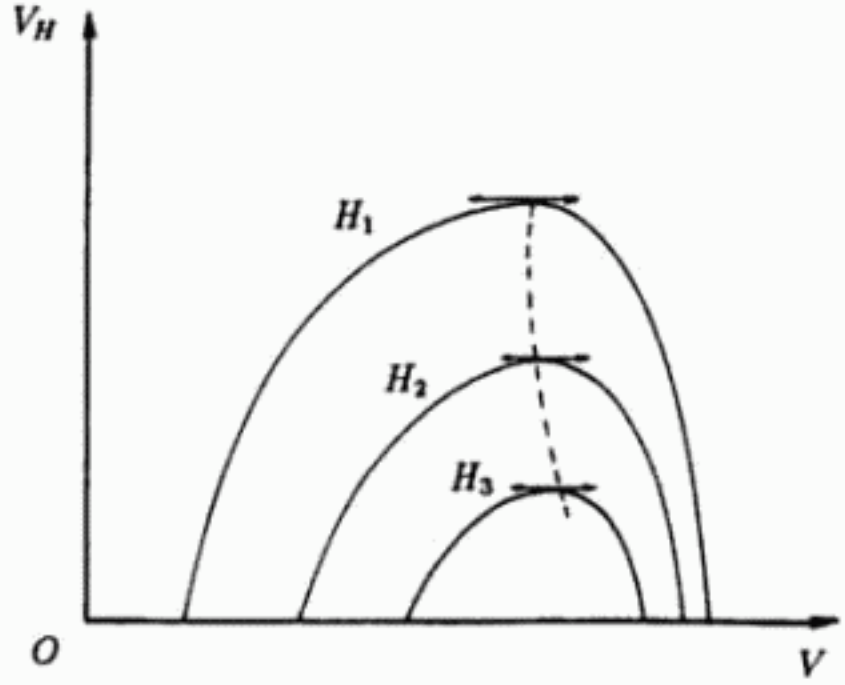

Figure 7.6: Variations of the rate of change of energy height as function of speed.

the aerodynamic characteristics $C_{D_0}(V,z)$ and $K(V,z)$. In general, as the altitude increases, the thrust decreases, but if we have high Mach number, we obtain higher thrust. On the other hand, when the Mach number increases, both C_{D_0} and K increase and hence they provide a higher drag coefficient C_D. Therefore, it is necessary to have an optimum energy management leading to a flight program $V = V(H) = V(z)$ as given in Eq. (7.100). The sucess of the solution in physical applications depends on a correct and realistic modeling of the functions $T_{max}(V,z)$, $C_{D_0}(V,z)$ and $K(V,z)$ which provides the plots in Fig. 7.6 upon transforming z into V and H.

On analyzing the graph, or solving Eq. (7.100), the optimum value $V = V(H)$ is used in the (V,z) space as shown in Fig. 7.5. The optimum climb follows the arcs for maximum rate of energy height such as the arc BC and the arc DF. To construct the overall minimum time to climb trajectory, we interpret the results as follows:

The initial point is at A and the initial speed V_1 is too low compared to the optimum speed at point B. The optimum trajectory starts with a dive at constant energy height to transform some potential energy into kinetic energy. Theoretically the change from A to B is instantaneous

and in practice, it involves a short duration. Then, we follow the optimum path from B to C. At point C, with higher altitude and lower value of T_{max} it is necessary to perform another dive along the constant energy height path to increase the speed to join the second extremum arc DF. This maneuver results in an increase of the thrust to complete the climb. At point F the final energy height H_f is reached, but at a higher speed and a lower altitude compared to the prescribed values V_f and z_f at the final point G. A zoom climb along the constant H_f line would lead to the prescribed point in a short duration.

The reason we have the two extremum arcs BC and DF is that for this example aircraft, in solving Eq. (7.100), we have two local maxima for V_H, one at low speed and one at high speed. Initially, at low altitude, we use the low speed solution giving higher maximum excess power. When the two maxima for V_H are equal, we switch the speed control to the higher value. Depending on the end-conditions and engine and aerodynamic characteristics of the aircraft, the dive from C to D at the middle of the trajectory may not exist.

This energy state approximation is useful in that it gives a simple solution to a complex problem. In practice, it gives a general idea of the optimum trajectory and we can use the solution as a starting trajectory for a refined computation to search for the true optimum. For example, if we start at point A' on Fig. 7.5 at sea level at a low speed, then it is clear that to reach a high altitude in a minimum time, it is first necessary to acquire the optimum climb speed by accelerating at constant altitude to join the climb path $B'C$, rather than starting to climb immediately. This initial delay in climbing can be easily caught up later with a higher rate of climb with higher speed and higher thrust.

7.6 Most economical climb

We now introduce the equation for the fuel consumption written as

$$\frac{dW}{dt} = -cT \tag{7.101}$$

We shall assume that the specific fuel consumption c is constant and the thrust depends only on the altitude. Hence for a fixed throttle setting, we have $T = T(z)$. To climb from an initial altitude, say at

$z = 0$, to a final altitude z_f, the weight of the fuel consumed is

$$\Delta W_1 = c \int_0^{t_f} T(z)\, dt = c \int_0^{z_f} T(z) \frac{dt}{dz}\, dz$$

Since $dz/dt = V_z$, the rate of climb, we obtain

$$\Delta W_1 = c \int_0^{z_f} \frac{T(z)}{V_z}\, dz \tag{7.102}$$

To minimize the fuel consumption, at each altitude, we must use the maximum rate of climb. Hence, the most economical climb to reach a prescribed altitude is also the fastest climb.

The most economical climb is of particular interest to commercial aviation and in general the climb portion is only the initial part of the trajectory. We reconsider this problem as follows. Let ΔW_f be the weight of the total amount of fuel available for a climb to a cruise altitude z_f, with fuel consumption ΔW_1, and a cruise at this altitude to travel an additional distance, with fuel consumption ΔW_2. Hence, we have

$$\Delta W_f = \Delta W_1 + \Delta W_2 \tag{7.103}$$

Let x_1 be the distance travelled during the climb, and x_2 be the additional distance for cruise leading to a total distance x_f as shown in Fig. 7.7.

$$x_f = x_1 + x_2 \tag{7.104}$$

We shall assume that during the cruise, the throttle is set at a fixed position providing a stabilized cruise speed V. The problem is to find a climb program, to the altitude z_f such that for a given total amount of fuel ΔW_f, the total distance travelled x_f is maximized.

For a large value of ΔW_f, that is in the case of long duration for the flight, it is apparent that the most economical program is to use the fastest climb to reach the final altitude for cruise as shown in the solid line leading to the maximum distance A. But for a small value of ΔW_f, that is for short range to the point B, it appears that we should use a smaller climb angle to extend the climb range x_1.

Mathematically, we first calculate x_1. We have

$$x_1 = \int_0^{t_1} V \cos\gamma\, dt = \int_0^{z_f} \frac{V \cos\gamma}{V_z}\, dz \tag{7.105}$$

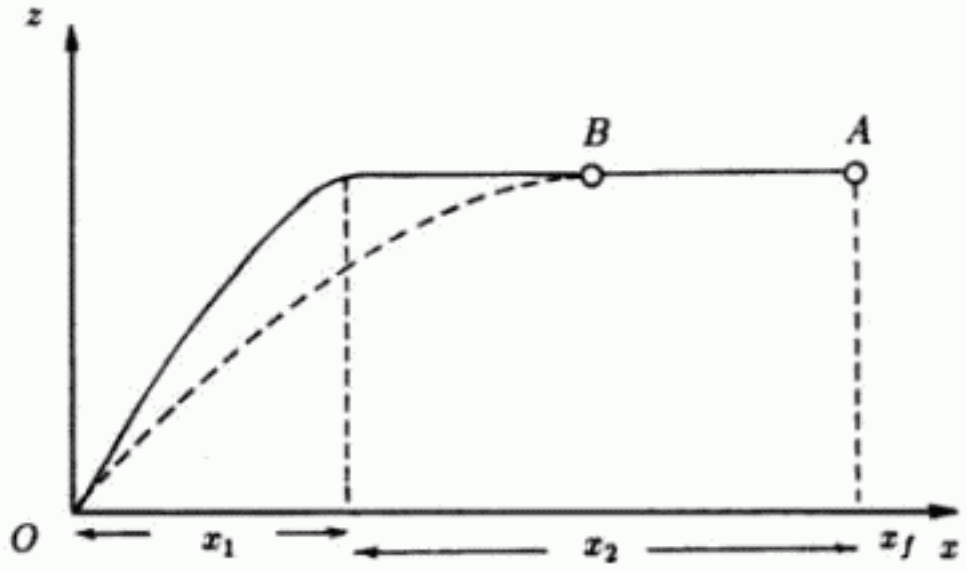

Figure 7.7: Climb and cruise for maximum distance.

During the cruise, we consider

$$\frac{dW}{dx} = \frac{dW}{dt}\frac{dt}{dx} = -\frac{cT}{V} = -\frac{1}{R} \tag{7.106}$$

For a prescribed throttle setting during the cruise, with the resulting nearly constant cruise speed, we can evaluate the constant R. Then, we have the cruise distance x_2 in terms of the fuel consumption

$$x_2 = R\Delta W_2 = R(\Delta W_f - \Delta W_1) \tag{7.107}$$

The total distance travelled to be maximized is

$$x_f = R\Delta W_f - Rc\int_0^{x_f} \frac{T(z)}{V_z}\,dz + \int_0^{x_f} \frac{V\cos\gamma}{V_z}\,dz \tag{7.108}$$

We recall that ΔW_f is given and both c and R are considered as constant. Since $V_z = V\sin\gamma$, it appears that to maximize x_f, at any altitude z, we must minimize the function

$$F(V) = Rc\frac{T(z)}{V_z} - \frac{1}{\tan\gamma} \tag{7.109}$$

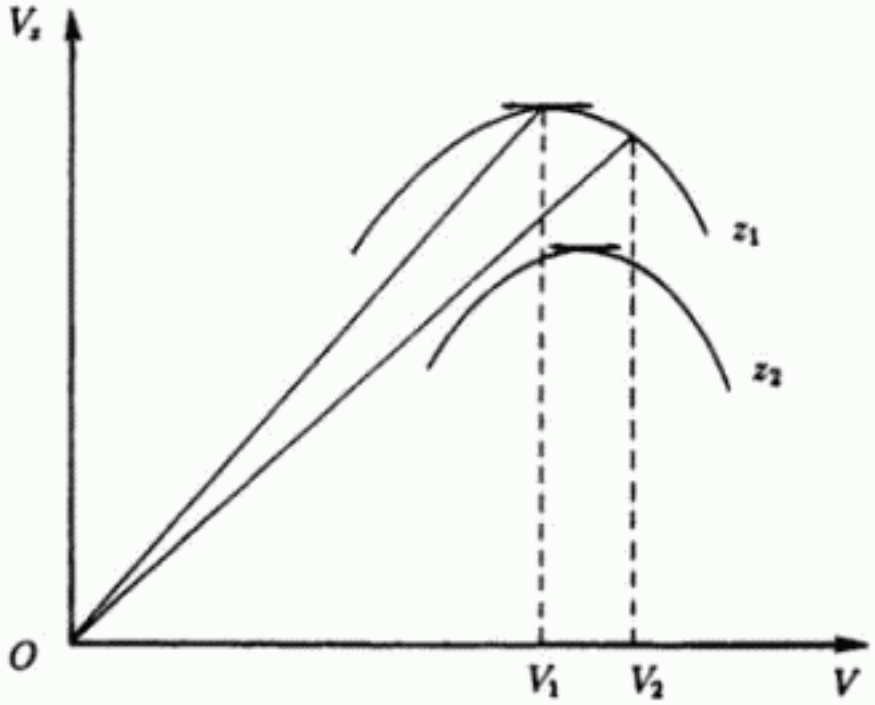

Figure 7.8: Plot of V_z versus V.

Figure 7.8 shows the plot of V_z versus V, using altitude as a parameter. We notice that $\sin\gamma = V_z/V$ is the slope of the line from the origin O to any operating point on the curve V_z.

We have discussed before that, at any current altitude, the rate of climb V_z is a function of the speed V, and hence $\tan\gamma$ is also a function of V. In Eq. (7.109), if only the first term is considered, to minimize F we should use the maximum rate of climb V_z. But the corresponding optimum speed at V_1, will give a high climb angle γ and if the second term in Eq. (7.109) is included, this will increase the value of F through a large value of γ. It appears that there is a trade-off providing an overall minimum value for F at a speed V_2 slightly larger than V_1 giving a smaller rate of climb and thus increasing the first term in Eq. (7.109), but at the same time giving a smaller climb angle such that the increase in the second term is larger than the increase in the first term. More explicitly, we take $\cos\gamma \approx 1$ and rewrite the function $F(V)$ to be minimized, in the form

$$F(V) = \frac{1}{V_z}(RcT - V) > 0 \tag{7.110}$$

The function F is minimized when

$$(RcT - V)\frac{dV_z}{dV} + V_z = 0 \tag{7.111}$$

We notice that $RcT - V > 0$ since this is equivalent to

$$T_{climb} > \frac{V_{climb}}{Rc} = T_{cruise}\frac{V_{climb}}{V_{cruise}}$$

Then, since during the climb $V_z > 0$, Eq. (7.111) is necessarily satisfied for $dV_z/dV < 0$ which corresponds to the speed V_2 in Fig. 7.8.

Exercises

7-1. Show that the maximum rate of climb for a propeller driven aircraft is

$$V_z = \frac{P_a}{W}\left(1 - \frac{P_r^*}{P_a}\right)$$

where P_r^* is the minimum power required

$$P_r^* = \frac{2}{3^{3/4}E_{max}}\sqrt{\frac{2W^3}{\rho S C_L^*}}$$

with $C_L^* = \sqrt{C_{D_0}/K}$ being the lift coefficient for maximum lift-to-drag ratio.

7-2. The ceiling is attained when at maximum throttle setting, we have $P_a = P_r^*$. Discuss the influence of the maximum power P_a, the weight W, the wing loading W/S and the maximum lift-to-drag ratio E_{max} on the absolute propulsive ceiling.

If the ceiling is above the critical altitude, using the modeling as given by Eq. (7.23), show that the density at the ceiling is given by the explicit equation

$$\frac{\rho}{\rho_c} = \left(\frac{P_r^*}{P_0}\right)^{2/3}$$

where both the maximum power available P_0 and the minimum power required P_r^* are evaluated at the critical altitude.

7-3. Below the critical altitude where P_a is constant, show that with an exponential atmosphere, the minimum time to climb is

$$t = \frac{2W}{\beta P_a}\left[\frac{\beta}{2}(z_f - z_1) + \text{Log}\left(\frac{V_{z_1}}{V_{z_f}}\right)\right]$$

7-4. In Eq. (7.32) for the optimum equivalent speed V_i for maximum climb angle, put $x = P_a\sqrt{\sigma}/\rho_0 S C_{D_0}$ and consider this equation as an implicit equation defining V_i as a function of x. Show that $dV_i/dx < 0$ and hence conclude that V_i is smaller at lower altitude where x is larger.

7-5. For a propeller driven aircraft, upon solving Eq. (7.32) for the optimum V_i which is a function of the altitude, the corresponding lift coefficient for maximum climb angle is given by the lift equation (7.28). Using this value in Eq. (7.34), show that the maximum climb angle is given by

$$\sin\gamma = \frac{1}{2E_{max}}\left(\lambda - \frac{3}{\lambda}\right)$$

where $\lambda = C_{L_{opt}}/C_L^*$.

7-6. It is curious that in the previous exercise, it appears that a high value of E_{max} decreases the climb angle. But we should realize that high values of E_{max} also lead to high values of λ which may be easily beyond the maximum value of λ for stalling. To explain this, show that the optimum equation (7.32), when expressed in terms of λ, has the form

$$\frac{1}{\lambda^2} + \frac{2P_a/P_r^*}{3^{3/4}\lambda^{1/2}} = 1$$

where P_r^* is the minimum power required as given in Exercise 7-1.

Using the approach in Exercise 7-4, it is readily seen that with high power available, at low altitude, with a high value of E_{max} and light weight the optimum value of λ is high.

7-7. The results in Exercises 7-5 and 7-6 constitute a universal solution to the problem of the maximum climb angle of a propeller driven aircraft.

First, at the ceiling, $P_a/P_r^* = 1$ and the smallest limiting value of λ is $\lambda = \sqrt{3}$, that is $C_L = \sqrt{3C_{D_0}/K}$ as expected. A table, or graph of $P_a/P_r^* \geq 1$ versus λ can be generated. Notice that λ quickly increases to unacceptable values even with a moderate ratio P_a/P_r^*.

Next, for each value of λ we can calculate $2E_{max}\sin\gamma$ for tabulation. The use of the tables or the graphs for any particular aircraft at any power available and altitude is evident.

7-8. Let V_{z_1} be the maximum rate of climb as given in Exercise 7-1. Let V_{z_2} be the rate of climb when the maximum climb angle is used. Show that

$$V_{z_2} = \frac{3^{3/4}P_r^*}{4W\lambda^{1/2}}\left(\lambda - \frac{3}{\lambda}\right)$$

where λ is as defined in Exercises 7-5 and 7-6. By forming the ratio V_{z_1}/V_{z_2} and then using the equation in Exercise 7-6 to eliminate P_a/P_r^*, show that

$$\frac{V_{z_1}}{V_{z_2}} = \frac{2}{3}\left[1 + \frac{2\bar{\lambda}^{3/2}}{(\bar{\lambda}+1)(\bar{\lambda}^{1/2}+1)}\right]$$

where $\bar{\lambda} = \lambda/\sqrt{3}$. For the realistic range of $\bar{\lambda}$ between 1 and 2, this ratio varies between 1 and 1.187. Hence, in practice, the fastest climb and the climb at maximum angle are essentially the same.

7-9. Let V_{z_1} be the maximum rate of climb of a jet aircraft with the magnified thrust-to-weight ratio τ_1. It is proposed to find the value τ_2 such that the new rate of climb is increased by a factor k, that is so that $V_{z_2} = kV_{z_1}$.

Define

$$u = \tau + \sqrt{\tau^2 + 3}$$

Show that

$$\frac{V_{z_2}}{V_{z_1}} = \frac{u_1^{1/2}(u_2^2 - 9)}{u_2^{1/2}(u_1^2 - 9)} = k$$

With the new factor

$$k_1 = \frac{k(u_1^2 - 9)}{u_1^{1/2}}$$

we solve the equation

$$u_2^2 - k_1 u_2^{1/2} - 9 = 0$$

for u_2 and deduce

$$\tau_2 = \frac{u_2^2 - 3}{2u_2}$$

Numerical examples: Take $\tau_1 = 2$. When $k = 1.2$, we obtain $\tau_2 = 2.177603 = 1.09\tau_1$. When $k = 1.3$, we obtain $\tau_2 = 2.264306 = 1.13\tau_1$.

7-10. Show that with the approximation $\cos\gamma \approx 1$, the lift control for maximum rate of climb is

$$\frac{C_L}{C_L^*} = \sqrt{\tau^2 + 3} - \tau$$

Hence, conclude that for a fixed throttle setting, as τ decreases during the climb, C_L increases until the final value C_L^* at the ceiling.

7-11. Use the definitions of u, V_{z_1}, V_{z_2} and k as in Exercise 7-9. For a certain throttle setting and maximum lift-to-drag ratio, let W_1 be the weight resulting in a value τ_1 with the corresponding maximum rate of climb V_{z_1}. Let W_2 be a smaller weight such that the rate of climb is increased to the new value $V_{z_2} = kV_{z_1}$.

Show that

$$\frac{V_{z_2}}{V_{z_1}} = \frac{(u_1\tau_1)^{1/2}(u_2^2 - 9)}{(u_2\tau_2)^{1/2}(u_1^2 - 9)} = \frac{(u_1^2 - 3)^{1/2}(u_2^2 - 9)}{(u_2^2 - 3)^{1/2}(u_1^2 - 9)} = k$$

With a new factor k_1 and a new unknown y such that

$$k_1 = \frac{k(u_1^2 - 9)}{(u_1^2 - 3)^{1/2}}, \qquad y = (u_2^2 - 3)^{1/2}$$

show that y is calculated from

$$y^2 - k_1 y - 6 = 0$$

Upon solving this quadratic equation, we obtain u_2 and

$$\tau_2 = \frac{u_2^2 - 3}{2u_2} = \frac{y^2}{2\sqrt{y^2 + 3}}$$

Then, calculate the ratio

$$\frac{\tau_2}{\tau_1} = \frac{W_1}{W_2}$$

Numerical examples: Take $\tau_1 = 2$. When $k = 1.2$, we obtain $\tau_2 = 2.237881$, $W_1/W_2 = 1.119$. When $k = 1.3$, we obtain $\tau_2 = 2.360014$, $W_1/W_2 = 1.180$.

7-12. Consider Eq. (7.68) for the case of a large value of the magnified thrust-to-weight ratio τ_0 at sea level. Let

$$\epsilon = \frac{3}{2E_{max}(T_0/W)\sigma} = \frac{3}{2\tau_0\sigma} \ll 1$$

Then, this equation becomes

$$t = \frac{\tau_0}{3\beta V_{s_0}} \operatorname{Log} \frac{(1-\epsilon_1)(1+\epsilon_f)}{(1+\epsilon_1)(1-\epsilon_f)}$$

Using the series expansion

$$\operatorname{Log} \frac{1+\epsilon}{1-\epsilon} = 2\left(\epsilon + \frac{\epsilon^3}{3} + \cdots\right)$$

show that we have Eq. (7.70)

$$t = \frac{1}{\beta V_{s_0}} \left(\frac{1}{\sigma_f} - \frac{1}{\sigma_1}\right)$$

7-13. Consider the exact formula (7.77) for the fastest time to climb. If τ is large, then from Eqs. (7.45) and (7.75), u and y are large and we can use the approximation,

$$y \approx u \approx 2\tau = 2\tau_0 \sigma.$$

Then show that to the order of $1/y$ we have for the logarithm term and the arc tangent term

$$\sqrt{2}\left(\frac{2\sqrt{6}}{y_f} - \frac{2\sqrt{6}}{y_1}\right) \qquad \text{and} \qquad \sqrt{3}\left(\frac{1}{y_f} - \frac{1}{y_1}\right)$$

respectively. Then, show that the formula is reduced to

$$t = \frac{1}{\beta V_{s_0}} \left(\frac{1}{\sigma_f} - \frac{1}{\sigma_1}\right)$$

7-14. By using $\cos\gamma = \sqrt{1 - \sin^2\gamma}$ in Eq. (7.82), show that we can calculate $\sin\gamma$ from the quadratic equation

$$(E^2+1)\sin^2\gamma - 2E\tau \sin\gamma + (\tau^2 - 1) = 0.$$

If $T \geq W$, we can have vertical climb, $\sin\gamma = 1$, with $E = 0$. For $T < W$, show that real solutions always exist regardless of the value of E. Solve for $\sin\gamma$ and show that it can be put in the form

$$\sin\gamma = \frac{\dfrac{T}{W} - \dfrac{1}{E}\left[1 + \dfrac{1}{E^2} - \dfrac{T^2}{W^2}\right]^{1/2}}{1 + (1/E^2)}$$

Hence, deduce that γ is larger for larger values of T/W and E. Conclude that the steepest climb is conducted with $E = E_{max}$.

Use the half tangent formula to calculate $\sin\gamma$ from Eq. (7.84) and compare it with the solution above. They should be identical.

7-15. Show that Eq. (7.84) can be put in the form

$$\tan\frac{\gamma}{2} = \frac{1}{(T/W)+(1/E)}\left[1-\sqrt{1+(1/E)^2-(T/W)^2}\right]$$

From this equation, it is seen that γ increases when the lift-to-drag ratio increases.

Let

$$z = \tan\frac{\gamma}{2}, \qquad x = \frac{1}{E}, \qquad y = \frac{T}{W}$$

Show that

$$z = \frac{y-x}{1+\sqrt{1+x^2-y^2}}$$

In this form, it is clear that when y increases z increases. Also when E increases, x decreases and z increases.

8

Turning performance

8.1 Introduction

The analysis of climbing flight at steep angles has displayed the curvature of the flight path due to the variation of the flight path angle. Because of this variation, the acceleration is not directed along the velocity vector and the resulting force deflects this velocity. Hence the trajectory is no longer rectilinear. The study of turning trajectories is the topic of this chapter and the following chapter. In turning, the direction of the velocity varies strongly along the flight path and the resulting acceleration must be included in the analysis.

As the velocity vector changes its direction, the aircraft turns. The turn can be effected in a horizontal plane, or in a vertical plane or with change in both the altitude and the heading. For example, heading changes after a take-off are representative of ascending turns. Altitude changes during holding patterns above airports involve descending turns. Heading changes for final approach before landing are descending turns. On the other hand, turning flight can be made at constant rate, that is a steady turn, or with a varying rate resulting in a non-steady turn.

Again, following the general plan, we shall analyze turning performance in increasing order of complexity. In the general case, for an aircraft considered as a dynamic system, the motion of its center of mass is defined by seven variables, namely the three position coordinates x, y and z, the speed V, the flight path angle γ, the heading angle ψ, and the mass m (Fig. 8.1). They are governed by seven differential

equations as derived in Chapter 2. Turning maneuvers are generally of short duration so that the weight $W = mg$ can be considered as

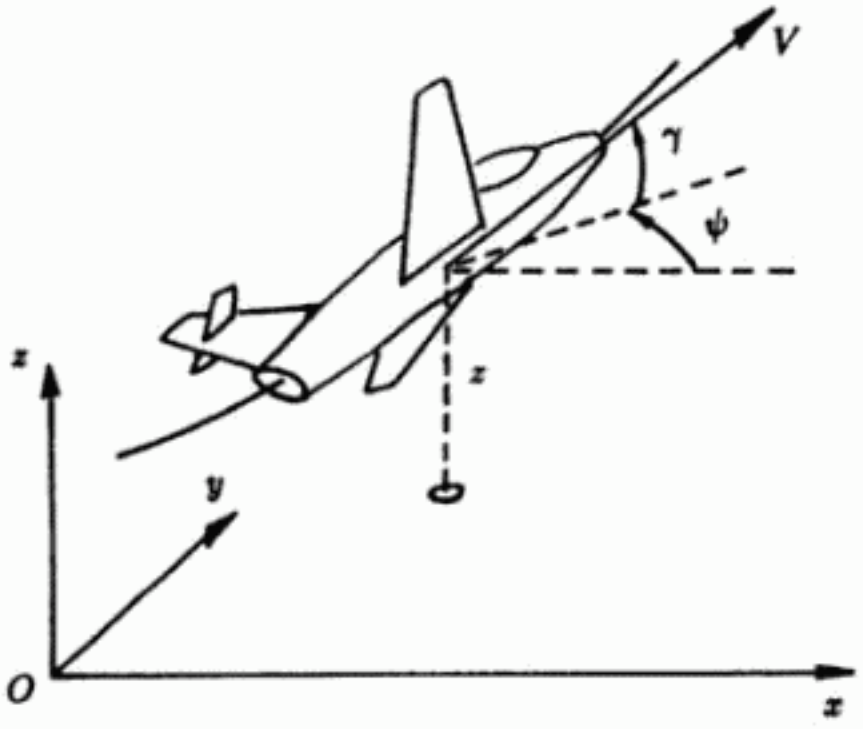

Figure 8.1: Three-dimensional trajectory.

constant. We have the remaining six equations

$$\begin{aligned}
\frac{dx}{dt} &= V\cos\gamma\cos\psi \\
\frac{dy}{dt} &= V\cos\gamma\sin\psi \\
\frac{dz}{dt} &= V\sin\gamma \\
\frac{dV}{dt} &= g\left[\frac{T}{W}\cos\varepsilon - \frac{D}{W} - \sin\gamma\right] \\
\frac{d\gamma}{dt} &= \frac{g}{V}\left[\left(\frac{L}{W} + \frac{T}{W}\sin\varepsilon\right)\cos\phi - \cos\gamma\right] \\
\frac{d\psi}{dt} &= \frac{g}{V}\left(\frac{L}{W} + \frac{T}{W}\sin\varepsilon\right)\frac{\sin\phi}{\cos\gamma}
\end{aligned} \tag{8.1}$$

In the equations, we have used ϕ to denote the bank angle, that is the

angle between the vertical plane and the plane of symmetry containing the lift and the thrust.

As usual, if we consider that the thrust **T** is nearly collinear with the velocity vector **V**, the approximation $\cos\varepsilon \approx 1$, and $\sin\varepsilon \approx 0$ in Eq. (8.1) can be made. The latter approximation can be further enhanced by the fact, as will be shown below, that for turning flight, the load factor $n = L/W$ is much greater than 1. We shall first consider the simplest maneuver of a steady turn in a horizontal plane.

8.2 Constant speed turn in a horizontal plane

The simplest maneuver is a turn in a horizontal plane at constant speed. The altitude is constant and hence, $\gamma = 0$. From the equation for γ in system (8.1) we have the lift equation

$$L\cos\phi = W \tag{8.2}$$

A steady turn is a turn in which the speed is constant. If the speed is constant, with $\gamma = 0$ and $dV/dt = 0$, we have the thrust equation

$$T = D \tag{8.3}$$

an equation which shows that the thrust is used to balance the drag. Figure 8.2 shows the force diagram for a coordinated turn in a horizontal plane. This means that there is no sideslip angle, and the velocity vector is in the plane of symmetry containing the aerodynamic force and the propulsive force. In a perfectly coordinated turn at constant speed, the thrust balances the drag and their common line of action is along the direction of the velocity which is perpendicular to the plane of the figure. In other words, the drag and the thrust are perpendicular to the plane formed by the lift **L** and the gravity force **W**. From the figure, it is seen that the weight is balanced by the vertical component of the lift force. This equilibrium of force is represented by Eq. (8.2). Because of the bank angle ϕ, the lift has a horizontal component with magnitude $L\sin\phi$ and directed toward the center of the turn in the horizontal plane. This force is balanced by a centrifugal force of magnitude mV^2/R, where R is the radius of curvature which, in this case, is the turning radius.

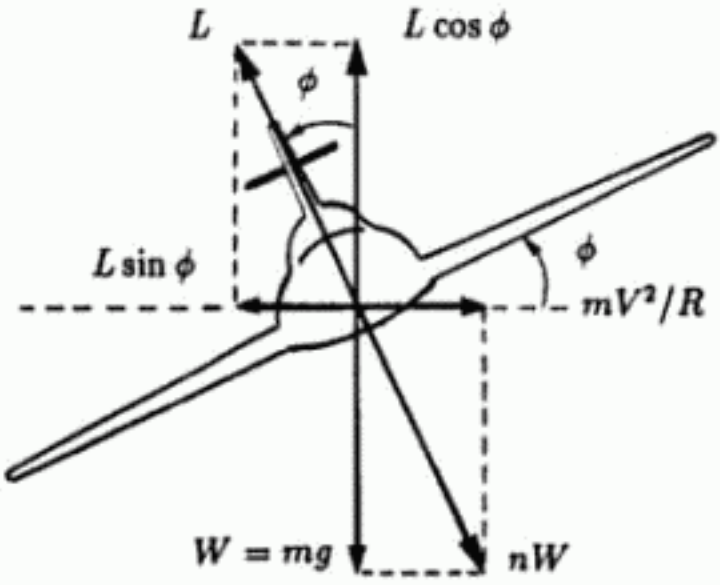

Figure 8.2: Coordinated turn in a horizontal plane.

8.2.1 The load factor

In Chapter 7, we have introduced the notion of the load factor, n, defined as the ratio of the lift force to the weight

$$n = \frac{L}{W} \tag{8.4}$$

This is a very important parameter in turning performance. From Eq. (8.2), it is related to the bank angle by the simple relation

$$n = \frac{1}{\cos\phi} \tag{8.5}$$

A plot of this equation in Fig. 8.3 displays the values of the load factor for different bank angles. Typical bank angles for fighter aircraft are 45°, 60° and 80°. As ϕ approaches 90°, the load factor becomes infinite.

By rewriting Eq. (8.2) as

$$L = nW \tag{8.6}$$

we see that nW is a combination of the weight and the centrifugal force and it is opposite to the lift force. This force is also called the apparent

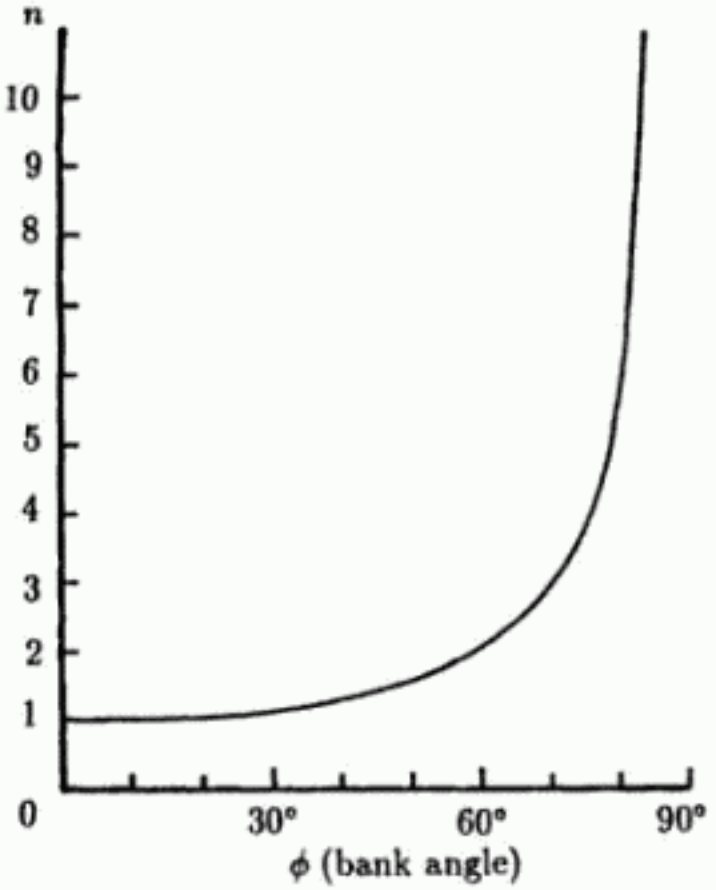

Figure 8.3: The load factor as a function of the bank angle.

weight. For high values of the load factor, the force becomes so severe that it reaches the physiological limit of the pilot, and passengers, or the structural limit of the airframe. Hence, in practice, there exists an upper limit n_s for the load factor and correspondingly, for horizontal turn, there is an upper limit ϕ_s for the bank angle. For example, if the structural limit is $n_s = 6$, the bank angle is limited at 80.406 degrees. Turning at this angle, the pilot is subjected to a force equal to six times his own weight.

8.2.2 *The control of turning*

As in Chapter 6 for the control of the cruise, we display the lift

equation and the thrust equation as follows

$$nW = \frac{1}{2}\rho S V^2 C_L$$

$$T = \frac{1}{2}\rho S V^2 C_D$$

For a propeller driven aircraft we replace the thrust equation by the power equation by multiplying the thrust equation by the speed V.

To control the turn, the pilot can vary the thrust available T_a, or the power available P_a, the angle-of-attack through the lift coefficient C_L, and the bank angle ϕ. From Eq. (8.5), controlling the bank angle is the same as controlling the load factor n. Assume that at a given altitude we want to turn at a certain prescribed load factor n, with a stabilized speed V. Then, from the lift equation, we have the corresponding lift coefficient C_L and through the drag polar, this results in a drag coefficient C_D. From the thrust equation, or the power equation, we calculate the necessary thrust, or power, to maintain the required speed. But, we should realize that, as a physical plant, the aircraft has its own limitations. First the load factor selected should be less than the structural limit n_s. Yet, with a high load factor, for a certain range of the selected stabilized speed, the resulting lift coefficient may exceed its maximum value $C_{L_{max}}$ for stall. Still, if this coefficient is restricted to $C_{L_{max}}$, the resulting drag coefficient C_D and the selected speed V for turning may lead to a thrust required that is higher than the maximum thrust the engine is capable of delivering. These various constraints, and in addition the influence of altitude and Mach number on aerodynamic and engine characteristics should be considered in the analysis of turning performance.

8.2.3 The turning rate

For transport aircraft, during an instrument flight in the vicinity of an airport, the control of turning rate to complete a turn in a prescribed time is important. For fighter aircraft, turning at a high rate is an essential design objective.

From the last equation in system (8.1), we have the turning rate, with $\varepsilon = 0$, $\gamma = 0$ as

$$\dot{\psi} = \frac{g}{V}\left(\frac{L}{W}\right)\sin\phi \tag{8.7}$$

Using the lift equation (8.2), we have the simple formula

$$\dot{\psi} = \frac{g}{V} \tan \phi \tag{8.8}$$

This formula can be used to calculate the turning rate with the selected bank angle and turning speed, with the assumption that no physical constraints on the load factor, the lift coefficient and the thrust available are violated. Using Eq. (8.5), we can express the turning rate in terms of the speed and the load factor as

$$\dot{\psi} = \frac{g\sqrt{n^2 - 1}}{V} \tag{8.9}$$

We have an alternate form by using Eq. (8.6) to express the speed in terms of the load factor and the lift coefficient. Then, we have

$$\dot{\psi} = g\sqrt{\frac{\rho S}{2W}}\sqrt{C_L}\sqrt{n - \frac{1}{n}} \tag{8.10}$$

These various formulas can be used to calculate the turning rate and to analyze turning performance subject to physical constraints.

8.2.4 The turning radius

The radius of a turn is obviously an important parameter in flight operations. Based on Fig. 8.2, by expressing the centrifugal force as equal to the lateral component of the lift force in turning and using Eq. (8.2), we have the expression for the turning radius

$$R = \frac{V^2}{g \tan \phi} \tag{8.11}$$

As with the turning rate, this formula can be used to calculate the turning radius with the selected bank angle and turning speed with the assumption that no physical constraints are violated. In terms of the speed and the load factor, we have

$$R = \frac{V^2}{g\sqrt{n^2 - 1}} \tag{8.12}$$

Finally, when the speed is expressed in terms of the load factor and the lift coefficient by the use of Eq. (8.6), we obtain

$$R = \left(\frac{2W}{g\rho S C_L}\right)\frac{n}{\sqrt{n^2-1}} \tag{8.13}$$

A simple examination of Eq. (8.10) reveals that to have a high turning rate, it is necessary to use a high value of the load factor n, that is a high bank angle ϕ, and also a high value of the lift coefficient C_L. By inspecting Eq. (8.13), we see that this is also true for a small turning radius. This dictates high engine performance to overcome the resulting high drag force and a complete discussion would involve its dependence on altitude and Mach number. Therefore, we shall complete this chapter with the analysis of turning performance of propeller driven aircraft and reserve a separate chapter to deal with the case of jet aircraft.

8.3 Power required for turning

We express the thrust equation (8.3) in terms of powers by multiplying it by the speed V. We have

$$P = \frac{1}{2}\rho S V^3 C_D \tag{8.14}$$

The right-hand side of this equation is the power required to turn at the prescribed speed V and angle-of-attack leading to the drag coefficient C_D. By the drag polar, controlling C_D is the same as controlling C_L. By the lift equation (8.6), we see that, ultimately, we can express the power required in terms of the load factor n, that is of the bank angle ϕ, and the lift coefficient. If this substitution is made, we have the power required for turning

$$P_{nr} = \sqrt{\frac{2W^3}{\rho S}}\, n^{3/2}\frac{C_D}{C_L^{3/2}} \tag{8.15}$$

We add the subscript n to the symbol P_r for the power required to emphasize the fact that this concerns the case of turning with the load factor n. For $n = 1$, we have the case of rectilinear level flight.

For comparison with the case of a jet aircraft, we consider the thrust required by combining Eqs. (8.3) and (8.4) to obtain

$$T_{nr} = nW\frac{C_D}{C_L} \tag{8.16}$$

Then, by using the same angle of attack, that is by keeping C_D and C_L the same, while the thrust required is proportional to nW, the power required is proportional to $(nW)^{3/2}$. For a propeller driven aircraft, the increase in power required for greater weight and higher load factor in turning is more severe than the increase in the thrust required for a jet aircraft.

If we use a parabolic drag polar to express C_D in terms of C_L^2 and use the lift equation (8.6) to express C_L in terms of n and V, then upon substituting into Eq. (8.14), we have

$$P_{nr} = \frac{\rho S V^3 C_{D_0}}{2} + \frac{2Kn^2W^2}{\rho SV} \tag{8.17}$$

For each value of the load factor n, the plot of the power required for turning versus the speed shows the same behavior as for the case of cruise with $n = 1$. In particular, as discussed in Chapter 6 for a realistic drag polar, the slope of the curve is infinite at the stall speed as shown in Fig. 8.4. In the same figure we also have the power available for a given throttle setting at that flight altitude.

Again, as has been mentioned in Chapter 6, for the convenience of an analytical discussion, we have used a parabolic drag polar to derive Eq. (8.17) for the power P_{nr} required to turn. It is physically correct except near the stall speed. In Fig. 8.4, the lowest curve is the plot of P_r versus V for rectilinear flight with $n = 1$. To obtain the curve for P_{nr} with arbitrary $n > 1$, at each point M on the curve of P_r with speed V, we have a new point M_n with speed $V\sqrt{n}$ and power $P_r\sqrt{n^3}$ (see Exercise 8-1). The highest curve is that for $n = n_s$, the imposed maximum value of the load factor. In the range of speed, along each curve P_{nr}, the minimum speed is the stall speed, which is obtained from the lift equation with $C_L = C_{L_{max}}$. We have

$$V_{stall} = \sqrt{\frac{2nW}{\rho S C_{L_{max}}}} \tag{8.18}$$

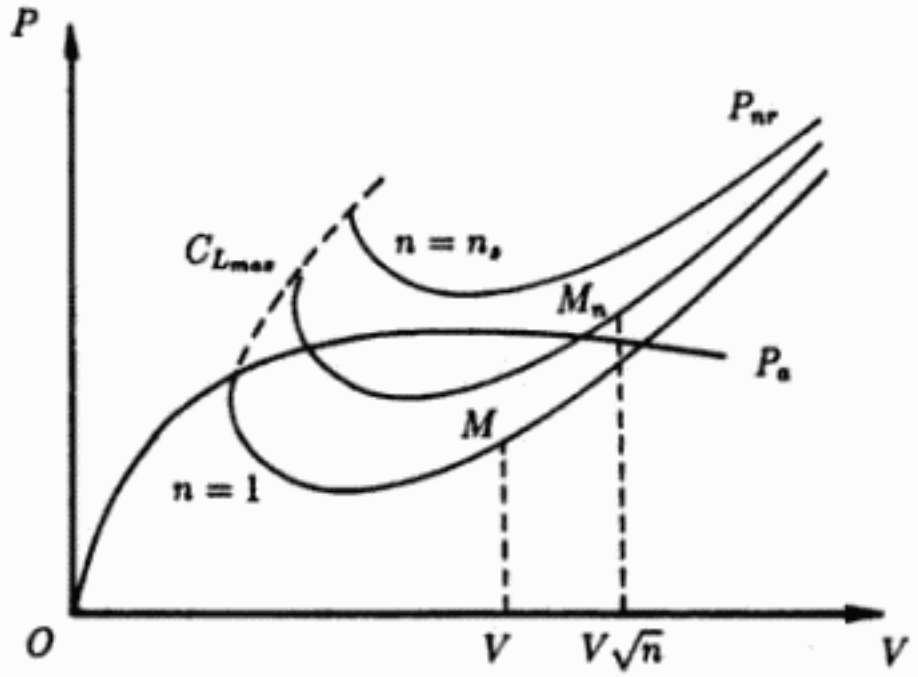

Figure 8.4: Power available and power required for turning.

Hence, in turning with the load factor n, the stall speed increases by the factor $\sqrt{n}$ as compared to the stall speed in rectilinear flight.

Consider a throttle setting resulting in a power available P_a as shown in Fig. 8.4. For steady turning, we have $P_a = P_{nr}$. For turning, we can arbitrarily select a bank angle ϕ, resulting in a load factor n. Turning at constant speed is possible if we have intersection between the curve P_a and the curve P_{nr} selected. Along the stall line, shown as a dashed curve in Fig. 8.4, there exists a value n such that the P_{nr} curve intersects the P_a curve at $C_L = C_{L_{max}}$, with the stall speed. The other intersection is at a higher speed with lower lift coefficient. For a higher value of n we have two intersecting points and just as in the case of cruise discussed in Chapter 6, the turning can be conducted at two flight regimes: one low speed regime with high angle-of-attack and one high speed regime with low angle-of-attack. By a similar discussion, we can show that the low speed regime is unstable while the high speed regime is stable. But the difference here is that, as will be shown later in this chapter, the use of low speed for turning yields a higher turning rate and a smaller turning radius. Then, in optimum maneuvers, the turn is conducted near the stall speed.

Figure 8.4 plots the power required for turning and the power avail-

able at a specified altitude with atmospheric density ρ. Just as in the case of rectilinear level flight, as discussed in Chapter 6, the power required increases by the factor $\sigma^{-1/2}$, where σ is the density ratio, when the attitude increases, while the power available decreases with altitude above the critical altitude for the reciprocating engine considered. By putting in Eq. (8.17) $P_{nr} = P_a$, the power available for the prescribed throttle setting for the turn, we can calculate the corresponding turning speed V, for any load factor n, by solving a quartic equation. A physical solution exists if P_a is greater than the minimum value of P_{nr} which is obtained from the equation $dP_{nr}/dV = 0$. Explicitly, we solve for the corresponding speed

$$\frac{1}{2}\rho V^2 = \frac{nW}{S}\sqrt{\frac{K}{3C_{D_0}}} = \frac{nW}{\sqrt{3}SC_L^*} \tag{8.19}$$

By comparison with to the lift equation (8.6), we have the lift coefficient $C_L = \sqrt{3}C_L^*$ for minimum power required. This is also obtained by minimizing P_{nr} as given by Eq. (8.15) with respect to C_L. If a parabolic drag polar is used, then we have its minimum value

$$P_{nr}^* = \frac{2}{3^{3/4}E_{max}}\sqrt{\frac{2n^3W^3}{\rho SC_L^*}} \tag{8.20}$$

Turn at the prescribed load factor at constant altitude with atmospheric density ρ is possible only if $P_a \geq P_{nr}^*$. If in Eq. (8.20) we replace P_{nr}^* by P_a, then on solving for n, we have the maximum possible value for the load factor to turn at the prescribed power available. We have then

$$n_{max} = \left[\frac{3^{3/2}}{8}\rho C_L^* \frac{E_{max}^2 (P_a/W)^2}{W/S}\right]^{1/3} \tag{8.21}$$

This maximum load factor increases if P_a increases. For fixed throttle setting, n_{max} decreases with altitude, since it is first proportional to $\rho^{1/3}$ and then it decreases with $P_a^{2/3}$ as the power available decreases above the critical altitude. With maximum throttle setting, when n_{max} is reduced to unity, we have reached the propulsive ceiling when only rectilinear flight at constant altitude is barely feasible.

At low altitude and with sufficient power, n_{max} is high and it may exceed the value n_s. In this case, for the given power available, we can

turn at any load factor up to the value n_s. At high altitude where n_{max} is small, we may reach n_{max} before the value n_s.

8.4 Optimum turn

In general, for propeller driven aircraft, turning is accomplished at low speed and we assume that the aerodynamic characteristics are independent of the Mach number. For a given aircraft we have the constant values W, S, C_{D_0} and K, and hence also E_{max} and C_L^*. Furthermore we assume that $C_{L_{max}}$ is known as is the imposed value n_s. At any operating altitude, as specified by the atmospheric density ρ, a steady turn can be done in an infinite number of ways. We first consider some straight forward calculations of the performance and then, in a sense, search for the optimum solutions.

We first notice that for steady turning, the trajectory is a circle in a horizontal plane and both the turning rate and the turning radius are constant.

8.4.1 Turning at a prescribed rate

If we want to change the direction, by any amount, in a prescribed time, this leads to specifying the turning rate $\dot{\psi}$. The turn can be accomplished in an infinite number of ways. This is because according to Eq. (8.9) we can select any combination for the pair n and V giving the value $\dot{\psi}$ subject to the constraints on n_s, $C_{L_{max}}$ and P_{max}, the maximum power available at the flight altitude. We can select a bank angle ϕ, providing the corresponding load factor $n \leq n_s$ and calculate the speed V for turning from the equation. This speed should be greater than the stall speed at the selected load factor as given by Eq. (8.18). Therefore, we have the first necessary condition for any prescribed turning rate, with the selected load factor,

$$\dot{\psi} \leq g\sqrt{\frac{\rho S C_{L_{max}}}{2W}}\sqrt{n - \frac{1}{n}} \tag{8.22}$$

If we put n_s in this inequality we have on the right-hand side an upper value $\dot{\psi}_{max}$ for the turning rate. The selected turning rate must be less than, or at most equal to this value which can also be obtained by

maximizing $\dot{\psi}$ as given by Eq. (8.10) with respect to C_L and n. This is the absolute maximum turning rate

$$\dot{\psi}_{max} = g\sqrt{\frac{\rho S C_{L_{max}}}{2W}}\sqrt{n_s - \frac{1}{n_s}} \tag{8.23}$$

This rate is achievable at low altitude with adequate propulsive power. It is seen that the maximum turning rate is high at low altitude, with high values of n_s and $C_{L_{max}}$ and low wing loading W/S.

Next, we assume that with the prescribed rate, the strict inequality $\dot{\psi} < \dot{\psi}_{max}$ is satisfied. Then, we can use any value of $n < n_s$ and calculate the corresponding speed from Eq. (8.9) to be used in Eq. (8.17) for the power required P_{nr}. The final condition is that this power required is less than the maximum power available produced by the engines at the flight altitude. The power required to turn at the specified rate $\dot{\psi}$ is

$$P_{nr} = \frac{\rho S C_{D_0} V^3}{2} + \frac{2KW^2\dot{\psi}^2 V}{g^2\rho S} + \frac{2KW^2}{\rho S V} \tag{8.24}$$

If the maximum power available at the flight altitude is greater than this value, turning at the prescribed rate with the selected load factor is feasible. But, if P_{max} is less than the value for P_{nr} from Eq. (8.24), it may still be possible to turn at the same prescribed rate $\dot{\psi}$ by selecting a lower value of the load factor providing a lower value of the corresponding speed as given in Eq. (8.9) to reduce the power required. This means that to achieve the prescribed turning rate $\dot{\psi}$, we can use the speed to control the flight and calculate the corresponding load factor from Eq. (8.9). Considered as a function of V, the power required for turning is a minimum when $dP_{nr}/dV = 0$. Explicitly, in terms of the dynamic pressure, $q = \rho V^2/2$, we have the quadratic equation

$$F(q) = q^2 + \frac{2(W/S)^2\dot{\psi}^2}{3g^2\rho C_L^{*2}}q - \frac{(W/S)^2}{3C_L^{*2}} = 0 \tag{8.25}$$

By taking the positive root of this equation, we have the dynamic pressure for turning at the prescribed rate $\dot{\psi}$ with minimum power. Solving for V and on substituting into Eq. (8.24), we have the minimum power, for comparison with P_{max}. The corresponding load factor is obtained from Eq. (8.9). Concerning the root of Eq. (8.25), we observe

that when $q = 0$, we have $F(q) < 0$. On the other hand, when q has the value as given by Eq. (8.19), we have

$$F(q) = \frac{2(n^2 - 1)(W/S)^2}{3C_L^{*2}} > 0$$

Since this value of q corresponds to $C_L = \sqrt{3}C_L^*$, we conclude that when the turning rate $\dot{\psi}$ is prescribed, the optimum lift coefficient for turning with minimum power required is greater than $\sqrt{3}C_L^*$. Theoretically if the lift-drag relationship, $C_D = C_D(C_L)$ is accurately modeled, it can be shown that

$$C_{L_3} < C_{L_{opt}} < C_{L_4} = C_{L_{max}} \tag{8.26}$$

where C_{L_3} is the lift coefficient which minimizes the function $C_D/C_L^{3/2}$. For a parabolic drag polar, we have seen that $C_{L_3} = \sqrt{3C_{D_0}/K}$, but then the condition $C_{L_{opt}} < C_{L_4}$ may not hold. This is because a parabolic representation of the drag polar is not valid near the stall speed.

Another way to interpret the results of this subsection is as follows. We consider again the plot of the power required to turn P_{nr} at the load factor n_1 versus the speed V as shown in Fig. 8.5. For a prescribed turning rate $\dot{\psi}$, let A be the operating point on the curve with the speed V_1 as calculated by Eq. (8.9). If we keep a constant load factor and decrease the speed along the curve, the turning rate increases up to a maximum value $\dot{\psi}_{max}(n_1)$, for the selected load factor, when the speed reaches the stall speed, with $C_L = C_{L_{max}}$, as given by Eq. (8.18). The condition for the existence of the point A is that $\dot{\psi} \leq \dot{\psi}_{max}(n_1)$ and it is denoted explicitly by the condition (8.22). At the point A, we have a high value for the power required to turn. We can keep the same turning rate $\dot{\psi}$ by using a lower value of n with a correspondingly lower value of V. As shown in Fig. 8.5, the dashed line is the line with constant $\dot{\psi}$. This is precisely the plot of Eq. (8.24) for a parabolic drag polar. Along the line, the power required first decreases as the speed decreases. The function $F(q)$, as given by Eq. (8.25) gives the sign for the slope of the curve P_{nr} for constant $\dot{\psi}$. At the point B, with load factor n_3 and speed V_3 satisfying Eq. (8.19), we still have $F(q_3) > 0$ as has been verified above. Hence, the lowest point on the dashed line, with constant $\dot{\psi}$, occurs at a speed which is less than V_3 and at a load factor less than n_3. By Eq. (8.10), for constant $\dot{\psi}$, it is

seen that $C_{L_{opt}} > C_{L_3}$. Finally, at the point C, we have with the same turning rate $\dot{\psi}$, the value $n_4 < n_3$, $V_4 < V_3$, with V_4 being the limiting stall speed as given by Eq. (8.18). Theoretically, the minimum for P_{nr} should occur between the points B and C.

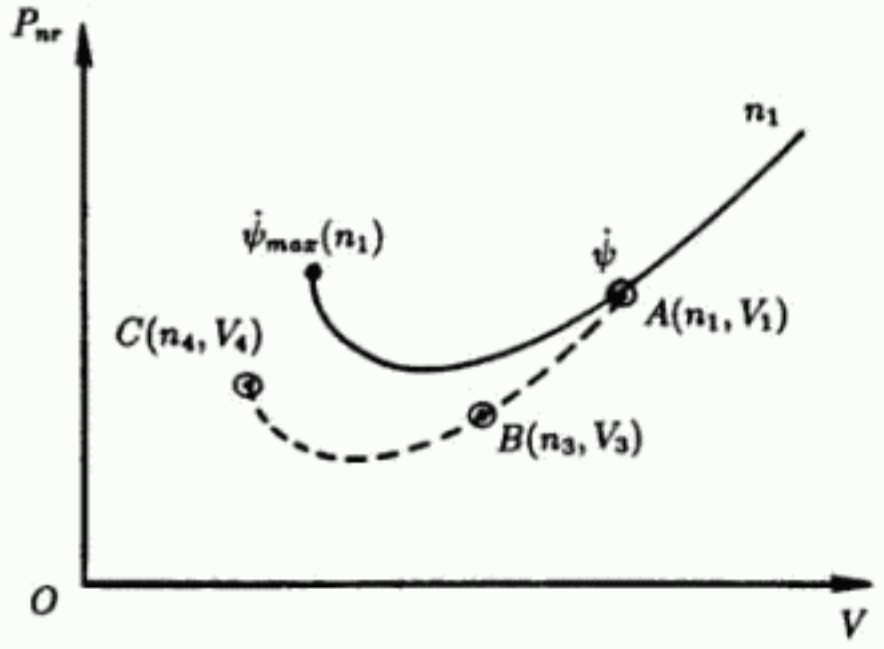

Figure 8.5: Power required to turn at a prescribed turning rate.

If we use the dynamic pressure, as calculated by the stall equation (8.18) to evaluate the slope $F(q)$ of the dashed curve, we have

$$F(q_4) = \frac{(W/S)^2}{C_{L_{max}}^2}\left[n_4^2\left(1 + \frac{C_{L_{max}}^2}{3C_L^{*2}}\right) - 2\frac{C_{L_{max}}^2}{3C_L^{*2}}\right] \tag{8.27}$$

If $F(q_4) < 0$, the root of Eq. (8.25) is between q_4 and q_3. But, using a parabolic drag polar, even if we enforce the condition that the value for P_{nr} for constant n, starts first to decrease at $C_L = C_{L_{max}}$, that is $C_{L_{max}} > \sqrt{3}C_L^*$, the condition that $F(q_4) < 0$ is not clearly settled. Nevertheless for a realistic drag polar, we can rigorously prove the condition (8.26), that is for turning with a prescribed rate $\dot{\psi}$, the optimum angle-of-attack is such that the corresponding lift coefficient is between $C_{L_{max}}$ and the value for minimum of $C_D/C_L^{3/2}$ (see Exercise 8-5).

8.4.2 Turning at a prescribed radius

We now consider the case where the turning radius R is prescribed. Again, according to Eq. (8.12), the turn can be accomplished in an infinite number of ways since we can select any combination for the pair n and V giving the same value R provided that the constraints on n_s, $C_{L_{max}}$ and P_{max} are respected.

We can select a bank angle ϕ, providing the corresponding load factor $n \leq n_s$ and calculate the speed V for turning from Eq. (8.12). This speed should be greater than the stall speed at the selected load factor as given by Eq. (8.18). Therefore, we have the first necessary condition for any prescribed turning radius R with the selected load factor n,

$$R > \left(\frac{2W}{g\rho SC_{L_{max}}}\right)\frac{n}{\sqrt{n^2-1}} \tag{8.28}$$

If we put $n = n_s$ in this inequality, we have on the right-hand side the expression for the smallest turning radius R_{min} provided that there is sufficient power to maintain the required speed at $n = n_s$ and $C_L = C_{L_{max}}$. We have

$$R_{min} = \left(\frac{2W}{g\rho SC_{L_{max}}}\right)\frac{n_s}{\sqrt{n_s^2-1}} \tag{8.29}$$

It is seen again that the minimum turning radius is small at low altitude, with high values of n_s and $C_{L_{max}}$ and low wing loading W/S.

Next, we assume that with the prescribed turning radius, the strict inequality $R > R_{min}$ is satisfied. Then, we can use any value $n < n_s$ and calculate the corresponding speed from Eq. (8.12) to be used in Eq. (8.17) for the power required P_{nr}. We have then

$$P_{nr} = \left(\frac{\rho SC_{D_0}}{2} + \frac{2KW^2}{g^2R^2\rho S}\right)V^3 + \frac{2KW^2}{\rho SV} \tag{8.30}$$

If the maximum power available at the flight altitude is greater than this value, turning at the prescribed radius, with the selected load factor is feasible. But if P_{max} is less than the value for P_{nr} from Eq. (8.30), it may still be possible to turn at the same prescribed radius by selecting a lower value of the load factor providing a lower value of the corresponding speed as given in Eq. (8.12) to reduce the power

required. This means that we can use the speed to control the flight and compute the corresponding load factor from Eq. (8.12). Considered as a function of V, the power required for turning with a prescribed radius is minimum when $dP_{nr}/dV = 0$. In terms of the dynamic pressure, we have the solution

$$q = \frac{W/S}{\sqrt{3}C_L^*}\left[1 + \frac{4(W/S)^2}{g^2R^2\rho^2C_L^{*2}}\right]^{-1/2} \tag{8.31}$$

With the prescribed turning radius, on solving for the optimum speed, Eq. (8.12) provides the corresponding load factor, and the lift equation (8.6) can be used to calculate the optimum lift coefficient for turning with minimum power. Theoretically, this lift coefficient should be between $C_{L_{max}}$ and $\sqrt{3}C_L^*$ as shown in condition (8.26). But if a parabolic drag polar is used, the condition $C_{L_{opt}} < C_{L_{max}}$ may not hold (see Exercise 8-6).

8.4.3 Turning at a prescribed throttle setting

In practice, to start a turn, we select a bank angle, providing a load factor $n > 1$. As seen in Eq. (8.17), to maintain the same speed, the power required P_{nr} is higher. Hence, it is necessary to increase the power available to sustain turning. We consider the case of turning at a prescribed power available. For a steady turn, $P_a = P_{nr}$ and we write Eq. (8.17) as

$$P_a = \frac{\rho S C_{D_0} V^3}{2} + \frac{2Kn^2W^2}{\rho SV} \tag{8.32}$$

Since P_a is a prescribed constant, if a bank angle is selected for turning, we have the corresponding value for the load factor n, and on solving the equation for V, we have the turning speed. Equation (8.9) will give the turning rate, while Eq. (8.12) provides the turning radius for the selected bank angle. Alternatively, we can choose a speed V for turning and use Eq. (8.32) to solve for n^2. Then, we can calculate the corresponding values for the turning rate and the turning radius (see Exercise 8-7). Concerning the physical contraints, the load factor selected must be less than the maximum load factor achievable, or the limiting structural load factor, and the turning speed must be greater than the stall speed. Since there is an arbitrary variable to be selected,

either in the load factor n, or in the speed V, as long as $P_a > P_r^*$, turning can be performed in an infinite number of ways. The turning rate $\dot{\psi}$ may vary between zero and a maximum value. Likewise the turning radius R can have any value greater than a certain minimum value. We propose to evaluate these extrema for a prescribed power available P_a.

First, based on Eq. (8.32), with constant P_a, we evaluate

$$\frac{dn^2}{dV} = \frac{1}{V}\left[n^2 - \frac{3q^2C_L^{*2}}{(W/S)^2}\right] \tag{8.33}$$

By setting $dn^2/dV = 0$, we have the condition for a maximum load factor achievable. It is the same as given in Eq. (8.19). Upon substituting into Eq. (8.32), we have the maximum load factor as given in Eq. (8.21).

Concerning the turning rate, we have noticed that Eq. (8.32) defines n^2 as a function of V. Hence the turning rate, as given in Eq. (8.9) is a function of the speed V. By writing the condition $d\dot{\psi}/dV = 0$, for a maximum turning rate, we obtain

$$\frac{dn^2}{dV} = \frac{2(n^2-1)}{V} \tag{8.34}$$

By equating the last two equations, we have the condition for the maximum turning rate

$$n^2 = 2 - \frac{3q^2C_L^{*2}}{(W/S)^2} \tag{8.35}$$

We notice that the optimum load factor is less than $\sqrt{2}$. It can also be shown that the optimum lift coefficient is greater than $\sqrt{3}C_L^*$ (see Exercise 8-9). By substituting back into Eq. (8.32), we have the equation for the optimum turning speed with maximum turning rate

$$V^4 + \frac{2E_{max}(P_a/W)(W/S)}{\rho C_L^*}V - \frac{4(W/S)^2}{\rho^2 C_L^{*2}} = 0 \tag{8.36}$$

After evaluating the optimum speed V_{opt} from this equation, the corresponding load factor is given by Eq. (8.35). We then evaluate the stall speed by Eq. (8.18) and verify the condition $V_{opt} \geq V_{stall}$. If V_{opt} is less than V_{stall}, the turn should be made at V_{stall}, that is with $C_L = C_{L_{max}}$. If this is the case, we use Eq. (8.15) with $P_{nr} = P_a$, and $C_L = C_{L_{max}}$

to evaluate the load factor at stall for the prescribed power available P_a. Using this load factor in Eq. (8.10) with $C_L = C_{L_{max}}$, we have the maximum turning rate.

Concerning the turning radius, we have a similar analysis. First, Eq. (8.32) defines n^2 as a function of V. Then the turning radius, as given in Eq. (8.12) is a function of the speed V. The condition for a minimum turning radius, $dR/dV = 0$, is then expressed as

$$\frac{dn^2}{dV} = \frac{4(n^2 - 1)}{V} \tag{8.37}$$

By equating this equation with Eq. (8.33), we have the condition for a minimum turning radius

$$n^2 = \frac{4}{3} - \frac{q^2 C_L^{*2}}{(W/S)^2} \tag{8.38}$$

Again, we notice that the optimum load factor for a turning with minimum radius is less than $2\sqrt{3}/3$. It is possible to show that the lift coefficient for a turn with minimum radius is greater than $\sqrt{3}C_L^*$ (see Exercise 8-9). By substituting back into Eq. (8.32), we have the equation for the optimum turning speed with minimum radius

$$V_{opt} = \frac{8K(W/S)}{3\rho(P_a/W)} \tag{8.39}$$

The corresponding load factor is given by Eq. (8.38). The condition that $V_{opt} \geq V_{stall}$ is set out as

$$\frac{1}{2}\rho V_{opt}^2 > \frac{2(W/S)}{\sqrt{3(C_L^{*2} + C_{L_{max}}^2)}} \tag{8.40}$$

In general, within the assumption of a parabolic drag polar, this condition is only satisfied for aircraft with very high values of $C_{L_{max}}$ using low P_a/W. Just as for the case of turning at maximum rate for a prescribed throttle setting, if the optimum speed is less than the stall speed, turning with minimum radius is conducted at stall speed. In this case, from Eq. (8.15) with $P_{nr} = P_a$, we calculate the load factor at stall by using $C_L = C_{L_{max}}$, $C_D = C_{D_{max}} = C_{D_0} + KC_{L_{max}}^2$. Then, we have

$$n_{stall} = \left[\frac{\rho(P_a/W)^2 C_{L_{max}}^3}{2(W/S)C_{D_{max}}^2}\right]^{1/3} \tag{8.41}$$

The stall turning speed is given by Eq. (8.18) and from these we evaluate the maximum turning rate and the minimum turning radius.

8.5 Numerical application

To have a better understanding of the analysis in the preceding section, let us consider a hypothetical propeller driven aircraft with the following data,

$$C_{D_0} = 0.025, \qquad K = 0.048, \qquad C_{L_{max}} = 1.8$$
$$W/S = 35 \text{ lb/ft}^2, \quad HP/W = 0.14 \text{ hp/lb}$$

For a turn at sea level, we take

$$\rho_0 = 2.3769 \times 10^{-3} \text{ lb}-\text{s}^2/\text{ft}^4, \quad g = 32.2 \text{ ft/s}^2$$

We calculate the corresponding parameters $C_L^* = (C_{D_0}/K)^{1/2}$, $E_{max} = 1/2(C_{D_0}K)^{1/2}$ for use in the various formulas.

First, if a propeller efficiency $\eta_p = 0.85$ is used, we have the power-to-weight ratio

$$\frac{P_a}{W} = 550 \times 0.85 \times 0.14 = 65.45 \text{ ft/s}$$

By Eq. (8.21), the maximum load factor achievable at sea level is

$$n_{max} = 3.05 \text{ g's}$$

Since n_{max} is proportional to $\sigma^{1/3}$, at say 10,000 ft where $\sigma = 0.629$, the maximum load factor is reduced to $n_{max} = 2.61$ g's. We have assumed that the power available remains the same up to the critical altitude somewhat above this altitude. At higher altitude, the value of n_{max} is further reduced and tends to $n = 1$ at the propulsive ceiling. If we impose a structural limit $n_s = 2.5$ for the load factor, then the limiting value for the load factor is $n = n_s$ at low altitude and at high altitude when $n_{max} < n_s$, the limiting value for the load factor is $n = n_{max}$.

Returning to turning at sea level, we have the maximum turning rate by using $n = n_s$ and $C_L = C_{L_{max}}$ in Eq. (8.23). We have

$$\dot{\psi}_{max} = 0.3648 \text{ rad/s} = 20.9 \text{ deg/s}$$

If we use the general expression (8.15) to calculate P_{nr}/W, with $n = n_s$, $C_L = C_{L_{max}}$, $C_D = C_{D_0} + KC^2_{L_{max}}$, we obtain

$$\frac{P_{nr}}{W} = 50.71 \; ft/s$$

This is less than the value P_a/W. Hence, the turn is possible. If we increase the structural limit for the load factor to $n_s = 3$, the maximum turning rate would be $\dot{\psi}_{max} = 23.55$ deg/s. But the new power required will increase to $P_{nr}/W = 66.66$ ft/s and the power available is not sufficient to maintain this turn at constant speed.

Similarly, we use $n_s = 2.5$ and $C_L = C_{L_{max}}$ in Eq. (8.29) to calculate the minimum turning radius

$$R_{min} = 554.39 \text{ ft}$$

The power required is the same as has been calculated above and the turn is possible. If we increase n_s to the new value $n_s = 3$, the new minimum turning radius is $R_{min} = 538.93$ ft. It is only a small reduction at the expense of a large increase in the power required which is now in excess of the power available.

We can repeat the numerical evaluation of the optimum performance at any other altitude provided that, at the selected altitude, n_{max}, as evaluated from Eq. (8.21) is greater than unity.

Now, at sea level, let us assume that we want to control the turn at the rate of $\dot{\psi} = 6$ deg/s so that we can complete a 180° turn in 30 seconds. Then, from Eq. (8.9), with $\dot{\psi}$ expressed in rad/s, a load factor of $n = 2.5$ would require a speed of $V = 704.5$ ft/s while turning with a bank angle of $\phi = 30°$, that is with a load factor of $n = 1.155$, would require a lower speed at $V = 177.71$ ft/s. Hence, we can use the speed to control the turning at the prescribed rate, provided that, at each speed selected, the corresponding load factor satisfies Eq. (8.9). The power required for turning at the prescribed rate is given by Eq. (8.24). The dynamic pressure for the minimum of P_{nr} is given by Eq. (8.25). With the numerical data, we solve this equation to obtain

$$q = 24.728 \text{ lb/ft}^2, \qquad V = 144.246 \text{ ft/s}$$

From Eq. (8.9), with the prescribed rate, the corresponding load factor is 1.1046. At this load factor, the stall speed, as computed from

Eq. (8.18) is 134.43 ft/s. The optimum speed, for turning at the prescribed rate with minimum power required, is greater than the stall speed. We can also use the lift equation (8.6) to calculate the optimum value for the lift coefficient, which is $C_L = 1.563$, and it is clearly between $C_{L_{max}} = 1.8$ and $\sqrt{3}C_L^* = 1.25$. Since we have calculated both the optimum lift coefficient and the optimum load factor, it is simpler to use Eq. (8.15) to calculate the minimum power required to be $P_{nr}/W = 14.505$ ft/s. By using the optimum speed, with the prescribed turning rate to calculate P_{nr}/W from Eq. (8.24), we obtain the identical result.

In a similar manner, it is possible to turn with any radius greater than the minimum value calculated above. Let us select the turning radius to be $R = 1200$ ft. Then, from Eq. (8.12), a load factor of $n = 2.5$ would require a speed of 297.55 ft/s, while turning with a load factor of $n = 1.155$ would require a lower speed at $V = 149.439$ ft/s. By selecting the speed to control the turning at the prescribed radius we have seen that the power required at the selected speed is given by Eq. (8.30), with the optimum value for the dynamic pressure given explicitly in Eq. (8.31). With the numerical data, we obtain

$$q = 19.2517 \text{ lb/ft}^2, \qquad V = 127.275 \text{ ft/s}$$

From Eq. (8.12), with the prescribed radius, the corresponding load factor is $n = 1.084$. At this load factor, the stall speed, as calculated from Eq. (8.18) is 133.17 ft/s. Therefore, in this example where we select the turning radius to be $R = 1200$ ft, the value of the speed which minimizes the power required is less than the stall speed. But, this is because we have used a parabolic drag polar for the analysis and as such its behavior near the stall angle-of-attack is not correct. It is fair to say that the minimum power required will occur near the stall and hence let us select $C_L = C_{L_{max}}$ for turning. By eliminating the speed V between Eqs. (8.12) and (8.18), we can calculate the corresponding load factor to be $n = 1.104$. The stall speed at this load factor is $V = 134.398$ ft/s. Using either Eq. (8.15) with n and $C_{L_{max}}$ or Eq. (8.30) we have the power required $P_{nr}/W = 14.88$ ft/s which is close to the true minimum.

Finally, with the given characteristics for the aircraft and at sea level, we evaluate the turning performance for the prescribed power-to-weight ratio of $P_a/W = 65.45$ ft/s. With this power, we can turn at any rate smaller than the maximum rate and at any radius greater

than the minimum radius. Let us evaluate these extrema. First, for the maximum turning rate we evaluate the optimum turning speed as given by Eq. (8.36). With the given data, we obtain $V = 43.11$ ft/s. From Eq. (8.35), the corresponding load factor is $n = 1.412$. The stall speed at this load factor is $V_{stall} = 151.99$ ft/s and it is much higher than the optimum speed. Hence turning is restricted at $C_L = C_{L_{max}}$.

Similarly, for the minimum turning radius, the optimum speed evaluated from Eq. (8.39) is 28.80 ft/s and it is much too low. Therefore the minimum turning radius is also achieved with the stall speed.

We evaluate the load factor with $C_L = C_{L_{max}}$ from Eq. (8.41), and then the stall speed from Eq. (8.18) to have the following optimum performances.

$$
\begin{aligned}
n &= 2.96369 \\
\phi &= 70.28^\circ \\
V_{stall} &= 220.20 \text{ ft/s} \\
\dot{\psi}_{max} &= 0.408 \text{ rad/s} = 23.37 \text{ deg/s} \\
R_{min} &= 539.75 \text{ ft}
\end{aligned}
$$

8.6 Non-steady turn

In order to obtain some simple and explicit formulas for the application, we have assumed that the speed is maintained constant during the turn and that the lift–drag relationship is parabolic. Let us now have a more realistic assessment of the dynamic process during a turn.

In general, at the start of a turn, with the bank angle set, the drag increases and it is necessary to increase the power available. Hence, we shall assume that P_a is prescribed and examine the top performance from this throttle setting. To stay in horizontal flight, the equilibrium in the forces as shown in Fig. 8.2 is valid and for convenience we rewrite the pertinent relations (8.6), (8.9) and (8.12). We have

$$qC_L = n(W/S) \tag{8.42}$$

$$n^2 = \frac{2\dot{\psi}^2 q}{\rho g^2} + 1 \tag{8.43}$$

$$n^2 = \frac{4q^2}{g^2 R^2 \rho^2} + 1 \tag{8.44}$$

where again $q = \rho V^2/2$ is the dynamic pressure and $\dot{\psi}$ is the turning rate while R is the turning radius. We first remove the condition of turning with constant speed so that, in general we have

$$m\frac{dV}{dt} = T - D \tag{8.45}$$

By multiplying this equation by the speed V to express it in terms of the power and considering m as practically constant, we have the equation

$$\frac{d}{dt}\left(\frac{1}{2}mV^2\right) = P_a - P_{nr} \tag{8.46}$$

where $P_a = TV$ is the power available, assumed constant in the speed range considered and P_{nr} is the power required for turn with the prescribed load factor. For a general drag polar, which is not parabolic, it is

$$P_{nr} = \sqrt{\frac{2W^3}{\rho S}}n^{3/2}f(C_L) \tag{8.47}$$

where

$$f(C_L) = \frac{C_D(C_L)}{C_L^{3/2}} \tag{8.48}$$

At any flight altitude we have the plots of P_a and P_{nr} versus the speed, for each value of n as shown in Fig. 8.6. Along each power required curve, with constant n, from Eq. (8.42) as C_L increases from a small value, the speed decreases. For each point of the curve, there is a corresponding well defined value for C_L resulting in a function $f(C_L)$ as defined in Eq. (8.48) for a general drag polar. For a realistic drag polar, that is if, when based on aerodynamic data, the function $C_D = C_D(C_L)$ is accurately modeled, the function $f(C_L)$ has the following properties:

At a value $C_L = C_{L_3}$, $f(C_L)$ is a minimum and consequently P_{nr} is a minimum. We have

$$\left(\frac{df}{dC_L}\right)_{C_L=C_{L_3}} = 0 \tag{8.49}$$

At the stall lift coefficient, $C_L = C_{L_4} = C_{L_{max}}$, when we consider C_L as a function of C_D, it passes through its maximum value, that is

$$\left(\frac{dC_L}{dC_D}\right)_{C_L=C_{L_4}} = 0 \tag{8.50}$$

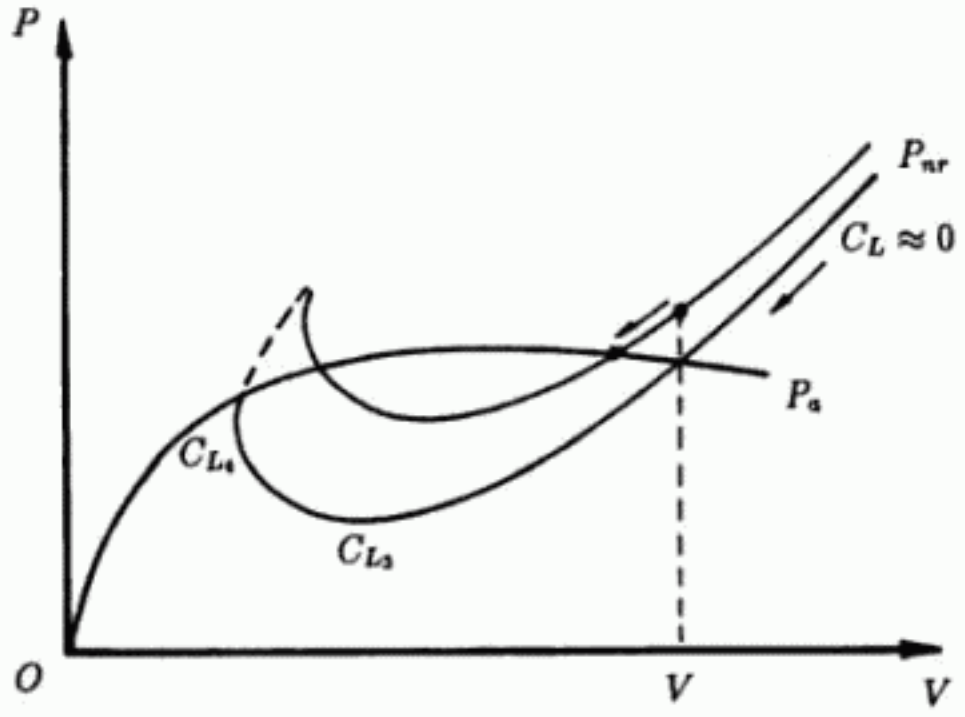

Figure 8.6: Power required for turning with a general drag polar.

For a turn at a load factor n, with a stabilized speed V, we have $P_a = P_{nr}$. If at this instant we increase the bank angle, and hence increase the load factor to a higher value, then to keep a coordinated turn, by Eq. (8.42) the lift coefficient C_L has to be proportionally increased. As shown in Fig. 8.6, we have a higher value of P_{nr}. Mathematically, this can be assessed from Eq. (8.47) since P_{nr} increases with n and furthermore $f(C_L)$ also increases with C_L since it has been assumed that the function $f(C_L)$ is minimized at the value $C_L = C_{L_3}$. With $P_a < P_{nr}$, from Eq. (8.46) the kinetic energy of the system decreases. The speed tends to a smaller stabilized speed. We have a decelerated turn. During this time, the instantaneous turning rate is calculated from Eq. (8.43) but if the load factor is maintained the same, while the speed decreases, the turning rate is increased. Likewise, the instantaneous turning radius is calculated from Eq. (8.44) and for constant load factor it decreases with speed.

We now consider the limiting case where the turn has been stabilized at its maximum turning rate. Then, with $P_a = P_{nr}$, we have

$$P_a = \sqrt{\frac{2W^3}{\rho S}} n^{3/2} f(C_L) \tag{8.51}$$

Since P_a is a prescribed constant, this equation defines the load factor n as a function of the lift coefficient C_L. By taking its derivative with respect to C_L, we have

$$\frac{dn}{dC_L} = -\frac{2n}{3f}\frac{df}{dC_L} \tag{8.52}$$

Since n is a function of C_L, by Eq. (8.42), the dynamic pressure q is also a function of C_L. We take the derivative of this equation with respect to C_L to obtain

$$C_L \frac{dq}{dC_L} + q = \frac{W}{S}\frac{dn}{dC_L} \tag{8.53}$$

Finally, when both n and q are expressed as functions of C_L, by Eq. (8.43) the turning rate is a function of C_L. By taking the derivative of this equation, we have

$$n\frac{dn}{dC_L} = \frac{\dot{\psi}^2}{\rho g^2}\frac{dq}{dC_L} + \frac{q}{\rho g^2}\frac{d\dot{\psi}^2}{dC_L} \tag{8.54}$$

With respect to C_L, the turning rate is maximized when $d\dot{\psi}^2/dC_L = 0$. We have the optimum relation

$$n\frac{dn}{dC_L} = \frac{\dot{\psi}^2}{\rho g^2}\frac{dq}{dC_L} \tag{8.55}$$

By using Eqs. (8.42) and (8.43) and also Eqs. (8.52) and (8.53), we have after simplification, the equation for the optimum value of the lift coefficient C_L for maximum turning rate

$$F(C_L) = \frac{n^2 - 1}{2C_L} - \frac{n^2 + 1}{3f}\frac{df}{dC_L} = 0 \tag{8.56}$$

This equation can also be expressed in terms of the optimum speed for turning. If a parabolic drag polar is used it leads to Eq. (8.35) as derived before.

We notice that since $n > 1$, the first term is positive. With a realistic drag polar, we use the properties of the function $f(C_L)$ as depicted in Eqs. (8.49) and (8.50) to locate the root $C_{L_{opt}}$ of Eq. (8.56). At $C_L = C_{L_3}$, $df/dC_L = 0$ and hence $F(C_{L_3}) > 0$. Furthermore, by the definition of $f(C_L)$, we have its derivative

$$\frac{df}{dC_L} = \frac{1}{C_L^{3/2}}\left(\frac{dC_D}{dC_L} - \frac{3C_D}{2C_L}\right) \tag{8.57}$$

When C_L is near $C_{L_4} = C_{L_{max}}$, $dC_L/dC_D \approx 0$ and the derivative df/dC_L is infinite. Then $F(C_{L_4}) < 0$ and we conclude that $C_{L_{opt}}$ is located between C_{L_3} and C_{L_4}. Although in the previous section on numerical application we have found that V_{opt} is less than V_{stall}, in reality, with a more accurate representation of the drag polar we should have $V_{opt} > V_{stall}$, and as such, for a prescribed P_a, using $V_{opt} = V_{stall}$, we have obtained a high turning rate.

Similarly, if the turning radius is considered, by taking the derivative of Eq. (8.44), we obtain

$$n\frac{dn}{dC_L} = \frac{4q}{g^2R^2\rho^2}\frac{dq}{dC_L} - \frac{4q^2}{g^2R^3\rho^2}\frac{dR}{dC_L} \tag{8.58}$$

When the turning radius is minimized, we have the optimum condition

$$n\frac{dn}{dC_L} = \frac{4q}{g^2R^2\rho^2}\frac{dq}{dC_L} \tag{8.59}$$

By using Eqs. (8.42) and (8.44), and also Eqs. (8.52) and (8.53), we have after simplification, the equation for the optimum value of the lift coefficient C_L for minimum turning radius

$$F(C_L) = \frac{n^2-1}{C_L} - \frac{2}{3f}\frac{df}{dC_L} = 0 \tag{8.60}$$

If a parabolic drag polar is used it leads to Eq. (8.38) as derived before and it is possible that the optimum value V_{opt} calculated may be less than the stall speed V_{stall}. But for a realistic drag polar, enforced by the conditions (8.49) and (8.50), we easily find that the optimum lift coefficient $C_{L_{opt}}$ for turning with minimum turning radius occurs between C_{L_3} and C_{L_4}.

Exercises

8-1. Based on Fig. 8.4, consider the power required for rectilinear flight, with $n = 1$

$$P_r = \frac{1}{2}\rho S V^3 C_{D_0} + \frac{2KW^2}{\rho S V}$$

with the corresponding lift equation

$$\frac{1}{2}\rho S V^2 C_L = W.$$

Deduce that to each point M on the plot of P_r with the speed V, there corresponds a unique value for the lift coefficient C_L resulting in a unique value for the angle-of-attack.

Next, consider the plot of the power required P_{nr} for turning at the load factor n as given by Eq. (8.17), with the lift equation (8.6). Show that the point M_n, with the same value for the lift coefficient, corresponds to a speed $V' = V\sqrt{n}$ and a power $P_{nr} = P_r\sqrt{n^3}$.

8-2. Along the curve P_r, with $n = 1$, show that at the stalling point we have

$$q_{stall} = \frac{W}{SC_{L_{max}}}$$

$$P_{r(stall)} = \sqrt{\frac{2W^3}{\rho S}}\frac{C_{D_{max}}}{C_{L_{max}}^{3/2}}$$

where $C_{D_{max}}$ is the value of the drag coefficient at $C_L = C_{L_{max}}$.

Show that, with a parabolic drag polar, at the lowest point on the curve P_r, we have

$$q^* = \frac{W}{\sqrt{3}SC_L^*}$$

$$P_r^* = \frac{2}{3^{3/4}E_{max}}\sqrt{\frac{2W^3}{\rho SC_L^*}}$$

From the results in Exercise 8-1, deduce the values of the dynamic pressure q and the corresponding power required P_{nr} to turn at the load factor n, at the stall point and at the lowest point on the power curve.

8-3. It is proposed to investigate the effects of $C_{L_{max}}$ and n_s on the absolute maximum turning rate.

Show that we can write Eq. (8.23) as

$$\bar{\dot{\psi}}_{max} = \left[\frac{C_{L_{max}}(n_s^2 - 1)}{n_s}\right]^{1/2}$$

where $\bar{\dot{\psi}}_{max}$ is by definition, the dimensionless maximum turning rate. Take several typical values for $C_{L_{max}} = 1.4$, 1.6, 1.8 and 2.0 and plot $\bar{\dot{\psi}}_{max}$ versus n_s in the range from 1 to 6. Observe that the maximum turning rate increases with $C_{L_{max}}$ and n_s. Also, notice that when n_s is high, the effect of increasing n_s on $\bar{\dot{\psi}}_{max}$ is small.

Show that

$$\frac{\Delta\bar{\dot{\psi}}_{max}}{\bar{\dot{\psi}}_{max}} = \frac{1}{2}\left[\frac{\Delta C_{L_{max}}}{C_{L_{max}}} + \frac{n_s^2 + 1}{n_s(n_s^2 - 1)}\Delta n_s\right]$$

Use this formula to explain the behavior of the plots.

8-4. Similarly, we investigate the effects of $C_{L_{max}}$ and n_s on the absolute minimum turning radius.

Show that we can write Eq. (8.29) as

$$\bar{R}_{min} = \frac{n_s}{C_{L_{max}}\sqrt{n_s^2 - 1}}$$

where $\bar{R}_{min}$ is by definition the dimensionless minimum turning radius. For $C_{L_{max}} = 1.4$, 1.6, 1.8 and 2.0, plot $\bar{R}_{min}$ versus n_s in the range from 1 to 6. Observe that $\bar{R}_{min}$ decreases when $C_{L_{max}}$ and n_s increase and when n_s is high, the effect of increasing n_s on $\bar{R}_{min}$ is small.

Show that

$$\frac{\Delta\bar{R}_{min}}{\bar{R}_{min}} = -\frac{\Delta C_{L_{max}}}{C_{L_{max}}} - \frac{\Delta n_s}{n_s(n_s^2 - 1)}$$

Use this formula to explain the behavior of the plots.

8-5. At the flight altitude, by taking the square root in Eq. (8.15) as unit power, we define the dimensionless power required to turn at the load factor n, and lift coefficient C_L as

$$P_{nr} = n^{3/2} f(C_L)$$

where

$$f(C_L) = C_D(C_L)/C_L^{3/2}$$

For a realistic drag polar, that is with an accurate modeling of the function $C_D = C_D(C_L)$, along the curve P_{nr}, for constant n, we have the following properties:

The function P_{nr}, for constant n, is minimized at a value C_{L_3} when $df/dC_L = 0$.

At the stall lift coefficient $C_L = C_{L_{max}} = C_{L_4} > C_{L_3}$, the lift coefficient C_L, considered as a function of C_D, is maximized, that is $dC_L/dC_D = 0$.

We propose to prove that, for any prescribed turning rate $\dot{\psi}$, the power required for turning is a minimum at a value $C_{L_{opt}}$ such that

$$C_{L_3} < C_{L_{opt}} < C_{L_4}$$

If q is the dynamic pressure, show that

$$qSC_L = nW, \qquad n^2 = \frac{2\dot{\psi}^2 q}{\rho g^2} + 1$$

Then, n is a function of q and consequently C_L is a function of q. This means that for a given turning rate, we can express P_{nr} as a function of q. Show that its derivative with respect to q is

$$\frac{dP_{nr}}{dq} = \frac{3\dot{\psi}^2}{2\sqrt{n}\rho g^2} f + \sqrt{n^3}\frac{df}{dq}$$

At $C_L = C_{L_3}$,

$$\frac{df}{dq} = \frac{df}{dC_L}\frac{dC_L}{dq} = 0$$

Hence $dP_{nr}/dq > 0$.

At $C_L = C_{L_{max}} = C_{L_4}$, first show that in general

$$\frac{df}{dq} = -\frac{(n^2+1)(W/S)}{2q^2 n C_L^{3/2}}\left(\frac{dC_D}{dC_L} - \frac{3C_D}{2C_L}\right)$$

Observe that near $C_L = C_{L_{max}}$, since C_L is nearing its maximum value $dC_L/dC_D = \varepsilon$ where ε is a very small positive quantity. Then, conclude that $dP_{nr}/dq < 0$. Hence P_{nr} is a minimum for a value of C_L between C_{L_3} and C_{L_4}.

8-6. Again, we consider the dimensionless power required P_{nr} as defined in Exercise 8-5, with the same properties for the functions $f(C_L)$ and $C_D(C_L)$.

For a turn with a prescribed turning radius R, show that

$$qSC_L = nW, \qquad n^2 = \frac{4q^2}{g^2R^2\rho^2} + 1$$

Then, n is a function of q and consequently C_L is a function of q. This means that, for a given turning radius, we can express P_{nr} as a function of q. Show that its derivative with respect to q is

$$\frac{dP_{nr}}{dq} = \frac{6q}{\sqrt{n}g^2R^2\rho^2}f + \sqrt{n^3}\frac{df}{dq}$$

Show that at $C_L = C_{L_3}$, $df/dq = 0$ and $dP_{nr}/dq > 0$. At $C_L = C_{L_{max}} = C_{L_4}$, show that

$$\frac{df}{dq} = -\frac{W/S}{q^2nC_L^{3/2}}\left(\frac{dC_D}{dC_L} - \frac{3C_D}{2C_L}\right)$$

Then using the same arguments as in Exercise 8-5, conclude that near $C_L = C_{L_{max}}$, df/dq is negative and large and $dP_{nr}/dq < 0$. Again the value of C_L which minimizes P_{nr} for a prescribed turning radius is between C_{L_3} and C_{L_4}.

8-7. Consider the case of turning with a prescribed power available P_a. Show that the load factor is a function of the speed V as given by

$$n = \left[\frac{\rho(P_a/W)}{2K(W/S)}V - \frac{\rho^2C_{D_0}}{4K(W/S)^2}V^4\right]^{1/2}$$

Then, the turning rate and the turning radius are also functions of the speed as given by

$$\dot{\psi} = \frac{g\sqrt{n^2-1}}{V}$$

and

$$R = \frac{V^2}{g\sqrt{n^2-1}}$$

Use the data for the hypothetical propeller driven aircraft as given in Section 8.5, and for turning at sea level, plot the variations of n, $\dot{\psi}$ and R with the speed V.

Observe that the value of V for a minimum turning radius is the smallest, while the value of V for a maximum load factor is the largest, with the value of V for a maximum turning rate in between these two occurences.

8-8. To explain the behavior of the plots in Exercise 8-7, derive the simple relations

$$R\dot{\psi} = V$$

and

$$n^2 = \frac{\dot{\psi}^2 V^2}{g^2} + 1$$

Show that

$$\dot{\psi}\frac{dR}{dV} + R\frac{d\dot{\psi}}{dV} = 1$$

and

$$\frac{dn^2}{dV} = \frac{2\dot{\psi}^2 V}{g^2} + \frac{2V^2\dot{\psi}}{g^2}\frac{d\dot{\psi}}{dV}$$

Then, show that when R is a minimum, $\dot{\psi}$ is still increasing and, when $\dot{\psi}$ reaches its maximum value, n is still increasing. Then, in the plots with increasing V, the minimum of R occurs first, while the maximum of n occurs last.

Since the speed V for minimum R is the smallest and for a prescribed power available, $P_a = \rho S V^3 C_D/2$, the lift coefficient for minimum R is the largest.

8-9. For turning with a prescribed power available, the condition for a maximum turning rate is given in Eq. (8.35). By using the lift equation (8.6), show that

$$n^2\left(1 + \frac{3C_L^{*2}}{C_L^2}\right) = 2$$

Then, based on the fact that for turning, $n > 1$, show that $C_L > \sqrt{3}C_L^*$.

By using Eq. (8.38) for a minimum turning radius, show that we have similar conclusion.

8-10. Using a parabolic drag polar, with $f = C_D/C_L^{3/2}$, show that Eq. (8.56) leads to Eq. (8.35), while Eq. (8.60) leads to Eq. (8.38).

9

Turning flight of jet aircraft

9.1 Turning flight in general

We shall consider in this chapter the turning flight of jet aircraft. This case deserves special attention for several reasons. First, from the point of view of the propulsion system, for jet aircraft, we consider the thrust available instead of the power available as in the case of propeller driven aircraft. For a prescribed throttle setting, the thrust produced depends on both the altitude and the Mach number and their effects should be considered in the analysis. Next, in terms of the aerodynamic characteristics, the drag polar, and in particular the maximum lift coefficient, $C_{L_{max}}$, depend strongly on Mach number. Finally, for high-performance fighter aircraft, the thrust-to-weight ratio is high, especially at low altitude, and the peak performance depends heavily on the aerodynamic and structural constraints and the discussion of optimum maneuvers is rather subtle.

We first reproduce the pertinent equations for a coordinated turn in a horizontal plane, and then use these equations for the discussion of turning performance.

As shown in Fig. 9.1, we have the equilibrium of the lift force

$$L = nW \tag{9.1}$$

where the load factor n is related to the bank angle ϕ by the simple relation

$$n = \frac{1}{\cos\phi} \tag{9.2}$$

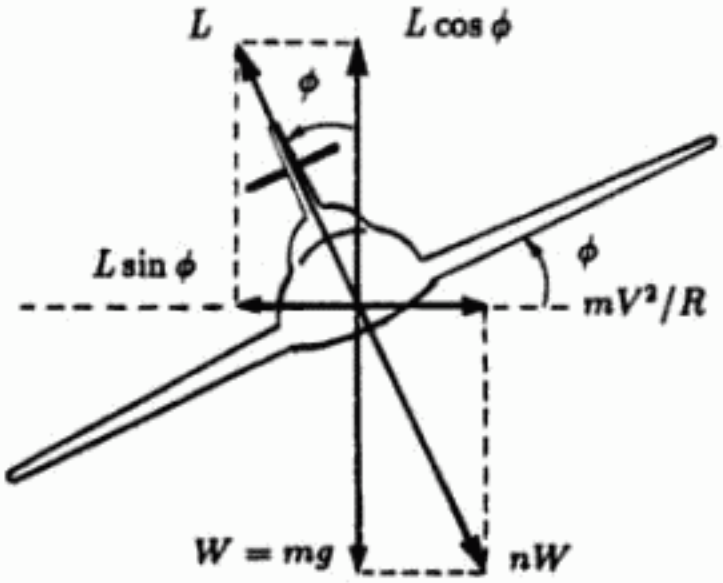

Figure 9.1: Coordinated turn in a horizontal plane.

In terms of the load factor n and the speed V, the turning rate is

$$\dot{\psi} = \frac{g\sqrt{n^2 - 1}}{V} \tag{9.3}$$

If in this equation, we use the speed as obtained from the lift equation (9.1), we have the alternate form

$$\dot{\psi} = g\sqrt{\frac{\rho S}{2W}}\sqrt{C_L}\sqrt{n - \frac{1}{n}} \tag{9.4}$$

On the other hand, as derived in Chapter 8, we have for the turning radius

$$R = \frac{V^2}{g\sqrt{n^2 - 1}} \tag{9.5}$$

If V^2 is calculated from the lift equation, we have the alternate form

$$R = \frac{2W}{g\rho S C_L}\frac{n}{\sqrt{n^2 - 1}} \tag{9.6}$$

These equations are valid for the general case of turning in the horizontal plane so that we have the equation for the variation of speed

$$m\frac{dV}{dt} = T - D \tag{9.7}$$

For the particular case of steady turn with a constant stabilized speed, we have the equilibrium condition

$$T = D \tag{9.8}$$

In general, the drag polar is a function of Mach number. If a parabolic assumption is used, then

$$C_D = C_{D_0}(M) + K(M)C_L^2 \tag{9.9}$$

where the zero-lift drag coefficient, C_{D_0}, and the induced drag factor, K, are assumed known functions of Mach number. These functions can always be modeled accurately by a certain polynomial representation if sufficient aerodynamic data are available. We assume that the maximum lift coefficient

$$C_{L_{max}} = C_{L_{max}}(M) \tag{9.10}$$

is also a known function of Mach number. In general, $C_{L_{max}}$ is constant at low Mach number, say for $M \leq 0.6$. At high Mach number, and for a subsonic aircraft, it decreases drastically as M is approaching unity. For a supersonic aircraft, at supersonic speeds, $C_{L_{max}}$ tends to a nearly constant value, lower than the value at low subsonic speeds.

For the evaluation of the peak performance, we consider the maximum thrust produced

$$T_{max} = T_{max}(z, M) \tag{9.11}$$

It is assumed that it is a known function of altitude and Mach number. From engine data, it is adequate to represent it as

$$T_{max} = T_0(M)\left(\frac{\rho}{\rho_0}\right)^x \tag{9.12}$$

where x is a constant exponent close to unity, ρ_0 is the density of the air at sea level and $T_0(M)$ is a simple polynomial in M denoting the maximum thrust at sea level.

Finally, we impose a physiological–structural constraint n_s, usually in the range from 3 to 9, for the load factor.

9.2 The maneuvering limit

We first consider the limit imposed by the aerodynamic characteristics, independent of the propulsion system. The discussion is similar to the one presented in Chapter 6. We rewrite the lift equation (9.1) in terms of Mach number by using the classical relations

$$M = \frac{V}{a}, \qquad a^2 = \frac{kp}{\rho} \tag{9.13}$$

where again a is the speed of sound, ρ is the density and p is the ambient pressure with the constant k being the ratio of the specific heats, having the value 1.4 for air. Then we have

$$n\omega = M^2 C_L \tag{9.14}$$

where ω is the dimensionless wing loading

$$\omega = \frac{2W}{kpS} \tag{9.15}$$

Since we treat the weight as constant, ω is constant at the selected flight altitude. When the altitude increases, p decreases and ω increases. Hence, we can use ω to denote the flight level.

According to the lift equation, in its new form (9.14), for each selected bank angle, that is a load factor n for turning, we can choose an arbitrary Mach number for turning and correspondingly adjust the appropriate lift coefficient. The turning rate is given by Eq. (9.3) while the turning radius is obtained from Eq. (9.5). For a steady turn, the thrust must be sufficient to cancel the high drag due to the increase in the induced drag. Also, the lift coefficient calculated must be less than the maximum lift coefficient. Hence, we define the maneuvering limit as the plot of $n\omega$ versus M from the limiting equation

$$n\omega = M^2 C_{L_{max}}(M) \tag{9.16}$$

This plot depends solely on the function $C_{L_{max}}(M)$, and it is the same as that for the flight envelope in Chapter 6, except that here, in the

ordinate, we have $n\omega$ instead of ω. Figure 9.2 presents such a plot and the curve limits the domain of flight for a typical subsonic aircraft. At low Mach number, $C_{L_{max}}$ is nearly constant, and the plot is parabolic. When M is near unity, $C_{L_{max}}$ is nearly zero and $n\omega$ is very small. Hence, we have a typical plot as shown in the figure.

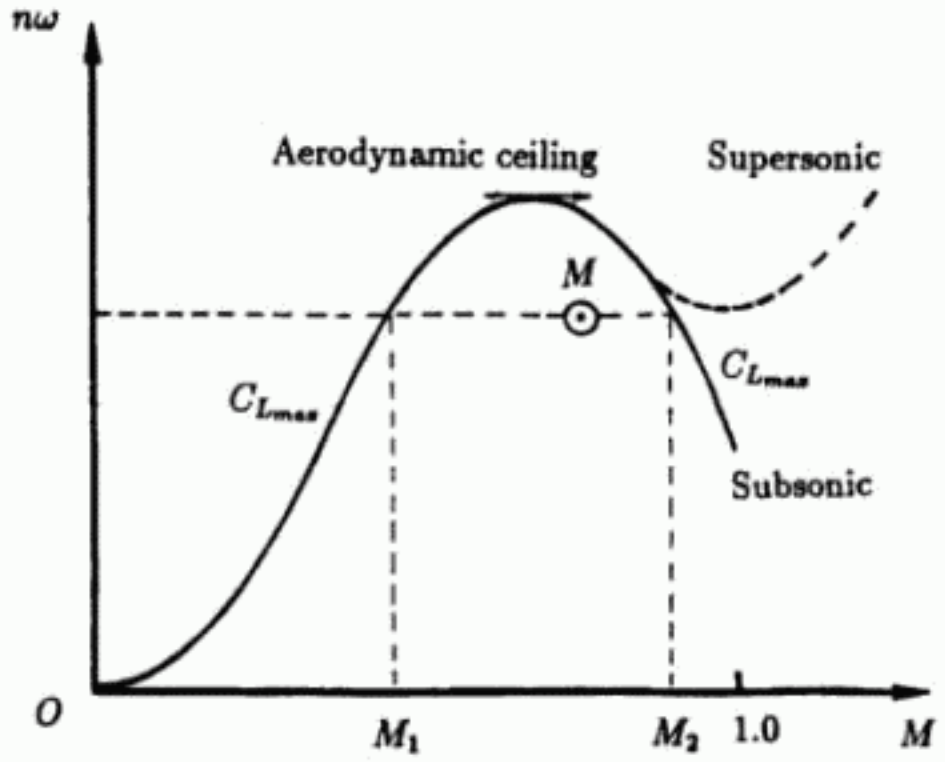

Figure 9.2: Domain of flight.

At any flight altitude, through the ambient pressure p, we have the value ω. With the selected load factor n, the line with the corresponding constant value $n\omega$ intersects the flight envelope, which is the plot of Eq. (9.16), at two points with Mach number M_1 and M_2. With sufficient thrust, turning at the prescribed altitude, with the selected load factor can be performed at any Mach number between M_1 and M_2. The aircraft stalls at both M_1 and M_2, where $C_L = C_{L_{max}}$. It stalls at $M = M_1$ because at that lower Mach number the lift coefficient has reached its maximum value necessary to satisfy the lift equation (9.14). But during the turn with the selected load factor n, if we increase the

Mach number by increasing the thrust, then M reaches the other limiting Mach number M_2. At this high value of the Mach number the maximum lift coefficient, $C_{L_{max}}(M)$, has a low value and as a consequence, we again reach the limiting condition (9.16). For a subsonic jet aircraft, stall during a turn may occur at both the low speed and the high speed regimes.

The horizontal line in Fig. 9.2 for determining M_1 and M_2 corresponds to a given value of $(2W/kpS)n$. We can vary this level in two ways:

First, for a prescribed value of the load factor n, the quantity $\omega = 2W/kps$ varies with altitude through the ambient pressure. This case has been discussed in Chapter 6 for level flight where $n = 1$. As the altitude increases, the level line moves up until it is a tangent to the flight envelope at a point corresponding to the maximum value of $C_{L_{max}}M^2$. This gives the aerodynamic ceiling for the prescribed load factor n, or equivalently, by Eq. (9.2) for a prescribed bank angle ϕ. The aerodynamic ceiling is then obtained by calculating the ambient pressure at the ceiling

$$p_{ceiling} = \frac{2W/kS}{(C_{L_{max}}M^2)_{max}}n \tag{9.17}$$

For any given function $C_{L_{max}}(M)$, the maximum value of $C_{L_{max}}(M)M^2$ is known and we can evaluate the value of p at the ceiling for each selected value of n (see Exercise 9-1). This value increases as n increases. Hence, the aerodynamic ceiling is lower for higher values of the load factor. Also, it is lower for higher values of the wing loading, W/S.

On the other hand, we can hold the altitude constant, that is setting a value of $2W/kpS$ and vary the load factor n. The horizontal line in Fig. 9.2 varies linearly with n. This leads us to Fig. 9.3 which plots the domain of flight for turning at a prescribed altitude.

The domain of flight, bounded by the plot of $C_{L_{max}}M^2$ versus M, is the same but the ordinate of the figure can be graduated in terms of the load factor n. At a given altitude, there exists a maximum load factor n_{max}, given by

$$n_{max} = \frac{kpS}{2W}(C_{L_{max}}M^2)_{max} \tag{9.18}$$

Turning flight at a given altitude cannot be performed beyond this maximum value of the load factor regardless of the power of the en-

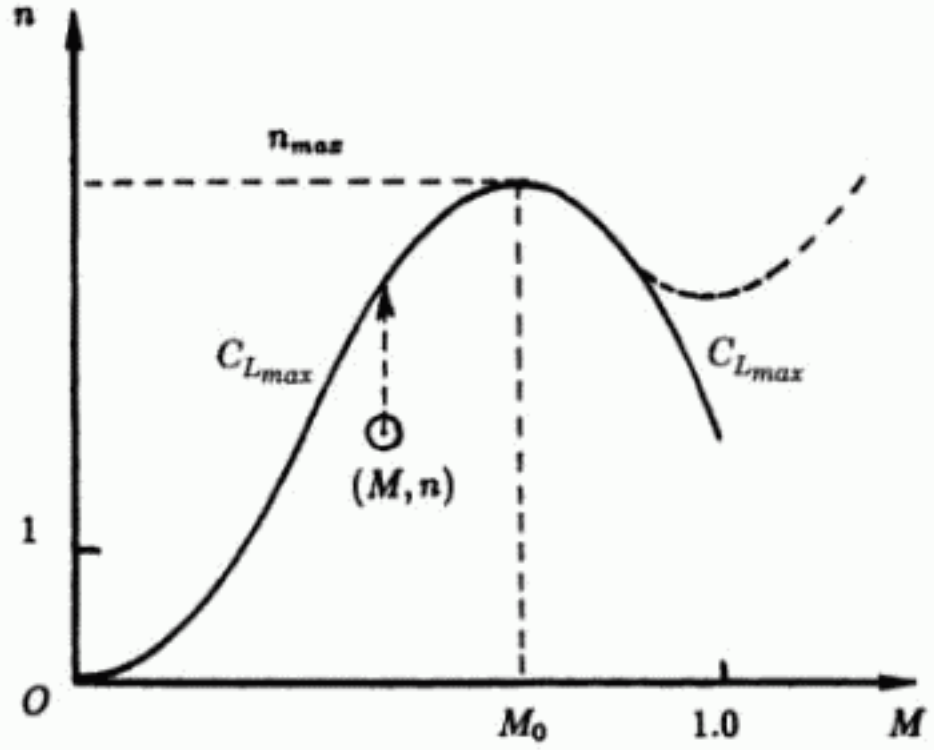

Figure 9.3: Domain of flight for turning at a prescribed altitude.

gine. This is due to the compressibility effect on the aerodynamic configuration of the aircraft.

In the case where the value n_{max}, as calculated by Eq. (9.18) exceeds the maximum value of the load factor n_s as imposed by the physiological and structural limit, then, the domain of flight is bounded at its upper limit by this new value of the maximum load factor as shown in Fig. 9.4.

At low Mach number, the domain of flight is restricted by the limit $C_L = C_{L_{max}}$. At high Mach number, it is restricted by the structural constraint, $n = n_s$.

The value M_c of the Mach number at the intersection of the flight envelope and the physiological/structural limit is called the corner Mach number and is obtained by solving the equation

$$M^2 C_{L_{max}}(M) = \frac{2W}{kpS} n_s \tag{9.19}$$

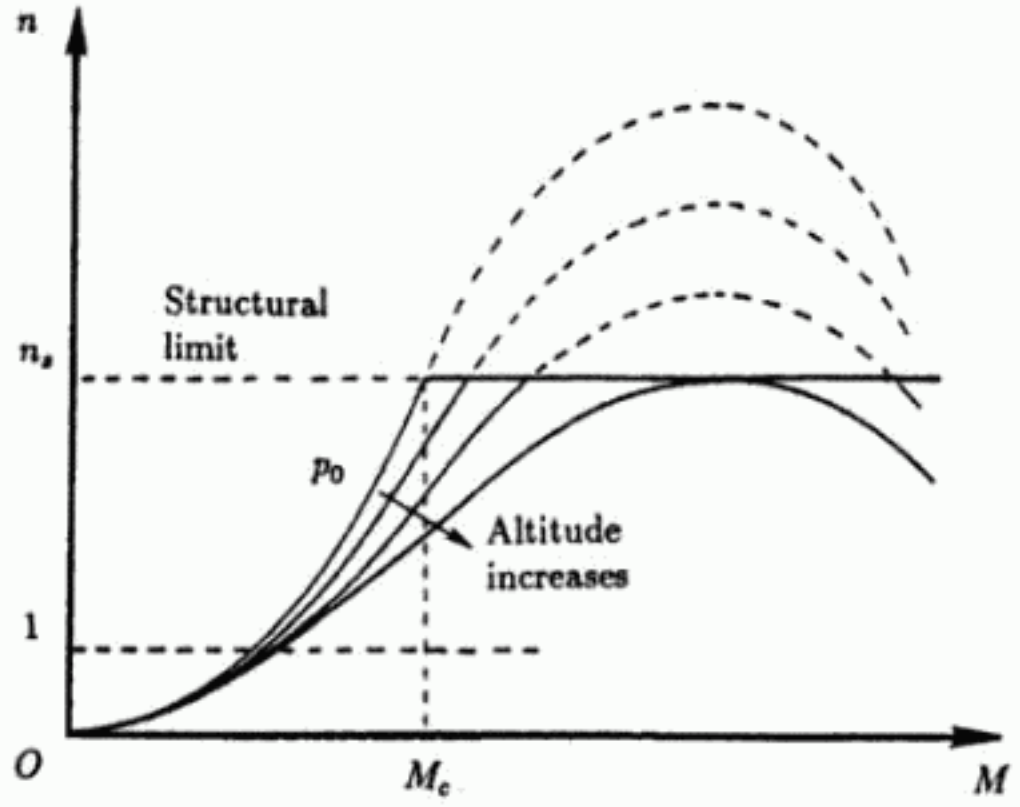

Figure 9.4: Domain of flight at various altitudes with structural limit.

where n_s is the imposed load factor.

In Fig. 9.4, the ordinate n can be calibrated for any flight altitude, starting from the condition at sea level, $p = p_0$, as follows. Plot the curve

$$n = \frac{M^2 C_{L_{max}}(M)}{2W/kp_0S} \tag{9.20}$$

for the given aircraft wing loading W/S, and aerodynamic characteristic function $C_{L_{max}}(M)$ at sea level, $p = p_0$. The curve, which is the outer curve, is the flight envelope for the aircraft at sea level and its intersection with the line $n = n_s$ gives the corner Mach number for the aircraft at sea level while its highest point gives the maximum load factor due to aerodynamic constraint at sea level. Next, in order to use the same scale for the n-axis for different altitude levels, say every 2 km, we reduce the sea-level curve, along the n-axis by the ratio p/p_0

where p is the pressure at the current altitude. Then, it is seen that the corner Mach number increases as the altitude increases. Also, the maximum aerodynamic load factor n_{max} decreases by the same ratio as the altitude increases. Hence, there exists an altitude beyond which $n_s > n_{max}$ and the physiological/structural limit is no longer enforced because the aircraft reaches its aerodynamic limit first. It is in this sense that we distinguish high altitude turning from low altitude turning.

9.3 The thrust required for turning

For a steady turn in a horizontal plane, the two equations (9.1) and (9.8) have to be constantly satisfied. So far, we have restricted the discussion to Eq. (9.1) which shows the lift requirement. We now turn our attention to Eq. (9.8) which shows the thrust requirement.

Again, we use the relations (9.13) to express the lift and the thrust equations in terms of the Mach number. We have

$$\frac{2W}{kpS} n = C_L M^2 \tag{9.21}$$

and

$$\frac{2T}{kpS} = C_D M^2 \tag{9.22}$$

We assume a lift-drag relationship as given in Eq. (9.9).

In turning, as the bank angle is set, we have a corresponding load factor $n > 1$. To keep the same Mach number, by Eq. (9.21), the lift coefficient, and hence the angle-of-attack, has to be increased proportionally. By Eq. (9.9) for the drag polar, this leads to an increase in the drag coefficient which, by Eq. (9.22), results in an increase in the thrust magnitude.

Turning can be performed at high speed, and low angle-of-attack, or at low speed and consequently at high angle-of-attack. Let us assume that we start with a rectilinear flight, $n = 1$, and at high speed, hence with a low value $C_L = C_{L_1}$. For turning with a load factor $n > 1$, the new value of the lift coefficient is $C_L = nC_{L_1}$, if we maintain the same speed. Then the thrust must increase with the new drag coefficient. For a typical, and realistic drag polar, the slope dC_L/dC_D is high when C_L is small. As a consequence, we have a small increase in C_D and the

relative increase in the thrust required is small. On the other hand, if we turn at high angle-of-attack, that is if we start with low speed and a high value of the lift coefficient C_L, near the stall, the slope dC_L/dC_D is small. Then, even with a low bank angle, a small increase in C_L in proportion to n, would lead to a large increase in the drag coefficient C_D. We then expect a large increase in the thrust required. A quantitative analysis, using a parabolic drag polar is depicted in Exercise 9-3.

By dividing the two equations (9.21) and (9.22), we have the thrust required for turning at the load factor n

$$T_{nr} = nW\frac{C_D}{C_L} \tag{9.23}$$

By keeping the same angle-of-attack for turning, the thrust required is proportional to the apparent weight nW. If we use a parabolic drag polar, and the lift equation written in terms of the dimensionless wing loading ω, as given in Eq. (9.14), we have the thrust-to-weight ratio in the form

$$\frac{T_{nr}}{W} = C_{D_0}\frac{M^2}{\omega} + n^2\frac{K\omega}{M^2} \tag{9.24}$$

Typical plots of this equation, using the load factor as parameter, are shown in Fig. 9.5. The lowest curve is the plot of the thrust required for rectilinear flight with $n = 1$. By Eq. (9.21), to each point N on this curve, with Mach number M, there corresponds a well defined lift coefficient C_L. Now, on the curve T_{nr}, with load factor n, for the same value of C_L, we have the corresponding point N' with Mach number $M' = M\sqrt{n}$ as seen from Eq. (9.21). If the drag polar is independent of the Mach number, then the drag coefficient C_D will be the same and from Eq. (9.23) we have the corresponding value $T_{nr} = nT_r$, where T_r is the value of the thrust required at the point N, with $n = 1$. On the same figure, we have the plot of the thrust available T_a for a certain throttle setting. For a steady turn at the selected load factor, we have $T_a = T_{nr}$. We have two possible points of intersection of the two curves T_a and T_{nr} at the Mach numbers M_1 and M_2. Using the same arguments as for the case of steady cruise in Chapter 6, we can see that the high speed regime at M_1 is stable, while turning with the same load factor and thrust available using the low speed regime at M_2 is unstable. We notice that if we use a realistic drag polar, showing

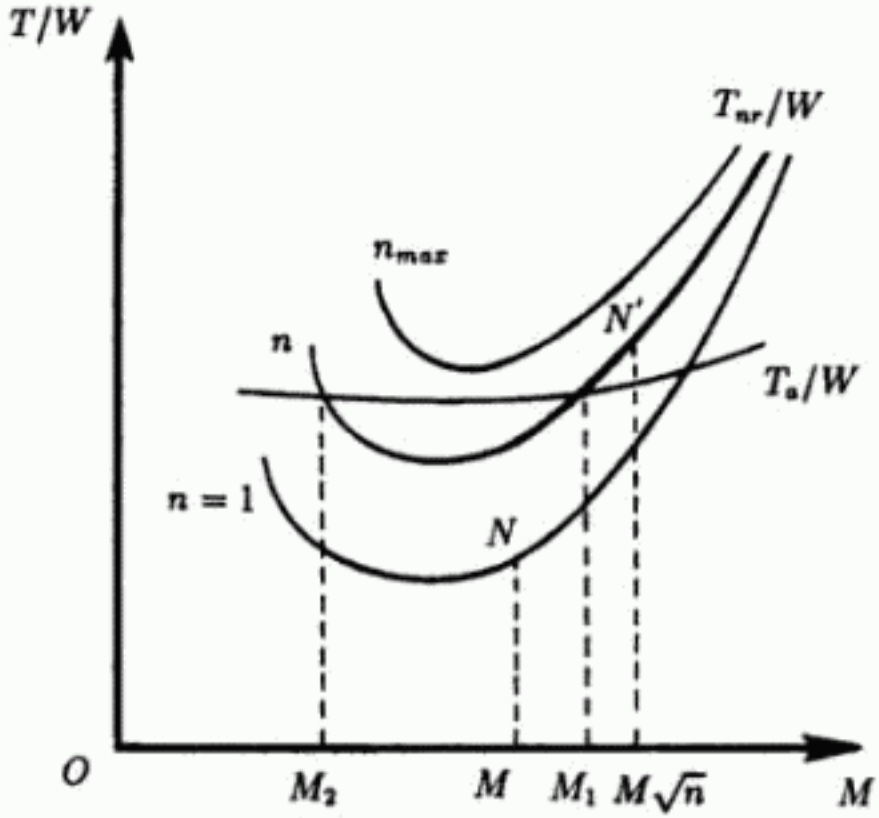

Figure 9.5: Thrust required for turning.

the effect that C_L is stationary at the stall angle-of-attack, then the slope of the T_{nr} curve at the stall Mach number is infinite. By keeping the throttle setting fixed, if we increase the load factor, the two Mach numbers M_1 and M_2 tend toward each other. When the curve T_a becomes a tangent to the highest T_{nr} curve, we attain the maximum load factor, n_T, for turning at the prescribed throttle setting. From the design standpoint, it is important to know the maximum value of the load factor n_T due to the limitation of thrust. If in Eq. (9.23), we set $T_{max} = T_{nr}$, we can calculate n_T from

$$n_T = \frac{T_{max}}{W}\left(\frac{C_L}{C_D}\right)_{max} \tag{9.25}$$

If we assume that the drag polar is independent of the Mach number, then the value of the maximum lift-to-drag ratio is constant. We recall that the minimum thrust to maintain level flight, with $n = 1$, is given

by

$$1 = \frac{T_{min}}{W}\left(\frac{C_L}{C_D}\right)_{max} \tag{9.26}$$

We deduce that

$$n_T = \frac{T_{max}}{T_{min}} \tag{9.27}$$

The evaluation of the maximum load factor n_T using a parabolic drag polar, function of the Mach number, is detailed in Exercise 9-5.

The maximum value n_T is the limit due to the engine characteristics and is known as the maneuvering margin. This is because when the thrust is already at its maximum value, for any value of the load factor n exceeding the maneuvering margin n_T, the thrust required is higher than the maximum thrust available and a steady turn at a higher load factor than n_T is not possible in a horizontal plane.

The maximum value n_T, as shown in Eq. (9.25) is high for high values of the thrust-to-weight ratio. But, at maximum throttle setting, for a typical model of the thrust, as assumed in Eq. (9.12), as the altitude increases, the value of T_{max} decreases. Then, there comes an altitude where $n_T = 1$. This altitude is the propulsive ceiling.

We now return to Eq. (9.24) which shows the variation of the thrust required T_{nr} to turn at the selected load factor n. For any throttle setting, by putting T_a/W equal to the right-hand side of this equation, we have an equation for evaluating the two Mach numbers M_1 and M_2 for a steady turn. When M_1 tends to M_2, we have the Mach number, for turning at the load factor n, with minimum thrust available. Since T_a is nearly independent of Mach number in the speed range where its minimum occurs, the operating point is in the vicinity of the lowest point on the curve T_{nr}. Then, we have the condition at minimum thrust by writing $dT_{nr}/dM = 0$. We have

$$2C_{D_0}\frac{M}{\omega} + C'_{D_0}\frac{M^2}{\omega} - 2n^2\frac{K\omega}{M^3} + n^2\frac{K'\omega}{M^2} = 0$$

where the prime denotes the derivative with respect to M. As in Chapter 6, we use the notation of the logarithmic derivative

$$y_M = \frac{d(\operatorname{Log} y)}{d(\operatorname{Log} M)} = \frac{M}{y}\frac{dy}{dM}$$

to put this equation in the form

$$n\omega = M^2 C_L^* \sqrt{\frac{2 + C_{D_0 M}}{2 - K_M}} \tag{9.28}$$

where, as usual we define $C_L^* = \sqrt{C_{D_0}/K}$, being the lift coefficient at maximum lift-to-drag ratio. This equation gives the Mach number for turning at the load factor n, with minimum thrust required. By substituting back into Eq. (9.24) we obtain

$$\left(\frac{T_{nr}}{W}\right)_{min} = \frac{n(2 + C_{L_M}^*)}{E_{max}\sqrt{(2 + C_{D_0 M})(2 - K_M)}} \tag{9.29}$$

If we neglect the effect of Mach number on C_{D_0} and K of the parabolic drag polar, then we see that the minimum thrust for turning is at $C_L = C_L^*$, that is at maximum lift-to-drag ratio.

9.4 Optimum turn

From the discussion in the preceding two sections, with the condition $n > 1$ for turning in a horizontal plane, we have seen that there are three types of constraints on the load factor at any flight altitude.

First, there is the maneuvering limit, due to the effect of compressibility of the air on the aerodynamic characteristics. For any given $\omega = 2W/kpS$, the maneuvering limit is the plot of n versus M according to Eq. (9.16). Next, there is the maneuvering margin, due to the limitation of the maximum thrust, according to Eq. (9.25). Figure 9.6 presents the plot of the maneuvering limit and also the plot of the maneuvering margin which is only enforced if the thrust is sufficiently low. Finally, there is the physiological/structural limit n_s on the load factor. Turning flight in a horizontal plane, for both the steady and the unsteady regimes, is necessarily within these limits.

In this section, we shall consider turning at peak performance by assuming constraints only on aerodynamic characteristics and a structural limit. This is to say that the thrust produced is sufficiently high to cancel the drag. Turning with a prescribed throttle setting will be the subject for discussion in the next section.

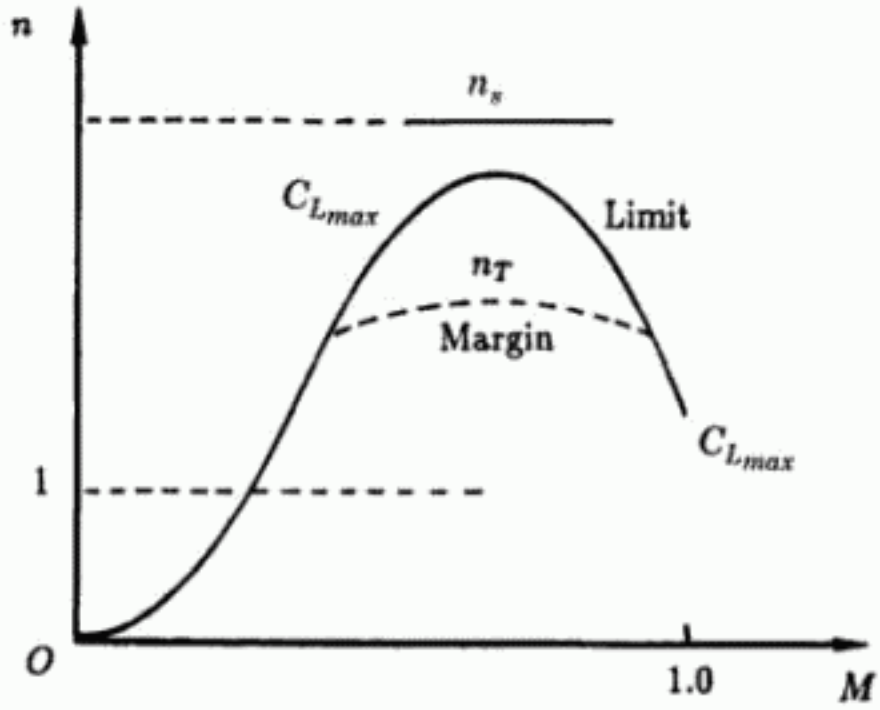

Figure 9.6: Various limits on the load factor for turning.

9.4.1 Turning rate

The turning rate is given by Eq. (9.3) and for each pair (n, V) or equivalently (n, M), we have a specified turning rate, provided that the constraints on the load factor, lift coefficient, and thrust available are satisfied. If the speed is expressed in terms of the load factor and the lift coefficient, we have the alternate form (9.4). Then, it is clear from this equation that a low wing loading W/S gives a high turning rate. Also turning is faster at lower altitude where the density is high.

It is proposed to select a load factor n, and a lift coefficient C_L to have the highest turning rate with the assumption that we have sufficient thrust to sustain the turn.

We first consider the case of turning at low altitude where the structural constraint n_s is enforced. The domain of flight is shown in the diagram (n, M) in Fig. 9.7.

At any Mach number, low enough, we must first use $C_L = C_{L_{max}}$ as clearly evident from Eq. (9.4). Still in the range of low Mach number

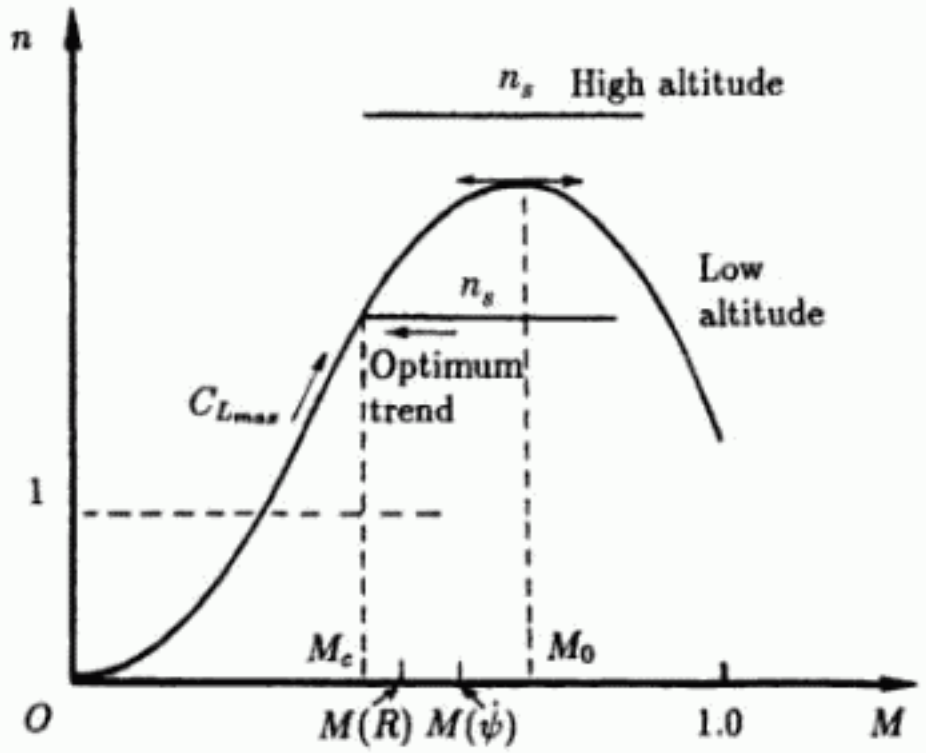

Figure 9.7: Domain of flight for turning.

where $C_{L_{max}}(M)$ is nearly constant, from this equation, the turning rate increases with the load factor and we must use $n = n_s$, at the corner Mach number M_c. Beyond this Mach number, with $n = n_s$, we rewrite Eq. (9.3)

$$\dot{\psi} = \frac{g\sqrt{n_s^2 - 1}}{aM} \tag{9.30}$$

According to this formula, since n_s is constant, the highest turning rate is attained with the minimum Mach number, and as a consequence, we keep $M = M_c$ for optimum turn. Again, we emphasize the fact that the conclusion has been reached with the assumption of a constant value for $C_{L_{max}}$.

For turning at high altitude, we refer to the same figure, but now the value n_{max}, at the highest point of the maneuvering limit, as calculated by Eq. (9.18), is low, because of a smaller value for the ambient pressure p. This leads to $n_{max} < n_s$ and the structural constraint is no longer enforced.

Again, we must use $C_L = C_{L_{max}}(M)$, and the optimum point is on the maneuvering limit, as given by Eq. (9.16). We write this equation as

$$n = \frac{1}{\omega} M^2 C_{L_{max}}(M) = f(M) \tag{9.31}$$

If sufficient aerodynamic data are available, we can always model the function $C_{L_{max}}(M)$ as a polynomial in M, and therefore, we assume that $f(M)$ is a known function of M. A property of the function $C_{L_{max}}$ is that it decreases as Mach number increases. Then, we consider the equation (9.3) for the turning rate in the form

$$\frac{g}{a\dot{\psi}} = \frac{M}{\sqrt{f^2(M) - 1}} = F_1(M) \tag{9.32}$$

This is a function of M, and the turning rate is maximized for a value $M = M_{opt}$ which minimizes the function $F_1(M)$. This optimum Mach number can only be found with an appropriate modeling of the function $f(M)$. But qualitatively, it can be assessed that $M_{opt} < M_0$, where M_0 is the Mach number which maximizes the function $M^2 C_{L_{max}} \sim f(M)$. This is because, for $M > M_0$, the function $n = f(M)$ decreases as M increases and hence the function $F_1(M)$ increases with M. The minimum of $F_1(M)$ must occur before M_0. Hence $n_{opt} < n_{max}$.

As a final note, we observe that when the constraint n_s is enforced, that is with the existence of the corner Mach number M_c, if the optimum Mach number computed is such that $M_{opt} < M_c$, turning with maximum rate is performed at $M = M_{opt}$, instead of at $M = M_c$.

9.4.2 Turning radius

We have a similar analysis for the turning radius. It is given by Eq. (9.5) and for each pair (n, V) or equivalently (n, M), we have a specified turning radius provided that the constraints on the load factor, lift coefficient, and thrust available are satisfied. If the speed is expressed in terms of the load factor and the lift coefficient, we have the alternate form (9.6). From this equation, it is clear that a low wing loading W/S gives a small turning radius. Also this radius is small for turning at low altitude where the density is high.

First for minimum turning radius, it is necessary that we use $C_L = C_{L_{max}}$. At low Mach number, where $C_{L_{max}}$ is nearly constant, as seen

from Eq. (9.6), the turning radius decreases as the load factor n increases. This leads to using $n = n_s$ if the structural limit is enforced at low altitude. The turning Mach number at $C_L = C_{L_{max}}$, $n = n_s$ is the corner Mach number, M_c. Beyond this corner Mach number, we write Eq. (9.5) with $n = n_s$.

$$R = \frac{a^2 M^2}{g\sqrt{n_s^2 - 1}} \tag{9.33}$$

With constant n_s, the turning radius increases as the Mach number increases. Hence the minimum of R occurs at $n = n_s$, $M = M_c$. This conclusion is reached with the assumption of a constant value for $C_{L_{max}}$.

For turning at high altitude, where $n_{max} < n_s$, with $C_L = C_{L_{max}}$ for minimum turning radius, we write Eq. (9.5) as

$$\frac{Rg}{a^2} = \frac{M^2}{\sqrt{f^2(M) - 1}} = F_2(M) \tag{9.34}$$

where the function $n = f(M)$ is defined in Eq. (9.31). Then the turning radius is minimized for a value M_{opt} which minimizes the function $F_2(M)$. This optimum Mach number can only be found with an appropriate modeling of the function $f(M)$. As in the discussion of the maximum turning rate, we see that $M_{opt} < M_0$ where M_0 is the Mach number which maximizes the function $n = f(M)$. Also we notice that when the constraint n_s is enforced, if $M_{opt} < M_c$, the value $M = M_{opt}$ must be used, instead of the value $M = M_c$, for minimum turning radius.

Without expliciting the function $f(M)$, we can find the relative position of the two optimum Mach numbers $M_{opt}(\dot{\psi})$ for maximum turning rate and $M_{opt}(R)$ for minimum turning radius. By the definitions (9.32) and (9.34) of the two functions $F_1(M)$ and $F_2(M)$, we notice that

$$F_2 = MF_1 \tag{9.35}$$

By taking the derivative of this equation with respect to M, we obtain

$$\frac{dF_2}{dM} = F_1 + M\frac{dF_1}{dM} \tag{9.36}$$

When the turning radius is a minimum, $dF_2/dM = 0$, and we have $dF_1/dM = -F_1/M < 0$. Hence the function F_1, which is proportional

to the time to turn is still decreasing. We conclude that the optimum Mach number for fastest turn is higher than the optimum Mach number for minimum radius turn. As a consequence of the lift equation (9.16) on the boundary $C_{L_{max}}$, the load factor for fastest turn is higher.

9.5 Numerical application

To have a better understanding of the analysis in the preceding sections, let us consider a hypothetical fighter aircraft with the following data.

$$C_{D_0} = 0.012, \qquad K = 0.208, \qquad W/S = 95 \text{ lb/ft}^2$$

In general, optimum turn is performed at low Mach number and we have used constant values for C_{D_0} and K. For a refined calculation of the performance, it is not difficult to use the aerodynamic data available to model these functions as polynomials in the Mach number M. On the other hand, to display explicitly the role of the maneuvering limit, we consider a maximum lift coefficient such that at subsonic speed, we have

$$C_{L_{max}} = \begin{cases} 1.0, & \text{if } M \leq 0.6 \\ 1.0 - 3.75(M - 0.6)^2, & \text{if } M > 0.6 \end{cases}$$

This is rather a simple model to ease the iteration in the numerical computation, but for a more elaborate modeling, the procedure for the evaluation of the optimum performance is the same.

At sea level, we have

$$k = 1.4, \quad p_0 = 2116 \text{ lb/ft}^2, \quad a_0 = 1116 \text{ ft/s}, \quad g = 32.2 \text{ ft/s}^2$$

With the function $C_{L_{max}}(M)$, we easily find that

$$\max[M^2 C_{L_{max}}(M)] = 0.5533 \quad \text{at} \quad M_0 = 0.8448$$

At sea level, we evaluate the dimensionless wing loading

$$\omega_0 = \frac{2W}{kp_0S} = 0.0641$$

Using Eq. (9.17), with $n = 1$, we see that at the aerodynamic ceiling $p/p_0 = 0.1159$ and this corresponds to an altitude near 50,000 ft.

Hence, if adequate thrust is available, turning is possible up to this altitude.

Now, using Eq. (9.18), we see that the maximum load factor at sea level is $n_{max} = 0.5533/0.0641 = 8.63$ g. At higher altitude, say at 30,000 ft where $p/p_0 = 0.297$, the maximum load factor is reduced proportionally to $n_{max} = 2.56$ g. Therefore, if we impose a physiological/structural constraint of $n_s = 5$, this constraint is enforced up to an altitude such that $p/p_0 = 5/8.63 = 0.579$, that is to about 14,000 ft.

At sea level, if we take $n_s = 5$, by Eq. (9.19), the corner Mach number is $M_c = 0.566$. We have used $C_{L_{max}} = 1$ for the calculation, and it is correct since $M_c < 0.6$. But if we increase n_s to $n_s = 6$, we have $M_c > 0.6$ and the function $C_{L_{max}}(M)$ has to be used in the evaluation of M_c.

With these preliminary evaluations, we now know that at sea level for maximum turning rate and minimum turning radius, we must use $n = n_s = 5$, and $M = M_c$, that is at a turning speed of $V_c = 631.66$ ft/s. From Eqs. (9.3) and (9.5), this gives

$$\dot{\psi}_{max} = 0.2497 \text{ rad/s} = 14.31 \text{ deg/s}$$
$$R_{min} = 2529 \text{ ft}$$

If we use Eq. (9.23) with $n = n_s$ and $C_L = C_{L_{max}}$, we see that to maintain a steady turn, it requires a thrust-to-weight ratio of $T/W = 1.1$. This is rather high, and we should emphasize the fact that the values $\dot{\psi}_{max}$ and R_{min} evaluated are the absolute extrema. In general, to achieve optimum performance in turning, we just use maximum thrust as will be analyzed in the next section.

Let us now evaluate the peak performance in turning of this aircraft at the flight altitude of 30,000 ft with the current value of the wing loading

$$\omega = \frac{2W}{kpS} = \omega_0 \frac{p_0}{p} = 0.2158$$

We have seen that the maximum load factor is $n_{max} = 2.56$ and the constraint $n_s = 5$ is no longer enforced.

For the maximum turning rate, we search for the minimum of the function $F_1(M)$, as defined in Eqs. (9.31) and (9.32). We find that

$$M_{opt}(\dot{\psi}) = 0.777 < M_0 = 0.8448$$
$$F_1(M) = 0.344205$$

$$\dot{\psi}_{max} = 0.09408 \text{ rad/s} = 5.39 \text{ deg/s}$$
$$n = 2.469$$

Notice that we have used the speed of sound of $a = 994.356$ ft/s at the current altitude for the evaluation of $\dot{\psi}$ using Eq. (9.32). With this optimum Mach number, we have $C_{L_{max}} = 0.8825$, $C_{D_{max}} = 0.1740$ and from Eq. (9.23) we obtain the required thrust-to-weight ratio $T_{nr}/W = 0.4868$. This value is also high since in the previous calculation at sea level, even if we assume that a maximum thrust-to-weight of $T_0/W = 1.1$ is attainable, by using a law for the thrust available which is proportional to the density ratio, at 30,000 ft where $\rho/\rho_0 = 0.374$, we have the thrust-to-weight ratio of only $T/W = 0.4114$.

Again, with the assumption of a sufficiently high thrust for optimum steady turn at altitude, we calculate the absolute minimum turning radius by minimizing the function $F_2(M)$ as defined in Eqs. (9.31) and (9.34). We find that

$$M_{opt}(R) = 0.685 < M_{opt}(\dot{\psi})$$
$$F_2(M) = 0.251709$$
$$R = 7729.06 \text{ ft}$$
$$n = 2.1154$$

With this optimum Mach number, we have $C_{L_{max}} = 0.9729$, $C_{D_{max}} = 0.2089$ and from Eq. (9.23) with the corresponding load factor, we obtain the required thrust-to-weight ratio $T_{nr}/W = 0.4542$.

To conclude this section, we observe that at the altitude of 30,000 ft the optimum load factor for turn at maximum rate is $n_1 = 2.469$ and the optimum load factor for turn with minimum radius is $n_2 = 2.1154$ while the maximum load factor at this altitude is $n_{max} = 2.56$. Then, if we impose the physiological constraint at $n_s = 2.0$ (a very hypothetical assumption for the illustration of the theory), the optimum turn is at the corner Mach number, with $C_L = C_{L_{max}}(M_c)$, and $n = n_s$ for both the fastest turn and the minimum radius turn. But if we take n_s to be between n_1 and n_2, then the fastest turn is at $n = n_s$, while the minimum radius turn is at $n = n_2 < n_s$.

9.6 Steady turn with constant thrust setting

The minimum turning radius and the maximum turning rate discussed in the previous sections are respectively the absolute minimum radius and the absolute maximum rate under the condition that, at the prescribed altitude, the thrust produced by the engine can deliver the required load factor to sustain the turn at the optimum speed.

We now discuss the optimum condition for steady turn of a jet aircraft with constant throttle setting, providing a constant thrust magnitude, assumed independent of the Mach number.

First, Eq. (9.23) can be solved for the load factor

$$n = \tau \frac{C_L}{C_D} \tag{9.37}$$

where τ is the thrust-to-weight ratio

$$\tau = \frac{T}{W} \tag{9.38}$$

By substituting into the general equation (9.6) for the turning radius, we have

$$R = \frac{2W\tau}{g\rho S} \frac{1}{\sqrt{\tau^2 C_L^2 - C_D^2}} \tag{9.39}$$

For a given altitude and thrust setting, the turning radius R is minimized by maximizing the function

$$F = \tau^2 C_L^2 - C_D^2 \tag{9.40}$$

where τ is constant and the aerodynamic coefficients are functions of the angle-of-attack. Hence, there exists an angle-of-attack that one can select to maximize the function F. We first give a qualitative analysis due to André Turcat, former chief test pilot of the French–British SST Concorde and President of the French National Academy of Air and Space (Turcat, 1960). The drag polar is realistic and arbitrary (Fig. 9.8). Since F is stationary, we have

$$2\tau^2 C_L dC_L - 2C_D dC_D = 0$$

The optimum condition is

$$\frac{dC_D}{dC_L} = \tau^2 \frac{C_L}{C_D} \tag{9.41}$$

With the angles δ and θ as defined in Fig. 9.8, we have

$$\tan\delta = \frac{dC_D}{dC_L}, \qquad \tan\theta = \frac{C_L}{C_D} \tag{9.42}$$

We notice that $\tan\delta$ is the slope of the tangent at the operating point measured with respect to the C_L axis and $\tan\theta$ is the lift-to-drag ratio at that point. The drag polar is plotted with the same scale on both axes. Then, from Eqs. (9.41) and (9.42)

$$\tan\delta = \tau^2 \tan\theta \tag{9.43}$$

For very high thrust, δ is large compared with θ and at the extreme limit, when $\tau \to \infty$, $\delta \to 90°$ and the operating point reaches $C_{L_{max}}$. By Eq. (9.37), the load factor becomes infinite. On the other hand, the minimum value of τ, also from Eq. (9.37), is the value for rectilinear flight, $n = 1$, at maximum lift-to-drag ratio

$$\tau_{min} = \frac{1}{(C_L/C_D)_{max}} \tag{9.44}$$

In this case, from Eq. (9.43) with $\tan\theta = (C_L/C_D)_{max}$ and Eq. (9.44) we have

$$\tan\delta = \frac{1}{\tan\theta} \tag{9.45}$$

Hence

$$\delta + \theta = 90° \tag{9.46}$$

a result which can be deduced directly from Fig. 9.8 by decreasing $\tan\delta$ and increasing $\tan\theta$ to find the minimum of their ratio. To conclude this qualitative discussion, since τ is obviously between the extreme limits, the operating point for minimum turning radius is between the value C_L^* for maximum lift-to-drag ratio and $C_{L_{max}}$. Analytically, if a parabolic drag polar independent of Mach number, is used, that is, if

$$C_D = C_{D_0} + KC_L^2$$

then, the optimum condition (9.41) gives the explicit solution

$$C_D = \frac{\tau^2}{2K} \tag{9.47}$$

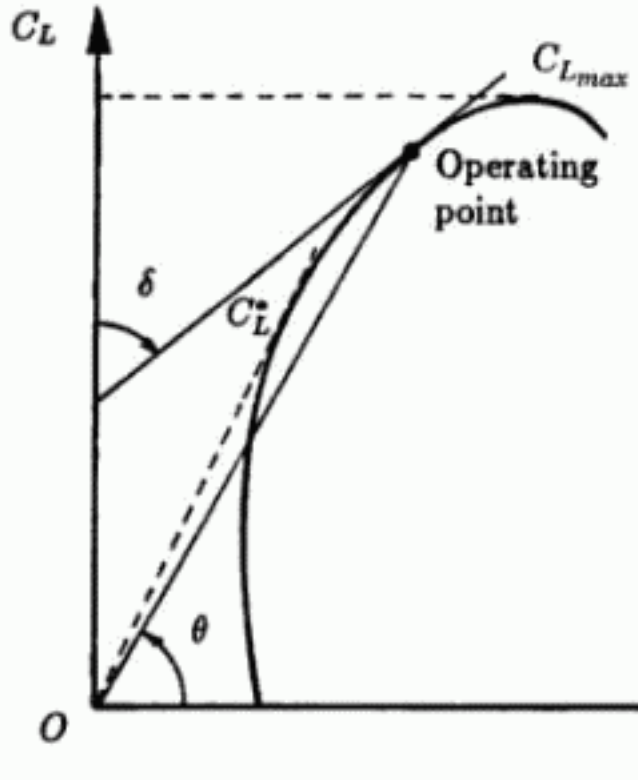

Figure 9.8: Graphical discussion of the operating point for minimum turning radius.

By substituting this solution into Eq. (9.39) we have the minimum turning radius

$$R_{min} = \frac{2W}{g\rho S C_L^*} \frac{1}{\sqrt{E_{max}^2 \tau^2 - 1}} \tag{9.48}$$

Hence, we observe again that low wing loading, high thrust-to-weight ratio and high maximum lift-to-drag ratio reduce the minimum turning radius. Also, the turning radius is smaller at lower altitude.

Next, we observe that, for a prescribed thrust-to-weight ratio, the maximum load factor is obtained from Eq. (9.37) by using maximum lift-to-drag ratio

$$n_{max} = \tau E_{max} \tag{9.49}$$

The corresponding maximum bank angle is simply

$$\cos \phi_{max} = \frac{1}{\tau E_{max}} \tag{9.50}$$

Finally, we consider the turning rate for a prescribed thrust setting. Using Eq. (9.37) in the expression (9.4) for the turning rate, we have

$$\dot{\psi} = g\sqrt{\frac{\rho S}{2W\tau}}\sqrt{\frac{\tau^2 C_L^2 - C_D^2}{C_D}} \tag{9.51}$$

For a prescribed thrust-to-weight ratio, τ, the turning rate $\dot{\psi}$ is maximized by maximizing the function

$$G = \frac{\tau^2 C_L^2 - C_D^2}{C_D} \tag{9.52}$$

As before, if we consider C_L as a function of C_D, by maximizing G with respect to C_D, we have the optimum condition for maximum turning rate

$$2\tau^2 \frac{C_L}{C_D}\frac{dC_L}{dC_D} = 1 + \tau^2\left(\frac{C_L}{C_D}\right)^2 \tag{9.53}$$

Using the definition (9.42), we have

$$\tau^2 \tan\theta\left(\frac{2}{\tan\delta} - \tan\theta\right) = 1 \tag{9.54}$$

When τ has its minimum value the equation is satisfied identically with $\tau = 1/E_{max} = 1/\tan\theta$, and $\tan\delta\tan\theta = 1$ as for the case of minimum turning radius. But here, when the thrust is infinitely large, we are led to the limiting condition $\tan\delta\tan\theta = 2$. From Fig. 9.8, we notice that $\tan\delta$ is infinite at $C_L = C_{L_{max}}$. Hence, we conclude that for any thrust setting between the extreme limits, the optimum operating point for maximum turning rate occurs at a value of C_L between C_L^* and $C_{L_{max}}$. As its relative position with respect to the operating point for minimum turning radius, we consider the function F, as defined in Eq. (9.40) and write

$$F = GC_D$$

where both F and G are positive. Then

$$\frac{dF}{dC_D} = C_D\frac{dG}{dC_D} + G \tag{9.55}$$

At the point of maximum turning rate $dG/dC_D = 0$ and $dF/dC_D = G > 0$. The function F is still increasing and has not reached its

maximum value corresponding to minimum radius turn. Hence, the optimum angle-of-attack for minimum radius turn is higher than the optimum angle-of-attack for maximum rate turn.

Using a parabolic drag polar in the optimum condition (9.53), we have the explicit solution

$$C_D = \tau\sqrt{\frac{C_{D_0}}{K}} \tag{9.56}$$

By substituting this solution into Eq. (9.51), we have the maximum turning rate

$$\dot{\psi}_{max} = g\sqrt{\frac{\rho S}{2WK}}\sqrt{\tau - \frac{1}{E_{max}}} \tag{9.57}$$

It is again seen that high maximum lift-to-drag ratio and high thrust increase the maximum turning rate. Also, turning is faster at low altitude and with low wing loading.

To summarize the discussion of the operating point on a parabolic drag polar, for a constant thrust setting horizontal turn, the following equations can be deduced from Eqs. (9.47), (9.50) and (9.56):

$$\begin{array}{ll} \text{Maximum bank turn,} & C_D = C_{D_1} = 2C_{D_0} \\ \text{Maximum rate turn,} & C_D = C_{D_2} = \tau\sqrt{C_{D_0}/K} \\ \text{Minimum radius turn,} & C_D = C_{D_3} = \tau^2/2K \end{array} \tag{9.58}$$

On the other hand, the minimum thrust-to-weight ratio to maintain rectilinear level flight is $\tau_{min} = 1/E_{max} = 2\sqrt{KC_{D_0}}$. Hence, for turning

$$\tau > 2\sqrt{KC_{D_0}} \tag{9.59}$$

Using this inequality in Eqs. (9.58), it is readily seen that

$$C_{D_3} > C_{D_2} > C_{D_1} \tag{9.60}$$

We conclude that, for the same thrust setting, the angle-of-attack for the minimum radius turn is higher than the angle-of-attack for the maximum rate turn which, in turn, is higher than the angle-of-attack for the maximum bank angle turn, a result in agreement with the qualitative discussion for an arbitrary drag polar.

Just as in the case of turning of a propeller driven aircraft discussed in Chapter 8, for a jet aircraft, we have found that when $\tau > \tau_{min}$, a

coordinated steady turn in a horizontal plane is always possible. For the case where the thrust is kept constant, the optimum solution for maximum turning rate, and the optimum solution for minimum turning radius are such that $C_{L_2} < C_{L_3} < C_{L_{max}}$, where the C_{L_i} are the respective lift coefficients. But, if we use a parabolic drag polar for the calculation, although the condition $C_{L_2} < C_{L_3}$ is always respected, one or both of these lift coefficients, for high values of the thrust-to-weight ratio, may exceed the value $C_{L_{max}}$. This is not because of the optimum characteristics of the turn but rather because of the inaccurate representation of the parabolic drag polar near to $C_{L_{max}}$. In this case, for an approximate evaluation of the peak performance, it is adequate to simply use $C_L = C_{L_{max}}$ in Eq. (9.39) for the minimum turning radius and in Eq. (9.51) for the maximum turning rate.

As an illustration of the analysis of turning with a prescribed thrust, we consider the previous fighter aircraft with the characteristics

$$C_{D_0} = 0.012, \quad K = 0.208, \quad C_{L_{max}} = 1.0$$

$$W/S = 95 \text{ lb/ft}^2$$

At sea level, we take $g = 32.2 \text{ ft/s}^2$, $\rho_0 = 2.3769 \times 10^{-3} \text{ lb-s}^2/\text{ft}^4$.

First, we have $C_{D_{max}} = 0.220$, $E_{max} = 10$. If we use $T/W = 0.3$, we find that

$$C_{D_3} = \tau^2/2K = 0.216 < C_{D_{max}}$$

The formulas for optimum turn are applicable and we find from Eqs. (9.48), (9.49) and (9.57) that

$$R_{min} = 3654.12 \text{ ft}$$
$$n_{max} = 3, \quad \phi_{max} = 70.53^\circ$$
$$\dot{\psi}_{max} = 0.1117 \text{ rad/s} = 6.4 \text{ deg/s}.$$

If we increase the thrust-to-weight ratio to the value $T/W = 0.65$, we find that $C_{D_2} < C_{D_{max}}$, but the value $C_{D_3} = 1.016$ is now too high. Therefore, equation (9.39) wiht $C_L = C_{L_{max}}$, $C_D = C_{D_{max}}$ must be used to evaluate approximately the minimum turning radius. With the new and high value of the thrust-to-weight ratio, we find that

$$R_{min} = 2638.19 \text{ ft}$$
$$n_{max} = 6.5, \quad \phi_{max} = 81.15^\circ$$
$$\dot{\psi}_{max} = 0.1852 \text{ rad/s} = 10.61 \text{ deg/s}.$$

If we use a higher thrust-to-weight ratio of $T/W = 1.0$, then $C_{D_2} = 0.240 > C_{D_{max}}$. The use of a parabolic drag polar leads to an optimum speed for turning for both the fastest turn and the minimum radius turn now below the stall speed. In this case, it is appropriate to use Eqs. (9.39) and (9.51) with $C_L = C_{L_{max}}$ to evaluate the optimum performance. Then, we obtain

$$R_{min} = 2544.83 \text{ ft}$$
$$n_{max} = 10, \quad \phi_{max} = 84.26°$$
$$\dot{\psi}_{max} = 0.2369 \text{ rad/s} = 13.57 \text{ deg/s}.$$

9.7 Non-steady turn

For fighter aircraft, in air-to-air combat, it is necessary for survival to use the fastest turn or the minimum radius turn at maximum thrust. With the lift coefficient near the stalling point and at high load factor, the maximum thrust at high altitude is usually not sufficient to overcome the high drag. For a coordinated turn, although the lift equation is satisfied, with $T < D$, the aircraft decelerates. When the speed has reached the stall speed, either the load factor or the altitude or both have to decrease.

For accelerating or decelerating turns at constant altitude, we use the lift equation (9.1) with a parabolic drag polar to rewrite the general equation (9.7) in the form

$$\frac{\rho S C_{D_0}}{m} dt = -\frac{2V^2 dV}{V^4 - \dfrac{2T}{\rho S C_{D_0}} V^2 + \dfrac{4Kn^2W^2}{(\rho S)^2 C_{D_0}}} \tag{9.61}$$

If we keep a constant load factor n, this equation can be integrated by quadrature if the thrust T and the aerodynamic characteristics C_{D_0} and K are assumed independent of the speed. This has been done for the case $n = 1$ in Section 6.8 when we studied the unsteady rectilinear flight at constant altitude. For the solutions with $n > 1$, it suffices to replace in the equations in Section 6.8, the weight W by the apparent weight nW. The detailed results are given in Exercises 9-11 and 9-12. Here, we shall give a qualitative discussion based on the (V, n)

diagram as shown in Fig. 9.9. At constant altitude, the speed of sound is constant and we use V instead of M in the abcissa. As usual, we have the flight envelope and the limit in the load factor either in n_s or n_{max}. On the same diagram, we have plotted the equation $T = D$,

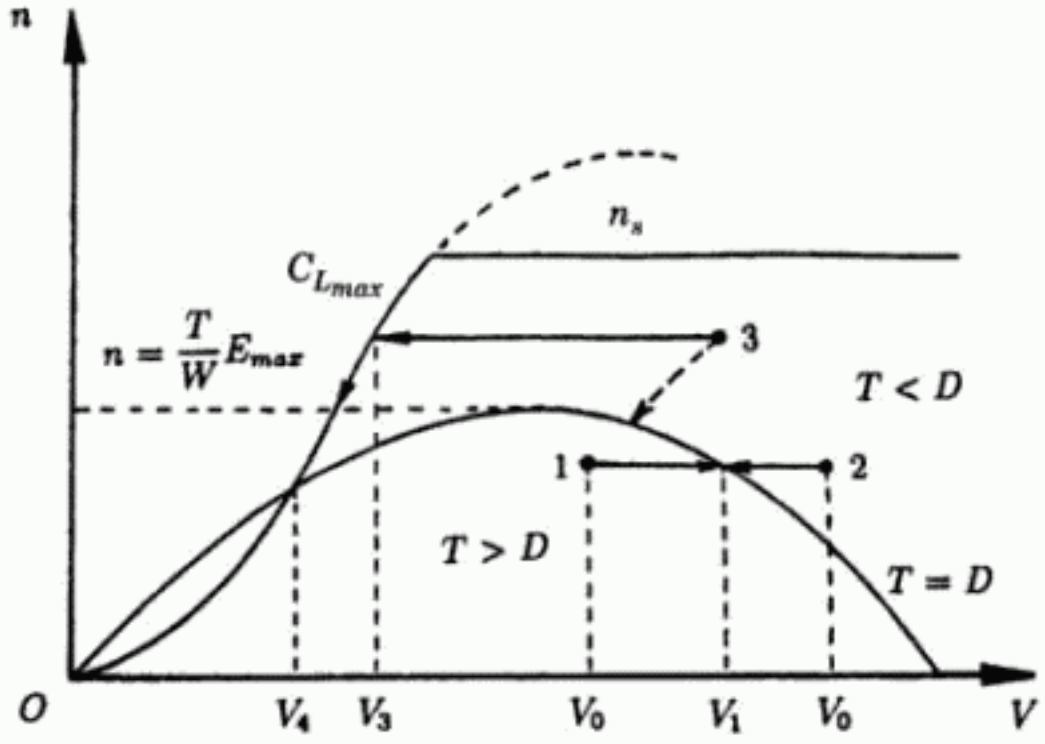

Figure 9.9: Accelerating and decelerating turn in a horizontal plane.

which is

$$V^4 - \frac{2T}{\rho S C_{D_0}} V^2 + \frac{4Kn^2W^2}{(\rho S)^2 C_{D_0}} = 0 \tag{9.62}$$

Let V_1 and V_2 be the two positive roots of this equation

$$\begin{aligned} V_1 &= \frac{1}{\sqrt{\rho S C_{D_0}}}\left[T + \sqrt{T^2 - \frac{n^2W^2}{E_{max}^2}}\right]^{1/2} \\ V_2 &= \frac{1}{\sqrt{\rho S C_{D_0}}}\left[T - \sqrt{T^2 - \frac{n^2W^2}{E_{max}^2}}\right]^{1/2} \end{aligned} \tag{9.63}$$

For real solutions, we must have $T \geq nW/E_{max}$, which is the minimum thrust required to turn at the load factor n. The speeds V_1 and V_2

are for steady turning at the prescribed and sufficiently high thrust available. The curve $T = D$ divides the (V, n) space into two regions. In one region, we have $T > D$ and the turn is accelerating. This is shown by the trajectory 1 starting with the initial speed V_0 less than the high and stabilizing speed V_1 for a steady turn. The aircraft accelerates from V_0 to V_1 with constant n. But as the speed V is approaching V_1, the excess thrust $T - D$, which is proportional to the acceleration, tends to zero. Then, theoretically the time to reach V_1 is infinite, and in practice we consider that the speed has been stabilized when it it is sufficiently near the value V_1. This phenomenon has been observed in Chapter 6 (also see Exercise 9-11). On the other hand, with the trajectory 2, we start with the initial speed $V_0 > V_1$ and hence $T < D$. The aircraft decelerates from V_0 to V_1, also in infinite time.

For the same thrust setting, if we use a high load factor for turning such that $n > TE_{max}/W$, Eq. (9.62) has no real roots. There are no stabilizing speeds, and we are constantly in the region $T < D$ with the selected high constant load factor, as shown in trajectory 3. The aircraft decelerates from the initial speed V_0 to the stall speed V_3 in a finite time. At V_3, we can no longer maintain the same high load factor. To maintain constant speed at $V = V_3$, we can reduce the load factor to satisfy the equation $T = D$. If we select to continue the turn at $C_L = C_{L_{max}}$, then as the speed continues to decrease since we are in the region where $T < D$, the load factor, that is the bank angle has to be constantly reduced to maintain the lift equation at $C_L = C_{L_{max}}$, until the speed V_4 is reached where $T = D$. Since V_4 is also a stabilizing speed, it is reached in infinite time (see Exercise 9-13).

9.8 Three-dimensional turn

When turning involves changes in the altitude, the discussion is more involved. Except for combat maneuvers of military aircraft, in climbing or descending turns, the pilot generally maintains a constant speed and a constant flight path angle with the thrust magnitude also held constant. In this section, we shall discuss the turn under these assumptions.

Referring back to the general equations (8.1) in Chapter 8, with $\dot{V} = 0$, $\dot{\gamma} = 0$ and $\varepsilon = 0$, and we have the simplified equations for

steady turning with variation in altitude

$$T = \frac{1}{2}\rho S V^2 C_D + W \sin\gamma \tag{9.64}$$

$$L\cos\phi = W\cos\gamma \tag{9.65}$$

$$\dot{\psi} = \frac{g}{V}\tan\phi \tag{9.66}$$

The load factor is still defined as $n = L/W$, but now, from the lift equation, Eq. (9.65), we have

$$n = \frac{\cos\gamma}{\cos\phi} \tag{9.67}$$

For the same bank angle ϕ, the load factor for climbing or desdending turns $\gamma \neq 0$, is smaller than in horizontal turns. For a flight path angle less than 20°, the difference is small.

We notice that, in terms of the load factor, the lift equation is the same as Eq. (9.1) with of course, as has been mentioned in Eq. (9.67), a smaller load factor for the same bank angle. Hence, the discussion of the lift equation is exactly the same as detailed in Section 9.2. We have the same conclusions for the maneuvering limit and the same pertinent formulas. The only change is that when the bank angle is calculated in terms of the load factor, Eq. (9.67) should be used.

On the other hand, the thrust equation is now Eq. (9.64) with the additional term $W\sin\gamma$. In this equation, the drag coefficient C_D is obtained from the drag polar with the lift coefficient C_L evaluated from the lift equation (9.1). As has been explained in Chapter 7 on climb performance, when an altitude change is involved, the discussion is most convenient in terms of power. Here, we shall restrict the analysis to the case of a jet powered aircraft with constant thrust. By multiplying Eq. (9.64) by the speed V to express it in terms of power, we have

$$P = TV = \frac{1}{2}\rho S V^3 C_D + WV\sin\gamma \tag{9.68}$$

In this equation

$$P_a = TV \tag{9.69}$$

is the power available as produced by the engine thrust and

$$P_{nr} = \frac{1}{2}\rho S V^3 C_D \tag{9.70}$$

is the power required for turning at the specified load factor. Since the vertical component of the velocity is $V_z = V \sin\gamma$, it is the rate of climb or the rate of descent depending on the sign of γ being positive or negative. Then, from Eq. (9.68), we have for the rate of change in altitude

$$V_z = \frac{P_a - P_{nr}}{W} \tag{9.71}$$

and for the flight path angle

$$\sin\gamma = \frac{P_a - P_{nr}}{VW} \tag{9.72}$$

In this form, we can see that the discussion in Chapter 7 on climb performance can be carried over for a climbing turn or a descending turn. It suffices to replace in the relevant formulas in Chapter 7 the weight W by the apparent weight nW to obtain the corresponding results for the case of turning with a load factor n.

For example, with a parabolic drag polar, and with excess power, the rate of climb is

$$V_z = \frac{1}{W}\left(TV - \frac{1}{2}\rho S C_{D_0} V^3 - \frac{2Kn^2W^2}{\rho SV}\right) \tag{9.73}$$

For maximum rate of climb, we have $dV_z/dV = 0$. This leads to the equation

$$\frac{3\rho S C_{D_0}}{W} V^4 - 2\frac{T}{W} V^2 - \frac{4Kn^2W}{\rho S} = 0 \tag{9.74}$$

The optimum speed for climb with maximum rate of climb is

$$V_{opt} = \frac{1}{\sqrt{3\rho S C_{D_0}}}\left[T + \sqrt{T^2 + \frac{3n^2W^2}{E_{max}^2}}\right]^{1/2} \tag{9.75}$$

If the thrust is maintained constant during the turning climb, the optimum speed increases as the density decreases during the climb, but the corresponding equivalent speed is constant. This is something of a contradiction to the assumption that $\dot{V} = 0$. But turning is generally of short duration and the assumption is valid.

The turning rate is given by Eq. (9.66) which can be calculated for any selected bank angle and speed.

We shall refer to Fig. 9.10 to obtain a geometric derivation of the turning radius. For a constant flight path angle γ, and speed V, the climbing or descending turn consists of a circular motion in the horizontal plane with constant radius R and constant speed $V\cos\gamma$, and a vertical translation with constant speed $V\sin\gamma$. The resulting trajectory is a circular helix traced on a circular cylinder of radius R. This is considered as the turning radius since it limits the turn in the physical space. It can be shown that the radius of curvature of the helix is longer given by

$$r = \frac{R}{\cos^2\gamma} \tag{9.76}$$

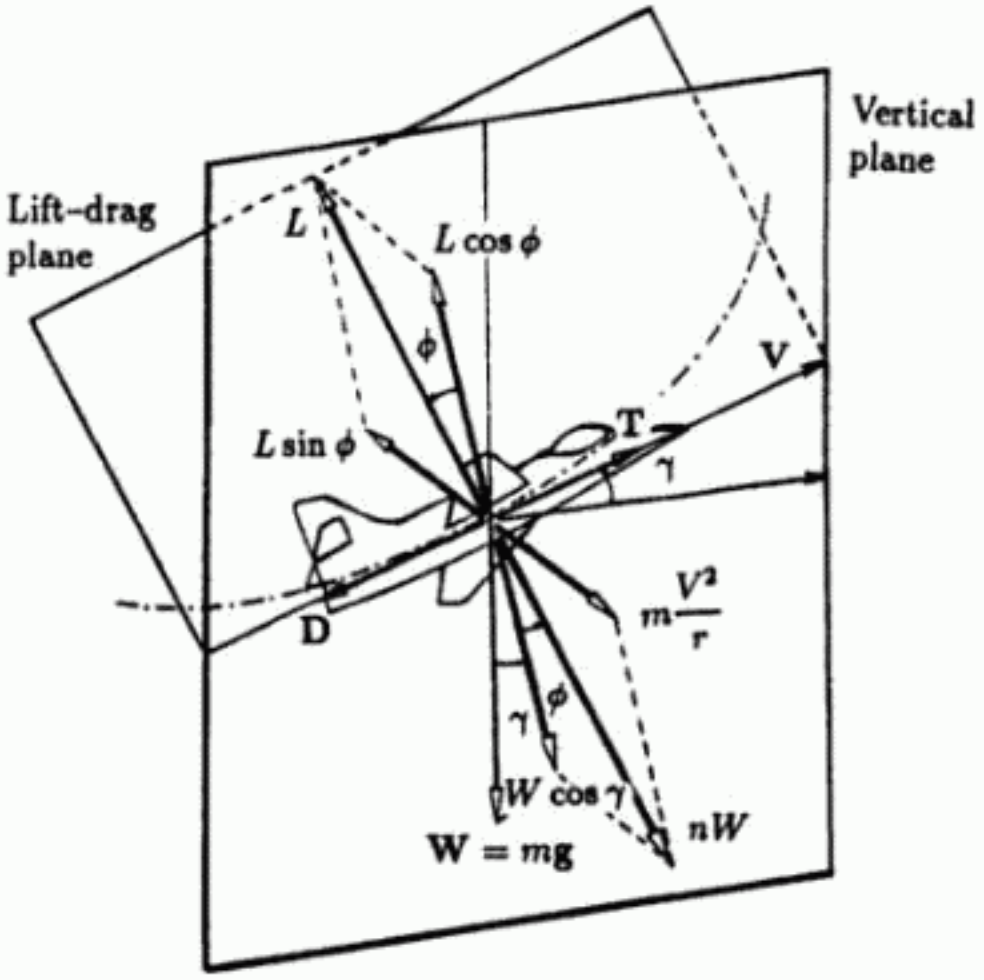

Figure 9.10: Geometry of a climbing turn.

The projection of the lift force in the horizontal plane is always

$L\sin\phi$. By writing that this force is balanced by the centrifugal force mV^2/r where r is the radius of curvature of the helical trajectory, we have

$$L\sin\phi = m\frac{V^2\cos^2\gamma}{R}$$

Using Eq. (9.65), we have the expression for the turning radius

$$R = \frac{V^2\cos\gamma}{g\tan\phi} \tag{9.77}$$

Again, we can use this formula to evaluate the turning radius for any selected bank angle, speed and climb angle. But, in terms of the load factor, we have from Eq. (9.67)

$$\sin\phi = \frac{\sqrt{n^2-\cos^2\gamma}}{n}, \qquad \tan\phi = \frac{\sqrt{n^2-\cos^2\gamma}}{\cos\gamma} \tag{9.78}$$

Hence, finally, we have

$$R = \frac{V^2\cos^2\gamma}{g\sqrt{n^2-\cos^2\gamma}} \tag{9.79}$$

If Eq. (9.1) is used, we can express the turning radius in terms of the two controls, namely the load factor n, and the lift coefficient C_L, as

$$R = \frac{2m}{\rho S C_L}\frac{n\cos^2\gamma}{\sqrt{n^2-\cos^2\gamma}} \tag{9.80}$$

Since γ is constant, the discussion on the minimum turning radius in terms of C_L and n can be carried out exactly in the same manner as in the case of a horizontal turn. From Eq. (9.80), it is seen that, compared to a horizontal turn, climbing or descending turns with large flight path angles can significantly reduce the turning radius. For example, for $n = 3$, and with a descent angle of $\gamma = 60°$, we have a ratio of turning radii equal to $\sqrt{2/35} = 0.239$. Similarly, by rewriting Eq. (9.66) for the turning rate in terms of the load factor and the lift coefficient, we obtain

$$\dot{\psi} = g\sqrt{\frac{\rho S}{2W}}\sqrt{C_L}\sqrt{\frac{n}{\cos^2\gamma}-\frac{1}{n}} \tag{9.81}$$

Since γ is constant, the discussion for maximum turning rate in terms of C_L and n can be carried out exactly in the same manner as in the case of the horizontal turn.

We notice that Eq. (9.81) gives the rate of change of heading ψ as measured in the horizontal plane of reference but not the rate of change of direction of the velocity vector. If χ is the angle between the instantaneous velocity vector $\mathbf{V}$ and the initial velocity vector $\mathbf{V}_c$, we have, by definition of the radius of curvature r

$$\frac{1}{r} = \frac{d\chi}{ds} = \frac{d\chi}{dt}\frac{dt}{ds} = \frac{\dot{\chi}}{V} \tag{9.82}$$

Hence, using Eqs. (9.76) and (9.79)

$$\dot{\chi} = \frac{V}{r} = \frac{V\cos^2\gamma}{R} = \frac{g}{V}\sqrt{n^2 - \cos^2\gamma} = \dot{\psi}\cos\gamma \tag{9.83}$$

Therefore

$$\dot{\chi} = g\sqrt{\frac{\rho S}{2W}}\sqrt{C_L}\sqrt{n - \frac{\cos^2\gamma}{n}} \tag{9.84}$$

From Eqs. (9.81) and (9.84), we can see that, compared to a horizontal turn, a large flight path angle improves significantly the turning rate of the heading but not the turning rate of the velocity vector itself. As a specific example, for $n = 3$ and $\gamma = 60°$, the ratio in $\dot{\psi}$ is $\sqrt{35/8} = 2.09$ while the ratio in $\dot{\chi}$ is only $\sqrt{35/32} = 1.05$. For fighter aircraft in combat, it is the change in the velocity vector that is important.

9.9 Turning in a vertical plane

Turning in a vertical plane involves zero bank angle, $\phi = 0$, and varying flight path angle, $\dot{\gamma} \neq 0$. If the horizontal distance is free from consideration, we consider the variations in the altitude, speed and flight path angle.

$$\frac{dz}{dt} = V\sin\gamma \tag{9.85}$$

$$m\frac{dV}{dt} = T - D - mg\sin\gamma \tag{9.86}$$

$$mV\frac{d\gamma}{dt} = L - mg\cos\gamma \tag{9.87}$$

By introducing the load factor $n = L/W$, we put the last equation in the form

$$\dot{\gamma} = \frac{g}{V}(n - \cos\gamma) \tag{9.88}$$

Just as in Chapter 7 for climb performance, we use the energy height which is proportional to the total energy of the dynamical system

$$H = z + \frac{V^2}{2g} \tag{9.89}$$

Its variation is then

$$\dot{H} = \frac{(T - D)V}{W} \tag{9.90}$$

These are the equations of interest to analyze turning in a vertical plane.

The maneuvers of special importance for fighter aircraft are the *loop*, the *Immelmann*, the *half loop* and the *split-S*, as shown in Fig. 9.11. In a loop, starting with $\gamma_0 = 0$, the maneuver consists of rotating the velocity vector by 360 degrees in a vertical plane. An *Immelmann* is a half-loop, followed by a half roll. It has the net effect of changing the heading by 180 degrees while gaining in altitude. On the other hand, if starting from level flight we perform a half roll to invert the aircraft, then complete the maneuver as for the second half of a loop, we achieve the split-S maneuver. It has the net effect of changing the heading by 180 degrees while loosing altitude.

We consider the case of the half loop which, mathematically, is equivalent to the *Immelmann*. In aerobatic maneuvers the fastest turn is of prime consideration. For this case, the initial value of γ is $\gamma_0 = 0$, while its final value is $\gamma_f = \pi$. During the maneuver, γ increases continuously, $\dot{\gamma} > 0$, and if the variation of H is not of prime importance, for the fastest maneuver, we are led to maximizing, at each instant, the turning rate $\dot{\gamma}$.

From the definition of the load factor

$$n = \frac{\rho S C_L V^2}{2W} \tag{9.91}$$

By obtaining the speed from this equation, and on substituting into Eq. (9.88), we have the turning rate in the vertical plane

$$\dot{\gamma} = g\sqrt{\frac{\rho S}{2W}}\sqrt{C_L}\left(\sqrt{n} - \frac{\cos\gamma}{\sqrt{n}}\right) \tag{9.92}$$

This equation is very similar to Eq. (9.4). Hence, the discussion of the maximum for $\dot{\gamma}$ is similar to the discussion of the maximum for $\dot{\psi}$.

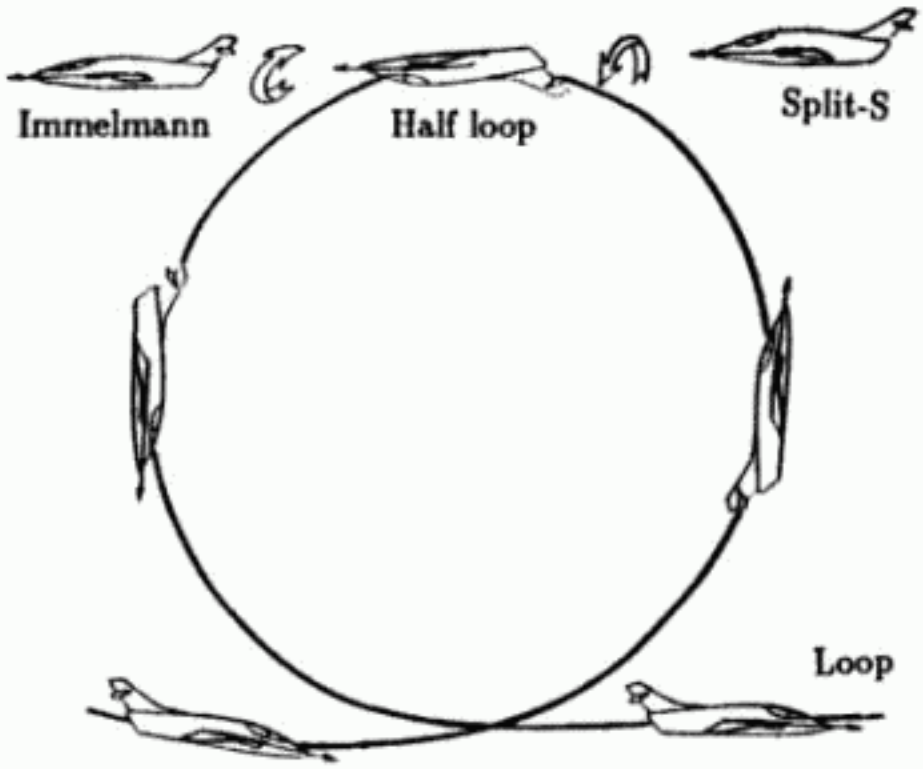

Figure 9.11: Aerobatic maneuvers in a vertical plane.

First, we observe that low wing loading, W/S, favors fast turning. Also, turning is faster for higher values of ρ, that is at low altitude.

The function $\dot{\gamma}$, as given in Eq. (9.92) is to be maximized with respect to C_L and n, considered as two controls.

Equation (9.91), expressed in terms of Mach number is identical to Eq. (9.14). This leads to the same flight envelope which is the plot of the equation, $n = M^2 C_{L_{max}}/\omega$, as shown in Fig. 9.4. The fact to notice here is that, with $\omega = 2W/kpS$, ω increases as the altitude increases. Therefore, during the maneuver, the boundary curve in this figure keeps becoming lower and lower.

As with the case of turning in the horizontal plane, we distinguish the turn at low altitude and the turn at high altitude.

At low altitude, the physiological/structural limit is enforced. The same discussion, as has been used in the case of the horizontal turn, leads to the selection of $n = n_s$, and $C_L = C_{L_{max}}$, where $C_{L_{max}}$ is evaluated at the corner Mach number, $M = M_c$. The maximum turning rate is

$$\dot{\gamma}_{max} = \frac{g}{a}\frac{n_s - \cos\gamma}{M_c} \tag{9.93}$$

The difference with the analogue $\dot{\psi}_{max}$ as given in Eq. (9.30) with $M = M_c$ is that $\dot{\gamma}_{max}$ is not constant. From Eq. (9.93) while the factor in the numerator increases from $n_s - 1$ to $n_s + 1$, in the denominator the term $aM_c = V_c$, which is the corner speed, also increases according to the relation

$$V_c = \sqrt{\frac{2n_sW}{\rho S C_{L_{max}}(M_c)}} \tag{9.94}$$

The reason that V_c increases is that the density ρ decreases during the half loop and also $C_{L_{max}}$ decreases as the corner Mach number increases. But in general, in Eq. (9.93) we have a faster increase in the numerator and as a consequence the turning rate increases (see Exercise 9-14). The thrust control is to be modulated to provide, at each instant, the necessary corner Mach number.

At high altitude the constraint $n \leq n_s$ is no longer enforced and we consider Eq. (9.88) in the form

$$\dot{\gamma} = \frac{g}{a}\frac{n - \cos\gamma}{M} \tag{9.95}$$

The operating point (M, n) is to be selected in the domain of flight in Fig. 9.3 to maximize the function $\dot{\gamma}$. At each Mach number, $\dot{\gamma}$ is maximized by using the maximum possible value for n. Hence the point is on the turning flight envelope. At each altitude, and flight path angle, with n as given by Eq. (9.16), the maximization of $\dot{\gamma}$ with respect to M, yields

$$F(M) = (C_{L_{max}})_M + 1 + \frac{\cos\gamma}{n} = 0 \tag{9.96}$$

On the other hand, the Mach number M_0 that gives the maximum load factor is obtained from (see Exercise 9-7)

$$(C_{L_{max}})_M + 2 = 0 \tag{9.97}$$

Concerning the root $M = M_{opt}$ of the equation $F(M) = 0$, we notice that at low Mach number since $C_{L_{max}}$ is nearly constant and $\cos\gamma/n < 1$, we have $F(M) > 0$. On the other hand at $M = M_0$, $(C_{L_{max}})_M = -2$, we have

$$F(M_0) = -1 + \frac{\cos\gamma}{n} < 0$$

Hence, we conclude that the optimum Mach number for the fastest turn is less than the optimum Mach number for the maximum load factor.

Exercises

9-1. For a high subsonic transport aircraft, we have the following data for the function $C_{L_{max}}(M)$.

M	0.1	0.2	0.3	0.4	0.5	0.6	0.7	0.8	0.9
$C_{L_{max}}$	1.33	1.33	1.31	1.22	1.08	0.99	0.96	0.90	0.68

(a) Plot the function $n\omega = M^2 C_{L_{max}}$ and find graphically the value $M = M_0$ for the maximum of this function.

(b) Evaluate graphically the maximum of this function. It appears that M_0 is near the value $M = 0.8$. Assume that in the vicinity of this value

$$C_{L_{max}} = c_1 M + c_2 M^2 + c_3 M^3$$

Use the points $M = 0.7$, 0.8 and 0.9 to evaluate the constants c_i. Then iterate to find an accurate value for M_0 and the corresponding maximum value of $M^2 C_{L_{max}}$.

9-2. Use the numerical results of Exercise 9-1, and consider the case where

$$W/S = 125\ \text{lb/ft}^2, \quad k = 1.4, \quad p_0 = 2116\ \text{lb/ft}^2$$

(a) Calculate $\omega_0 = 2W/kp_0S$. Then, take $n = 1$ and evaluate the pressure ratio p/p_0 at the aerodynamic ceiling. From the tables of the standard atmosphere, evaluate the altitude of the ceiling.

(b) Calculate n_{max} at sea level.

(c) Take the value $n_s = 2$ for the structural limit. Calculate the maximum altitude for possible turning at this load factor.

9-3. Let subscript 1 denote the condition for rectilinear flight and subscript 2 the condition for horizontal turning flight at the load factor n.

(a) For the same speed, show that

$$\frac{T_2}{T_1} = \frac{C_{D_2}}{C_{D_1}}$$

$$\text{and} \qquad n = \frac{C_{L_2}}{C_{L_1}}$$

Hence, using a parabolic drag polar, as given in Eq. (9.9), show that

$$\frac{T_2}{T_1} = \frac{1 + n^2(C_{L_1}/C_L^*)^2}{1 + (C_{L_1}/C_L^*)^2}$$

where $C_L^* = \sqrt{C_{D_0}/K}$ is the lift coefficient corresponding to maximum lift-to-drag ratio.

(b) Plot the function T_2/T_1 versus C_{L_1}/C_L^* for several values of $n = 1, 2, 3, 4$ and observe that the function increases as C_{L_1}/C_L^* increases for $n > 1$. Hence, conclude that for any $n > 1$, a higher ratio T_2/T_1 corresponds to a higher value of C_{L_1} for initial rectilinear flight. Explain this analytically by showing that the derivative of T_2/T_1 with respect to $(C_{L_1}/C_L^*)^2$ is positive.

9-4. When C_{D_0} and K are independent of Mach number, by putting $T_{nr}/W = y$ and using subscript 1 for the case of rectilinear flight and subscript 2 for the case of turning flight with load factor n, show that we have the functions

$$y_1 = AM_1^2 + \frac{B}{M_1^2}, \qquad y_2 = AM_2^2 + \frac{n^2 B}{M_2^2}$$

where A and B are two constants. Then, show that these functions can be deduced from one another by the transformation

$$M_2 = \sqrt{n} M_1, \qquad y_2 = n y_1$$

9-5. Equation (9.25) is a quick evaluation of the maneuvering margin due to the limitation of the maximum thrust. When the influence of Mach number on the drag polar is considered, as assumed in Eq. (9.9),

n_T is obtained by setting $n = n_T$, $T_{max} = (T_{nr})_{min}$ in Eq. (9.29). Then, show that

$$\frac{T_{max}}{W} = \frac{n_T(2 + C^*_{L_M})}{E_{max}\sqrt{(2 + C_{D_{0M}})(2 - K_M)}}$$

$$\frac{2W}{kpS} = \frac{M^2}{n_T}\sqrt{\frac{C_{D_0}}{K}}\sqrt{\frac{2 + C_{D_{0M}}}{2 - K_M}}$$

Hence, we first obtain the Mach number from

$$\frac{T_{max}}{kpS} = M^2 C_{D_0}\frac{2 + C^*_{L_M}}{2 - K_M}$$

and then deduce n_T.

9-6. Consider the Eqs. (9.31) and (9.32)

$$n = \frac{1}{\omega}C_{L_{max}}(M)M^2 = f(M)$$

$$\frac{g}{a\dot{\psi}} = \frac{M}{\sqrt{f^2(M) - 1}}$$

Assume that the function $C_{L_{max}}(M)$ is known. Show that the Mach number for maximum turning rate is obtained from the equation

$$(C_{L_{max}})_M + \frac{n^2 + 1}{n^2} = 0$$

where subscript M denotes the logarithmic derivative.

9-7. Consider Eqs. (9.31) and (9.34)

$$n = \frac{1}{\omega}C_{L_{max}}(M)M^2 = f(M)$$

$$\frac{Rg}{a^2} = \frac{M^2}{\sqrt{f^2(M) - 1}}$$

(a) Again assume that the function $C_{L_{max}}(M)$ is known by an appropriate modeling. Show that, at high altitude, the Mach number for minimum turning radius is obtained from the equation

$$(C_{L_{max}})_M + \frac{2}{n^2} = 0$$

where subscript M denotes the logarithmic derivative.

(b) Show that the maximum of the function f, that is of the load factor n, occurs at a Mach number M_0 given by the equation

$$(C_{L_{max}})_M + 2 = 0$$

9-8. In summarizing the results in Exercises 9-6 and 9-7, let M_0, M_1 and M_2 be respectively the Mach numbers for maximum load factor, maximum turning rate and minimum turning radius. Define the functions

$$n = \frac{1}{\omega} C_{L_{max}}(M) M^2$$

$$C = (C_{L_{max}})_M = \frac{M}{C_{L_{max}}} \frac{dC_{L_{max}}}{dM}$$

Furthermore, we have obtained the optimum relations

$$F_0(M) = C + 2 = 0, \quad \text{for maximum } n,$$

$$F_1(M) = C + \frac{n^2 + 1}{n^2} = 0, \quad \text{for maximum } \dot{\psi},$$

$$F_2(M) = C + \frac{2}{n^2} = 0, \quad \text{for minimum } R.$$

It is proposed to show that

$$M_0 > M_1 > M_2$$

and

$$n_0 > n_1 > n_2.$$

(a) Concerning the function n, since it is a maximum at $M = M_0$, before this value, it is increasing and hence $n_i > n_j$ implies that $M_i > M_j$ and vice versa.

(b) If we evaluate the function $F_1(M)$ at low Mach number, where $C_{L_{max}}$ is nearly constant and hence $C \approx 0$, we obtain $F_1 > 0$. On the other hand, show that at $M = M_0$ where $C(M_0) = -2$, $n = n_0 > 1$, we have $F_1(M_0) < 0$. Then conclude that the root M_1 of the equation $F_1(M) = 0$ occurs before the value M_0.

(c) Using the same arguments, show that the root M_2 of the equation $F_2(M) = 0$ occurs before the value M_0.

(d) Finally, by using $M = M_1$ in the function $F_2(M)$, show that

$$F_2(M_1) = \frac{1 - n_1^2}{n_1^2} < 0.$$

Therefore, the root M_2 of the equation $F_2(M) = 0$ occurs before the value M_1.

9-9. From the solutions (9.48), (9.50) and (9.57) for the minimum turn radius, the maximum bank angle and the maximum turning rate for the case of a prescribed thrust setting and without violation of the constraint $C_{L_{max}}$ for a parabolic drag polar, derive the following relation

$$R_{min}\dot{\psi}_{max}^2 = 2g\tan(\phi_{max}/2)$$

which is completely independent of the aerodynamic and engine characteristics of the aircraft. Furthermore it is independent of the thrust level used, provided that $T > T_{min}$.

9-10. Show that we have in general

$$R\dot{\psi}^2 = g\tan\phi$$

Hence, deduce that for turning at low altitude, subject to the structural limit n_s, the optimum performances are related by

$$R_{min}\dot{\psi}_{max}^2 = g\tan\phi_s$$

where ϕ_s is the maximum bank angle corresponding to the load factor n_s.

9-11. If Eq. (9.62) has the real roots V_1 and V_2, as given by Eq. (9.63) with $V_1 > V_2$, we can write the differential equation (9.61) as

$$\frac{\rho S C_{D_0}}{m}dt = -\frac{2V^2 dV}{(V^2 - V_1^2)(V^2 - V_2^2)}$$

Let

$$-\frac{2V^2}{(V^2 - V_1^2)(V^2 - V_2^2)} = \frac{A}{V^2 - V_1^2} + \frac{B}{V^2 - V_2^2}$$

Evaluate the constants A and B in terms of V_1 and V_2 and perform the integration from $t = 0$, $V = V_0$ to obtain the time to turn

$$t = \frac{m}{\rho S C_{D_0}(V_1^2 - V_2^2)}\left[V_1 \operatorname{Log}\frac{(V_1 + V)(V_1 - V_0)}{(V_1 - V)(V_1 + V_0)} + V_2 \operatorname{Log}\frac{(V - V_2)(V_0 + V_2)}{(V + V_2)(V_0 - V_2)}\right]$$

This formula is valid for both the accelerating turn from V_0 to V_1, and decelerating turn from V_0 to V_1. Notice that when $V = V_1$ the time is infinite.

9-12. When $n > E_{max}(T/W)$, Eq. (9.62) has no real roots. We have the trajectory 3 in Fig. 9.9. To evaluate the time for a decelerating turn from V_0 to V_3, let

$$k_1^2 = \frac{1}{2\rho S C_{D_0}}\left(\frac{nW}{E_{max}} + T\right)$$
$$k_2^2 = \frac{1}{2\rho S C_{D_0}}\left(\frac{nW}{E_{max}} - T\right)$$

where the constants k_1 and k_2 have the dimensions of speed.

(a) Show that Eq. (9.62) can be rewitten as

$$V^4 - 2(k_1^2 - k_2^2)V^2 + (k_1^2 + k_2^2)^2 = [(V + k_1)^2 + k_2^2][(V - k_1)^2 + k_2^2] = 0$$

With this relation, show that the differential equation (9.61) has the form

$$\frac{\rho S C_{D_0}}{m} dt = \left[\frac{V}{(V + k_1)^2 + k_2^2} - \frac{V}{(V - k_1)^2 + k_2^2}\right]\frac{dV}{2k_1}$$

(b) Integrate the equation from the initial speed V_0 to obtain the solution

$$t = \frac{m}{4\rho S C_{D_0}}\left\{\frac{1}{k_1}\,\mathrm{Log}\left[\frac{(V_0 - k_1)^2 + k_2^2}{(V_0 + k_1)^2 + k_2^2}\,\frac{(V + k_1)^2 + k_2^2}{(V - k_1)^2 + k_2^2}\right]\right.$$
$$\left. + \frac{2}{k_2}\tan^{-1}\left[\frac{2k_2(V_0 - V)(V_0 V + k_1^2 + k_2^2)}{[V_0^2 - (k_1^2 + k_2^2)]V^2 + 4k_2^2 V_0 V - (k_1^2 + k_2^2)[V_0^2 - (k_1^2 + k_2^2)]}\right]\right\}$$

(c) Evaluate the final stall speed V_3 in terms of n and $C_{L_{max}}$ and conclude that the time to reach V_3 is finite.

9-13. It is intended to maintain the turn in the horizontal plane at $C_L = C_{L_{max}}$, but with constant thrust such that $T < D$. Hence, from Fig. 9.9, the turn is decelerating from a certain speed V_3 to the stabilizing speed V_4 when $T = D$.

(a) Using the lift equation (9.1) at $C_L = C_{L_{max}}$, show that the equation for the variation of the speed is

$$\frac{\rho S C_{D_{max}}}{2m} dt = -\frac{dV}{V^2 - k_3^2}$$

where

$$C_{D_{max}} = C_{D_0} + KC_{L_{max}}^2$$

and

$$k_3^2 = \frac{2T}{\rho S C_{D_{max}}} = V_4^2$$

(b) By integrating the equation, show that the time to turn is

$$t = \frac{m}{\rho S V_4 C_{D_{max}}} \operatorname{Log} \frac{(V_3 - V_4)(V + V_4)}{(V_3 + V_4)(V - V_4)}$$

Notice that the time to stabilize at V_4 is infinite.

(c) Show that the speed decreases as a function of the time according to

$$\frac{V}{V_4} = \frac{be^{at} + 1}{be^{at} - 1}$$

where

$$a = \frac{\rho S V_4 C_{D_{max}}}{m}$$

$$b = \frac{V_3 + V_4}{V_3 - V_4}$$

Then, again $V \to V_4$ when $t \to \infty$.

9-14. From Eqs. (9.93) and (9.94), by neglecting the variation of $C_{L_{max}}(M)$ for low speed turning, show that the ratio of the turning rate at the final point and the initial point of an *Immelmann* is

$$\frac{\dot{\gamma}_{max}(f)}{\dot{\gamma}_{max}(0)} = \sqrt{\sigma} \frac{n_s + 1}{n_s - 1}$$

where $\sigma = \rho_f / \rho_0$ is the density ratio between the final altitute and the initial altitude.

By using an exponential atmosphere, show that when the final rate is higher than the initial rate, we have

$$\beta(z_f - z_0) \leq 2 \operatorname{Log} \frac{n_s + 1}{n_s - 1}$$

In general, since $1/\beta \approx 23{,}500$ ft, this condition is satisfied by a small difference in the altitude and a moderate load factor.

9-15. Consider Eq. (9.73) for the rate of climb in turning in the case where C_{D_0} and K are functions of Mach number. Use the dimensionless quantities

$$\omega = \frac{2W}{kpS}, \qquad K_T = \frac{2T}{kpS}$$

where ω is the dimensionless wing loading and K_T is the dimensionless thrust. Show that we have

$$\omega \frac{V_z}{a} = K_T M - C_{D_0} M^3 - n^2 K \frac{\omega^2}{M}$$

At each current altitude, show that the optimum Mach number for the maximum rate of climb in turning is obtained by solving the equation

$$C_{D_0}(3 + C_{D_{0M}})M^4 - K_T M^2 - n^2 K(1 - K_M)\omega^2 = 0$$

Show that when the effect of Mach number is neglected, this equation reduces to Eq. (9.74).

With the optimum Mach number evaluated, show that the maximum rate of climb is

$$\left(\frac{V_z}{a}\right)_{max} = M\left[\frac{M^2}{\omega} C_{D_0}(2 + C_{D_{0M}}) - \frac{n^2 \omega K}{M^2}(2 - K_M)\right]$$

Deduce that at the propulsive ceiling where $n = 1$, $V_z = 0$, $T = T_{max}$, we have

$$\omega = M^2 C_L^* \sqrt{\frac{2 + C_{D_{0M}}}{2 - K_M}}$$

$$\frac{T_{max}}{W} = \frac{2 + C_{L_M}^*}{E_{max}\sqrt{(2 + C_{D_{0M}})(2 - K_M)}}$$

where as usual $C_L^* = \sqrt{C_{D_0}/K}$.

10

Take-off and landing performance

10.1 Introduction

With the development of heavy military and commercial transport aircraft and the coming of age of the supersonic transport aircraft, the available take-off field lengths in various large metropolitan areas around the world become one of the key design requirements.

Any flight mission necessarily starts with a take-off from an airfield or from the deck of an aircraft carrier. Likewise, a successful flight is completed with a smooth landing. Take-off is an accelerated maneuver while landing is a decelerated maneuver. They both consist of two phases: a ground run phase and an airborne phase. In the following, we shall start with a description of the take-off and then analyze the forces involved in the equations of motion for each phase in order to obtain the pertinent solutions for the evaluation of its performance. The same plan is followed for the evaluation of the landing performance.

10.2 Description of a take-off

The take-off of a conventional aircraft is here defined as a series of maneuvers from the moment of brake release when the aircraft starts to accelerate along a horizontal, or nearly horizontal runway until, in a clean configuration with all the landing gear and flaps retracted, a steady climb to cruising altitude is established. The ground run phase starts at the initial time, $t = 0$, and ends at the time $t = t_g$ when the

aerodynamic lift becomes equal to the weight and the aircraft becomes airborne. During this phase, the main landing gear is in contact with the ground and the velocity of the aircraft is parallel to the runway. During the ground run, the airspeed accelerates from the initial speed V_0 to the lift-off speed V_{LOF}. If the air is calm, the initial speed is zero. With a head wind with speed V_W, the starting airspeed is $V_0 = V_W$. The ground run distance x_g is the distance from rest to the point of lift-off. We shall use the thrust line as the reference line to measure the angle-of-attack. At the beginning of the ground run, the angle-of-attack remains fixed being the one which is defined by the attitude of the aircraft. This attitude is dictated by the geometry of the landing gear. However, when, with a sufficient speed, the control surfaces become effective for directional and attitude control, the pilot may rotate the aircraft to obtain an angle-of-attack most favorable for the ground run. Therefore, for all practical purposes, to evaluate the ground run distance, we can resolve it into two parts and in each part use a constant angle-of-attack for the integration of the equations of motion.

For most aircraft, we have a tricycle landing gear which consists of two main groups of wheels and a nose wheel or a tail wheel (Fig. 10.1). With a nose wheel, during the initial portion of the ground run, the angle-of-attack is nearly zero and both the drag and the lift are minimized. At a sufficient speed, it is helpful to lift up the nose wheel for a smooth run and at the same time to increase the angle-of-attack to achieve an optimum value. As will be discussed below, this is designed to provide a significant lift force to reduce the reaction force of the runway and hence minimize the friction force to provide higher acceleration.

With a tail wheel, during the initial portion of the ground run, the angle-of-attack is high and both the drag and the lift are maximized. At a speed when the control surfaces are effective, a rotation of the aircraft downward to release the contact of the tail wheel with the runway for a smooth run and at the same time to decrease the angle-of-attack in order to reduce the drag for higher acceleration is dictated.

Theoretically, the aircraft can be airborne when the airspeed reaches the stall speed, $V = V_{stall}$. At that point, a rotation of the aircraft to bring the angle-of-attack to the value α_{max}, with the resulting $C_L = C_{L_{max}}$ would satisfy the lift equation for pure atmospheric flight. But, for safety reasons, civilian and military specifications require that the

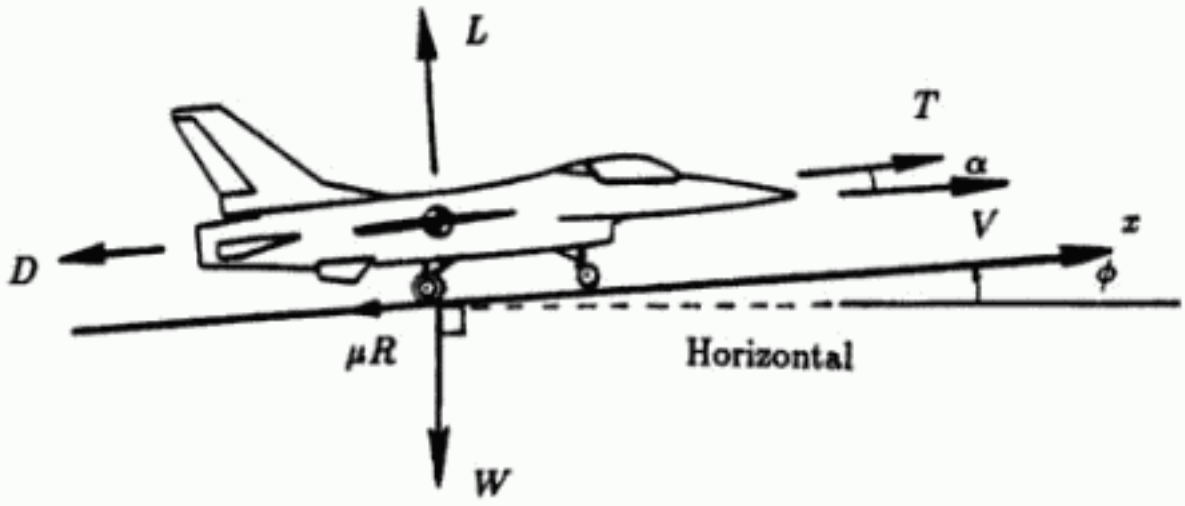

Figure 10.1: Forces acting on the aircraft during the ground phase.

lift-off speed is higher. Usually, it is set as

$$V_{LOF} = k_1 V_{stall} \tag{10.1}$$

with the value $k_1 = 1.10$. This coefficient k_1 may vary with the type of aircraft.

After lift-off, during the airborne phase, the trajectory consists of three subarcs, each of these adds a horizontal distance to the total take-off length (Fig. 10.2). The first subarc is a rotation to deflect the velocity from a nearly horizontal direction to a few degrees upward. The duration of this rotation is about 1–2 seconds. After this initial rotation is the transition period at the end of which the aicraft is required to clear a hypothetical obstacle. This obstacle height is 50 feet for military aircraft and 35 feet for civilian aircraft. The speed at the clearance of the obstacle is usually specified as

$$V_2 = k_2 V_{stall} \tag{10.2}$$

with the value $k_2 = 1.20$. We should mention that the notation V_1

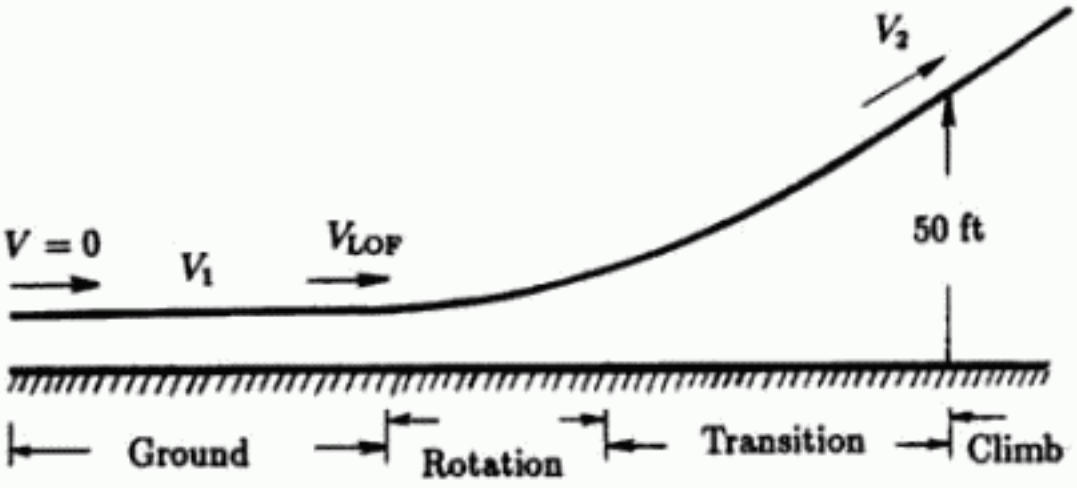

Figure 10.2: Different phases of a take-off.

is commonly reserved to denote the so-called decision speed which is defined as the speed during the ground run, beyond which for multi-engine aircraft the take-off should be continued even with the failure of one engine. The take-off field length is defined as the total distance from rest to the point of clearance of the obstacle. The final portion of the airborne phase is the climb out which covers the period from the time of the clearance of the obstacle to the time when the aircraft has reached approximately 500 feet altitude with the throttle adjusted from take-off power to climb power. With the flaps retracted, the take-off phase is completed at this altitude.

10.3 Equations of motion

For the ground run phase, with x being the distance along the runway, V_g the ground speed, a the net acceleration and t the time, we

have the equations

$$\frac{dx}{dt} = V_g \tag{10.3}$$

and

$$\frac{dV_g}{dt} = a \tag{10.4}$$

For a head wind with speed V_W, the ground speed is

$$V_g = V - V_W \tag{10.5}$$

where V is the usual airspeed. The performance characteristics of interest are the ground run distance x_g and the time to lift-off t_g. We shall obtain the solutions for the case of calm air, $V_W = 0$ and later on modify them to include the case with wind speed.

By eliminating time between the Eqs. (10.3) and (10.4) and then integrating the resulting equation with respect to V, we obtain for the ground run distance

$$x_g = \int_0^{V_{LOF}} \frac{V}{a} dV \tag{10.6}$$

To perform this quadrature analytically we shall make explicit the expression for the acceleration by considering the total force applied as depicted in Fig. 10.1. We have

$$F = ma = T\cos\alpha - D - \mu R - W\sin\phi \tag{10.7}$$

where as usual, T is thrust, D the drag and α the angle-of-attack which is here defined as the angle between the thrust line and the velccity. For generality, we assume that the runway is making a small angle ϕ with respect to the horizontal with $\phi > 0$ for a positive slope. Of course, m is the mass and $W = mg$ is the weight which we assume as constant during the relatively short duration for the take-off. A new force which is added here for the ground phase is the rolling friction force μR which is proportional to the runway reaction force R. The dimensionless coefficient μ is called the rolling friction coefficient. It depends on many factors such as the condition of the runway, the tire material, tread, pressure and loading, the condition of the wheel bearings and to some extends, the speed. To ease the integration, μ is taken as constant during the ground run with some average value. Typical values for various runways are:

Runway	μ
Concrete, asphalt	0.02
Hard turf	0.04
Average field, short grass	0.05
Average field, long grass	0.10
Soft field, sand	0.10–0.30

The reaction force of the runway exists when there is a normal force applied to the runway. Hence, we consider

$$R = W\cos\phi - L - T\sin\alpha \geq 0 \tag{10.8}$$

where L is the lift. Using the small angle approximation for the runway slope and this expression for R in Eq. (10.7) we have the net accelerating force

$$F = T(\cos\alpha + \mu\sin\alpha) - \frac{1}{2}\rho SV^2(C_D - \mu C_L) - (\mu + \phi)W \tag{10.9}$$

In this equation, the standard expressions for the lift and the drag have been used.

During the ground run, the pilot controls the direction, to be always along the axis of the runway, the thrust throttle setting and the angle-of-attack. To obtain a short ground run distance, the accelerating force must be maximized and the thrust throttle setting is at its maximum allowable value. In general, at fixed throttle setting, T decreases when the speed increases. Propeller thrust shows a most marked decrease while the thrust of a turbojet engine is almost constant. The turbofan and the turboprop engines represent an intermediate case. In any case, T can be modeled as a quadratic function of the speed V.

At the beginning of the ground run, at low speed when the elevator control is not effective, it is not possible to change the attitude of the aircraft. Then, the angle-of-attack is constant. In Eq. (10.9), the last term on the right-hand side is constant. At a sufficiently high speed, when it is possible to use elevator control to change the angle-of-attack, while the first term can be increased with an appropriate selection of the angle-of-attack, the change in the second term is more significant (see Exercises 10-2 and 10-3). Then, it is more advantageous to use an angle-of-attack which minimizes $(C_D - \mu C_L)$. This leads us to selecting a new angle-of-attack for the second portion of the ground run. This

explains the standard technique for take-off as described in Section 10.2.

With the assumption that the ground run can be appropriately divided into two or even three segments and in each segment a constant angle-of-attack is maintained for the run, then since the thrust is a function of the speed, the net acceleration is also a function of the speed. The solution for each segment of the ground run is obtained by quadrature. We have

$$t = \int_{V_0}^{V_1} \frac{dV}{a(V)} \tag{10.10}$$

and

$$x = \int_{V_0}^{V_1} \frac{V\,dV}{a(V)} \tag{10.11}$$

where V_0 and V_1 are respectively the speeds at the initial time and the final time of each segment.

Based on engine data, we may model the thrust as a function of the speed in the form

$$T = T_0(1 + c_1 V + c_2 V^2) \tag{10.12}$$

where c_1 and c_2 are two constants appropriately evaluated and T_0 is the constant thrust magnitude at the initial time where $V = 0$. For accurate analysis we may also model the rolling friction coefficient as a linear or quadratic function of the speed. In the following integration we use constant values for α and μ in each segment of the ground run. Then, the net acceleration is a quadratic function of the speed

$$a(V) = A + BV + CV^2 \tag{10.13}$$

The quadratures in Eqs. (10.10) and (10.11) are usually in one of the following two cases (George, 1969):

a) $B = 0$, $C = 0$. This is when, for a quick estimate, we assume a constant acceleration for the ground run segment. This may occur with a high thrust, and also in the segment where the drag and the friction force can be neglected or used at a constant average value. We have the solutions

$$t = \frac{1}{A}(V_1 - V_0) \tag{10.14}$$

and

$$x = \frac{1}{2A}(V_1^2 - V_0^2) \tag{10.15}$$

b) $\Delta = B^2 - 4AC > 0$. This is for the general case of the quadratic expression (10.13), and the reason that we usually have $\Delta > 0$ comes from the fact that in general $AC < 0$. We have the solutions

$$t = \frac{1}{\sqrt{\Delta}} \operatorname{Log} \left[\frac{2CV_1 + B - \sqrt{\Delta}}{2CV_0 + B - \sqrt{\Delta}} \right] \left[\frac{2CV_0 + B + \sqrt{\Delta}}{2CV_1 + B + \sqrt{\Delta}} \right] \tag{10.16}$$

and

$$\begin{aligned} x = {} & \frac{1}{2C} \operatorname{Log} \left[\frac{A + BV_1 + CV_1^2}{A + BV_0 + CV_0^2} \right] \\ & - \frac{B}{2C\sqrt{\Delta}} \operatorname{Log} \left[\frac{2CV_1 + B - \sqrt{\Delta}}{2CV_0 + B - \sqrt{\Delta}} \right] \left[\frac{2CV_0 + B + \sqrt{\Delta}}{2CV_1 + B + \sqrt{\Delta}} \right] \end{aligned} \tag{10.17}$$

This integration can also be performed in terms of elementary functions in the case where $\Delta = B^2 - 4AC < 0$.

10.4 Practical solutions for the ground run

For a preliminary estimate of the ground run distance x_g and the time to lift-off t_g, it is sufficient to consider an average constant angle-of-attack for the whole duration. Furthermore, in Eq. (10.12), we can take $c_1 = 0$ and if the thrust angle-of-attack is neglected in Eq. (10.9), we shall have the net accelerating force

$$F = T_0(1 + c_2 V^2) - \frac{1}{2}\rho S(C_D - \mu C_L)V^2 - (\mu + \phi)W \tag{10.18}$$

By multiplying Eq. (10.13) by the mass m and comparing with this equation, we deduce that $B = 0$. As for the coefficients A and C, we have

$$\begin{aligned} mA &= T_0 - (\mu + \phi)W \\ mC &= c_2 T_0 - \frac{1}{2}\rho S(C_D - \mu C_L) \end{aligned} \tag{10.19}$$

Let F_0 be the initial accelerating force and F_{LOF} the accelerating force at lift-off, that is

$$\begin{aligned} F_0 &= T_0 - (\mu + \phi)W \\ F_{\text{LOF}} &= T_0 - (\mu + \phi)W + \left[c_2 T_0 - \frac{1}{2}\rho S(C_D - \mu C_L) \right] V_{\text{LOF}}^2 \end{aligned} \tag{10.20}$$

We should mention that, if at the time of lift-off the angle-of-attack is instantaneously changed to α_{LOF}, we would have $L = W$ and the coefficient of μ in F_{LOF} is zero. But this term is retained here for the calculation for the assumed case of using an average optimum angle-of-attack for the ground run. Then it is clear that

$$\begin{aligned} mA &= F_0 \\ mC &= -\frac{F_0 - F_{LOF}}{V_{LOF}^2} \end{aligned} \tag{10.21}$$

With $B = 0$, and when $F_0 > F_{LOF}$, we have $AC < 0$, and the solutions (10.16) and (10.17) apply. With the expressions (10.21) for A and C, we have by setting $V_0 = 0$ and $V_1 = V_{LOF}$ the solutions

$$t_g = \frac{WV_{LOF}}{2gF_0\sqrt{1-\eta}} \operatorname{Log} \frac{1+\sqrt{1-\eta}}{1-\sqrt{1-\eta}} \tag{10.22}$$

and

$$x_g = \frac{WV_{LOF}^2}{2gF_0(1-\eta)} \operatorname{Log} \frac{1}{\eta} \tag{10.23}$$

In these formulas, for simplicity of notation, we have defined the constant ratio of the accelerating forces

$$\eta = \frac{F_{LOF}}{F_0} \tag{10.24}$$

For the discussion of take-off performance, we put the solutions in the form (Buning, 1986)

$$x_g = \frac{WV_{LOF}^2}{2gF_0} K_1(\eta) \tag{10.25}$$

and

$$t_g = \frac{WV_{LOF}}{gF_0} K_2(\eta) \tag{10.26}$$

where K_1 and K_2 are functions of the ratio η with

$$K_1 = \frac{1}{1-\eta} \operatorname{Log} \frac{1}{\eta} \tag{10.27}$$

and

$$K_2 = \frac{1}{2\sqrt{1-\eta}} \operatorname{Log} \frac{1+\sqrt{1-\eta}}{1-\sqrt{1-\eta}} \tag{10.28}$$

We notice that, in the solution (10.25), the coefficient of K_1 is the ground run distance with a constant accelerating force F_0. Hence, the factor K_1 denotes the effect of the variation of the force as a function of the speed during the ground run. Likewise, in the solution (10.26), the coefficient of K_2 is the time to lift-off with a constant accelerating force F_0. Hence, the factor K_2 denotes the effect of the variation of the force during the ground run. These solutions were obtained from the general equations (10.16) and (10.17). The function $K_1(\eta)$, as given in Eq. (10.27), is valid for arbitrary values of η while the function $K_2(\eta)$, as given in Eq. (10.28), is restricted to the case where $\eta \leq 1$. For the case where $\eta > 1$, that is when the accelerating force is such that it is higher at the end of the run, K_2 has a different functional form. This case should not be ruled out because from the definition (10.20) of F_0 and F_{LOF}, although c_2 is generally negative, it may be small or even positive in some special cases where a boosting jet assistance is added for take-off and also for a high rolling friction coefficient, the optimum angle-of-attack for the ground run may be such that $(C_D - \mu C_L) < 0$. These cases add up to make $F_{LOF} > F_0$. Then, when $\eta > 1$, by direct integration of the equation for the time t, or simply by a transformation using complex numbers, we have the relevant expression for the function K_2 as (see Exercise 10-5)

$$K_2 = \frac{1}{\sqrt{\eta - 1}} \text{Arc tan} \sqrt{\eta - 1} \tag{10.29}$$

The main performance characteristic for take-off is the ground run distance. First, it is proportional to V_{LOF}^2. By writing that, at take-off, the lift is equal to the weight, we obtain

$$V_{LOF}^2 = \frac{2k_1^2 W}{\rho S C_{L_{max}}} \tag{10.30}$$

where as specified above, $V_{LOF} = k_1 V_{stall}$ with $k_1 = 1.10$. Therefore, the ground run distance is proportional to W^2 and inversely proportional to $\rho C_{L_{max}}$. A high value of $C_{L_{max}}$, through the use of flaps, decreases the ground run distance. A high value of the weight, which includes the weight of the fuel at take-off will increase considerably the ground run distance. For a specified take-off weight, although the dynamic pressure, that is the indicated speed for low speed, at take-off is the same, taking-off at airfields at high altitude where the actual value of

the atmospheric density is low, requires longer ground run distance. At any airfield altitude, a high temperature on the runway also decreases the value of ρ and increases the ground run distance. Finally, from Eq. (10.25), it is apparent that the value of F_0, as defined in Eq. (10.20), plays a fundamental role in take-off performance. A high thrust T_0 will decrease the ground run distance. The rolling friction coefficient μ and the positive runway slope ϕ have cumulatively the opposite effect.

By considering Eq. (10.26) for the time to lift-off we have similar conclusions.

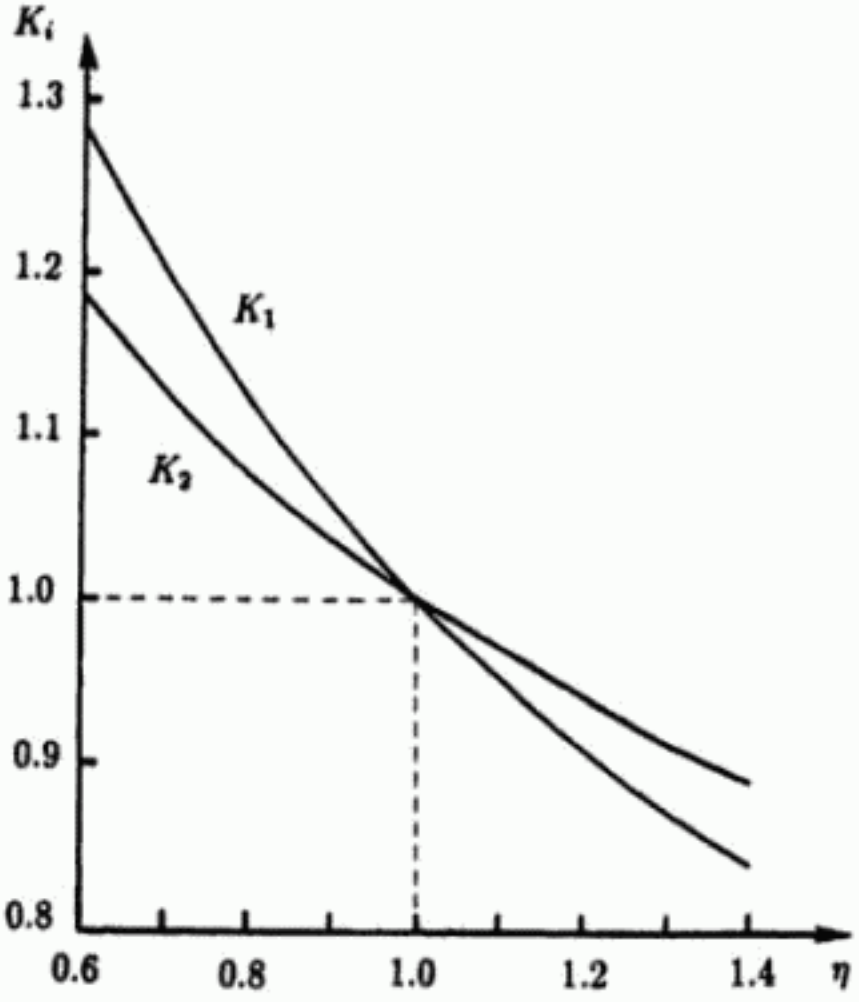

Figure 10.3: Variations of the functions K_1 and K_2 with respect to the thrust ratio $\eta = F_{LOF}/F_0$.

Concerning the influence of the parameter η, from the solutions (10.25) and (10.26), it is seen that the minima of x_g and t_g correspond

respectively to the minima of the functions $K_1(\eta)$ and $K_2(\eta)$. These functions are plotted in Fig. 10.3 in the range of interest of the ratio η of the accelerating forces. When $\eta = 1$, the functions have an indeterminate form but it can be easily shown that their common limit is unity. With respect to η, both functions are decreasing, and hence, for an optimum solution, the maximum value of η is dictated (see Exercise 10-6 and 10-7). With a prescribed value of F_0, using of course the maximum thrust T_0, we are led to maximizing F_{LOF} as defined in Eq. (10.20). The angle-of-attack selected for the ground run is the one which minimizes $(C_D - \mu C_L)$. It has been suggested in Exercises 10-2, 10-3 and 10-4 that this is also the case when the effect of the thrust angle-of-attack is included in the analysis. For a parabolic drag polar, the optimum angle-of-attack for the ground run is such that

$$C_L = \frac{\mu}{2K} \tag{10.31}$$

The corresponding value of the coefficient of the aerodynamic force in Eq. (10.20) is

$$C_D - \mu C_L = C_{D_0} - \frac{\mu^2}{4K} \tag{10.32}$$

and it can be negative for high values of the rolling friction coefficient. Therefore, if the thrust is nearly constant during the ground run, we may have $F_{LOF} > F_0$.

10.5 Ground effect and wind effect on ground run

In the proximity of the ground, with flaps extended for take-off, at any angle-of-attack, the lift coefficient is slightly higher as shown in Fig. 10.4. This is commonly known as the ground effect. With good wind tunnel data available, this effect can be included to reevaluate the lift–drag relationship for the computation of the ground run performance. The ground effect depends on the height of the wings above the ground. For wing heights of one-half the wing span or above, the ground effect can be ignored (Miller, 1976).

In practice, the runway selected for take-off is the one heading into the wind. By assuming that during the ground run the pilot maintains a straight line for the run, only the wind velocity component V_W parallel to the trajectory of the aircraft influences the ground run distance and

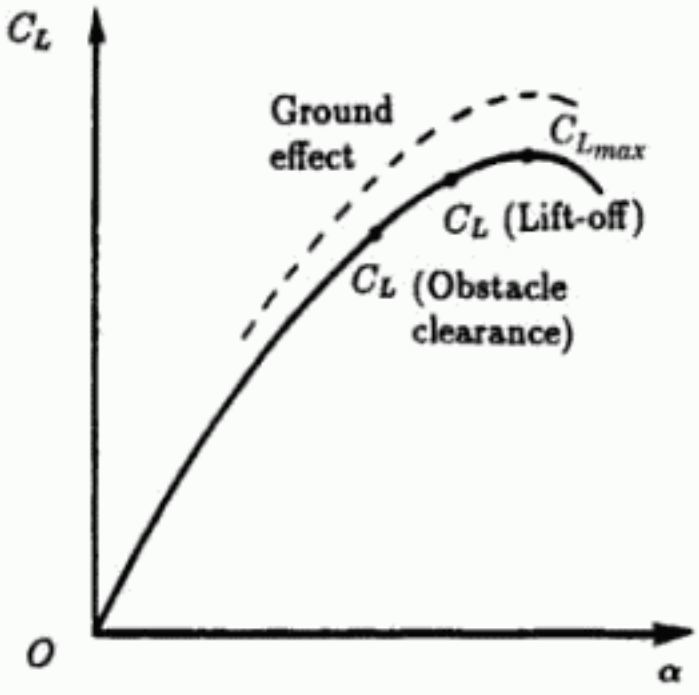

Figure 10.4: The lift curve with ground effect.

the time to lift-off. For the case of a head wind, $V_W > 0$, by using subscript W to denote the performance characteristics with the wind, we have the integrals,

$$t_W = \int_{V_W}^{V_{LOF}} \frac{d(V - V_W)}{a(V)} \tag{10.33}$$

and

$$x_W = \int_{V_W}^{V_{LOF}} \frac{(V - V_W)}{a(V)} d(V - V_W) \tag{10.34}$$

For constant wind speed, $d(V - V_W) = dV$, we first evaluate the time to lift-off with wind by an appropriate change of the limits of the integration. We have

$$t_W = t_g - \int_0^{V_W} \frac{dV}{a(V)} \tag{10.35}$$

The rule for the modification is simple. The time to lift-off with a head wind is the difference between the time without wind and the time to accelerate from $V = 0$ to $V = V_W$. The integral in this equation is

obtained from Eq. (10.26) with V_{LOF} replaced by V_W and, of course, η evaluated from Eq. (10.24) with the same substitution. If the wind speed is not too strong we can take $\eta = 1$, $K_2(\eta) = 1$ in this calculation and obtain

$$t_W = \frac{WV_{LOF}}{2gF_0}\left[\frac{1}{\sqrt{1-\eta}}\,\mathrm{Log}\,\frac{1+\sqrt{1-\eta}}{1-\sqrt{1-\eta}} - 2\frac{V_W}{V_{LOF}}\right] \tag{10.36}$$

where in this expression η is defined in Eq. (10.24). Equation (10.36) is valid for the case where $F_{LOF} < F_0$. The relevant formula when $F_{LOF} > F_0$ is

$$t_W = \frac{WV_{LOF}}{gF_0}\left[\frac{1}{\sqrt{\eta-1}}\,\mathrm{Arc\ tan}\,\sqrt{\eta-1} - \frac{V_W}{V_{LOF}}\right] \tag{10.37}$$

For the ground run distance we first expand the integral (10.34) to obtain

$$x_W = \int_{V_W}^{V_{LOF}} \frac{V\,dV}{a(V)} - V_W \int_{V_W}^{V_{LOF}} \frac{dV}{a(V)}$$

We notice that the second integral in this equation is t_W. Again, by an appropriate change of the limits of integration, we have the solution for the ground run distance with wind

$$x_W = x_g - \int_0^{V_W} \frac{V\,dV}{a(V)} - V_W t_W \tag{10.38}$$

The rule for the modification is simple. The presence of a head wind reduces the ground run distance by two amounts:

i) The length it takes to accelerate without wind from $V = 0$ to $V = V_W$.

ii) The length travelled with wind speed during the time to lift-off with wind.

The integral in Eq. (10.38) is obtained from Eq. (10.25) with V_{LOF} replaced by V_W and also η from Eq. (10.24), with the same substitution. If the wind speed is not too strong, we calculate this integral with $\eta = 1$, and use Eq. (10.36) for t_W to have the solution for the case $\eta < 1$,

$$x_W = \frac{WV_{LOF}^2}{2gF_0}\left[\frac{1}{1-\eta}\,\mathrm{Log}\,\frac{1}{\eta} + \frac{V_W^2}{V_{LOF}^2} - \frac{V_W}{V_{LOF}}\frac{1}{\sqrt{1-\eta}}\,\mathrm{Log}\,\frac{1+\sqrt{1-\eta}}{1-\sqrt{1-\eta}}\right] \tag{10.39}$$

with η as defined in Eq. (10.24). For the case where $\eta > 1$, the relevant formula is

$$x_W = \frac{WV_{LOF}^2}{2gF_0}\left[\frac{1}{1-\eta}\,\mathrm{Log}\,\frac{1}{\eta} + \frac{V_W^2}{V_{LOF}^2} - \frac{V_W}{V_{LOF}}\frac{2}{\sqrt{\eta-1}}\,\mathrm{Arc\ tan}\,\sqrt{\eta-1}\right] \tag{10.40}$$

10.6 The transition phase

At the end of the ground run, when the speed attains the lift-off speed, V_{LOF}, with action on the elevator control, by bringing the angle-of-attack from the optimum value for the ground run to the value α_{LOF}, we achieve equilibrium of the vertical forces, $L = W$, and the aircraft becomes airborne. We assume that this maneuver is achieved instantaneously. From the time of lift-off, we have the standard equations for pure atmospheric climbing flight

$$\begin{aligned}
\frac{dx}{dt} &= V\cos\gamma \\
\frac{dz}{dt} &= V\sin\gamma \\
m\frac{dV}{dt} &= T\cos\alpha - \frac{1}{2}\rho SV^2C_D - mg\sin\gamma \\
mV\frac{d\gamma}{dt} &= T\sin\alpha + \frac{1}{2}\rho SV^2C_L - mg\cos\gamma
\end{aligned} \tag{10.41}$$

The drag coefficient C_D and the lift coefficient C_L are functions of the angle-of-attack α, as measured from the thrust line. The thrust setting is at the take-off value providing $T = T(V)$, and the motion after lift-off depends on piloting technique in terms of the modulating of the angle-of-attack as a function of time.

As mentioned above, the take-off field length is the total distance from rest to the point of clearance of a hypothetical obstacle with a height specified at 35 feet or 50 feet. The ground run distance has been evaluated in the previous section. To calculate the additional distance from lift-off to the point of clearance of the obstacle, we consider the following flight program for the transition phase (Miller, 1976; Lan, 1981).

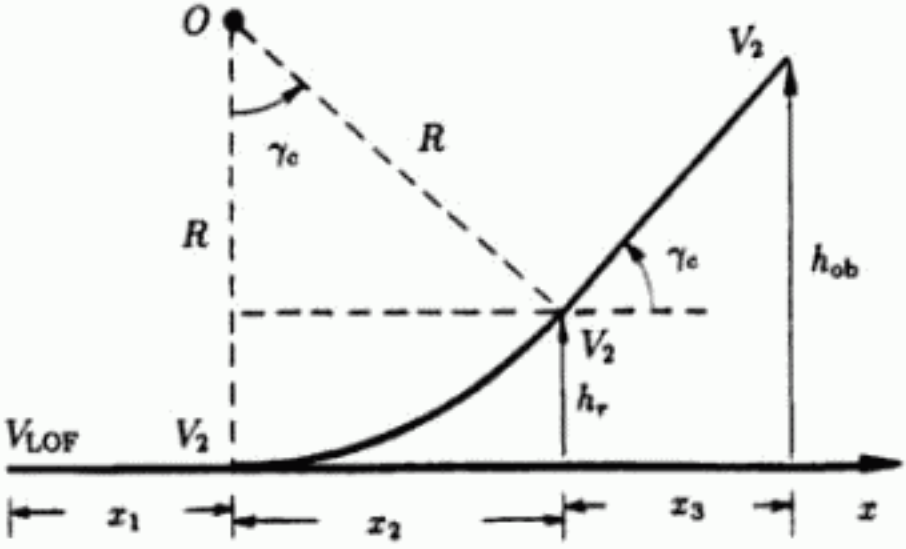

Figure 10.5: Rotation and climb to clear the obstacle.

After lift-off at speed $V_{LOF} = k_1 V_{stall}$, with $k_1 = 1.10$, the aircraft accelerates at nearly constant altitude to the speed $V_2 = k_2 V_{stall}$, with $k_2 = 1.20$ before actual rotation. The time of flight can be calculated from Eq. (6.158) of Chapter 6 with the appropriate subscripts used. In practice, it is known by experience and if t_1 is the time of flight, the field length includes the distance

$$x_1 = V t_1 \tag{10.42}$$

for this phase. The speed is the average of V_{LOF} and V_2.

The rotation and climb to clear the obstacle are shown in Fig. 10.5. It is assumed that the speed remains constant at $V = V_2$ during this phase. Furthermore, we neglect the thrust angle-of-attack and use small angle approximation for the flight path angle. From the figure, the flare arc is assumed to be a circular arc described at constant angular rate. At the end of the circular arc, the flight path angle reaches the steady climb angle γ_c. By setting $dV/dt = 0$ in the third

of the equations (10.41), we can evaluate this angle as

$$\gamma_c = \frac{T - D}{W} = \frac{T}{W} - \frac{1}{C_L/C_D} \tag{10.43}$$

In this equation $T = T(V)$ is evaluated at $V = V_2$ with throttle setting at take-off, and the drag coefficient from the lift-drag relationship, and the lift coefficient from the lift equation

$$\frac{1}{2}\rho S V_2^2 C_L = W \tag{10.44}$$

Hence, the climb angle γ_c is well defined.

Let R be the radius of the circular flare arc. From the geometry of the figure, the horizontal distance for the rotation is

$$x_2 = R \sin \gamma_c \tag{10.45}$$

To evaluate the radius R, we write that during the steady turn in the vertical plane with small flight path angle, the lift is equal to the sum of the weight and the centrifugal force, that is

$$L = W + m\frac{V_2^2}{R} \tag{10.46}$$

Therefore, we obtain

$$R = \frac{V_2^2}{g(n-1)} \tag{10.47}$$

where, as usual, we define the load factor as the ratio of the lift to the weight

$$n = \frac{L}{W} \tag{10.48}$$

with $n > 1$ for turning. The constant n is actually the control for rotation and it depends on piloting technique. To get an idea about its range of magnitude, we refer to Exercise 10-1 which points to the fact that the lift coefficient in Eq. (10.44) is such that $C_L = C_{L_{max}}/k_2^2$. Then we rewrite this equation as

$$\frac{1}{2}\rho S V_2^2 C_{L_{max}} = k_2^2 W \tag{10.49}$$

On the other hand, in Eq. (10.48), let C_{L_r} be the lift coefficient during the rotation. Then, we write this equation as

$$\frac{1}{2}\rho S V_2^2 C_{L_r} = nW \tag{10.50}$$

By comparing the last two equations , we deduce that

$$n = k_2^2 \frac{C_{L_r}}{C_{L_{max}}} \tag{10.51}$$

The ratio $C_{L_r}/C_{L_{max}}$ is frequently assumed to be 0.8. Then if $k_2 = 1.2$, we have on average $n = 1.15$.

The duration of the rotation can be evaluated by writing the last of the equations (10.41) as

$$\frac{d\gamma}{dt} = \frac{g}{V_2}(n-1) \tag{10.52}$$

By integrating this constant rate from $\gamma = 0$ to γ_c, we have

$$\gamma_c = \frac{g}{V_2}(n-1)t_2 \tag{10.53}$$

Again, based on the geometry of the Fig. 10.5, the height at the end of the flare arc is

$$h_r = R - R\cos\gamma_c = 2R\sin^2\frac{\gamma_c}{2} \tag{10.54}$$

If h_r is greater than the prescribed height h_{ob} of the obstacle, then the obstacle has been cleared before reaching the climb angle. For high performance aircraft, this is usually the case and the additional distance x_2 in the field length calculation is evaluated up to the point where $h = h_{ob}$ (see Exercise 10-10). If at the end of the rotation, $h_r < h_{ob}$, the aircraft climbs to this height with constant climb angle γ_c. This adds the distance

$$x_3 = \frac{h_{ob} - h_r}{\tan\gamma_c} \tag{10.55}$$

to the field length. The time to climb with the rate of climb $V_2\sin\gamma_c$ is

$$t_3 = \frac{h_{ob} - h_r}{V_2\sin\gamma_c} = \frac{x_3}{V_2\cos\gamma_c} \tag{10.56}$$

As a numerical example, we consider the case of an aircraft with $V_{stall} = 92\,\text{mph} = 134.96\,\text{ft/s}$. Then, with $k_1 = 1.10$, $k_2 = 1.20$, we have $V_{LOF} = 148.46\,\text{ft/s}$ and $V_2 = 161.95\,\text{ft/s}$.

If the acceleration from V_{LOF} to V_2 takes $t_1 = 2\,\text{s}$, the distance travelled at the average speed of $155\,\text{ft/s}$ is $x_1 = 310\,\text{ft}$.

By using a load factor of $n = 1.15$ for the rotation, with $g = 32.2\,\text{ft/s}^2$, the radius of the flare arc from Eq. (10.47) is $R = 5430\,\text{ft}$. If the climb angle, as calculated from Eq. (10.43) is $\gamma_c = 0.1396\,\text{radians} = 8\,\text{deg}$, the distance covered during the rotation, as calculated from Eq. (10.45) is $x_2 = 756\,\text{ft}$. The duration of the rotation, as calculated from Eq. (10.53) is $t_2 = 4.68\,\text{s}$. At the end of the rotation, the height calculated from Eq. (10.54) is $h_r = 52.84\text{ft}$. The aircraft then just clears a 50 ft high obstacle. The total field length is $x = x_g + x_1 + x_2$ and the total time for take-off with clearance of obstacle is $t = t_g + t_1 + t_2$.

If, with a slightly smaller thrust-to-weight ratio at take-off, the climb angle is at $\gamma_c = 7\,\text{deg}$, while with the same load factor $n = 1.15$, the radius R is the same, the distance during the rotation is now $x_2 = 662\,\text{ft}$, with the corresponding time $t_2 = 4.10\,\text{s}$. The height at the end of the rotation is only $h_r = 40.47\,\text{ft}$. From Eq. (10.55), the additional distance to the obstacle is $x_3 = 77.62\,\text{ft}$. The additional time from Eq. (10.56) is $t_3 = 0.48\,\text{s}$.

Here, some explanations are in order. From Chapter 7 on Climb Performance, and as evidenced from Eq. (10.43), a high thrust-to-weight ratio will give a higher climb angle. Yet, with the numerical example, with $\gamma_c = 8\,\text{deg}$, we obtain $x_2 = 756\,\text{ft}$, while with $\gamma_c = 7\,\text{deg}$, we have a total of $x_2 + x_3 = 740\,\text{ft}$ to be included in the field length calculation. Theoretically, the latter figure should be higher (see Exercise 10-10). The discrepancy comes from the fact that in the high thrust case, the 50 ft high obstacle is actually reached before the value $x_2 = 740\,\text{ft}$. A reevaluation of this distance at exactly the point where the height is 50ft, as detailed in Exercise 10-10, will provide $x_2 = 735\text{ft}$. Although the difference is small, the main effect of the higher thrust in field length calculation is in the sharp decrease in the ground run distance x_g, and also in the accelerating distance x_1.

The same remark can be made about the time required to clear the obstacle. In the numerical example, at lower thrust when $\gamma_c = 7\,\text{deg}$, the total time for rotation and climb to the obstacle is $t_2 + t_3 = 4.58\,\text{s}$. For the case of higher thrust with $\gamma_c = 8\,\text{deg}$, the actual time at

clearance of the obstacle is not 4.68 s but it is at $t_2 = 4.55$ s according to the formulas given in Exercise 10-11. The difference is small and the main effect of high thrust on the time for take-off is on the time to lift-off t_g, and to some extent on the accelerating time t_1.

10.7 Description of a landing

The landing is also made in two phases: the approach over a hypothetical obstacle with a flare to touch-down and the ground run to a full stop. This is illustrated in Fig. 10.6 and the field length for landing is defined as the distance from the obstacle to the full stop position.

Before coming to the obstacle, the aircraft makes an approach along the axis of the runway with a glide slope standardized between -2.5deg and -3.5 deg. For the calculation, we can use a -3 deg glide slope. Depending on the type of aircraft, the speed during the approach and the transition phase may be taken as the speed V_2 or slightly higher. Let subscript a denote the condition during approach. We rewrite the equations (10.43) and (10.44) as

$$\gamma_a = \frac{T}{W} - \frac{1}{C_L/C_D} < 0 \tag{10.57}$$

and

$$\frac{1}{2}\rho S V_2^2 C_L = W \tag{10.58}$$

From the last equation, the speed is controlled by the lift coefficient, that is the angle-of-attack. The corresponding drag coefficient is deduced from the lift–drag relationship, with the aerodynamic configuration for landing. With the lift-to-drag ratio well defined, from Eq. (10.57), the flight path angle during approach is controlled by the thrust-to-weight ratio.

After passage of the obstacle, a combination of thrust and angle-of-attack control would, theoretically, bring the aircraft to the touch-down speed V_{TD}, with the velocity direction parallel to the runway, and the main landing gear in contact with the runway. From this point the ground run starts, during which the braking forces will bring the aircraft to a full stop. To shorten the ground run distance, reversed thrust and/or drag chutes may be used.

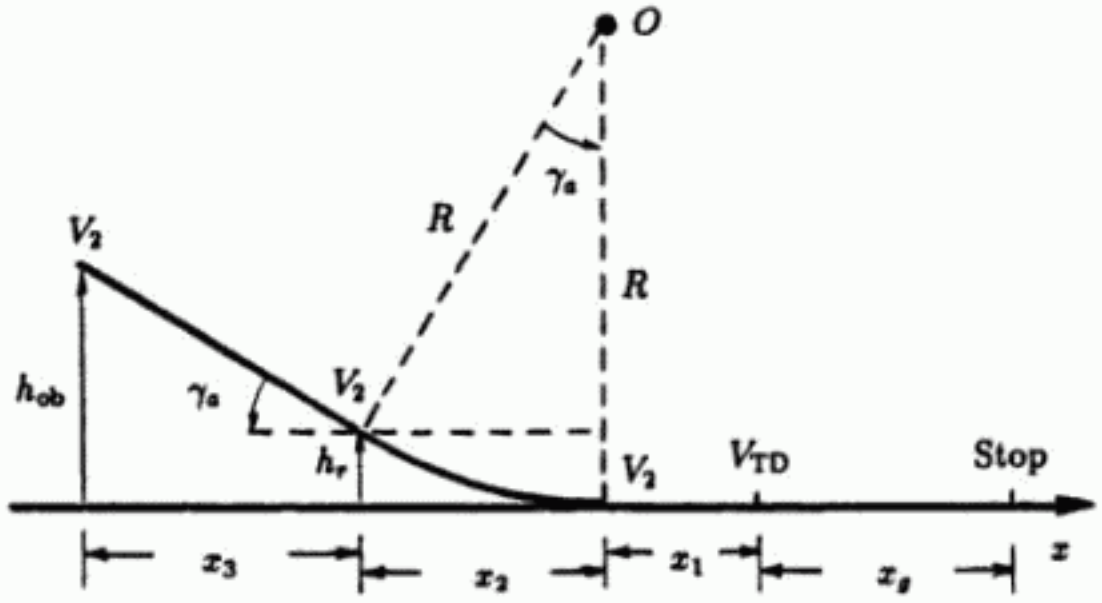

Figure 10.6: Different phases of a landing.

Since the landing is something of a reverse operation to the take-off, we shall first analyze the transition phase and then, consider the ground run phase.

10.8 Transition to touch-down

We consider the following flight program for the transition phase.

After passage of the obstacle at the height h_{ob} of the landing gear, the aircraft follows a straight line at the angle γ_a until the height h_r for the rotation. Since $\gamma < 0$, to simplify the notation, we adopt the convention of always using absolute value. Then, the distance travelled is

$$x_3 = \frac{h_{ob} - h_r}{\tan \gamma_a} \tag{10.59}$$

Since the horizontal component of the velocity is $V_2 \cos \gamma_a$, the time of

flight is

$$t_3 = \frac{x_3}{V_2 \cos \gamma_a} \tag{10.60}$$

The flare arc is assumed to be a circular arc with radius R. Then, just as for the case of the take-off, we have

$$R = \frac{V_2^2}{g(n-1)} \tag{10.61}$$

where n is the load factor used as the control.

From the geometry in Fig. 10.6, we obtain

$$h_r = R - R\cos\gamma_a = 2R\sin^2\frac{\gamma_a}{2} \tag{10.62}$$

The distance travelled during the flare is

$$x_2 = R\sin\gamma_a \tag{10.63}$$

The duration for the flare arc is given by

$$\gamma_a = \frac{g}{V_2}(n-1)t_2 \tag{10.64}$$

As a numerical example, as has been done in the previous section, we consider the case of $V_2 = 161.95$ ft/s, and $n = 1.15$, and hence a radius of $R = 5430$ ft. With a glide slope of $\gamma_a = 3$ deg, we have $h_r = 7.44$ ft. Therefore $x_2 = 284$ ft and $x_3 = 812$ ft. The corresponding times are respectively $t_2 = 1.76$ s and $t_3 = 5$ s.

If we consider a gentler maneuver using a load factor of only $n = 1.10$, we obtain a larger flare radius of 8145ft. With the same glide slope of 3 deg, we have $h_r = 11.16$ ft. Therefore, $x_2 = 426$ ft and $x_3 = 741$ ft. The corresponding times are respectively $t_2 = 2.63$ s and $t_3 = 4.58$ s. With a lower load factor for the flare, both the total distance $x_2 + x_3$ and the total time $t_2 + t_3$ are larger (see Exercise 10-12). In practice, a value of $n = 1.08$ is resonable for landing.

At the end of the flare arc, the velocity is parallel to the runway with magnitude V_2 and the main landing gear is slightly above the surface of the runway. The thrust is theoretically at its minimum value. A decelerated horizontal flight is maintained to reduce the speed V_2 to the touch-down speed V_{TD}. The deceleration time t_1 can be calculated

from Eq. (6.158) of Chapter 6 with the appropriate subscripts used. In practice, it is estimated by experience and the field length includes the distance

$$x_1 = Vt_1 \tag{10.65}$$

using an average speed between V_{TD} and V_2.

The transition phase, as described above, is a simplified scheme for the purpose of evaluating the total distance travelled and the total time of flight during this phase. In reality, from the point of clearance of the obstacle until the touch-down position, both the speed and the flight path angle continuously vary from V_2 to V_{TD} and from γ_a to the final value zero.

10.9 The ground run during landing

We have the same equations as for the ground run during take-off, except for the fact that the magnitudes of the various decelerating forces are different.

The force F, as given in Eq. (10.18) is now negative for a deceleration to a full stop, with the speed V varying from the initial speed V_{TD} to the final value zero. The touch-down speed can be taken practically as the lift-off speed or slightly lower. Most frequently, the thrust is zero, but taking account of a possible reverse thrust, used as additional braking force, we replace this term by a constant value $-T_0$, with $T_0 = 0$ if no reverse thrust is used.

We shall assume that during the ground run, the attitude of the aircraft is constant. Hence, we have constant angle-of-attack and as a consequence, constant values for C_D and C_L. These values are evaluated with the aerodynamic configuration for the ground run during landing which includes the flaps and the spoilers in extended position. If drag chutes are used to slow down the aircraft, they are released at some time after touch-down. To handle this situation, we can divide the landing ground run into two segments, and in each segment use a different value for the drag coefficient C_D for the evaluation of the different integrals involved. The rolling coefficient μ is now higher, of the order of $\mu = 0.3 - 0.4$, due to the landing gear braking force. In practice, this braking force develops progressively during the ground run. If μ is modeled as a function of speed, it would change the quadratic

formulation of the net decelerating force. A simple way to handle this is again to divide the ground run into segments, and in each segment use a different constant value for the friction coefficient μ.

In the following, we shall assume constant values for C_D, C_L and μ, and hence represent the net decelerating force for the whole duration of the ground run as

$$F = -\left[T_0 + (\mu + \phi)W + \frac{1}{2}\rho S(C_D - \mu C_L)V^2\right] \tag{10.66}$$

Inside the square brackets the constant term is positive. Even without reverse thrust, $T_0 = 0$, and with a negative slope, we usually have $\mu + \phi > 0$. For a landing gear with a nose wheel, the lift coefficient during the ground run is nearly zero and the coefficient of the aerodynamic term is positive. Only for the case of a tail wheel in contact with the runway during the ground run (hence for the aircraft at high angle-of-attack, with a high value of the friction coefficient and with insufficient drag devices) can the coefficient $C_D - \mu C_L$ be negative.

Although here we have a decelerating force, by analogy with the pertinent formulas for the take-off, we consider its absolute value and define, with $T_0 > 0$ for reverse thrust,

$$\begin{aligned} F_{\mathrm{TD}} &= T_0 + (\mu + \phi)W + \frac{1}{2}\rho S(C_D - \mu C_L)V_{\mathrm{TD}}^2 \\ F_0 &= T_0 + (\mu + \phi)W \end{aligned} \tag{10.67}$$

to be respectively the decelerating force at touch-down and the decelerating force at full stop. Also, we define the ratio

$$\eta = \frac{F_{\mathrm{TD}}}{F_0} \tag{10.68}$$

Then, the solutions for the ground run during landing are

$$x_g = \frac{WV_{\mathrm{TD}}^2}{2gF_0}K_1(\eta) \tag{10.69}$$

and

$$t_g = \frac{WV_{\mathrm{TD}}}{gF_0}K_2(\eta) \tag{10.70}$$

with the same function $K_1(\eta)$ as given in Eq. (10.27) and the function $K_2(\eta)$ as given in Eq. (10.28) when $\eta < 1$ and Eq. (10.29) when $\eta > 1$.

The influence of the touch-down speed on the ground run distance is the same as the influence of the lift-off speed for the take-off. A high value of $C_{L_{max}}$ through the use of flaps to lower V_{TD} decreases the ground run distance. The influences of altitude and temperature on the runway are the same, namely an airfield at high altitude and with high temperature on the runway will increase the length of the ground run. A higher weight at landing has the same effect.

It should be noted here that a high-lift aerodynamic configuration is used to obtain lower touch-down speed, but after contact with the ground, the pilot may change the aerodynamic characteristics of the aircraft so that different data are used to evaluate the drag coefficient C_D and the lift coefficient C_L in Eq. (10.67) for F_{TD}, with the ground effect included.

Again, from Eq. (10.69), to have a short ground run distance, a maximum value of F_0 is dictated. This will lead to using reverse thrust, if possible, and high braking coefficient μ. For given F_0, the functions $K_1(\eta)$ and $K_2(\eta)$ are minimized with the maximum value of η, and hence the maximum value of F_{TD}. A high value of the drag coefficient C_D, coupled with a low value of the lift coefficient C_L will increase F_{TD}. Since the angle-of-attack remains constant during the ground run, drag devices for the ground run are designed to achieve this improvement in the sense that C_D can be increased without significant increase in C_L.

Exercises

10-1. From the definitions (10.1) and (10.2), show that the lift coefficient at take-off is

$$C_L = \frac{C_{L_{max}}}{k_1^2}$$

and the lift coefficient at clearance of the hypothetical obstacle is

$$C_L = \frac{C_{L_{max}}}{k_2^2}$$

These formulas are used to evaluate the attitudes of the aircraft at the respective points.

10-2. Consider the expression for the net accelerating force during the ground run

$$F = T(\cos\alpha + \mu\sin\alpha) - \frac{1}{2}\rho S V^2(C_D - \mu C_L) - (\mu + \phi)W$$

Here, T is a function of the speed V and the last term is constant.

We use a parabolic drag polar

$$C_D = C_{D_0} + KC_L^2$$

and assume that

$$C_L = C_{L_\alpha}\alpha$$

where C_{L_α} is the slope of the lift curve and is constant.

a) If the angle-of-attack α is selected uniquely to maximize the effect of the thrust, show that we have a solution

$$\tan\alpha = \mu$$

and

$$T(\cos\alpha + \mu\sin\alpha) = T\sqrt{1+\mu^2} \approx T\left(1 + \frac{1}{2}\mu^2\right)$$

with the approximation coming from the fact that α is small. Show that we have an identical solution by first expanding $\cos\alpha + \mu\sin\alpha$ to the second order in α before maximizing this term.

b) With the optimum value of α, show that the resulting accelerating force is

$$F_1 = T\left(1 + \frac{1}{2}\mu^2\right) - \frac{1}{2}\rho SV^2(C_{D_0} + KC_{L_\alpha}^2\mu^2 - C_{L_\alpha}\mu^2) - (\mu + \phi)W$$

10-3. By continuing the previous exercise, it is now intended to select the optimum angle-of-attack to minimize the coefficient $C_D - \mu C_L$ of the aerodynamic force.

a) Show that we have the solution

$$\alpha = \frac{\mu}{2KC_{L_\alpha}} = k\mu$$

where, by definition, $k = 1/2KC_{L_\alpha}$.

Show that the resulting accelerating force is

$$F_2 = T\left(1 - \frac{1}{2}k^2\mu^2 + k\mu^2\right) - \frac{1}{2}\rho SV^2\left(C_{D_0} - \frac{1}{2}kC_{L_\alpha}\mu^2\right) - (\mu + \phi)W$$

b) Using F_1 from the previous exercise, deduce the difference

$$F_2 - F_1 = \frac{1}{2}\mu^2(k-1)^2 P$$

where, by definition

$$P = \frac{1}{2}\rho S V^2 \frac{C_{L_0}}{k} - T$$

Therefore, if $P > 0$, that is for a low or moderate value of the thrust, it is better to select the angle-of-attack for the ground run which minimizes the coefficient $C_D - \mu C_L$. Only for the case of a very high take-off thrust is the optimum angle-of-attack the one which favors the thrust term. Furthermore, since $F_2 - F_1$ is proportional to μ^2, the effect is more pronounced with higher values of the rolling friction coefficient.

10-4. It is possible to assess the sign of the function P in Exercise 10-3 in a more explicit way. It has been shown in Chapter 6 that the minimum thrust for cruise of a turbojet aircraft is obtained by using the angle-of-attack for maximum lift-to-drag ratio, that is with $\alpha = \alpha^*$, $C_L = \sqrt{C_{D_0}/K} = C_L^*$, $C_D = 2C_{D_0} = C_D^*$. Show then that

$$P = \frac{T_{min}}{\alpha^{*2}} - T$$

where, of course, the value of T is its maximum for take-off. An alternate expression is

$$P = \frac{W}{E_{max}\alpha^{*2}} - T$$

Therefore, for P to be negative, we must have a thrust-to-weight ratio at take-off such that

$$\frac{T}{W} > \frac{1}{E_{max}\alpha^{*2}}$$

with α^* in radians, usually of the order of $\pi/20$. Since E_{max} is about 15, this is clearly not the case.

10-5. From Eq. (10.18) with constant angle-of-attack for the ground run and when the thrust is a linear function in V^2, show that

$$ma(V) = F = F_0 - (F_0 - F_{\text{LOF}})\left(\frac{V}{V_{\text{LOF}}}\right)^2$$

a) By substituting into Eqs. (10.10) and (10.11) for a direct integration, show that we have

$$t_g = \frac{WV_{LOF}}{gF_0} \int_0^1 \frac{du}{1 - \varepsilon u^2}$$

and

$$x_g = \frac{WV_{LOF}^2}{2gF_0} \int_0^1 \frac{du^2}{1 - \varepsilon u^2}$$

where u is the normalized speed defined as

$$u = \frac{V}{V_{LOF}}$$

and

$$\varepsilon = 1 - \frac{F_{LOF}}{F_0} = 1 - \eta$$

b) Perform the quadratures and show that

$$K_1(\eta) = \int_0^1 \frac{du^2}{1 - \varepsilon u^2} = \frac{1}{1 - \eta} \operatorname{Log} \frac{1}{\eta} \tag{1}$$

for arbitrary values of η and

$$K_2(\eta) = \int_0^1 \frac{du}{1 - \varepsilon u^2} = \frac{1}{2\sqrt{1 - \eta}} \operatorname{Log} \frac{1 + \sqrt{1 - \eta}}{1 - \sqrt{1 - \eta}} \tag{2}$$

for $\epsilon = 1 - \eta > 0$, and

$$K_2(\eta) = \frac{1}{\sqrt{\eta - 1}} \operatorname{Arc\,tan} \sqrt{\eta - 1} \tag{3}$$

for $\epsilon = 1 - \eta < 0$.

c) Consider the expression (2) for $K_2(\eta)$ in the case where $1 - \eta < 0$. Use the imaginary number $i^2 = -1$ and show that

$$K_2(\eta) = -\frac{i}{2\sqrt{\eta - 1}} \operatorname{Log} \frac{1 + i\sqrt{\eta - 1}}{1 - i\sqrt{\eta - 1}}$$

Put

$$\sqrt{\eta - 1} = \tan \beta$$

and use the Euler's formulas

$$e^{i\beta} = \cos\beta + i\sin\beta$$
$$e^{-i\beta} = \cos\beta - i\sin\beta$$

to show that

$$K_2(\eta) = -\frac{i}{2\tan\beta}\operatorname{Log} e^{2i\beta} = \frac{\beta}{\tan\beta}$$

Then, deduce the expression (3) for $K_2(\eta)$ for the case where $\eta > 1$.

10-6. Consider the expression (10.25) for the ground run distance

$$x_g = \frac{WV_{LOF}^2}{2gF_0}K_1(\eta)$$

where by definition

$$K_1(\eta) = \frac{1}{1-\eta}\operatorname{Log}\frac{1}{\eta}$$

with $\eta = F_{LOF}/F_0$. The function has the indeterminate form when $\eta = 1$. Let $1 - \eta = \epsilon$, and use series expansion to show that, in the interval of convergence, $|\epsilon| < 1$, we have

$$K_1(\epsilon) = 1 + \frac{1}{2}\epsilon + \frac{1}{3}\epsilon^2 + \frac{1}{4}\epsilon^3 + \frac{1}{5}\epsilon^4 + \cdots$$

Then deduce that, with respect to ϵ, the function K_1 is monotonically increasing and, as a consequence, with respect to η, it is monotonically decreasing. The minimum of K_1 is attained with the largest value of η. Furthermore, when $\eta = 1$, $K_1 = 1$, $dK_1/d\eta = -1/2$. This explains the behavior of the function $K_1(\eta)$ as shown in Fig. 10.3.

10-7. Consider the expression (10.26) for the time to lift-off

$$t_g = \frac{WV_{LOF}}{gF_0}K_2(\eta)$$

where, by definition, for $\eta < 1$

$$K_2(\eta) = \frac{1}{2\sqrt{1-\eta}}\operatorname{Log}\frac{1+\sqrt{1-\eta}}{1-\sqrt{1-\eta}} \tag{1}$$

and for $\eta > 1$

$$K_2(\eta) = \frac{1}{\sqrt{\eta - 1}} \text{Arc tan} \sqrt{\eta - 1} \tag{2}$$

with $\eta = F_{LOF}/F_0$. Again, in general, for arbitrary η, let $1 - \eta = \varepsilon$. Notice that both the expressions (1) and (2) have the indeterminate form when $\eta = 1$.

a) When $\eta < 1$, put $\varepsilon = \varepsilon'^2$ in Eq. (1), and in the interval of convergence, $\varepsilon < 1$, use series expansion to show that

$$K_2(\varepsilon) = 1 + \frac{1}{3}\varepsilon + \frac{1}{5}\varepsilon^2 + \frac{1}{7}\varepsilon^3 + \cdots \tag{3}$$

b) When $\eta > 1$, put $\varepsilon = -\varepsilon'^2$ in Eq. (2), and in the interval of convergence, $|\varepsilon| < 1$, use series expansion to show that, we have the same formula (3).

c) The reason that we have the same expansion (3) for both the functional forms (1) and (2) can be explained by considering the integral form of $K_2(\varepsilon)$ as defined in Exercise 10-5, for both positive and negative values of ε.

$$K_2(\varepsilon) = \int_0^1 \frac{du}{1 - \varepsilon u^2} \tag{4}$$

In the interval of convergence, $|\varepsilon u^2| < 1$, use binomial expansion for $(1 - \varepsilon u^2)^{-1}$, and upon integrating, deduce that we have the solution (3).

From the general expression (3), deduce that with respect to ε, the function K_2 is monotonically increasing and, as a consequence, with respect to η, it is monotonically decreasing. The minimum of K_2 is attained with the largest value of η. Furthermore, when $\eta = 1$, $K_2 = 1$, $dK_2/d\eta = -1/3$. This explains the behavior of the function $K_2(\eta)$ as shown in Fig. 10.3.

10-8. As applications of the results in Exercises 10-6 and 10-7, show that when the wind speed V_W is small, $\eta = F_{V_W}/F_0 \approx 1$, $\varepsilon \approx 0$, and we have approximately the values for the following integrals

$$t = \int_0^{V_W} \frac{dV}{a(V)} \approx \frac{WV_W}{gF_0}$$

$$x = \int_0^{V_W} \frac{V\,dV}{a(V)} \approx \frac{WV_W^2}{2gF_0}$$

They are the approximations used in Eqs. (10.36) and (10.39).

10-9. To have a simple estimate of the time to lift-off and the ground run distance with wind, use a constant acceleration $a = F_0/m$ in Eqs. (10.33) and (10.34) for the integration and show that

$$t_W = \frac{W V_{LOF}}{g F_0}\left(1 - \frac{V_W}{V_{LOF}}\right)$$

and

$$x_W = \frac{W V_{LOF}^2}{2 g F_0}\left(1 - \frac{V_W}{V_{LOF}}\right)^2$$

Show that we have identical results with the more general solutions (10.36) and (10.39) by using the limit $\eta \to 1$.

10-10. We refer to Fig. 10.5 for this problem. In the case where the obstacle height h_{ob} is reached along the circular flare arc, let $\gamma_2 \leq \gamma_c$ be the flight path angle at the point of clearance.

a) Show that we have the following relations at the point of clearance

$$h_{ob} = 2R\sin^2(\gamma_2/2)$$
$$x_2 = R\sin\gamma_2$$

where

$$R = \frac{V_2^2}{g(n-1)}$$

Since the constant speed V_2 for the rotation is given, for any load factor n used for the turning, the turning radius R can be calculated. Then, with the prescribed obstacle height h_{ob} we can calculate γ_2 and x_2. Use the numerical example in Section 10.6 with $V_2 = 161.95$ ft/s, $n = 1.15$ and $h_{ob} = 50$ ft for the calculation and find that we have indeed $x_2 < 740$ ft.

b) Derive the explicit relation

$$x_2^2 = 2Rh_{ob} - h_{ob}^2$$

Again, with the numerical example, calculate $x_2 = 735$ ft.

c) Assume that, with a lower thrust-to-weight ratio, the circular flare arc is terminated at the climb angle $\bar{\gamma}_c < \gamma_2$, hence before reaching

the obstacle height. Let $\bar{x}_2$ be the horizontal distance for the flare arc, and x_3 be the additional distance to reach the obstacle height. Show that the distance for the transition phase for this case is

$$\bar{x}_2 + x_3 = \frac{h_{ob}}{\tan \bar{\gamma}_c} + R \tan \frac{\bar{\gamma}_c}{2}$$

d) Let $\Delta = \gamma_2 - \bar{\gamma}_c \geq 0$. By comparing the two transition distances in a) and c), show that the difference is

$$(\bar{x}_2 + x_3) - x_2 = \frac{2R}{\sin \bar{\gamma}_c} \sin^2 \frac{\Delta}{2}$$

The difference is indeed non-negative and small.

10-11. We have the same considerations as in the Exercise 10-10.

a) Show that if the obstacle height h_{ob} is reached along the circular flare arc, at the angle $\gamma_2 \leq \gamma_c$, the time of flight to the obstacle is

$$t_2 = \frac{R}{V_2} \gamma_2$$

b) Assume that, with a lower thrust-to-weight ratio, the circular flare arc is terminated at the climb angle $\bar{\gamma}_c < \gamma_2$, hence before reaching the obstacle height. Let $\bar{t}_2$ be the time for the flare arc, and t_3 be the additional time to reach the obstacle height. Show that the total time for the transition phase for this case is

$$\bar{t}_2 + t_3 = \frac{h_{ob}}{V_2 \sin \bar{\gamma}_c} + \frac{R}{V_2} \left(\bar{\gamma}_c - \tan \frac{\bar{\gamma}_c}{2} \right)$$

c) By comparing with the time of flight in a) and using the results in the previous exercise, show that the difference in the times of flight is

$$(\bar{t}_2 + t_3) - t_2 = \frac{R}{V_2} \left[(\sin \Delta - \Delta) + \frac{2}{\tan \bar{\gamma}_c} \sin^2 \frac{\Delta}{2} \right]$$

where $\Delta = \gamma_2 - \bar{\gamma}_c \geq 0$. Since $\sin \Delta - \Delta$ is of the order of Δ^3, and $\tan \bar{\gamma}_c$ is small, we have practically for the difference

$$(\bar{t}_2 + t_3) - t_2 = \frac{2R}{V_2 \tan \bar{\gamma}_c} \sin^2 \frac{\Delta}{2}$$

It is indeed non-negative and very small.

10-12. a) For the transition phase during landing, by using the glide angle with its absolute value, show that the combined distance for the descent from the obstacle and the flare arc is

$$x_2 + x_3 = \frac{h_{ob}}{\tan \gamma_a} + R \tan \frac{\gamma_a}{2}$$

Therefore, with given h_{ob} and γ_a this is a linear function of R, and it is a minimum for a maximum permissible value of the control load factor n for the flare arc.

b) Show that the combined time is

$$t_2 + t_3 = \frac{h_{ob}}{V_2 \sin \gamma_a} + \frac{R}{V_2}\left(\gamma_a - \tan \frac{\gamma_a}{2}\right)$$

This is also a minimum for the maximum value of n.

c) The largest value of R is obtained when the flare arc starts at $h_r = h_{ob}$. Show that the minimum of the load factor is

$$n = 1 + \frac{2V_2^2}{g h_{ob}} \sin^2 \frac{\gamma_a}{2}$$

Then, show that the longest transition distance is such that $x_3 = 0$ and

$$x_2 = \frac{h_{ob}}{\tan(\gamma_a/2)}$$

while theoretically, with $R = 0$, the shortest transition distance is such that $x_2 = 0$ and

$$x_3 = \frac{h_{ob}}{\tan \gamma_a}$$

Show that the ratio of the limiting distances is

$$\frac{\min x}{\max x} = \frac{1}{2}\left(1 - \tan^2 \frac{\gamma_a}{2}\right) \approx \frac{1}{2}.$$

d) Show that the longest time for the transition is such that $t_3 = 0$, and

$$t_2 = \frac{h_{ob} \gamma_a}{V_2(1 - \cos \gamma_a)}$$

while theoretically, with $R = 0$, the shortest time for the transition is such that $t_2 = 0$ and

$$t_3 = \frac{h_{ob}}{V_2 \sin \gamma_a}$$

Show that the ratio of the limiting times is

$$\frac{\min t}{\max t} = \frac{1}{\gamma_a} \tan \frac{\gamma_a}{2} \approx \frac{1}{2}.$$

11

Performance of hypervelocity reentry vehicles

11.1 Introduction

To complete the analysis of flight performance at high speed of an aerodynamic lifting vehicle inside a planetary atmosphere, in this last chapter we shall consider the case of an aerospace vehicle which, upon completing its mission in the vacuum space about the earth, reenters the atmosphere at a speed of the order of the orbital speed. Hence, as has been discussed in Chapter 2, $V \approx \sqrt{gr}$ and the term V^2/gr must be retained in the equations of motion.

We shall assume that the earth and its atmosphere are non-rotating and the planar flight is effected in the plane of a great circle. For a non-rotating lifting reentry vehicle, we consider the equations of motion of its center of mass, as have been derived in Chapter 2.

$$\begin{aligned}
\frac{dr}{dt} &= V \sin\gamma \\
\frac{d\theta}{dt} &= \frac{V\cos\gamma}{r} \\
\frac{dV}{dt} &= -\frac{\rho S C_D V^2}{2m} - g\sin\gamma \\
V\frac{d\gamma}{dt} &= \frac{\rho S C_L V^2}{2m} - \left(g - \frac{V^2}{r}\right)\cos\gamma
\end{aligned} \tag{11.1}$$

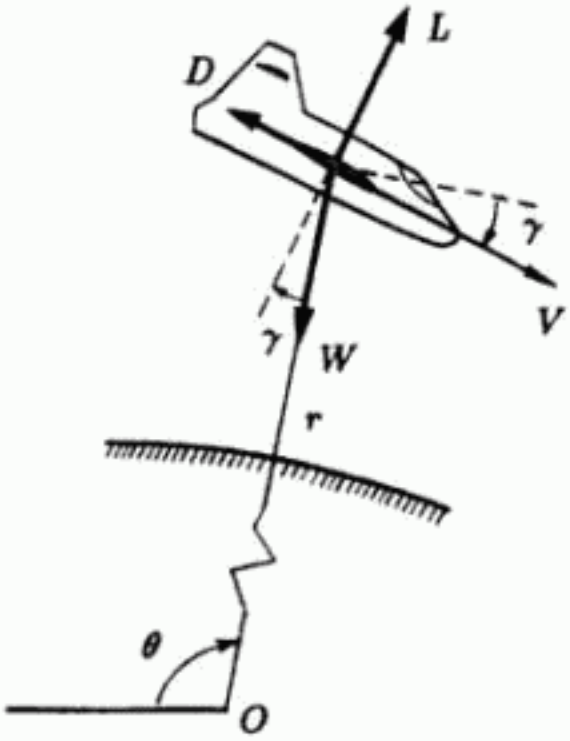

Figure 11.1: Nomenclature.

We refer to Fig. 11.1 for the nomenclature. The position is now defined by the radial distance r from the center of attraction of the planet and the longitude θ, expressed in radians. The velocity is represented by its magnitude V and the flight path angle γ as measured from the local horizontal which is now constantly changing in direction. Since there is no thrusting force during reentry, we consider the mass m as constant if the ablation of the material is negligible.

The gravitational field is taken to be a central, inverse-square force field, with the acceleration given by

$$g = g_0\left(\frac{r_0}{r}\right)^2 \tag{11.2}$$

where subscript zero denotes the condition at sea level. We shall use a locally exponential atmosphere for the variation of the density according to the law

$$\frac{d\rho}{\rho} = -\beta dr \tag{11.3}$$

where β is the inverse of the local scale height and, for any specified planetary atmosphere, it is a function of the radial distance r.

The physical phenomena of interest in the analysis of reentry trajectories are the strong variations in the speed, the deceleration and the heating during entry. These occur during the main portion of the trajectory between the reentry altitude of approximately 95 km where the deceleration is being felt and a final altitude at the level of the tropopause. Below this altitude, the speed has been reduced to the range where the flat earth assumption can be applied. The treatment of flight performance at this speed regime has been adequately covered in the previous chapters. In particular, Chapter 5 presents an in-depth analysis of glide performance at low speed.

In this chapter, we shall first derive a set of dimensionless equations of motion, valid for an arbitrary reentry vehicle of arbitrary shape, size and mass. Then, depending on the type of trajectories, we shall make the appropriate simplifying assumptions and integrate the equations of motion to obtain the laws of variation for different physical quantities of interest.

11.2 Dimensionless equations of motion

It has been found convenient for the analysis of reentry trajectories to use the following dimensionless variables

$$Z = \frac{\rho S C_D}{2m}\sqrt{\frac{r}{\beta}} \qquad u = \frac{V^2}{gr} \tag{11.4}$$

The variable Z, which has been first introduced by Chapman in his classical analysis (Chapman, 1959), is proportional to the atmospheric density ρ, and hence it can be used as the altitude variable. It varies from a near zero value at the entry altitude to a much higher value at sea level. The variable u is the speed variable. It is simply the square of the ratio of the current speed V to the local circular speed which is $V_c = \sqrt{gr}$.

Using the longitudinal range θ to replace the time, we rewrite

Eqs. (11.1)

$$\begin{aligned}\frac{dr}{d\theta} &= r\tan\gamma \\ \frac{dV^2}{d\theta} &= -\frac{r\rho SC_D V^2}{m\cos\gamma} - 2gr\tan\gamma \\ \frac{d\gamma}{d\theta} &= \frac{r\rho SC_L}{2m\cos\gamma} + \left(1 - \frac{gr}{V^2}\right)\end{aligned} \tag{11.5}$$

By taking the derivative of u with respect to θ, using its definition (11.4) and Eqs. (11.2) and (11.5), we obtain

$$\frac{du}{d\theta} = -\frac{r\rho SC_D}{m\cos\gamma}\frac{V^2}{gr} - 2\tan\gamma + \frac{V^2}{gr}\tan\gamma$$

By using the definition (11.4) for Z and u, we have the equation for u

$$\frac{du}{d\theta} = -\frac{2\sqrt{\beta r}Zu}{\cos\gamma} - (2-u)\tan\gamma \tag{11.6}$$

On the other hand, by taking the derivative of Z with respect to θ, using the exponential law (11.3) for ρ, we obtain for the case where C_D is constant

$$\frac{dZ}{d\theta} = -\beta r\left(1 - \frac{1}{2\beta r} + \frac{1}{2\beta^2}\frac{d\beta}{dr}\right)Z\tan\gamma \tag{11.7}$$

In this equation for Z, if a strictly exponential atmosphere is used, β = constant and $d\beta/dr = 0$. On the other hand, if an isothermal atmosphere is considered, β/g = constant and $(1/2\beta^2)(d\beta/dr) = -1/\beta r$. In both cases, in the equations for u and Z, the variables β and r enter as the dimensionless product βr. For the earth's atmosphere, for altitude below 120 kilometers, the mean value of βr is about 900. The deviation of βr from its mean value is large. In the same region βr varies from a low of about 750 to a high of about 1300. It is however a better assumption to use a mean value for βr than simply to put β constant and use the strictly exponential atmosphere in the calculation. Hence, we shall take $\beta r = 900$, and also since $1/\beta r$ is small, we can neglect this term in the equation for Z.

Finally, with the definition (11.4), the equation for γ is

$$\frac{d\gamma}{d\theta} = \frac{\sqrt{\beta r}Z}{\cos\gamma}\frac{C_L}{C_D} + 1 - \frac{1}{u} \tag{11.8}$$

In summary, to analyze reentry trajectories, we have the following dimensionless equations

$$\begin{aligned}\frac{dZ}{d\theta} &= -\beta r Z \tan\gamma \\ \frac{du}{d\theta} &= -\frac{2\sqrt{\beta r} Z u}{\cos\gamma} - (2-u)\tan\gamma \\ \frac{d\gamma}{d\theta} &= \frac{\sqrt{\beta r} Z}{\cos\gamma}\frac{C_L}{C_D} + 1 - \frac{1}{u}\end{aligned} \tag{11.9}$$

For the earth's atmosphere we use the average value $\beta r = 900$ and the equations are valid for any arbitrary vehicle regardless of its size, shape and mass.

Several useful physical quantities during entry can be expressed in terms of the variables u and Z. First, from the equation for V in system (11.1), with the definitions (11.4) of u and Z, we have the tangential deceleration

$$-\frac{1}{g}\frac{dV}{dt} = \sqrt{\beta r} Z u + \sin\gamma \tag{11.10}$$

For small flight path angle, this deceleration is equal to the deceleration due to the drag force (see Exercise 11-1),

$$\frac{a}{g} = -\frac{1}{g}\frac{dV}{dt} \approx \sqrt{\beta r} Z u \tag{11.11}$$

Hence, the deceleration during entry is proportional to the product Zu. The deceleration due to the aerodynamic force, that is the combined lift and drag forces, as felt by the crew or an accelerometer during entry is

$$\frac{a}{g} = \sqrt{\left(\frac{L}{mg}\right)^2 + \left(\frac{D}{mg}\right)^2} = \sqrt{\beta r} Z u \sqrt{1 + \left(\frac{C_L}{C_D}\right)^2} \tag{11.12}$$

Hence, for entry at small angles, the deceleration due to aerodynamic force is obtained by simply multiplying the vehicle deceleration, given by Eq. (11.11) by the constant factor $\sqrt{1 + (C_L/C_D)^2}$.

The Z function provides the flight altitude of the vehicle, once the drag parameter $SC_D/2m$ is specified. For an arbitrary atmosphere, the altitude is most conveniently expressed in terms of the local atmospheric density ρ. Let subscript zero denote the condition at sea

level. From the definition (11.4) of Z, and using a strictly exponential atmosphere, we have

$$\frac{\rho}{\rho_0} = \frac{2m}{SC_D r \rho_0}\sqrt{\beta r}Z = e^{-\beta h} \tag{11.13}$$

In this equation, the strong variation is in the density and hence we can use $r \approx r_0$. Then, we have for the flight altitude

$$h = \frac{1}{\beta}\mathrm{Log}\left(\frac{SC_D r_0 \rho_0}{2m}\frac{1}{\sqrt{\beta r}Z}\right) \tag{11.14}$$

Another quantity of interest is the dynamic pressure exerted on the vehicle

$$\frac{1}{2}\rho V^2 = \frac{W}{SC_D}\sqrt{\beta r}Zu \tag{11.15}$$

Hence the dynamic pressure is proportional to the deceleration of the vehicle.

Relatively simple expressions can also be obtained for the aerodynamic heating rate per unit area, q, and the total heat absorbed per unit area, Q/A.

According to the local similarity law, the heating rate q at any point on the body is equal to a fraction of the heating rate q_s at a stagnation point of radius of curvature R. Thus, the local heating rate is expressed as

$$q = k_1 q_s \tag{11.16}$$

where k_1 is a constant and the heating rate in hypersonic flow at a stagnation point, q_s, can be expressed as

$$q_s = \frac{C}{\sqrt{R}}\left(\frac{\rho}{\rho_0}\right)^n\left(\frac{V}{\sqrt{gr}}\right)^m \tag{11.17}$$

where the constants C, n and m depend on the type of boundary layer flow. For laminar flow, $n = 1/2$. A simple power law $m = 3$ for the speed, together with Eq. (11.13) for the density ratio, gives the expression for the laminar convective heat transfer rate, in terms of the variables u and Z

$$q = \left[C\left(\frac{\beta}{r_0\rho_0^2}\right)^{1/4}\right]\left[k_1\sqrt{\frac{2m}{SC_D R}}\right]\bar{q} \tag{11.18}$$

where

$$\bar{q} = Z^{1/2} u^{3/2} \tag{11.19}$$

The expression for the heat transfer rate has been written in the form of the product of three factors. The first factor represents the effect on heat flux of the particular planetary atmosphere. The second factor represents the effect of the physical characteristics of the vehicle, that is the mass, dimensions and shape of the vehicle. The last factor represents the effect of the particular type of reentry trajectory. For any arbitrary vehicle, we only need to compute the dimensionless quantity $\bar{q}$ as defined by Eq. (11.19).

Equation (11.18) for the heating rate is useful in studying vehicles designed to operate at radiation equilibrium temperature. For heat-sink type vehicles, an equation for the total heat absorbed, Q, during entry is of more interest. This quantity is expressed in the form of an integral

$$Q = \iint q \, dt \, dA = \iint k_1 q_s \, dt \, dA \tag{11.20}$$

where A is the whole surface wetted by the boundary layer. Let

$$k_2 = \frac{1}{A} \int k_1 \, dA = \frac{1}{A} \int \frac{q}{q_s} \, dA \tag{11.21}$$

where k_2 is the factor which takes into account the variations in heat flux over the whole surface A. For a hemisphere we have $k_2 \approx 0.5$. With the definition of k_2, we have

$$Q = k_2 A \int q_s \, dt \tag{11.22}$$

Using Eq. (11.18) for $q_s = q/k_1$ in this integral, we have

$$Q = \left[C \left(\frac{\beta}{r_0 \rho_0^2} \right)^{1/4} \right] \left[k_2 A \sqrt{\frac{2m}{S C_D R}} \right] \int Z^{1/2} u^{3/2} \, dt \tag{11.23}$$

The integration can be performed with respect to the speed variable u by noticing that in Eq. (11.6) for small flight path angle, we have

$$\frac{du}{d\theta} = -\frac{2\sqrt{\beta r} Z u}{\cos \gamma}$$

On the other hand

$$\frac{d\theta}{dt} = \frac{V\cos\gamma}{r} = u^{1/2}\sqrt{\frac{g}{r}}\cos\gamma$$

Hence

$$\frac{du}{dt} = -2\sqrt{\beta g}Zu^{3/2} \tag{11.24}$$

By substituting into Eq. (11.23) and integrating from the initial speed u_i, we have the total heat absorbed between u_i and u

$$Q = \left[\frac{C}{2}\left(\frac{1}{\beta g^2 r_0 \rho_0^2}\right)^{1/4}\right]\left[k_2 A\sqrt{\frac{2m}{SC_D R}}\right]\bar{Q} \tag{11.25}$$

where

$$\bar{Q} = \int_u^{u_i} \frac{du}{Z^{1/2}} \tag{11.26}$$

Finally, from Eq. (11.24), we have the time of flight between u_i and u

$$t = \frac{1}{2\sqrt{\beta g}}\int_u^{u_i} \frac{du}{Zu^{3/2}} \tag{11.27}$$

11.3 Gliding entry at small flight path angles

The general equations of motion (11.9) are convenient for an accurate analysis of reentry trajectories. The variables are completely non-dimensionalized and the results apply to any vehicle regardless of its size, shape and mass. The planetary atmosphere is specified by the constant value of βr which, for the earth, can be taken as $\beta r = 900$. The parameters to be specified for the calculation of the reentry trajectory are the lift-to-drag ratio C_L/C_D, assumed constant, the initial flight path angle γ_i and the initial speed variable u_i, while the initial value of Z is nearly zero.

For some types of reentry trajectories, using physical assumptions, the general equations can be simplified and subsequently their integration will provide first order solutions which are adequate for a preliminary estimate of different physical quantities of interest such as the deceleration and the heating during entry. In this section, we shall consider the case of gliding entry at small flight path angles.

The main assumption for this type of entry trajectory is that the flight path angle is small, that is we have approximately

$$\sin\gamma \approx \gamma, \qquad \cos\gamma \approx 1 \tag{11.28}$$

and furthermore that during the main portion of the trajectory, its variation is slow so that we have approximately $d\gamma/d\theta \approx 0$. This is the assumption of equilibrium glide and from the equation for γ in system (11.9), we have

$$\frac{C_L}{C_D} + \frac{\cos\gamma}{\sqrt{\beta r}Z}\left(1 - \frac{1}{u}\right) = 0 \tag{11.29}$$

Putting $\cos\gamma \approx 1$, and solving for Z, we have

$$Z = \frac{1-u}{\sqrt{\beta r}(C_L/C_D)u} \tag{11.30}$$

This is the relation between the speed and the altitude during the glide. We put this relation in the form

$$\frac{1}{\sqrt{\beta r}Z} = \frac{\dfrac{C_L}{C_D}\dfrac{V^2}{V_c^2}}{1 - \dfrac{V^2}{V_c^2}} \tag{11.31}$$

It is appropriate to evaluate the circular speed $V_c = \sqrt{gr} \approx \sqrt{g_0 r_0}$ at a reference altitude, say at sea level (see Exercise 11-2). We have plotted $1/\sqrt{\beta r}Z$ versus $V/\sqrt{g_0 r_0}$ in Fig. 11.2 for different values of the lift-to-drag ratio C_L/C_D. In the figure, the abcissa represents the speed ratio V/V_c and the ordinate $1/\sqrt{\beta r}Z$ varies in the same direction as the altitude. It is clear that as the altitude decreases, the speed decreases. The plots can be used to determine the speed–altitude relationship for any vehicle. For example, once we specify the lift-to-drag ratio C_L/C_D for glide entry, at any speed ratio we have the corresponding value $\sqrt{\beta r}Z$. For any particular vehicle, with given drag parameter SC_D/mg, the actual altitude is given by Eq. (11.14). At any speed ratio, higher lift-to-drag ratio gives higher altitude. Also, a lower wing loading W/S leads to higher altitude during the glide.

From Eq. (11.30), since $Z > 0$, and at entry $Z_i \approx 0$, we see that the equilibrium glide applies to the case where the entry speed is nearly equal to the circular speed.

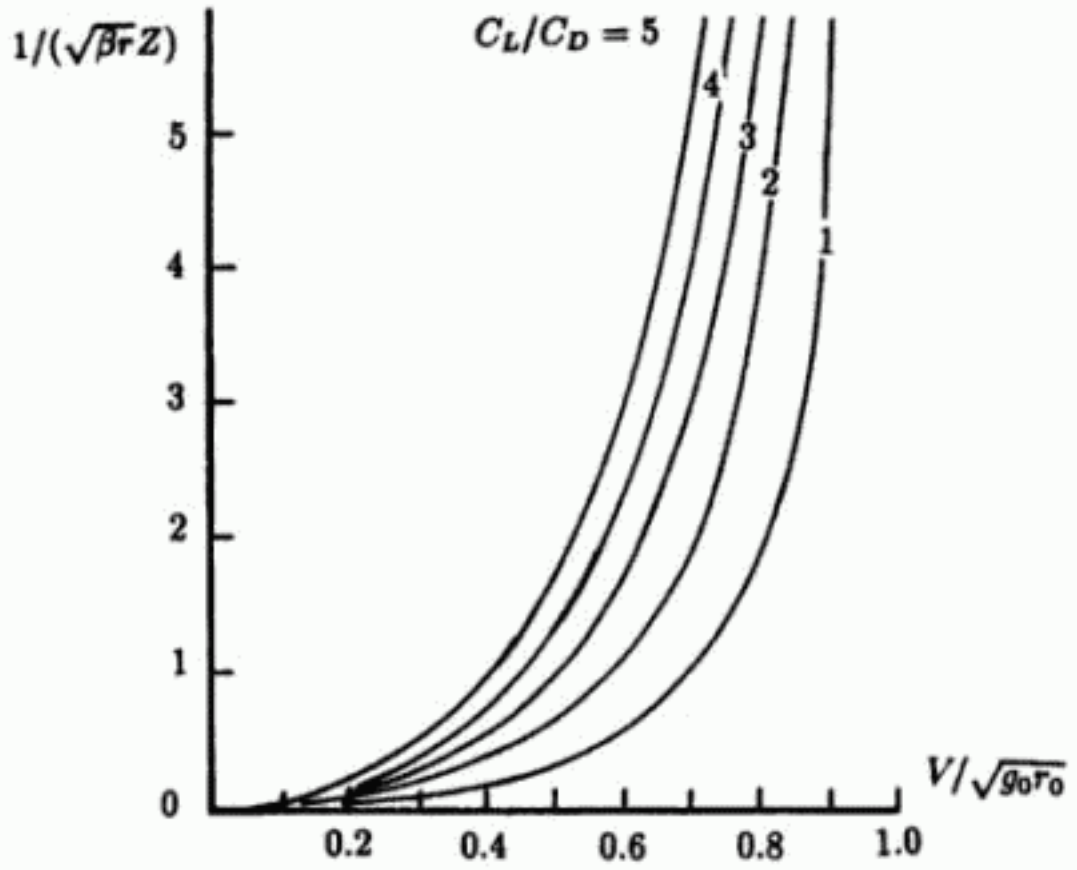

Figure 11.2: Velocity–altitude relationship during equilibrium glide.

To evaluate the variation in the flight path angle we use the equilibrium solution (11.30) to rewrite the equation for u in the system (11.9),

$$\frac{du}{d\theta} = -\frac{2(1-u)}{(C_L/C_D)\cos\gamma} - (2-u)\tan\gamma \tag{11.32}$$

By dividing this equation by the equation for Z and using solution (11.30), we obtain

$$\frac{du}{dZ} = \frac{u}{\sqrt{\beta r}}\left(\frac{2}{\sin\gamma} + \frac{2-u}{1-u}\frac{C_L}{C_D}\right) \tag{11.33}$$

On the other hand, from the solution (11.30) we have

$$\frac{du}{dZ} = -\sqrt{\beta r}\,\frac{C_L}{C_D}\,u^2 \tag{11.34}$$

Equating the last two equations and solving for $\sin\gamma$, we have

$$\sin\gamma = -\frac{2(1-u)}{(C_L/C_D)[\beta r u(1-u)+(2-u)]} \tag{11.35}$$

Because of the large factor βr in the denominator, the glide angle remains negligibly small until near the end when u tends to near zero. The limiting equations is

$$\sin\gamma = -\frac{1}{C_L/C_D} \tag{11.36}$$

for glide at low speed as has been derived in Chapter 5. The relation (11.35) for γ as a function of the speed ratio $V/\sqrt{g_0 r_0}$ is plotted in Fig. 11.3 for several values of the lift-to-drag ratio. It is clear from the solution that a higher lift-to-drag ratio yields a smaller glide angle.

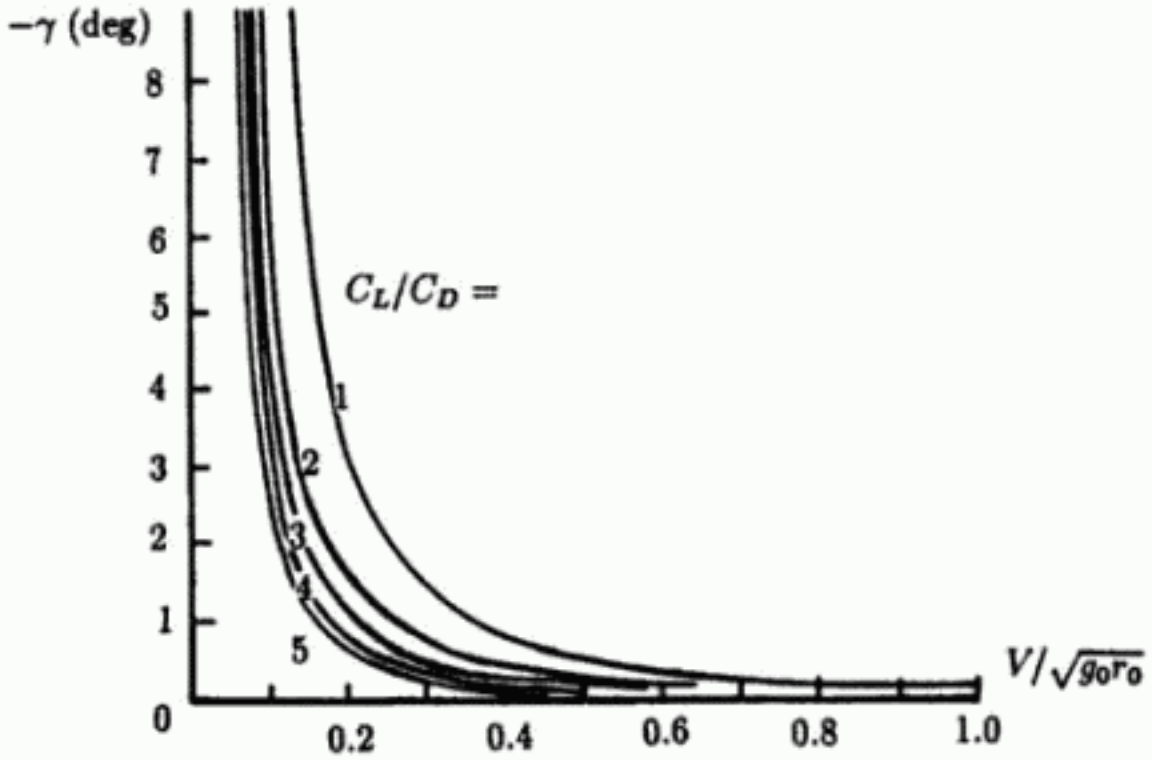

Figure 11.3: Glide angle as a function of the speed ratio

Glide entry is a flight program used to extend the range. To calculate the range, for small flight path angle, $\sin\gamma \approx 0$, and Eq. (11.6)

can be simplified to yield

$$\frac{du}{d\theta} = -2\sqrt{\beta r} Z u \tag{11.37}$$

Using the solution (11.30) in this equation, we have the equation for range θ

$$\frac{d\theta}{du} = -\frac{1}{2}\frac{C_L}{C_D}\frac{1}{1-u} \tag{11.38}$$

Integrating from the initial value of speed u_i, we obtain

$$\theta = \frac{1}{2}\frac{C_L}{C_D}\,\mathrm{Log}\,\frac{1-u}{1-u_i} \tag{11.39}$$

It is obvious from this equation that glide with maximum range is obtained with maximum lift-to-drag ratio.

The time of flight is obtained by integrating Eq. (11.27) using the equilibrium glide solution (11.30). We have

$$\sqrt{\frac{g}{r}}t = \frac{1}{2}\frac{C_L}{C_D}\int_u^{u_i} \frac{du}{(1-u)u^{1/2}} \tag{11.40}$$

By performing the integration, we obtain

$$\sqrt{\frac{g}{r}}t = \frac{1}{2}\frac{C_L}{C_D}\,\mathrm{Log}\left(\frac{1+\sqrt{u_i}}{1-\sqrt{u_i}}\,\frac{1-\sqrt{u}}{1+\sqrt{u}}\right) \tag{11.41}$$

Finally, the deceleration during the glide is given by Eq. (11.11) which, from the solution (11.30), is simply

$$\frac{a}{g} = \frac{1 - V^2/g_0 r_0}{C_L/C_D} \tag{11.42}$$

For gliding entry, as the speed decreases, the deceleration increases continuously along the descending trajectory and it is minimized by using the maximum lift-to-drag ratio.

11.4 Ballistic entry at large flight path angles

For ballistic entry, $C_L = 0$. The basic equations (11.9) become

$$\begin{aligned} \frac{dZ}{d\theta} &= -\beta r Z \tan\gamma \\ \frac{du}{d\theta} &= -\frac{2\sqrt{\beta r} Z u}{\cos\gamma} - (2-u)\tan\gamma \\ \frac{d\gamma}{d\theta} &= -\frac{1-u}{u} \end{aligned} \tag{11.43}$$

By dividing the last equation by the first, we obtain

$$\frac{d}{dZ}(\operatorname{Log}\cos\gamma) = -\frac{1-u}{\sqrt{\beta r}(\sqrt{\beta r} Z u)} \tag{11.44}$$

The equation is written in this form to show that, although initially $Z_i \approx 0$, for ballistic entry, the deceleration quickly becomes severe so that its magnitude, $\sqrt{\beta r} Z u$, will rapidly have a finite value rendering the right-hand side of Eq. (11.44) negligibly small. By putting this term equal to zero, we obtain, on integrating the equation, the first-order solution for ballistic entry

$$\cos\gamma = \cos\gamma_i \tag{11.45}$$

where γ_i is the initial entry angle.

For ballistic entry, the flight path angle remains nearly constant and the trajectory is essentially a small arc of a logarithmic spiral.

In the second equation of the system (11.43) the first term on the right-hand side is the drag force and it is much larger than the second term which comes from the gravity force and its effect due to the inverse square force field used to derive the equation for u. The basic assumption for ballistic entry is to neglect the gravity force, as compared to the very high drag force. If this is done, then on using the equation for Z to change the independent variable from θ to Z, we have

$$\frac{du}{dZ} = \frac{2u}{\sqrt{\beta r}\sin\gamma} \tag{11.46}$$

By putting $\gamma = \gamma_i$, this equation can be integrated from the initial condition to give

$$\frac{u}{u_i} = \exp\frac{2(Z - Z_i)}{\sqrt{\beta r}\sin\gamma_i} \tag{11.47}$$

Equations (11.45) and (11.47) constitute the first-order solution for ballistic entry at large flight path angles.

Equation (11.47), with the approximation $Z_i \approx 0$ at the initial entry altitude, can be written as

$$\frac{V}{V_i} = \exp \frac{Z}{\sqrt{\beta r} \sin \gamma_i} \tag{11.48}$$

From this equation, it is seen that, as altitude decreases, Z increases and the speed V decreases as the radius of a logarithmic spiral. The speed V decreases more rapidly with altitude for larger initial flight path angles. On the other hand, by the definition of Z, for each value of altitude, Z is larger for larger values of the drag coefficient and smaller values of the wing loading mg/S. Hence, the speed decreases more rapidly with a larger drag coefficient and a smaller wing loading.

The deceleration is given by Eq. (11.11). We have, using the solution (11.47) for u, the expression for the deceleration as a function of altitude

$$\frac{a}{g} = \sqrt{\beta r}\, u_i Z \exp \frac{2(Z - Z_i)}{\sqrt{\beta r} \sin \gamma_i} \tag{11.49}$$

The maximum deceleration occurs at the altitude Z_* obtained by solving the equation $da/dZ = 0$. Explicitly, we have

$$\frac{Z_*}{\sqrt{\beta r}} = -\frac{1}{2} \sin \gamma_i \tag{11.50}$$

From the definition of Z, this critical altitude is positive if and only if

$$-\sin \gamma_i \leq \frac{SC_D \rho_0}{m\beta} \tag{11.51}$$

where ρ_0 is the value of ρ at sea level. If this inequality is not satisfied, the deceleration continues to increase and reaches a maximum at the altitude zero. In this case, the maximum deceleration is

$$\left(\frac{a}{g}\right)_{max} = \sqrt{\beta r}\, u_i Z_0 \exp \frac{2(Z_0 - Z_i)}{\sqrt{\beta r} \sin \gamma_i} \tag{11.52}$$

where Z_0 is the value of Z at sea level

$$Z_0 = \frac{\rho_0 SC_D}{2m} \sqrt{\frac{r_0}{\beta}} \tag{11.53}$$

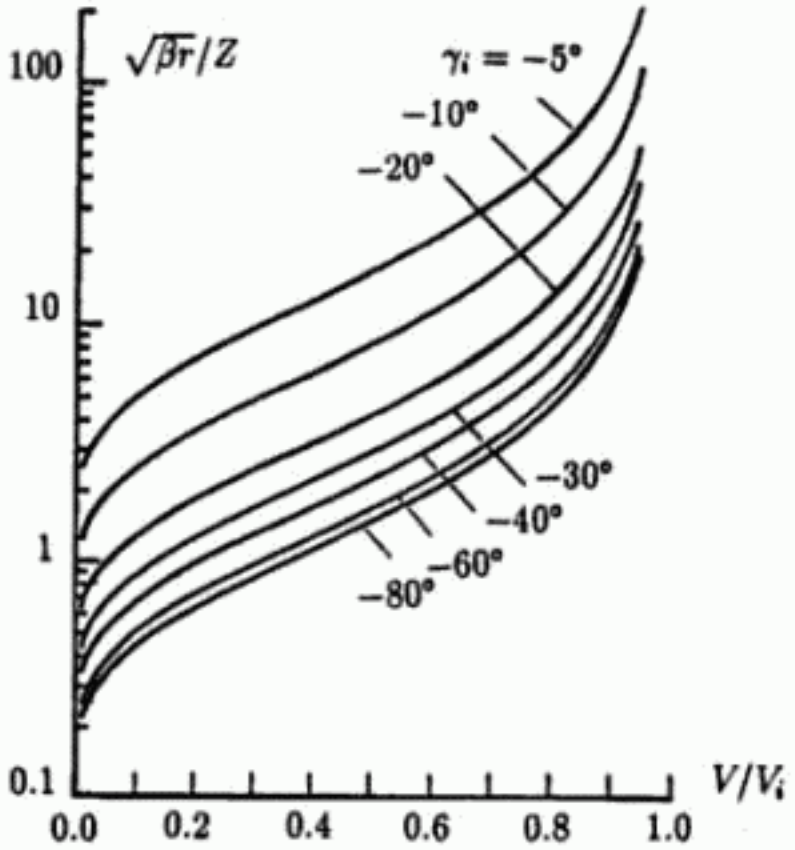

Figure 11.4: Altitude–velocity diagram for ballistic entry.

In the case where the strict inequality in Eq. (11.51) is satisfied, the maximum deceleration occurs at an altitude h_* above the surface of the earth. The corresponding value of Z is given by Eq. (11.50). Using this value in Eq. (11.47) with $Z_i = 0$, we have

$$\frac{u_*}{u_i} = \frac{1}{e}$$

Therefore

$$V_* = \frac{V_i}{\sqrt{e}} = 0.607 V_i \tag{11.54}$$

Thus, the point on the entry trajectory where the speed has decreased to about 60.7% of its initial value is the point of maximum deceleration. The maximum value of the deceleration is obtained from Eq. (11.49) with Z_* as given by Eq. (11.50). We have

$$\frac{a_*}{g} = -\frac{\beta r u_i}{2e} \sin \gamma_i \tag{11.55}$$

We see that the maximum deceleration is proportional to the quantity $u_i \sin \gamma_i$ and, according to the first-order solution, it is independent of the physical characteristics of the vehicle.

Figure 11.4 presents the velocity–altitude relationship, Eq. (11.48), for different values of the initial flight path angle. The use of the dimensionless quantity $\sqrt{\beta r}/Z$ as ordinate is convenient since the diagram applies to any type of vehicle regardless of its physical characteristics. For each specified vehicle, one can calculate its sea level value Z_0 by Eq. (11.53) and deduce the speed ratio at this level. This also applies to any altitude level by using the corresponding value of ρ.

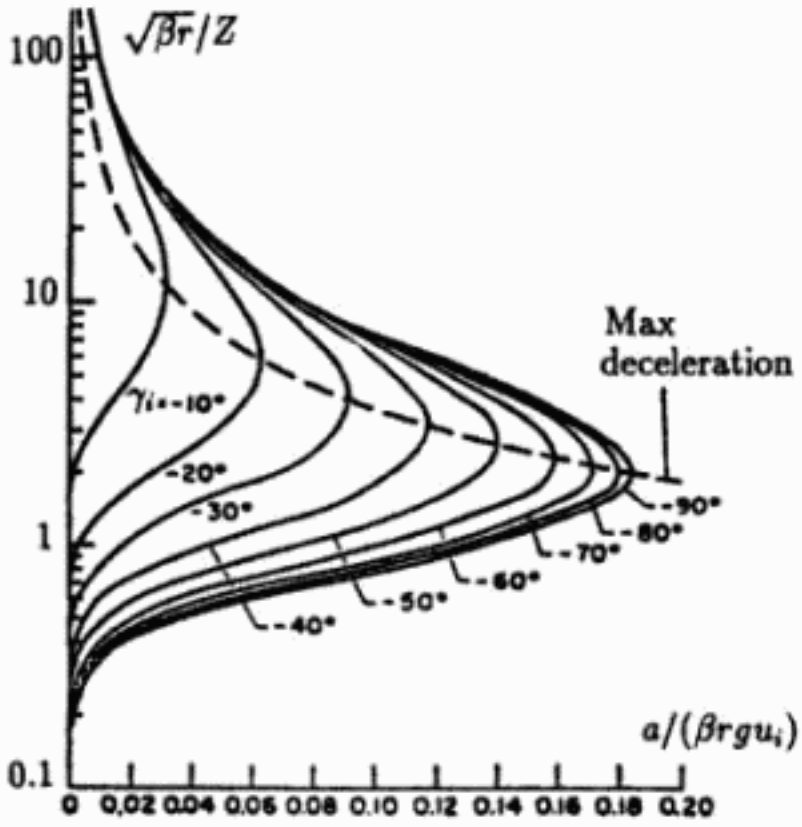

Figure 11.5: Altitude–deceleration diagram for ballistic entry.

Figure 11.5 presents the deceleration–altitude relationship, Eq. (11.49), for different values of the initial flight path angle. It is convenient for the plot to write this equation as

$$\frac{a}{(\beta r) g u_i} = \frac{Z}{\sqrt{\beta r}} \exp \frac{2Z}{\sqrt{\beta r} \sin \gamma_i} \tag{11.56}$$

Then by plotting $\sqrt{\beta r}/Z$ versus $a/(\beta r)gu_i$, the diagram can be used for any type of entry vehicle at any initial speed. The line of maximum deceleration, the dashed line in the figure, is the hyperbola

$$\frac{\sqrt{\beta r}}{Z}\frac{a}{\beta r g u_i} = \frac{1}{e} = 0.36788 \tag{11.57}$$

11.5 Skip entry

A trajectory of interest for a lifting hypervelocity vehicle is the skip trajectory. In the skipping phase, the vehicle enters the atmosphere, negotiates a turn, and is ejected from the atmosphere (Fig. 11.6).

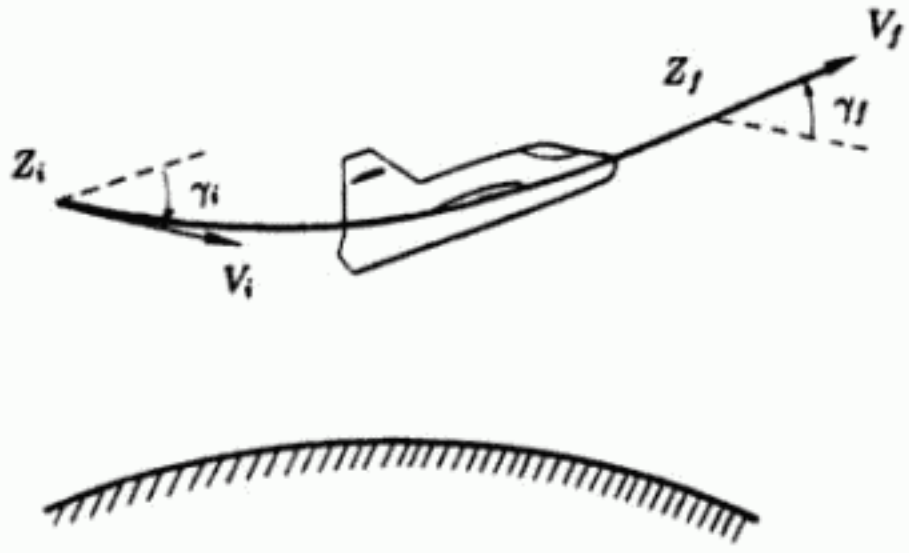

Figure 11.6: Geometry of the skip trajectory.

This type of maneuver can be used to achieve a change in the orbital plane. Only the maneuver at constant lift-to-drag ratio in a vertical plane will be analyzed in this section. The skip trajectory involves a short longitudinal range. Hence, the flat earth assumption will be used and the centrifugal force in the equation for γ can be neglected. Furthermore, since the gravitational force is, on average, much smaller

than the aerodynamic force, we can also neglect the gravitational force in the equations of motion.

With these assumptions, we deduce from the general equations (11.9) the equations of motion governing a skip trajectory

$$\begin{aligned} \frac{dZ}{d\theta} &= -\beta r Z \tan\gamma \\ \frac{du}{d\theta} &= -\frac{2\sqrt{\beta r} Z u}{\cos\gamma} \\ \frac{d\gamma}{d\theta} &= \frac{\sqrt{\beta r} Z}{\cos\gamma} \frac{C_L}{C_D} \end{aligned} \tag{11.58}$$

If the altitude Z is used as an independent variable to replace θ, we have the equations for u and γ

$$\begin{aligned} \frac{du}{dZ} &= \frac{2u}{\sqrt{\beta r}\sin\gamma} \\ \frac{d\gamma}{dZ} &= -\frac{C_L}{C_D} \frac{1}{\sqrt{\beta r}\sin\gamma} \end{aligned} \tag{11.59}$$

The second equation can be integrated to give

$$\cos\gamma - \cos\gamma_i = \frac{C_L}{C_D} \frac{Z - Z_i}{\sqrt{\beta r}} \tag{11.60}$$

The vehicle exits at a final altitude level Z_f equal to the initial altitude level Z_i. Hence $\cos\gamma_f = \cos\gamma_i$ and

$$\gamma_f = -\gamma_i \tag{11.61}$$

This shows that, for a skip maneuver at constant angle-of-attack, the exit angle is equal to the opposite of the entry angle.

At the lowest point of a skip trajectory, $\gamma = 0$. The minimum altitude is then

$$\frac{Z}{\sqrt{\beta r}} = \frac{Z_i}{\sqrt{\beta r}} + \frac{1 - \cos\gamma_i}{C_L/C_D} \tag{11.62}$$

For this altitude to be positive, from the definition of Z, it is necessary that

$$\frac{1 - \cos\gamma_i}{C_L/C_D} < \frac{SC_D\rho_0}{2m\beta}$$

where the condition $Z_i = 0$ has been assumed. We can write the condition as

$$\sin^2 \frac{\gamma_i}{2} < \frac{g\rho_0 C_L}{4\beta(mg/S)} \tag{11.63}$$

This inequality provides the altitude safety limit on the entry angle for a vehicle with specified lift capability and wing loading condition.

To obtain the velocity distribution along a skip trajectory, we combine the two equations (11.59) in the form

$$\frac{du}{d\gamma} = -\frac{2u}{C_L/C_D} \tag{11.64}$$

On integrating this equation, we obtain

$$\frac{u}{u_i} = \exp \frac{2(\gamma_i - \gamma)}{C_L/C_D} \tag{11.65}$$

or, in terms of V

$$\frac{V}{V_i} = \exp \frac{\gamma_i - \gamma}{C_L/C_D} \tag{11.66}$$

Since at exit $\gamma_f = -\gamma_i$, we obtain the final speed

$$V_f = V_i \exp \frac{2\gamma_i}{C_L/C_D} \tag{11.67}$$

Equations (11.60) and (11.65) constitute the first-order solution for a skip trajectory.

The range is given by the last of the Eqs. (11.58) which, with the solution (11.60) becomes

$$\beta r \frac{d\theta}{d\gamma} = \frac{\cos\gamma}{\cos\gamma - \cos\gamma_0} \tag{11.68}$$

where the modified initial angle γ_0 is defined by

$$\cos\gamma_0 = \cos\gamma_i - \frac{C_L}{C_D} \frac{Z_i}{\sqrt{\beta r}} \tag{11.69}$$

The integration from the initial angle γ_i gives the solution

$$\beta r\theta = \gamma - \gamma_i + \cot\gamma_0 \operatorname{Log} \frac{\tan(\gamma_0/2) + \tan(\gamma/2)}{\tan(\gamma_0/2) - \tan(\gamma/2)} \frac{\tan(\gamma_0/2) - \tan(\gamma_i/2)}{\tan(\gamma_0/2) + \tan(\gamma_i/2)} \tag{11.70}$$

In the calculation, the angle γ_0 as defined by Eq. (11.69) should be evaluated with its positive argument. Furthermore, the small term $(\gamma - \gamma_i)$ can be neglected. For example, the total range, at $\gamma_f = -\gamma_i$ is seen to be

$$\beta r \theta_f = -2\gamma_i + 2\cot\gamma_0 \operatorname{Log}\left[\frac{\tan(\gamma_0/2) - \tan(\gamma_i/2)}{\tan(\gamma_0/2) + \tan(\gamma_i/2)}\right] \tag{11.71}$$

With an entry angle of $\gamma_i = -5$ degrees, and for the angle γ_0 nearly the same but with a positive argument, say $\gamma_0 = 5.2$ degrees. The range angle is $\theta_f = 0.096$ rad $= 5.5$ deg. The distance travelled is indeed small, and the flat earth assumption for the skip trajectory is justified.

Again, we use Eq. (11.11) for the tangential deceleration. Using the solution (11.60) with $Z_i \approx 0$, for Z and the solution (11.65) for u, we write it as

$$\frac{a}{g} = \frac{\beta r u_i(\cos\gamma - \cos\gamma_i)}{C_L/C_D} \exp\frac{2(\gamma_i - \gamma)}{C_L/C_D} \tag{11.72}$$

By this expression, the deceleration is a function of γ alone. The maximum deceleration occurs at a value of γ obtained by solving the equation $da/d\gamma = 0$. We have

$$\frac{1}{2}\frac{C_L}{C_D}\sin\gamma = \cos\gamma_i - \cos\gamma \tag{11.73}$$

This can be written as a quadratic equation in $\tan(\gamma/2)$

$$2\cos^2\frac{\gamma_i}{2}\tan^2\frac{\gamma}{2} - \frac{C_L}{C_D}\tan\frac{\gamma}{2} - 2\sin^2\frac{\gamma_i}{2} = 0 \tag{11.74}$$

The equation has two roots, one positive and one negative. For a descending trajectory, we take the negative root

$$\tan\frac{\gamma}{2} = \frac{1}{4\cos^2(\gamma_i/2)}\left[\frac{C_L}{C_D} - \sqrt{\left(\frac{C_L}{C_D}\right)^2 + 4\sin^2\gamma_i}\right] \tag{11.75}$$

Using this critical value for γ in Eq. (11.65) and Eq. (11.72), we have the corresponding speed and the maximum deceleration. The altitude at which the maximum deceleration occurs in given by Eq. (11.60) with γ as given by Eq. (11.75).

Let subscript $*$ denote the condition at the point of peak deceleration. We have

$$\frac{C_L}{C_D}\frac{Z_* - Z_i}{\sqrt{\beta r}} = \cos\gamma_* - \cos\gamma_i = -\frac{1}{2}\frac{C_L}{C_D}\sin\gamma_* \tag{11.76}$$

Since $Z_* > Z_i$, $\gamma_* < 0$, and the peak deceleration occurs during the descending portion of the trajectory. From Eq. (11.76)

$$\frac{Z_* - Z_i}{\sqrt{\beta r}} = -\frac{\tan(\gamma_*/2)}{1 + \tan^2(\gamma_*/2)} \tag{11.77}$$

To reduce the deceleration, a skip trajectory is flown with small flight path angle with a certain moderate lift-to-drag ratio. Hence, we have

$$\frac{4 \sin^2 \gamma_i}{(C_L/C_D)^2} \ll 1$$

and the square root in Eq. (11.75) is approximated by

$$\sqrt{(C_L/C_D)^2 + 4 \sin^2 \gamma_i} \approx \frac{C_L}{C_D}\left[1 + \frac{2 \sin^2 \gamma_i}{(C_L/C_D)^2}\right]$$

Using this approximate relation in Eq. (11.75), we have the expression for the critical flight path angle where maximum deceleration occurs

$$\tan \frac{\gamma_*}{2} = -\frac{2 \sin^2(\gamma_i/2)}{C_L/C_D} \tag{11.78}$$

With this approximate solution for small flight path angle, we see that the peak deceleration occurs during descent and near the lowest point of the trajectory.

From Eq. (11.77), we see that the approximate critical altitude is

$$\frac{Z_* - Z_i}{\sqrt{\beta r}} = \frac{2 \sin^2(\gamma_i/2)}{C_L/C_D} \tag{11.79}$$

For small flight path angle, we write Eq. (11.78) as

$$\gamma_* = -\frac{\gamma_i^2}{C_L/C_D} \tag{11.80}$$

Since γ_* is of the second order in γ_i, we deduce from Eq. (11.66) the critical speed at the peak deceleration

$$V_* = V_i \exp \frac{\gamma_i}{C_L/C_D} \tag{11.81}$$

This speed is also the speed at the lowest point of the skip trajectory. With the same approximation, we calculate the maximum deceleration

$$\left(\frac{a}{g}\right)_{max} = \sqrt{\beta r} Z_* u_* = \frac{\beta r \gamma_i^2 V_i^2}{2V_c^2(C_L/C_D)} \exp \frac{2\gamma_i}{C_L/C_D} \tag{11.82}$$

In this explicit formula, $\beta r = 900$ and V_c is the circular speed at sea level. By inspecting the formula we see that higher initial speed and larger entry angle increase the maximum deceleration while higher lift-to-drag ratio decreases it (see Exercise 11-8).

11.6 Aerodynamic heating

The various first-order solutions presented above are now employed to analyze the thermal problems encountered in hypersonic flight. The study is of fundamental interest to scientists and engineers involved in the design of aerospace vehicles and in the planning of flight operations for a given mission. In space flight, achieving a maximum payload is always a factor of prime consideration. A relatively important fraction of this payload is used in the protection and cooling process during entry if the spacecraft is to be recovered. A detailed discussion of aerodynamic heating can be found in specialized text on reentry trajectories (Vinh, 1980). Here, in flight performance, we are interested in evaluating the various thermal quantities involved in the heating process during entry.

According to Allen and Eggers (1958), the three most important parameters in aerodynamic heating during entry are:

1. The heating rate q and its maximum heating rate q_{max} at any point on the body.
2. The average rate of heat input per unit area q_{av} from the air to the surface of the reentry body and its maximum value.
3. The total heat absorbed Q.

In terms of the dimensionless atmospheric density Z, and speed variable u, we have derived Eq. (11.19) for the dimensionless heating rate $\bar{q}$ and the integral (11.26) for the dimensionless total heat absorbed $\bar{Q}$.

The time rate of average heat input per unit area is given by

$$q_{av} = \frac{1}{4} C_F \rho V^3 \tag{11.83}$$

where C_F is termed the equivalent skin friction coefficient and will be assumed constant at a mean value for a particular vehicle. Then, in dimensionless form, we consider the function

$$\bar{q}_{av} = Z u^{3/2} \tag{11.84}$$

The variations of these thermal quantities will be evaluated separately for each type of entry trajectory.

11.6.1 Gliding entry

Along an equilibrium glide path, the density is given by Eq. (11.30). For the heating rate, we use Eq. (11.19) to obtain

$$\bar{q} = \frac{(1-u)^{1/2} u}{(\beta r)^{1/4} (C_L/C_D)^{1/2}} \tag{11.85}$$

Considered as a function of u, the heating rate passes through a maximum when $u = 2/3$. This corresponds to a maximum value of

$$\bar{q}_{max} = \frac{2}{3(\beta r)^{1/4} [3(C_L/C_D)]^{1/2}} \tag{11.86}$$

We conclude that the peak heating rate occurs when the speed is equal to 81.6% of the initial circular entry speed, and that the maximum rate is lower with higher lift-to-drag ratio.

If the solution (11.30) is used in Eq. (11.84), we have for the average rate of heat input

$$\bar{q}_{av} = \frac{(1-u) u^{1/2}}{(\beta r)^{1/2} (C_L/C_D)} \tag{11.87}$$

Considered as a function of u, the average rate of heat input passes through a maximum when $u = 1/3$. This corresponds to a maximum value of

$$(\bar{q}_{av})_{max} = \frac{2}{3(3\beta r)^{1/2} (C_L/C_D)} \tag{11.88}$$

The rate of heat input is a maximum when the speed has decreased to 57.7% of the initial circular entry speed, and this maximum rate is lower with higher lift-to-drag ratio.

If we use the solution (11.30) in the integral (11.26), we have the total heat absorbed

$$\bar{Q} = (\beta r)^{1/4}\left(\frac{C_L}{C_D}\right)^{1/2} \int_{u_f}^{u_i} \frac{u^{1/2}du}{(1-u)^{1/2}} \tag{11.89}$$

By using the end-point values $u_i = 1$ and $u_f = 0$, we have

$$\bar{Q} = \frac{1}{2}(\beta r)^{1/4}(C_L/C_D)^{1/2}\pi \tag{11.90}$$

The total heat absorbed is higher with higher value of the lift-to-drag ratio. This is because with higher lift-to-drag ratio, the time of flight is longer, and as a consequence, the total heat absorbed is larger.

11.6.2 Ballistic entry

For ballistic entry, we use the solution (11.47) with $Z_i \approx 0$ to evaluate the function (11.19). We have

$$\bar{q} = u_i^{3/2} Z^{1/2} \exp \frac{3Z}{\sqrt{\beta r}\sin\gamma_i} \tag{11.91}$$

Considered as a function of Z, this heating rate passes through a maximum at the density altitude

$$Z = -\frac{\sqrt{\beta r}}{6}\sin\gamma_i \tag{11.92}$$

On substituting into Eq. (11.91), we have the maximum rate

$$\bar{q}_{max} = (\beta r)^{1/4} u_i^{3/2}\left(-\frac{\sin\gamma_i}{6e}\right)^{1/2} \tag{11.93}$$

This rate increases with higher entry speed and steeper entry angle.

Concerning the average rate of heat input, as given by Eq. (11.84), for ballistic entry we have

$$\bar{q}_{av} = u_i^{3/2} Z \exp \frac{3Z}{\sqrt{\beta r}\sin\gamma_i} \tag{11.94}$$

The maximum of this average rate occurs when

$$Z = -\frac{\sqrt{\beta r}}{3}\sin\gamma_i \tag{11.95}$$

On substituting into Eq. (11.94) we have the maximum value

$$(\bar{q}_{av})_{max} = -\frac{\sqrt{\beta r}}{3e}u_i^{3/2}\sin\gamma_i \tag{11.96}$$

Again, we see that this maximum rate is higher with higher entry speed and steeper entry angle. For the total heat absorbed, we use Eq. (11.46) in the integral (11.26) to change the variable from u to Z and then substitute the solution (11.47) to obtain

$$\bar{Q} = \frac{2u_i}{\sqrt{\beta r}\sin\gamma_i}\int_{z_f}^{z_i} Z^{-1/2}\exp\frac{2Z}{\sqrt{\beta r}\sin\gamma_i}dZ \tag{11.97}$$

Let

$$\frac{2Z}{\sqrt{\beta r}\sin\gamma_i} = -\nu^2 \tag{11.98}$$

It is seen that, with this transformation, we can put the expression for $\bar{Q}$ in the form

$$\bar{Q} = u_i\sqrt{\frac{2\pi}{-\sqrt{\beta r}\sin\gamma_i}}\,\mathrm{erf}(\nu_f) \tag{11.99}$$

where the error function is defined as

$$\mathrm{erf}(x) = \frac{2}{\sqrt{\pi}}\int_0^x e^{-\nu^2}d\nu \tag{11.100}$$

and is a tabulated function (Abramowitz, 1964).

11.6.3 Skip entry

For a skip trajectory, we use the solutions (11.60) with $Z_i \approx 0$ and (11.65) in Eq. (11.19) to obtain

$$\bar{q} = \frac{(\beta r)^{1/4}u_i^{3/2}}{(C_L/C_D)^{1/2}}(\cos\gamma - \cos\gamma_i)^{1/2}\exp\frac{3(\gamma_i - \gamma)}{C_L/C_D} \tag{11.101}$$

Considered as a function of the flight path angle γ, this heating rate reaches a maximum when

$$6(\cos\gamma - \cos\gamma_i) + \frac{C_L}{C_D}\sin\gamma = 0 \tag{11.102}$$

Since the first term is positive, the solution is obtained for $\sin\gamma < 0$, that is during the descending part of the skip trajectory. By using the half-tangent formulas, we obtain a quadratic equation for $\tan(\gamma/2)$ which can be solved to give

$$\tan\frac{\gamma}{2} = \frac{1}{12\cos^2(\gamma_i/2)}\left[\frac{C_L}{C_D} - \sqrt{\left(\frac{C_L}{C_D}\right)^2 + 36\sin^2\gamma_i}\right] \tag{11.103}$$

By following the same discussion as in Section 11.5 for the maximum deceleration, for small entry flight path angle, we obtain the approximate solution

$$\tan\frac{\gamma}{2} = -\frac{6\sin^2(\gamma_i/2)}{C_L/C_D} \tag{11.104}$$

Since $\gamma \approx \gamma_i^2$, we use this approximation to evaluate the maximum heating rate as

$$\bar{q}_{max} = -\frac{(\beta r)^{1/4}u_i^{3/2}\gamma_i}{\sqrt{2C_L/C_D}}\exp\frac{3\gamma_i}{C_L/C_D} \tag{11.105}$$

By repeating the same analysis with the average heat input per unit area, we first obtain the expression

$$\bar{q}_{av} = \frac{(\beta r)^{1/2}u_i^{3/2}}{C_L/C_D}(\cos\gamma - \cos\gamma_i)\exp\frac{3(\gamma_i - \gamma)}{C_L/C_D} \tag{11.106}$$

The maximization of this quantity with respect to γ leads to the equation

$$3(\cos\gamma - \cos\gamma_i) + \frac{C_L}{C_D}\sin\gamma = 0 \tag{11.107}$$

By taking the negative root we obtain the solution for the flight path angle where the maximum rate of heat input occurs

$$\tan\frac{\gamma}{2} = \frac{1}{6\cos^2(\gamma_i/2)}\left[\frac{C_L}{C_D} - \sqrt{\left(\frac{C_L}{C_D}\right)^2 + 9\sin^2\gamma_i}\right] \tag{11.108}$$

For small entry angle, we have the approximate solution

$$\tan\frac{\gamma}{2} = -\frac{3\sin^2(\gamma_i/2)}{C_L/C_D} \tag{11.109}$$

Again since this critical value for γ is very small, we have the maximum value of $\bar{q}_{av}$ in the form

$$(\bar{q}_{av})_{max} = \frac{(\beta r)^{1/2} u_i^{3/2} \gamma_i^2}{2(C_L/C_D)} \exp\frac{3\gamma_i}{C_L/C_D} \tag{11.110}$$

As for the integral (11.26) for the total heat absorbed, if Eq. (11.64) is used to change the variable for integration from u to γ, and the solutions (11.60) and (11.65) substituted, we have

$$\bar{Q} = \frac{2u_i}{(\beta r)^{1/4}(C_L/C_D)^{1/2}} \int_{\gamma_i}^{\gamma_f} \frac{1}{(\cos\gamma - \cos\gamma_0)^{1/2}} \exp\frac{2(\gamma_i - \gamma)}{C_L/C_D}\, d\gamma \tag{11.111}$$

Here, to avoid the singularity at the initial and the final points, just as in the integration of Eq. (11.68) for the range, we have replaced $\cos\gamma_i$ by $\cos\gamma_0$ as defined in Eq. (11.69). Still, the integral cannot be expressed in terms of elementary functions. A simple way to perform the quadrature is to use an average value for $\cos\gamma$, and it is the same as using an average value for the density during the skip. In this case, we have by integrating Eq. (11.26) with $Z = Z_{av}$

$$\bar{Q} = \frac{u_i - u_f}{(Z_{av})^{1/2}} = \frac{u_i}{(Z_{av})^{1/2}}\left(1 - \exp\frac{4\gamma_i}{C_L/C_D}\right) \tag{11.112}$$

From the solution (11.60) for skip trajectory, the average value of Z is

$$Z_{av} = \frac{1}{\gamma_f - \gamma_i}\int_{\gamma_i}^{\gamma_f} Z\, d\gamma = Z_i + \frac{\sqrt{\beta r}}{C_L/C_D}\left(\frac{\sin\gamma_i}{\gamma_i} - \cos\gamma_i\right) \tag{11.113}$$

As a numerical example, with $\beta r = 900$, and for $C_L/C_D = 1.0$, and an entry angle of $\gamma_i = -5$ deg, while in the exact integral the density variable Z increases from the initial value Z_i to a maximum value of $Z_i + 0.114$ at the lowest point of the trajectory where $\gamma = 0$, and then returns to the value Z_i at exit, by Eq. (11.113), the average value of Z is $Z_i + 0.076$.

11.7 Comparative analysis of performance

At the beginning of the space flight era, space vehicles were designed for ballistic entry. With the advent of the space shuttle, glide entry has become a reality. Aerospace vehicles of the future will be more versatile and can enter a planetary atmosphere in any of the three entry modes that have been discussed in this chapter. Thus, it is of interest to compare the performance of these typical entry modes.

First, from the range standpoint, ballistic entry is the least effective mode. For skip entry, the range for each separate skipping phase is short but each atmospheric portion of the flight trajectory is followed by a Keplerian portion in space adding a significant distance to the total range. As a matter of fact, with a high initial entry speed a skip trajectory can achieve infinite range while a glide trajectory totally immersed in the atmosphere is condemned to a finite range. Thus, there exists an initial speed such that there is equal range for skip entry and glide entry, with gliding flight achieving the longer range at lower initial speed (see Exercise 11-12).

From considerations of aerodynamic heating, with the possible exception of the relatively dense vehicle in the ballistic mode, in all three modes, the hypervelocity vehicle expends the major part of its kinetic energy in flight and receives in exchange heat by convection. For a purely ballistic vehicle, this total heat input can be reduced by using high pressure-drag shapes, that is, blunted shapes. On the other hand, in the skip and glide modes, the geometric configuration of the vehicle will be slender to provide a moderate lift-to-drag ratio and as a consequence the heat load may be too high for the vehicle materials to absorb. In skip or glide mode one must, therefore, consider the possibility of the vehicle radiating a significant part of this heat back to the surrounding atmosphere. This problem has been extensively discussed in the literature and it is found that in a high lift-to-drag ratio glide mode, if the surface temperature is allowed to reach a high level, the vehicle can radiate heat at a rate equal to the maximum average convective heat transfer rate. Furthermore, in the glide mode, the vehicle may require less coolant than in the ballistic mode. The reason for this is that although in the glide mode the same vehicle will receive more heat, the gliding time is much longer. Therfore, with a sufficiently high radiant heat transfer rate the glide vehicle can return to the atmosphere

most of the heat it receives by convection.

In general, for a lifting hypervelocity vehicle, a combination of an initial entry at a high angle-of-attack using a nearly ballistic mode, followed by a tip over to lower the angle-of-attack, and continued with a high lift-to-drag ratio glide mode, would provide an adequate control of aerodynamic heating.

For manned flights, another factor to be considered is the peak deceleration. It has been shown before that this is essentially measured by the dynamic pressure. In structural analysis, this is also a factor to be considered for the selection of the material used for the protective wall of the vehicle exposed to the oncoming airstream.

Along each entry trajectory, we have obtained the explicit solutions for the points where the quantities $\bar{q}$, $\bar{q}_{av}$, and a/g reach their respective maximum values. These solutions are now summarized in Table 11.1.

Table 11.1: Points of maximum $\bar{q}$, $\bar{q}_{av}$ and a/g.

	Ballistic	Skip	Glide
$(\bar{q})_{max}$	$Z = -\frac{\sqrt{\beta r}}{6}\sin\gamma_i$	$\tan\frac{\gamma}{2} = -\frac{6\sin^2(\gamma_i/2)}{C_L/C_D}$	$\frac{V}{\sqrt{g_0 r_0}} = \frac{\sqrt{6}}{3}$
$(\bar{q}_{av})_{max}$	$Z = -\frac{\sqrt{\beta r}}{3}\sin\gamma_i$	$\tan\frac{\gamma}{2} = -\frac{3\sin^2(\gamma_i/2)}{C_L/C_D}$	$\frac{V}{\sqrt{g_0 r_0}} = \frac{\sqrt{3}}{3}$
$(a/g)_{max}$	$Z = -\frac{\sqrt{\beta r}}{2}\sin\gamma_i$	$\tan\frac{\gamma}{2} = -\frac{2\sin^2(\gamma_i/2)}{C_L/C_D}$	$\frac{V}{\sqrt{g_0 r_0}} = 0$

In the ballistic mode at nearly constant angle γ, the maximum of $\bar{q}$ occurs first, at the lowest value of Z, (hence at the highest altitude), then comes the maximum of $\bar{q}_{av}$, and finally the maximum of a/g.

In the skip mode the negative flight path angle increases from the initial value γ_i to $\gamma = 0$ when the vehicle reaches the lowest point. From the Table, the three maxima occur in the same order.

Finally in the glide mode, as the speed decreases continuously along the flight trajectory, again the vehicle reaches $\bar{q}_{max}$ first, and then $(\bar{q}_{av})_{max}$. In the meantime the deceleration builds up to reach its maximum at the final time.

We should notice that these conclusions were based on the first-order solutions obtained from a simplified system of equations with constant angle-of-attack. But it turns out that this is also true if we

use an arbitrary angle-of-attack varying as a function of time in the exact equations of motion for the integration. The general rule is as follows. By the definition of $\bar{q}$, $\bar{q}_{av}$ and a/g and similar functions, we can always raise them to a proper power and consider the maximum of the function

$$F = KZu^m \tag{11.114}$$

where K is a constant coefficient and m is a positive exponent not necessarily an integer. Then, for unpowered, three dimensional reentry trajectories with arbitrary modulation of the angle-of-attack and the bank angle as functions of time, the maximum of the function F, with $m > 0$, occurs during the descending phase. Furthermore, if we consider two functions F_1 and F_2, with exponents $m_1 > m_2$, then the maximum of F_1 occurs before the maximum of F_2. Obviously, at the limit where $m = 0$, the maximum of the density altitude Z occurs last at $\gamma = 0$ when the vehicle reaches the lowest point of the trajectory. The proof of this very general property was given by Vinh and Lu (1988).

As a final note, the definition of the dimensionless atmospheric density Z to be used as the altitude variable, as shown in Eq. (11.4), is appropriate for analyzing entry at constant angle-of-attack. For the case where the lift coefficient C_L, and consequently the drag coefficient C_D are allowed to vary as functions of time, we simply replace C_D in Eq. (11.4) by a reference constant aerodynamic coefficient. It has been found that we can use a new modified Chapman's Z variable defined as

$$Z = \frac{\rho S C_L^*}{2m}\sqrt{\frac{r}{\beta}} \tag{11.115}$$

where C_L^* is the lift coefficient at maximum lift-to-drag ratio for a parabolic drag polar

$$C_L^* = \sqrt{\frac{C_{D_0}}{K}} \tag{11.116}$$

With this, the equation for Z remains the same, while by simple adjustment of the variable Z in the system of dimensionless equations,

we have the new system

$$\begin{aligned}
\frac{dZ}{d\theta} &= -\beta r Z \tan\gamma \\
\frac{du}{d\theta} &= -\frac{\sqrt{\beta r} Z u(1+\lambda^2)}{E_{max}\cos\gamma} - (2-u)\tan\gamma \\
\frac{d\gamma}{d\theta} &= \frac{\sqrt{\beta r} Z \lambda}{\cos\gamma} + 1 - \frac{1}{u}
\end{aligned} \tag{11.117}$$

In these equations, E_{max} is the maximum lift-to-drag ratio which is a performance characteristic of the hypervelocity lifting vehicle while λ is now the normalized lift coefficient which is defined as

$$\lambda = \frac{C_L}{C_L^*} \tag{11.118}$$

This system and its three-dimensional generalization can be used to analyze optimal reentry trajectories with lift and bank modulation. The solution to these problems requires the use of variational calculus (Vinh, 1981).

Exercises

11-1. Consider the tangential deceleration

$$a = -\frac{dV}{dt} = \frac{D}{m} + g\sin\gamma$$

If we neglect the term $g\sin\gamma$, show that the relative error in evaluating the deceleration is

$$\frac{\Delta a}{a} = \frac{\sin\gamma}{(D/W)+\sin\gamma} \approx \frac{\sin\gamma}{D/W}$$

For $\gamma = -5°$, evaluate the percentage errors for a drag-to-weight ratio of D/W =4, 6, and 8.

11-2. Show that the ratio of the local circular speed at the altitude h to the circular speed at sea level is

$$\frac{V_c}{\sqrt{g_0 r_0}} = \left(1+\frac{h}{r_0}\right)^{-1/2} = 1 - \frac{1}{2}\frac{h}{r_0} + \frac{3}{8}\left(\frac{h}{r_0}\right)^2 - \cdots$$

Hence, $V_c \approx \sqrt{g_0 r_0}$ if $h/r_0 \ll 1$.

11-3. Consider Eq. (11.29) for equilibrium glide at small flight path angles

$$\frac{C_L}{C_D} + \frac{1}{\sqrt{\beta r} Z}\left(1 - \frac{1}{u}\right) = 0$$

For glide with super circular speed, $u > 1$, it is necessary to use negative lift to satisfy this equation. Let $u_i > 1$ be the initial value of the speed variable and $C_{L_{max}}$ be the maximum value of $|C_L|$.

Show that the highest altitude which can be satisfied by this equation is obtained by solving the equation

$$\frac{1}{2m}(r_0 + h)\rho(h) S C_{L_{max}} = 1 - \frac{1}{u_i}$$

for h.

If we continue to glide at this maximum altitude, the speed decreases from the initial speed u_i to the stall speed u_f while the lift coefficient increases from $-C_{L_{max}}$ to $C_{L_{max}}$. Show that

$$u_f = \frac{u_i}{2u_i - 1}$$

11-4. For ballistic entry, if we include the gravitational force by keeping the small term $(2 - u)\tan\gamma$ in the equation for u, Eq. (11.46) would become with constant γ,

$$\frac{du}{dZ} = \frac{u}{\sqrt{\beta r}}\left(\frac{2}{\sin\gamma_i} - \frac{1}{\sqrt{\beta r} Z}\right) + \frac{2}{\beta r Z}$$

(a) Show that the general solution of this linear differential equation is

$$u = \frac{2}{\beta r} Z^{-1/\beta r} \exp\frac{2Z}{\sqrt{\beta r}\sin\gamma_i}\,[I(Z) + C]$$

Where C is a constant of integration and the integral $I(Z)$ is defined as

$$I(Z) = \int Z^{\frac{1}{\beta r} - 1} \exp\left(-\frac{2Z}{\sqrt{\beta r}\sin\gamma_i}\right) dZ$$

(b) Let $n = 1/\beta r$. Show that this integral can be reduced to the integration of

$$I_n(x) = \int e^x x^{n-1} dx, \qquad x = -\frac{2Z}{\sqrt{\beta r}\sin\gamma_i}$$

If we take $n = 0$ approximately, the integral is the exponential integral

$$I = E_i(x) = \int_{-\infty}^{x} \frac{e^t}{t} dt$$

If $n \neq 0$, by integration by parts, derive the recurrence formula

$$I_n(x) = x^{n-1}e^x - (n-1)I_{n-1}$$

Then, by repeated application of this formula, deduce the series solution

$$I_n(x) = x^{n-1}e^x\left[1 - \frac{n-1}{x} + \frac{(n-1)(n-2)}{x^2} - \frac{(n-1)(n-2)(n-3)}{x^3} + \cdots\right]$$

11-5. For a skip trajectory, without making the assumption of small flight path angle, use Eqs. (11.74) and (11.75) in the expression (11.77) to express the critical altitude where maximum deceleration occurs as

$$\frac{Z_* - Z_i}{\sqrt{\beta r}} = \frac{2\sin^2(\gamma_i/2)}{C_L/C_D} \frac{\sqrt{1+2\epsilon} - 1}{\epsilon + \tan^2(\gamma_i/2)(1 + \epsilon - \sqrt{1+2\epsilon})}$$

where

$$\epsilon = \frac{2\sin^2\gamma_i}{(C_L/C_D)^2}$$

For very small flight path angle, $\epsilon \ll 1$, by binomial expansion, show that

$$\frac{Z_* - Z_i}{\sqrt{\beta r}} = \frac{2\sin^2(\gamma_i/2)}{C_L/C_D}\left[1 - \frac{\epsilon}{2\cos^2(\gamma_i/2)} + O(\epsilon^2)\right]$$

Hence, a higher order modification to Eq. (11.79) is

$$\frac{Z_* - Z_i}{\sqrt{\beta r}} = \frac{2\sin^2(\gamma_i/2)}{C_L/C_D}\left[1 - \frac{4\sin^2(\gamma_i/2)}{(C_L/C_D)^2}\right]$$

11-6. Consider the solution (11.47) for ballistic entry. Let A and B be two physical quantities such that

$$A = Zu^{\alpha} \quad \text{and} \quad B = Zu^{\beta}$$

where α and β are two positive exponents. Show that during entry, the peak value of A occurs before the peak value of B if $\alpha > \beta$.

11-7. We recall that for a skip trajectory $\gamma_f = -\gamma_i$.

(a) Let V_i, V_b, and V_f be respectively the speeds at the entry point, the lowest point and the exit point. Show that

$$V_b^2 = V_i V_f$$

(b) Let V_{f_1} be the speed and γ_{f_1} be the flight path angle at exit after the first skip. Then, after exit into the vacuum, the vehicle will follow a Keplerian trajectory and reenter the atmosphere for another skip. By symmetry of the trajectory, the new entry angle is $\gamma_{i_2} = -\gamma_{f_1} = \gamma_i$, and the new entry speed is $V_{i_2} = V_{f_1}$. Show that the speed at exit of the nth skip is

$$V_{f_n} = V_i \exp \frac{2n\gamma_i}{C_L/C_D}$$

(c) Let subscript n denote the elements durning the nth skip. Show that

$$V_{b_n} = \sqrt{V_{f_{n-1}} V_{f_n}} = V_i \exp \frac{(2n-1)\gamma_i}{C_L/C_D}$$

Then, deduce that the peak deceleration during the nth skip is

$$\left(\frac{a}{g}\right)_{max(n)} = \frac{\beta r \gamma_i^2 V_i^2}{2V_c^2 (C_L/C_D)} \exp \frac{2(2n-1)\gamma_i}{C_L/C_D}$$

11-8. By inspecting Eq. (11.82), for a skip trajectory, it is seen that the peak deceleration a_{max} increases as the square of the entry speed. It is proposed to determine the influence of γ_i and C_L/C_D on the peak deceleration.

Let

$$x = -\gamma_i > 0, \qquad y = \frac{1}{C_L/C_D}$$

and put the expression for a_{max} in the form

$$a_{max} = Kx^2y\exp(-2xy)$$

where K is a constant.

(a) By keeping y constant, show that a_{max} increases as x increases if $xy < 1$, that is if

$$\frac{C_L}{C_D} > -\gamma_i$$

a condition which is generally true for a skip trajectory.

(b) Similarly, by keeping x constant, show that a_{max} decreases as y decreases if $2xy < 1$, that is if

$$\frac{C_L}{C_D} > -2\gamma_i$$

a condition which is also generally true for a skip trajectory.

11-9. (a) By using the half-tangent formula, transform Eq. (11.102) into the quadratic equation

$$3(1+\cos\gamma_i)\tan^2\frac{\gamma}{2} - \frac{C_L}{C_D}\tan\frac{\gamma}{2} - 3(1-\cos\gamma_i) = 0$$

Deduce the solution (11.103).

(b) Similarly, transform Eq. (11.107) into the quadratic equation

$$3(1+\cos\gamma_i)\tan^2\frac{\gamma}{2} - 2\frac{C_L}{C_D}\tan\frac{\gamma}{2} - 3(1-\cos\gamma_i) = 0$$

Deduce the solution (11.108).

11-10. By inspecting Eq. (11.105), it is seen that, for a skip trajectory, the peak heating rate $\bar{q}_{max}$ increases as the cube of the entry speed V_i. As for the effect of γ_i and C_L/C_D, show that

$$\bar{q}_{max} = Kxy\exp(-3xy^2)$$

where K is a constant and by definition

$$x = -\gamma_i \quad \text{and} \quad y = \frac{1}{\sqrt{C_L/C_D}}$$

(a) By keeping y constant, show that $\bar{q}_{max}$ increases as x increases if $3xy^2 < 1$, that is if

$$\frac{C_L}{C_D} > -3\gamma_i$$

a condition which is generally true for a skip trajectory.

(b) Similarly, by keeping x constant, show that $\bar{q}_{max}$ increases as y increases if $6xy^2 < 1$, that is if

$$\frac{C_L}{C_D} > -6\gamma_i$$

a condition which is also generally true.

We conclude that the peak heating rate $\bar{q}_{max}$ is higher with higher entry speed, steeper entry angle and lower lift-to-drag ratio.

11-11. Concerning the function $(\bar{q}_{av})_{max}$ as given in Eq. (11.110), it has the same functional form as the function $(a/g)_{max}$ as given by Eq. (11.82). Hence, using the same definition for x and y as in Exercise 11-8, we conclude that for a skip trajectory, $(\bar{q}_{av})_{max}$ is higher with higher entry speed, steeper entry angle and lower lift-to-drag ratio.

Carry out the analysis and show that $(\bar{q}_{av})_{max}$ increases as x increases if $(C_L/C_D) > -1.5\gamma_i$ and that it increases as y increases if $(C_L/C_D) > -3\gamma_i$.

11-12. In the case of multiple-skip trajectory, we can visualize the vehicle as making several bounces on the top of the atmosphere of a spherical planet. We recall from Eq. (11.67) that, if V_i is the initial entry speed and γ_i is the initial entry angle, the exit speed V_{f_1} after the first skip is

$$V_{f_1} = V_i \exp \frac{2\gamma_i}{C_L/C_D}$$

and the exit angle is $\gamma_{f_1} = -\gamma_i$. With this velocity vector, the vehicle will travel in the vacuum for a distance x_1 before reentering the atmosphere with the speed $V_{i_2} = V_{f_1}$ and entry angle $\gamma_{i_2} = -\gamma_{f_1} = \gamma_i$ for the second skip.

(a) To obtain a simple estimate of the longitudinal distance travelled x_1 during the first hop of the vehicle in the vacuum, we use the equations for flight in a uniform gravitational field

$$\ddot{x} = 0$$

$$\ddot{z} = -g$$

where z is the altitude above the atmosphere. Integrate the equations with the initial conditions at $t = 0$, $x = z = 0$, $\dot{x} = V_{f_1} \cos \gamma_i$, $\dot{z} = -V_{f_1} \sin \gamma_i$ to obtain the range

$$x_1 = -\frac{V_{f_1}^2}{g} \sin 2\gamma_i$$

Similarly, by changing the subscript we have the distance travelled during free flight after the nth skip

$$x_n = -\frac{V_{f_n}^2}{g} \sin 2\gamma_i$$

(b) By neglecting the small ranges during the atmospheric skipping phases and using the result of Exercise 11-7, show that the total range for a skip trajectory is

$$x = \sum_{n=1}^{\infty} x_n = -\frac{V_i^2}{g} \sin 2\gamma_i \exp \frac{4\gamma_i}{C_L/C_D} \left(1 - \exp \frac{4\gamma_i}{C_L/C_D}\right)^{-1}$$

This equation is obtained by applying the formula for the infinite sum of a geometric progression. As an example, consider the case where $\gamma_i = -5$ deg, and $C_L/C_D = 3$. Show that to have a range of a quarter of a great circle, that is for $x = \pi r_0/2$, we must have an initial entry speed of $V_i = 1.0565 V_c$.

(c) To see the influence of γ_i on the total range, consider the case of very small values for the entry angle. By using series expansion show that we have approximately

$$x = \frac{V_i^2}{2g} \frac{C_L}{C_D} \left(1 + \frac{4\gamma_i}{C_L/C_D}\right)$$

Use this formula to recalculate the numerical example in part (b).

APPENDIX 1

Atmospheric and gravity data

Distribution of temperature, speed of sound, dynamic viscosity, density, and pressure in the standard atmosphere.

h (kft)	T/T_0	a/a_0	μ/μ_0	ρ/ρ_0	p/p_0
0	1	1	1	1	1
5	0.9656	0.9827	0.9731	8.617×10^{-1}	8.320×10^{-1}
10	0.9312	0.9650	0.9457	7.385	6.877
15	0.8969	0.9470	0.9178	6.292	5.643
20	0.8625	0.9287	0.8894	5.328	4.595
25	0.8281	0.9100	0.8605	4.481	3.711
30	0.7937	0.8909	0.8311	3.741	2.970
35	0.7594	0.8714	0.8011	3.099	2.353
36.089	0.7519	0.8671	0.7945	2.971	2.234
40	0.7519	0.8671	0.7945	2.462	1.851
45	0.7519	0.8671	0.7945	1.936	1.455
50	0.7519	0.8671	0.7945	1.522	1.145
55	0.7519	0.8671	0.7945	1.197	9.000×10^{-2}
60	0.7519	0.8671	0.7945	9.414×10^{-2}	7.078
65	0.7519	0.8671	0.7945	7.403	5.566
65.800	0.7519	0.8671	0.7945	7.124	5.356

Standard values for air at sea level:

$$T_0 = 288.150^\circ \text{ K}$$
$$p_0 = 1.01325 \times 10^5 \text{ N/m}^2 \quad (2116.22 \text{ lb/ft}^2)$$
$$\rho_0 = 0.12492 \text{ kg-s}^2/\text{m}^4 \quad (0.002377 \text{ lb-s}^2/\text{ft}^4)$$
$$a_0 = 340.294 \text{ m/s} \quad (1116.45 \text{ ft/s})$$
$$g_0 = 9.80665 \text{ m/s}^2 \quad (32.174 \text{ ft/s}^2)$$
$$\rho_0 g_0 = 1.225 \text{ kg/m}^3 \quad (0.0765 \text{ lb/ft}^3)$$
$$\mu_0 = 1.7894 \times 10^{-5} \text{ N-s/m}^2 \quad (3.7373 \times 10^{-7} \text{ lb-s/ft}^2)$$

Exponential atmosphere:

$$\rho = \rho_0 \exp(-\beta z)$$

An average value for the inverse of the scale height is

$$\frac{1}{\beta} = 23,500 \text{ ft} = 7,163 \text{ m}$$

APPENDIX 2

Typical aircraft characteristics

Main equations used for the definitions of various symbols:

Parabolic drag polar:

$$C_D = C_{D_0}(M) + K(M)C_L^2$$

$$C_L^* = \sqrt{\frac{C_{D_0}}{K}}$$

$$E_{max} = \frac{1}{2\sqrt{KC_{D_0}}}$$

Lift equation for nearly horizontal cruise:

$$W = \frac{1}{2}\rho S V^2 C_L$$

Breguet range equation for propeller driven aircraft:

$$x = \frac{\eta_p}{c_p} E_{max} \operatorname{Log} \frac{1}{1-\zeta}$$

Breguet range equation for turbojet aircraft:

$$x = \frac{VE}{c} \operatorname{Log} \frac{1}{1-\zeta}$$

Fuel weight fraction:

$$\zeta = \frac{\text{fuel weight}}{\text{initial weight}} = \frac{\Delta W}{W_1}$$

Aircraft A

Twin engine propeller driven aircraft:

$$C_{D_0} = 0.025$$
$$K = 0.048$$
$$C_{L_{max}} = 1.8$$
$$W_1 = 8,000 \text{ lb}$$
$$S = 220 \text{ ft}^2$$

We can also take various values for S such that the wing loading W_1/S (lb/ft^2) is in the range 20 to 40.

Max $P = 960$ hp $= 550 \times 960$ lb-ft/s, at sea level
$\eta_p =$ propeller efficiency, in the range 0.80 to 0.90
$c_p = 0.45$ lb/h/hp
$\zeta = 0.15$ to 0.25

If, in Breguet range equation the distance travelled x is in statute miles, the corresponding value for c_p is 0.45/375.

Aircraft B

Medium range turbojet transport aircraft:

$$W_1 = 100,000 \text{ lb}$$
$$S = 825 \text{ ft}^2$$

We can also take various values for S such that the wing loading W_1/S (lb/ft^2) is in the range 80 to 130.

Max $T = 32,000$ lb, at sea level
$c = 0.80$ to 1.1 hr^{-1}
$\zeta = 0.15$ to 0.30

Aircraft aerodynamic data:

M	C_{D_0}	K	$C_{L_{max}}$
0	1.230×10^{-2}	6.056×10^{-2}	1.80
0.60	1.230	6.056	1.80
0.65	1.233	6.100	1.70
0.70	1.236	6.250	1.60
0.75	1.239	6.500	1.40
0.80	1.245	6.850	1.20
0.85	1.260	7.400	0.90
0.90	1.320	8.200	0.60

In take-off and landing configuration, use $C_{L_{max}} = 2.0$.

Aircraft C

Supersonic turbojet fighter aircraft:

$$W_1 = 36,000 \text{ lb}$$
$$S = 500 \text{ ft}^2$$
$$\text{Max } T = 25,000 \text{ lb, at sea level}$$
$$c = 0.80 \text{ to } 1.20 \text{ hr}^{-1}$$
$$\zeta = 0.15 \text{ to } 0.20$$

Aircraft aerodynamic data:

M	C_{D_0}	K	$C_{L_{max}}$
0	0.55×10^{-2}	0.420	1.20
0.4	0.55	0.420	1.20
0.6	0.56	0.424	1.20
0.8	0.60	0.427	0.85
1.0	0.92	0.450	0.45
1.2	1.20	0.463	0.50
1.4	1.16	0.475	0.55
1.6	1.10	0.490	0.60
1.8	1.00	0.505	0.65
2.0	0.86	0.520	0.66

In take-off and landing configuration, use $C_{L_{max}} = 1.8$.

APPENDIX 3

Conversion table

Length

1 inch	= 0.0254 m
1 foot	= 0.3048 m
1 statute mile	= 1609.344 m
1 nautical mile	= 1852 m
1 meter	= 3.28084 ft

Mass

1 slug	= 14.5939 kg
1 kilogram	= 0.06852 slug

Force

1 pound	= 0.453592 kg
1 pound force	= 4.44823 newtons
1 kilogram	= 2.204623 lb
1 kilogram	= 9.807 newtons

References

1. Abramowitz, M., and Stegun, I. A. (1964). *Handbook of Mathematical Functions*. National Bureau of Standards.

2. Allen, H. J., and Eggers, A. J., Jr. (1958). "A study of the Motion and Aerodynamic Heating of Missile Entering the Earth's Atmosphere at High Supersonic Speeds". *NACA Report*, No. 1381.

3. Anderson, J. D., Jr. (1978). *Introduction to Flight*. McGraw-Hill, New York.

4. Buning, H. (1986). *Flight Mechanics Lecture notes*. The University of Michigan.

5. Chapman, D. R. (1959). "An Approximate Analytical Method for Studying Entry into Planetary Atmosphere.". *NASA TR R-11*.

6. Dommasch, D. O., Sherby, S. S., and Connolly, T. F. (1967). *Airplane Aerodynamics*. (Fourth Edition). Pitman Publishing Corp., New York.

7. George, L., Vernet, J. F., and Wanner, J. C. (1969). *La Mécanique du Vol-Performances des Avions et des Engins*. Dunod, Paris.

8. Hale, F. J. (1984). *Aircraft Performance, Selection, and Design*. John Wiley & Sons, New York.

9. Kerrebrock, J. L. (1977). *Aircraft Engines and Gas Turbines*. MIT Press, Cambridge, Massachusetts.

10. Kuethe., A. M., and Chow, C. Y. (1976). *Foundations of Aerodynamics*. John Wiley, New York.

11. Lan, C. T. E., and Roskam, J. (1981). *Airplane Aerodynamics and Performance*. Roskam Aviation and Engineering Corp., Ottawa, Kansas.

12. McCormick, B. W. (1979). *Aerodynamics, Aeronautics, and Flight Mechanics*. John Wiley & Sons, New York.

13. Miele, A. (1962). *Flight Mechanics—Theory of Flight Path*. Addison-Wesley, Reading , Massachusetts.

14. Miller, L. E., and Koch, P. G. (1976). "Aircraft Flight Performance Methods". *AFFDL-TR-75-89*. Wright-Patterson Air Force Base, Dayton, Ohio.

15. Turcat, A. (1960). *Cours de Mécanique du Vol*. Dunod, Paris.

16. *U.S. Standard Atmosphere*. (December, 1962). Prepared under the sponsorship of the National Aeronautics and Space Administration, the United States Air Force and the United States Weather Bureau, Washington, D.C.

17. Vinh, N. X., Busemann, A., and Culp, R. D. (1980). *Hypersonic and Planetary Entry Flight Mechanics*. The University of Michigan Press, Ann Arbor, Michigan.

18. Vinh, N. X. (1981). *Optimal Trajectories in Atmospheric Flight*. Elsevier Scientific Publishing Co., Amsterdam, Holland.

19. Vinh, N. X., and Lu, P. (1988). "Chebyshev Minimax Problems for Skip Trajectories". *The Journal of the Astronautical Sciences*, 36(1–2):179–197.

Index

absolute reference, 9
absorbed heat, 338
acceleration
  absolute, 12
  Coriolis, 12
  gravitational, 21, 333
  relative, 12
  transport, 12
actuator disk, 65
advance ratio, 70
aerodynamic ceiling, 118
aerodynamic efficiency, 39
aerodynamic forces, 8, 33
aerodynamic force components
  drag, 15, 34
  lift, 15, 34
aerodynamic heating for
  ballistic entry, 355
  glide entry, 354
  skip entry, 356
afterburning, 76
airspeed, 44
  calibrated, 45
  equivalent, 52
  indicated, 46
  indicator, 45
  true, 44
altitude
  critical, 125
  optimum cruise, 160, 164
  pressure, 48
angle-of-attack, 34
  stall, 35
  optimum, 37
angular velocity, 9
aspect ratio, 38
atmosphere
  exponential, 30
  isothermal, 335
  standard, 28
atmospheric
  density, 21, 29
  pressure, 28
  temperature, 28
  viscosity, 32

ballistic entry
  aerodynamic heating, 355
  deceleration, 345
  trajectory, 344
bank angle, 16, 222
  maximum, 225, 275
Bernouilli's equation, 44
best endurance, 146, 153

best range, 144, 154, 157
Breguet equation
  for endurance, 146
  for range, 144, 155

calibrated airspeed, 45
ceiling
  absolute, 190
  aerodynamic, 118
  cruise, 126, 131
  service, 191
Chapman variable, 334
climb angle, 192, 205
climbing flight
  most economical, 211
  non-steady, 205
  of propeller driven aircraft, 187
  of turbojet, 194
  zoom, 207
coefficient of
  drag, 21, 34
  lift, 21, 34
  lift at stall, 35, 299
  lift at take-off, 322
  rolling friction, 302, 320
control of flight, 114
coordinate systems
  geocentric, 23
  inertial, 9
  rotating, 9
  topocentric, 23
coordinated turn, 223
Coriolis acceleration, 12
critical
  altitude, 125
  Mach number, 41

deceleration during entry, 336
  ballistic, 345
  glide, 343
  skip, 351
descent, 100
  maximum endurance, 101
  maximum range, 101, 104
drag
  coefficient, 21, 34
  force, 34
  polar, 35
dynamic pressure, 50, 337

endurance factor, 175, 176
energy height, 206
equation of state, 29
equations of motion
  climbing flight, 184
  cruising flight, 112
  flat earth, 23–25
  flight in a vertical plane, 92
  reentry, 332
  spherical earth, 11, 20
  turning flight, 222
equivalent airspeed, 52
equivalent skin friction coefficient, 354
error function , 356
excess
  power, 186
  thrust, 281
exponential atmosphere, 30
exponential integral, 364

fastest climb, 189, 197
fastest turn, 238, 267, 276
filed length, 301
flare arc, 313, 319
flattest glide, 94
flight envelope, 116, 256
flight in a vertical plane, 92

flight over a flat earth
  coordinate systems, 23
  dynamical relations, 23
  kinematic relations, 24–25
flight over a spherical earth
  coordinate systems, 13
  dynamical relations, 20
  kinematic relations, 18
flight path angle, 14
  approach, 318
  climb, 186, 314
  glide, 94
  reentry, 333
forces
  aerodynamic, 8, 33
  centrifugal, 223
  gravitational, 15, 21
  propulsive, 8, 59
  rolling friction, 302, 320
fuel consumption, 59
fuel weight fraction, 139

gas constant, 29
gas turbine engine, 72
geocentric coordinates, 23
glide angle, 94
gliding entry
  aerodynamic heating, 354
  deceleration, 343
  trajectory, 339
gliding flight, 93
  maximum endurance, 97
  maximum range, 94
gravitational acceleration, 21, 333
ground effect, 309
ground run distance, 302

half loop, 287
heading angle, 14
heating rate, 337
horsepower, 63
hypervelocity vehicles, 332

Immelmann, 287
induced drag factor, 38

kinematic relations
  flat earth, 24–25
  spherical earth, 18
  vector, 9

laminar stagnation point, 337
landing, 317
  gear, 299
  ground run, 320
  transition, 318
latitude, 13
level flight, 112
lift coefficient, 21, 34
  at take-off, 322
  maximum, 35, 43
  stall, 35, 229
lift force, 21, 34
lift-off speed, 300
lift-to-drag ratio, 39
  maximum, 40
liquid propellant rocket, 60
load factor, 209, 224
  climbing turn, 282
  flight in a horizontal plane, 224
  flight in a vertical plane, 209
  landing, 319
  maximum, 258
  physiological-structural limit, 225, 259
  take-off, 314
logarithmic derivative, 118

longitude, 13
loop, 287

Mach number, 31
  corner, 259
  critical, 41
  drag divergence, 41
  optimum cruise, 160
  stall, 117
Machmeter, 46
maneuvering limit, 256
mass flow
  equation, 59, 63
  rate, 2, 60
maximum
  climb angle, 192, 205
  endurance, 146, 153
  range, 144, 154, 157
  rate of climb, 187, 196
  turning rate, 233, 267, 277
minimum
  time to climb, 189, 202, 207
  turning radius, 236, 269, 277
most economical climb, 211
multiflow propulsion systems, 60

normal acceleration, 107

obstacle height, 300
Oswald's efficiency factor, 39

parabolic drag polar, 38
peak deceleration, 343, 345, 353
peak heating rate, 355–358
piston-prop engines, 63
  aspirated, 63
  turbocharged, 64
pitch angle, 68
Pitot-static system, 44
Poisson's formula, 10
position vector, 8
power
  available, 119
  coefficient, 71
  equivalent shaft, 78
  minimum, 123, 231
  required, 120, 186, 228
  shaft, 63
power setting, 125
pressure
  altitude, 48
  atmospheric, 28
  dynamic, 50, 337
  stagnation, 44
  static, 44
propeller, 64
  efficiency, 66, 141
  theory, 67
propulsion systems, 59
  ramjet, 77
  reciprocating engine, 63
  rocket, 60
  turbofan, 78
  turbojet, 73
  turbojet with afterburner, 75
  turboprop, 77
propulsive force, 1, 8

radius
  flare, 314, 319
  of curvature, 107
  turning, 227, 254
ramjet, 77
range
  cruise, 143, 154
  maximum, 144, 154
  factor, 174, 177

rate
  heating, 337, 354
  of climb, 187, 195
  of descent, 97
  of fuel consumption, 60, 63
  turning, 226, 254
ratio
  advance, 70
  lift-to-drag, 39
  specific heats, 31
  thrust-to-weight, 101, 196, 262, 273
  weight, 145
Rayleigh formula, 47
reciprocating engines
  aspirated, 63
  supercharged, 64
reentry trajectories
  ballistic, 344
  glide, 339
  skip, 348
Reynolds number, 34
rocket
  climb, 198
  engine, 60
  powered aircraft, 194

Saint-Venant formula, 46
scale height, 30
sinking speed, 97
skin friction coefficient, 354
skip entry
  aerodynamic heating, 356
  deceleration, 351
  trajectory, 348
specific fuel consumption
  power, 63, 141
  thrust, 21, 148
speed
  circular, 23, 334
  decision, 301
  entry, 339
  lift-off, 300
  of sound, 31
  stall, 229
  touchdown, 317, 320
  wind, 142, 302
split-S, 287
stall
  lift coefficient, 35, 229
  speed, 229, 300
standard atmosphere, 28
steepest climb
  piston-prop, 192
  turbojet, 205
stratosphere, 28
  cruising flight, 163
  optimum altitude, 164
subsonic aircraft
  aerodynamic characteristics, 38
  flight envelope, 116
supersonic aircraft
  aerodynamic characteristics, 41
  flight envelope, 117

take-off, 298
  ground run, 305
  transition, 312
  wind effect, 309
tangential
  acceleration, 106
  deceleration, 336
  force, 15
throttle setting, 59
thrust
  angle-of-attack, 15

available, 127
coefficient, 71, 135
curves, 128
jet, 78, 165
magnitude, 21
minimum, 129, 171, 196
required, 127, 261
reverse, 320
static, 304
thrust-to-weight ratio, 101, 196, 262, 273
topocentric coordinates, 23
touchdown speed, 317, 320
transonic region, 43, 133
transport acceleration, 12
tropopause, 28, 164
troposphere, 28
cruising flight, 163
optimum altitude, 164
true airspeed, 44
turbofan, 78
turbojet, 73
turboprop, 77
turning flight, 223, 253
maximum bank angle, 275
maximum load factor, 275
maximum turning rate, 233, 268, 277
minimum turning radius, 236, 269, 275
power required, 228
thrust required, 261
turning radius, 227, 268
turning rate, 226, 266

velocity vector, 8

weight
apparent, 224
ratio, 145
wind effects on
optimum angle-of-attack, 142
take-off and landing, 309
wing
aspect ratio, 38
loading, 100, 116, 148, 156, 163, 199
reference area, 34, 38
span, 38

zero-lift drag coefficient, 38

Printed in the United Kingdom
by Lightning Source UK Ltd.
9711000001B/241-249



This text, written at a level accessible to advanced undergraduate and beginning graduate students, covers all aspects of flight performance of modern day high-performance aircraft, from take-off to landing, through different phases of flight in climb, cruise, turning and descent.

The book begins with an introduction to equations of motion, aerodynamic forces, and propulsion systems and then goes on to apply what has been learned to performance during descent and glide, cruising, climb, turning and take-off and landing. A final chapter discusses the performance of hypervelocity re-entry vehicles. Challenging exercises are included at the ends of chapters. These are designed to give readers a deeper understanding of the material covered in the text.

This text will serve as an introductory text for advanced undergraduates and beginning graduate students. It will also be of value to researchers in universities and industry.

Nguyen Vinh has been a Professor of Aerospace Engineering at the University of Michigan since 1972, and is a prolific author of books and technical papers on flight dynamics. For his contribution to aerospace engineering sciences, he was elected a foreign member of the French Academy of Air and Space in 1984. He has received the Excellence in Teaching and Excellence in Research Awards from the College of Engineering at the University of Michigan.

The cover photograph shows a General Dynamics F-16, and is reproduced by kind permission of General Dynamics.



CAMBRIDGE
UNIVERSITY PRESS

ISBN 0-521-47852-9
90000
9 780521 478526